African Railway Center of Excellence (ARCE)

A Comparative Analysis of the Effect of Section Loss on Section Performance of Cast-In-Place Railway Bridge Girder

A Thesis in Railway Civil Infrastructure Engineering

Joseph Fallah

Addis Ababa

A thesis submitted as a partial fulfilment of the requirements of Master of Science

January 2022

Declaration and approval

I, **Joseph Fallah**, to the best of my knowledge do hereby declare that this work is my original work and that everything contained herein is mine except wherein duly stated (acknowledged, and or referenced). Henceforth, this work has never been submitted no issued any academic qualification.

Signed: ___________ ___________________

Joseph Fallah Date (MM/DD/YYYY)

In testament of the above declaration, we the undersigned, do recommend that the thesis completed by the student above, in partial fulfillment of the degree requirements, be accepted by the Addis Ababa Institute of Technology for deposit.

Advisors' Approval:

Abrham Gebre, (PhD)	________________	____________________
Advisor	Signature	Date (MM/DD/YYYY)
Victor B. Smith, (MSCeng)	________________	____________________
Co-advisor	Signature	Date (MM/DD/YYYY)

Examiners' Approvals:

Zewdie Moges	________________	____________________
Internal Examiner	Signature	Date (MM/DD/YYYY)
Anteneh Zewdu	________________	____________________
External Examiner	Signature	Date (MM/DD/YYYY)

Departmental Approval

Zewdie Moges	________________	____________________
Chairperson	Signature	Date (MM/DD/YYYY)

Preface

This research work is written as a core partial fulfilment to obtaining the degree **Master of Science in Civil Infrastructure**. I'm a Liberia, a 2014 Civil Engineering degree graduate from the Stella Maris Polytechnic (now Stella Maris Polytechnic University), Monrovia. Prior to taking up undergraduate studies, I had been an ardent admirer and lover of the field of engineering and while there I started taking up light jobs in the construction industry, including internship, etc. Upon graduation, I had the opportunity to immediately get started as a junior staff. Approximately five years later, with a wealth of practical engagements and experiences, I travelled here to start a graduate program in Railway Engineering.

Nowadays, countries that have built a large and viable railway system have in some sense boosted their transportation sector. From this backdrop, ARCE was established to give that opportunity to young African engineers acquire the basic knowledge that would lead to them making impacts in the development of a railway system in their various countries. With the above mandate, and being from the Civil Infrastructure (CI), I decided taking up this research because of its link to several works I had previously undertaken and completed. Let me emphasize here also that my advisor was an ideally instrumental architect during the formulation and structuring of this research topic.

This research was written with the aim to assist railway engineers and civil/bridge engineers at large who are strategically into the infrastructural maintenance division, bridge design section, etc. to tap into this work and understand engineering backgrounds of cracks and how they can be controlled and maintained. It is worthwhile mentioning that this work is my original work!

Let me personally thank all the institutions and individuals who directly and indirectly contributed to my studies for their immense support that have culminated in the writing of this research. Notwithstanding, I would like to seize the opportunity to mention a few:

No.	Name	Contribution
1.	AALRT	Provision of data
2.	ERC	Provision of data
3.	ERA	Provision of data
4.	ArcelorMittal Liberia	Provision of data
5.	Winnie M. Siakor	Miscellaneous supports (Liberia)
6.	H. Athelstan F. K. Tambah	Miscellaneous supports (Liberia)
7.	Vivian T. Fallah (sister)	Miscellaneous supports (Liberia)
8.	Dabby P. Zeogar	Contribution to a research publication, Miscellaneous supports (USA)
9.	Tommy F. Kpakio	Miscellaneous supports (USA)

I'm extremely grateful to the Bestman family (landlord) for the enormous support they provided my home while I undertook this study. Finally, my family, you've always dearly remained special to my heart: you are awesome!

Joseph Fallah
Addis Ababa
December 2021

Dedication

This work is dedicated to my late mother **Hawa Yawah Ansumana Fallah** who was commonly referred to as **Mary-Go-Round** and my late father **John Fallah.**

Abstract

Section loss is a general term associated with reduction in the cross-sectional area of a member due to extreme loading, repeated load cycles, rebar carbonation, etc. To ascertain this magnitude of loss, this study strived to understand the parameters involved. In reinforced concrete (RC) members, section loss may begin with the steel and then the effect spilled over to the concrete or vice versa which then gets affected by atmospheric influents. In any case, technically the section (T-girder, rectangular section, etc.) is reduced or compromised, thus reducing its capacity and leading to an irreversible path to structural inefficiency. A building-block deficiency, crack from either extreme or repeated loading is a major contributor to section loss. Cracks were then thoroughly analyzed and a crosscheck was then authenticated against similar research (i.e., virtual laboratory) and finally LISA FEA was used to model and simulate the cracked design to monitor the response of the section in term of capability and performance. This research then derived and presented a direct relationship between flexural crack width and deflection. The proposed equation is in good agreement with the output of the finite element software.

Traditionally made of reinforcing bars and concrete, RC members have over the years been studied to investigate the particulate nature of the constituent elements acting as a unit. The analysis and design of cast-in-place railway bridges, like many other railway bridges, incorporates the application of several load types that are usually of very high magnitudes. The combination of these loads depicts the large depth-to-width ratios of flexural members. These loads include: dead load, live load, impact, Centrifugal force, Earth pressure, Buoyancy, Wind Load on Structure, Wind load on Live Load, Longitudinal force from Live Load, Longitudinal force due to Friction, or Shear Resistance at Expansion Bearing, Seismic, Stream Flow Pressure, Ice Pressure, Temperature, Rib Shortening, Shrinkage, Settlement of supports etc. Here, a railway superstructure is analyzed, and the load-carrying flexural member is designed. This research focused on the engineering that leads to cracks and the performance of the member considered. Cracks are one of the building blocks of long-term deformation in a structural member. This research employed several analytically comparative methods that investigated the trends and magnitude of section loss on the girder of a cast-in-place railway bridge by completely analyzing the girder manually under several static and dynamic loading conditions utilizing different materials strength parameters. The analysis informed the research about key characteristics of the girder to include: girder depth, girder width, and area of steel. These structural parameters were then used against a symbolic beam that were tested in the laboratory. Results from a virtual laboratory, to include crack dimensions, stiffness, were then used in the model of the cracked girder to understand the mode of response of the girder of these cracks.

Using the LISA FEA 8.0.0, approximate representations of crack widths were simulated into the model using the same material strength parameters as contained in the manual computational analysis. The performance of the girder was then rated based on allowable capacities as given in several references, regulatory materials, codes, and standards. It was observed and noted that up to the design crack width, the cracked section deflected steadily, and that the deflected cracked section is as twice as the uncracked section.

Table of Contents

List of figures

List of Tables

1. Introduction

This section, divided into sub-sections, paves the way in undertaking this research.

1.1 Overview

Over the years, bridges and culverts have been the predominant structures for curbing obstacle-crossing hindrances such as waterways and valleys. These structures are so important that they make transportation possible across. In railway transportation, the mode of contact between the vehicle and that of the path (i.e., the rail) is different from other modes of transportation. The fixed narrow path of the track makes way for a stricter load application point than their highway counterpart thus calling for high punching shear. Normally, rail services commercialized for passenger services are normally lighter than those dedicated to freight hauling services. For instance, nowadays most fast-growing cities, population wise, have adopted to using light right transportation to account for older modes such as streetcars and trolleys to ease the congestion problems faced by urbanization [1]. For longer distance travels, highspeed rail significantly reduces travel time and increases efficiency. However, highspeed rail costs the infrastructural component of the system a very high investment. All of these improvements need to be reflected in the principal load-carrying elements of the structure – the girder.

The bonding mechanisms associated with a reinforced concrete member do have an estimated length of time at which they might be structurally effective. Notwithstanding, impromptu and above-rated loads and/or conditions may abruptly destabilize those parameters. Due to some of those unforeseen circumstances, one of the main defects that normally pops out as early as possible is crack. Cracks, which are technically referred to as section loss in this research, weaken the overall estimated and anticipated strength of the section. It is important to mention that cracks on infrastructural projects like brides, especially railway bridges, should be at their minimal best. Researchers have evolved several theories and conducted experimental works on different types of engineering structures and have provided substantial evidence in trying to analyze the bonding properties associated with a section.

For railway areal structures undergo several loadings and under severe magnitude, damping elements and materials are installed to mitigate the compromise of load effects on principal load-carrying members. In ballasted tracks, the ballasts and pads serve as the primary dampers whereas in ballastless tracks, pads and suspension fasteners appreciably solve these problems. Nonetheless, these materials come with their limitations as well – may serve as weak points. To curb the effects of structural nonperformance, it is advisable heavier vehicles move on their designed lines in lieu of the consequences thereafter. The railway code [2] calls for a very heavier Copper E-360 axle load that may not necessarily be usefully economical for a light rail. In this way, some states within the United States (US) are quickly shifting to a more lighter loading condition in the neighborhood of an HS32 Truck [1] but with a very detailed engineering analysis computation. Railway Bridges are principally the key obstacle-crossing structures for which detailed analysis is to be run to enable them carry across a rolling stock effectively and safely. The functionality of a railway bridge will exhibit some level of ill-performances when some of the component members start to, at some extent, lose their individual capacities. The principal consideration in this case is the girder. From this backdrop concerning ill-performace, it was necessary to then devise the relationship between the ill-performance and the ill-performance factor, which is load in this case. This would then mitigate the problem.

1.2 Background of the Study

One of the most common failure mechanisms in structures is crack propagation. This study was undertaken to weigh in on the subject matter of figuring out cracks in a railway bridge wherein the magnitude and pattern would be determined and measured to know the effects on the section. Detecting some of the effects associated with the impacts of railway loads on a railway bridge girder is then given a great deal of consideration. Initially, a general look at researches that have been conducted in the area of concrete behavior sets the pace for conducting this research. Further, a more consolidated effort is made in reviewing railway bridge specific papers that focus on the load–structure interaction of the superstructure and then finally to the girder.

1.3 Aim and Objectives

In railway engineering, but specifically railway bridge engineering, only a few of such studies have been undertaken hence they are not readily available. Against this backdrop, this study tends to investigate the structural effects that cracks pose to a cast-in-place railway bridge girder by simulation of cracks into the girder while manipulating the material and sectional properties and then providing concluding statements.

The following points summarize the aim and objective of this research:

a. Analysis and design of the girder of a cast-in-place reinforced concrete railway bride
b. Probable causes associated with the types of structural cracks
c. The triggered down effects of cracks on a structural member

In the context of specificity, the objective of the research is to understand the degree of impact that cracks have on a cast-in-place railway bridge girder and provide measures of remedy.

1.4 Scope

This work followed three separate procedures as outlined in the methodology to obtain the objectives.

1.5 Hypothesis

If a definite relationship between flexural crack and deflection exists, then the causes and propagation of flexural crack would be so direct that the expression could be iterated in any way possible to suit the needed condition.

1.6 Limitations of the study

In this study, like any other study, a couple limitations are encountered. However, the major limitation is the inability to conduct an experiment in which a pseudo-moving load would have been tested on a symbolic girder. This is primarily due to the unavailability of the requisite laboratory setup that effectively undertakes such experiment. However, other studies that were undertaken in this form and manner are referenced.

2 Review of the Literature

Here, a systematic review of reinforced concrete materials and structures is done across several published research projects. Traditionally, reinforced concrete is composed of reinforcing bars and concrete – which is also a mixture of cement, sand, and crushed stones. However, advancement has had it evolved over the years that several other materials are nowadays used in the proportioning of reinforced concrete.

2.1 General Review of Reinforced Concrete

The general purpose of reinforcing a concrete section is to account for tension when the section is loaded, [3]. Nowadays, reinforcement in concrete may not singlehandedly be of the traditional steel rebar module. Carbon, fiberglass, natural, aramid, etc. are a few common types of composites used for reinforcement purposes in the construction industry. Each of these reinforcement methodologies have their strengths and limitations that make them unique to specific purposes.

[4] provides insight on the probable amount of splitting and or tensile strengths (up to 100%) that steel reinforcement bars could add to a section compared to the fiber. An improvement of more than 100% in displacement ductility of the beam specimens is achieved by the employment of 0.5% steel as compared to the 1% fiber element. [5] finds out that for salinity has damaging effect on steel rebars, members reinforced primarily with FRP bars could provide long-term solution to such. In this light, with the probable termination of corrosion related failure, it can be correlated also that good bonding exists even in the long-term. Furthermore, with said good bonding, failures associated with crack profiling is proportional. However, mechanical properties such as strength, roughness, toughness, etc. are comparably lower. Table 2-1 is quoted from [6].

Standard designation	**Description**
EN 14889-1:2006	Fibres for Concrete. Steel Fibres. Definitions, specifications & conformity
EN 14845-1:2007	Test methods for fibres in concrete
ASTM A820-16	Standard Specification for Fiber-Reinforced Concrete (superseded)
ASTM C1116/C1116M	Standard Specification for Fiber-Reinforced Concrete
ASTM C1018-97	Standard Test Method for Flexural Toughness and First-Crack Strength of Fiber-Reinforced Concrete (Using Beam With Third-Point Loading) (Withdrawn 2006)
CSA A23.1-19 Annex U	Ultra High Performance Concrete (with and without Fiber Reinforcement)
CSA S6-19, 8.1	Design Guideline for Ultra High Performance Concrete

Table 2-1: Basic properties of reinforcing steel

When a structure is under sustained self-weight or imposed load, creep settles in and affects the overall performance of the member. In brittle materials such as concrete, such long-term continuous deformation is common in occurrence. FRP concrete serves well against creep, most papers report. Table 2-2 and Table 2-3 contain some basic material properties of steel and concrete respectively:

Density (ρ) (kg/m^3)	**Poisson ratio (μ)**	**Tensile strength (f_t) (MPa)**	**Yield strength (f_y) (MPa)**	**Elastic Modulus (E_c) (GPa)**
7850	0.27 – 0.30	Depends on steel grade	Depends on tensile strength	200

Table 2-2: Basic properties of reinforcing steel

Compressive strength (f'_c) (MPa)	**Tensile strength (f_t) (MPa)**	**Elastic Modulus (E_c) (GPa)**	**Shear Modulus (G_c) (GPa)**	**Shrinkage strain (ε)**	**Creep (ϵ)**
From UTM test	$0.62\sqrt{f_c'}$	$4700\sqrt{f_c'}$	$\frac{E_c}{2(1+\mu)}$	0.0003	$\frac{E_c}{1+\theta}$

Table 2-3: Basic properties of concrete

It should be noted that though some of these material properties are unique to individual elements, in some elastic analyses they are applicable to a reinforced section – e.g., E_c.

2.1.1 Reinforced concrete structural members

Different types of structures may contain different types of members that may somehow provide additional safety/stiffness to the overall performance of the structure. Here, focusing on specific perspectives, the substructure and superstructure of a bridge are the two basic divisions of classification. To put it in context, the substructure basically serves as the support/reaction component which the superstructure provides the platform for crossing.

2.1.2 General review of reinforced concrete road and railway bridges

New concrete bridges must all be designed to incorporating parameters that account for reliability while existing ones must be regularly checked and maintained. Rebar corrosion, continued traffic, etc., on longitudinal members subjecting the member to flexure and shear etc. are amongst the most considerable [7].

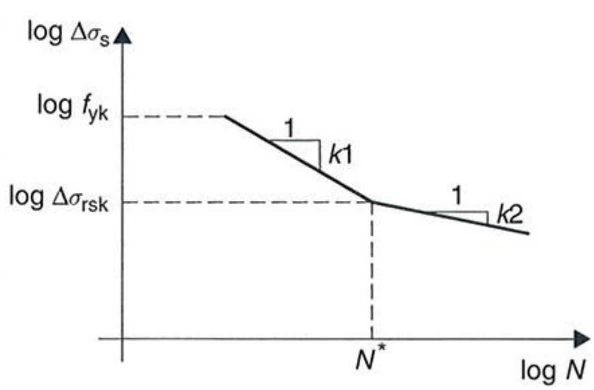

Fig. 2.1: A typical rebar stress – cycle curve

Bridges are some of the key civil structures that experience severe fatigue – due to the orientation and the repetitive load on the bridge. Railway loads are extra high and the vulnerability of these bridges thereof is directly related to the shortness in span [8]. The trend that fatigue occurs in the reinforcement bars of an RC member may be illustrated as in Fig. 2.3. Yielding of rebar in any structural member signals an impending failure. For bridges, traffic/axle load predominantly causes fatigue and the resulting annual degradation caused is a function of the number of cycles till failure occurs (N_i) and the total number of annual cycles (N_t).

$$D_{annual} = \sum_{i}^{N_t} \frac{1}{N_i} \quad \text{Eqn 2-1}$$

Finally, fatigue life (FL)

$$FL = \frac{1}{D_{annual}} \quad \text{Eqn 2-2}$$

As these repeated loads pass over time, natural frequency too does not remain constant. It then varies periodically as well [9]. A practical way to determining the structural response/adequacy of the bridge after construction as well as all cycles of loads and of creep for deflection, crack, strain etc., is by using proof-load test [10] where the acceptance or stop criteria would then dictate how much load the bridge can then be subjected to for safety, reliability, and economic purposes. Engineers should bear in mind that an adverse effect of proof load test may lead to an irreversible damage to the bridge hence a proportionate cost should be factored in for any eventuality [11].

2.2 Cracks

Mostly considering the interaction existing between corrosion member and concrete cover, most of those works delve into trying to somehow estimate the relationship between these two parameters. In papers of some renowned engineers and researchers who contributed immensely to the development of the understanding of cracks, rebars, corrosion and concrete cover, have all mentioned that the strength of a designed member decays overtime with the application of the design load. Some researches backed by experimental findings point to the chemical composition of the rebars which when constituent elements start to diffuse off the rebars sometimes necessitated by load effects, weakens the bond between the steel and the concrete. Weakening of the bond by effusion of these elements into the concrete is the key factor leading to microcracks and then to surface cracks to spalling and then finally to long-term deflection. However, some of these cracks are exhibited not due to the depletion of the reinforcing bars but due to sudden loading or unloading as well as due to an inadequacy of a member inappropriately designed. When corrosion is initiated to the reinforcement, the steel begins to get overstressed. – because of the decrease in the diameter of the rebar. Under such condition, cracks due to fatigue starts to propagate with some high intensity [12] as the bond starts to deteriorate.

In a static laboratory investigation conducted by [13], cracks of various types and magnitudes and causes were studied and reported on. Notably, the authors indicated that the mode of load application plays a significant role in the determination of the strength of concrete. This implies that the method of incrementality slowly compromises the brittleness of the member. However, everything in this research is strictly static. Using analytical model, [14] on the other hand focused on the chemical implications of section loss in a reinforced concrete member. Therein, it is noted that the final rust that suffices as the product of rebar deformation/or corrosion is a conglomeration of several oxides mostly due to chemical interactions affecting the bonding parameters and that in this condition, cracking is highly sensitive. These findings are usually made possible using hypothetical corrosion equation to estimate the rate of corrosion.

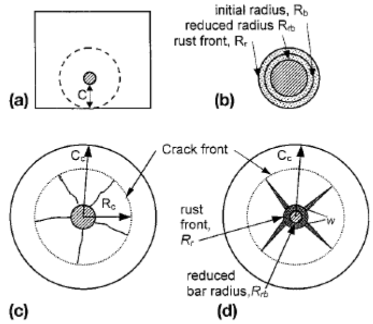

Fig. 2.2: Model of concrete cover as a thick-walled cylinder: (a) cylinder model; (b - c) definition of terms; (d) rust deposited within open cracks

Some decades ago, in a quest to understand corrosion to some extent, [15] conducted research in several phases considering different parameters to establish the relationship between rebar and concrete cover. It is noted in this work that because concrete has a pH value of at least 12.5, corrosion intensity which is a linear section loss factor, is dependent on the cover-to-bar diameter ratio. As serviceability requirement for reinforced concrete is a critical design parameter, concrete cover plays a cardinal role in achieving such requirement. [16] has been a very key structural reference material in the study of reinforced concrete. Despite the structure that may be under consideration may not necessarily be that of a typical “building”, the three major types of covers presented in the code: ground cover, atmospheric cover, and non-atmospheric cover will usually control the minimum cover criterion for such work – be it cast-in-place, precast, or deep foundation. In almost similar fashion, [17] and [18] conducted similar research like that of [14] but with a slight difference in setup and procedure.

[17] establishes that the more active the electro-potential was, the more intense the change in electrical resistance or the steel corrosion rate. However, a test setup solely intended to investigate corrosion that is carried out using electrical current might produce results that may be far too astronomically exaggerated based on the manner and form in which electric current reacts with metal. Furthermore, without the application of an external or live load, an important contributing factor leading to cracking which in turn causes corrosion, was lacking. This research considers the effects of railway live load. Most of the works described above were conducted on the normal shallow beams. However, another approach was considered when [19] studied deep beams wherein it was established that all the patterns of crack of the deep beams were same as those for simple struts of supports and their applied loads. In this paper, the results obtained from the experimental corroborate with results of the finite element model. [16] section 9.9 considers a beam deep if it is loaded and that it should satisfy at least one of two main conditions:

1. Total height of the beam is less than four (4) times the clear span
2. Concentrated loads be placed within a half of the clear span, i.e., within two times the total height of the beam.

The maximum length-to-thickness ratio (l/t) is always less than or equal to 4. This implies that the smaller the l/t ratio the deeper the beam is, holding the rule constant. The instrumentation in [19] well met this criterion.

The indirect loading scenario discussed in [19] considers loading the beam out of its rectangular section as shown in Fig. 2.3 – which could well be in violation of section 9.9 [16].

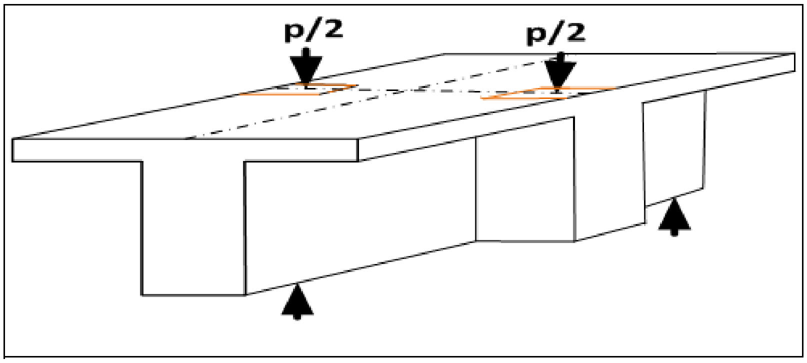

Fig. 2.3: Indirect loading of deep beam

Despite all the negatives/shortcomings associated with cracks to a flexural member, concrete may still provide useful strength contribution to the member. With the voids created at the cracks, concrete situated in the tension zone between those cracks is capable of providing some strength that can readily be of significance to the overall stiffness of the beam. When assessed, this implies that because the block of uncracked section is still being carried by the steel proves a logical point going forward. The profile of cracks is not likely identical from its tension face (mouth) towards the compression face (concrete-rebar interface), [20] reports. Several mechanisms to appreciably control cracks exist. Addition of composites like fibers is one. Accordingly, [21] notes that although fibers enhance the section against cracks, increasing the span decreases such enhancement.

2.3 Specific review on railway bridge section loss

The magnitude of load on a bridge has a direct impact on its life span. [22] reports that with sustained load there is always room for continued deflection over time. However, the deflection pattern is more severe at the onset than at its maximum. In the case of prestressed concrete girders, dilation plays a key role in crack propagation [23] – for the load emitted from the vehicle as well as the in-body temperature of the section [24]. It can thus be seen on Fig. 2.4 that several patterns of cracks are observed as compared to that of a non-prestressed reinforced concrete beam.

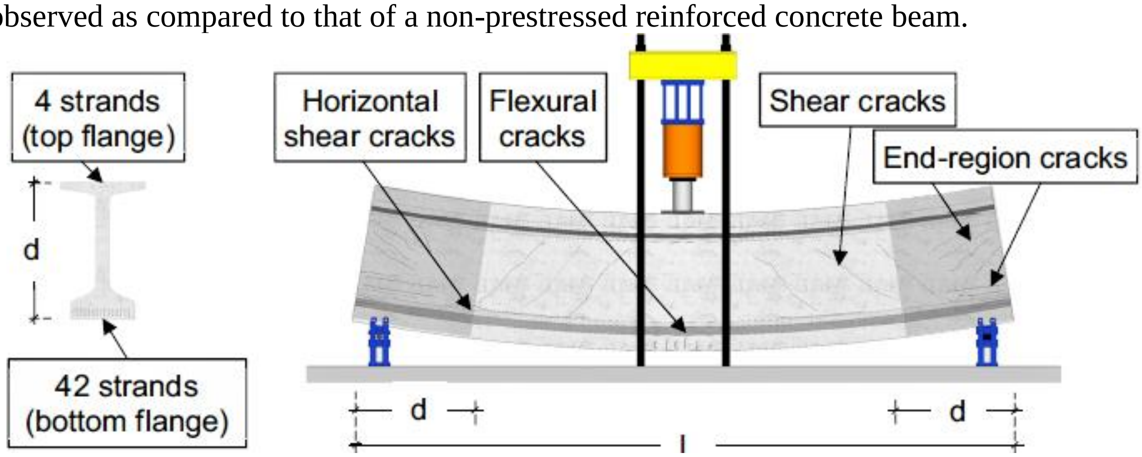

Fig. 2.4 Section and cracking pattern of prestressed concrete girder { [23]}

3 The Research Methodologies

This research encompasses numerical analysis and design, virtual experimentation, Software simulations as well as professional views. Mostly analytical, appropriate design discussions are held concomitantly. A separate general discussion section is also included to account for the conglomerated and synchronized discussion which also considers the findings of each method.

1. **Analytical** ~ Here, equations/calculations are presented a step-by-step detail of each method used in this research.

    - **Analytical Method 1: Structural Calculations** ~ A symbolic railway girder was designed incorporating all necessary parameters with the use of various codes, standards, and texts. This section contains a brief overview, material and sectional details, results, discussion and conclusions.

    - **Analytical Method 2: Verification of experiment ~** As above, verification of experiment was undertaken to validate procedures, assumptions and findings in Analytical Method 1.

2. **Validation (Software) of analytical results** ~ to compare findings from the analytics/computation and the output from the software.
3. **Summary of discussion on research findings** ~ A comprehensive comparative analysis amongst all analytical methods used in the research is presented, as well as the limitations and advantages of each method.

4. **Conclusion ~ C**onsolidated statements for the research from all conclusions of each method are presented.

5. **Recommendation ~** The objective is to provide concise information of what needs to be adopted or done by future researchers.

6. **References ~** Every material cited during the research are clearly given in this section.

Appendicle ~ Tables, figures, charts, graphs, all other items coned, and those generated that do not necessarily need to be included in the work are shifted here.

4 Analytical

This chapter is the core chapter dealing with the analytical design philosophies contained in this research.

4.1 Analytical 1: Analysis and Design and Discussion of methods

Railway bridges, like many other structural members, are basically designed by at least knowing some principal dimensions that structure has. However, in a fresh-start project, engineers would have to do preliminary sizing based on the results from site reconnaissance or investigation. In the case of bridges, be it highway or railway, the span is one of such principal data needed - this is the unsupported length of the bridge, though there might be a little modification in the applicability of this definition, it runs from abutment to abutment for single span bridges and abutment to pier for multiple span bridges. By adopting one of the key definitions of what a bridge relative to its span length is, the 6-m minimum limiting value is used to design this railway girder and then investigate the thematic area – cracks. A single-track railway bridge is what is being considered herein. The rudimentary chapter in [2] or sizing the required flange dimensions associated with the girder span is Chapter 8-2.23.10. However, there seems to be some little differences amongst codes with respect to a particular subject but results may be assessed based on the criticality of the parameter under consideration.

4.1.1 Flange dimensions

A flanged section (commonly referred to as T-section) is one which consists of a slab and a beam integrally acting as a single structural member based on the several controlling factors involved. Thus, a physical look cannot substantiate that the section is actually a flanged section. However, from the initial stage of analysis up to the determination of the depth of stress block, the actual shape of the section may be designed as regular rectangular section. For this research, a girder of 10-m clear span is selected and a girder-to-girder spacing is then chosen based on the dimension of the adopted sleeper which allows it to run over the girders. These are key design data used in the analysis of this Railway bridge superstructure. These data, especially material parameters, may be modified where necessary. Part 8-2.23.10b(1) of [2] states that "The effective slab width acting as a T-girder flange shall not exceed one-fourth of the span length of the girder, and its overhanging width on either side of the girder shall not exceed six times the thickness of the slab or one-half the clear distance to the next girder*"*. Thus, the effective slab width should be:

$$b_{eff} \ngtr \frac{1}{4}s \qquad \text{Eqn 4-1}$$

$$b_{eff} \ngtr \frac{1}{4}(10) \ngtr 2.5\ m$$

$$b_{ow} \ngtr 6t_{slab} \qquad \text{Eqn 4-2}$$

$$b_{ow} \ngtr 6(0.28) = 1.68\ m$$

$$b_{eff} \ngtr \frac{1}{6}s_{g0} \qquad \text{Eqn 4-3}$$

$$b_{eff} \ngtr \frac{1}{2}(2.1) \ngtr 1.05\ m$$

However, Table 6.3.2.1 of [16] also outlines that the web's flange for a double-sided flange system shall be the least of

$$b_{eff} \ngtr 8h \qquad \text{Eqn 4-4}$$

$b_{eff} \ngtr 8(0.28) \ngtr 2.24\ m$

$$b_{ow} \ngtr \frac{s_w}{2} \qquad \text{Eqn 4-5}$$

$b_{ow} \ngtr \frac{2.1}{2} = 1.05\ m$

$$b_{eff} \ngtr \frac{l_n}{8} \qquad \text{Eqn 4-6}$$

$b_{eff} \ngtr \frac{10}{8} \ngtr 1.255\ m$

Note that these limiting values are compared with those of the structural drawing and the appropriate ones selected.

4.1.2 The Basic Structural and Material properties

Table 4-1 gives the basic structural dimensions of the section and provides some universally accepted basic properties associated with each material. The description field provides a name synopsis of each sectional or material properties, the magnitude presents the numerical value associated with each element, the unit gives the name of the system of measurement associated with property, and finally, the remarks section is used to provide brief information about the particular line item.

#	Description	Mag.	Unit	Remark
s	Clear span between support	10	m	Designer's pick due to site condition
s_g	Girder-to-girder o/c span	2.6	m	Designer's pick, girder length
s_t	Spacing of ties/sleepers	600	mm	Designer's pick, due to track stiffness parameter
L_t	Length of ties	2.6	m	German B70 sleepers details
w_t	Weight of ties	1.3	kN/m	German B70 sleepers details + add-ons
w_b	Unit weight of ballast	19	kN/m^3	AREMA 8-2.2.3 b. (2)
w_r	Weight of rail (w_r)	3	kN/m	AREMA 8-2.2.3 b. (2)
f'_c	Compress. strength of concr.	40	MPa	METROLINX RC-0506-04STR Part 3-11.1
f_y, f_{yk}	Yield strength of steel	420	MPa	AREMA 8-2.3.2 (c., d.), 19.4.2.2.2
E_c	Elast. Mod. of concrete	30	GPa	AREMA 8-2.32.4a
E_s	Elast. Mod. of steel	200	GPa	AREMA 8-2.32.4b
sb#	Main bar # used in slab	25	mm	Designer's pick
gb#	Main bar # used in girder	32	mm	Designer's pick
cc	Concrete Cover	50	mm	AREMA 2010 Chapt. 8-2.6.1 (Table 8-2-7)
ρ	Weight density of concrete	24	kN/m^3	AREMA 2.2.3 b. (2)
Ø	Flex. Strength Reduct. factor	0.90		AREMA 2.30.2 b.
ψ	Shear. Strength Reduct. factor	0.85		AREMA 2.30.2 b.
LL	Live load	120	kN	AREMA 2.2.3 c.
		120	kN/m	AREMA 2.2.3 c.

Table 4-1: Basic dimensions and material properties used in the design

Selecting some key data from the table, the thickness of each component can be calculated. [2] Chapter 8-2.23.9 and Chapter 8-2.23.10 allow for the adoption of a T-girder construction method for railway bridges. However, one of the first analyses that is usually carried out in load-carrying structures is to determine the thickness of the slab. This is usually a non-load dependent criterion - it is a length related criterion! Referencing [2] chapter 8-2.23.6c(1) and Table 8-2-10 "Recommended Minimum Thickness For Constant Depth Members" to compute its adequacy, the minimum thickness of the Bridge slab/flange with main reinforcement perpendicular to traffic can be calculated as below:

A) Girder

$$t_g = \frac{clear\ span + 2.75}{15} \qquad \text{Eqn 4-7}$$

$$t_g = \frac{s + 2.75}{15} = \frac{10 + 2.75}{15} = \frac{12.75}{15} = 0.85 \approx 0.9\ m$$

B) Flange

$$t_f = \frac{girder - to - girder\ o/c\ spacing + 3}{20} \qquad \text{Eqn 4-8}$$

$$t_f = \frac{s_g + 3}{20} = \frac{2.6 + 3}{20} = \frac{5.6}{20} = 0.28\ m$$

For serviceability requirements as contained in [16] chapter 9.3.1.2, the depth of the girder is increased up to 900 mm from the calculated 850 mm.

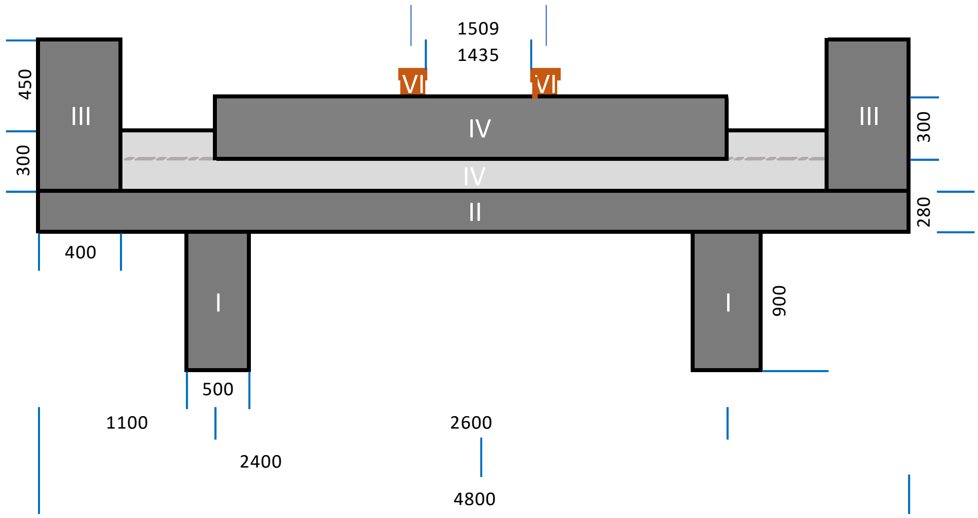

Fig. 4.1 Cross-section of a typical railway bridge

NB: For any 3-D Design purpose, take a flange width dimension of 1.0 m

4.1.3 Shear and Moment of the Flange

Analysis of the top flange for flexure

A. DEAD LOAD (DL)

Desig.	*l* (m)	*w* (m)	*t* (m)	*ρ* (kN/m³)	w_t (kN/m)	P (kN)	Remark
II.		1.0	0.28	24	6.72		Associated with the flange/deck
III.	1.0	0.4	0.3	24		3.08	Associated with the curb/barrier
IV.		1.0	0.3	19	5.7		Associated with the ballast
V.					1.3		Associated with the tie/sleeper
VI.	1.0		1.0		3.0	3.0	Associated with the rail

Table 4-2: A simple dead load calculation table

In the table above, the weight of the various components is calculated, except for the girder itself. In this procedure, the girder is serving as the support to the flange hence it is justifiable in this context. Further, because of the difference in the orientation of the component elements while considering the axis of analysis, some weights are converted to a concentrated load while the majority is converted to uniformly distributed load.

$$Density\ (\rho_{wt}) = \frac{force\ (P)}{volume\ (V)} \qquad \text{Eqn 4-9}$$

Thus, the concentrated load (P) for components analyzed in this category (i.e., running parallel to traffic) is given by the equation

$P = \rho_{wt}V = \rho_{wt}(lwt)$

On the other hand, the uniformly distributed load (UDL) applies to components whose spans structurally run in the perpendicular direction. Thus, the equation:

$w_t = \rho_{wt}(wt)$

The table above simplifies the various load in the form to be used for structural calculations.

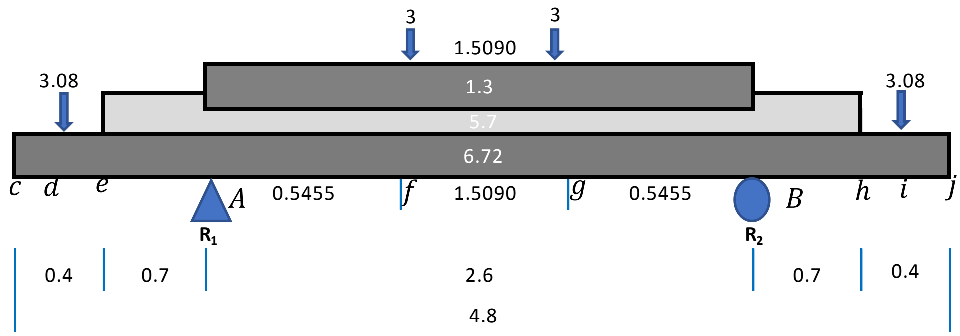

Fig. 4.2 Representation of dead load on a determinate beam

Calculation of reactions

NB: Because of the symmetry in the loading condition, both reactions are equal.

$$R_1 = R_2$$

…and the sign convention be "Clockwise is POSITIVE" (See *SoE 10-1*). Thus, the reaction force is obtained.

$$R_1 = \frac{\sum M}{s_g} \qquad \text{Eqn 4-10}$$

$R_1 = \dfrac{91.77\ kN.m}{2.6\ m} = 35.30\ kN$

By symmetry, $R_2 = 35.30\ kN$, and the shear calculation is contained in *SoE 10-2*

Points of zero shear

The point of zero shear occurs where the shear transitions from negative to positive shear or vice versa practically excluding those at the supports.

$$X_{V=0} = \frac{M_{prev.}}{w_{t_{next}}} \qquad \text{Eqn 4-11}$$

$$X_{V=0} = \frac{10.37}{13.72} = 0.76\ m$$

Bending Moment calculation

Bending moment, in any structural member, is the primary quantity used to carry on a full design of the required reinforcement. Normally, in structural analysis for structures like bridges and several heavy-load-carrying structures, the designers would likely use the maximum moment capacity across the member. This is the same analogy used herein. See *SoE 10-3*. Hence, the Shear Force Diagram (SFD) and Bending Moment Diagram (BMD).

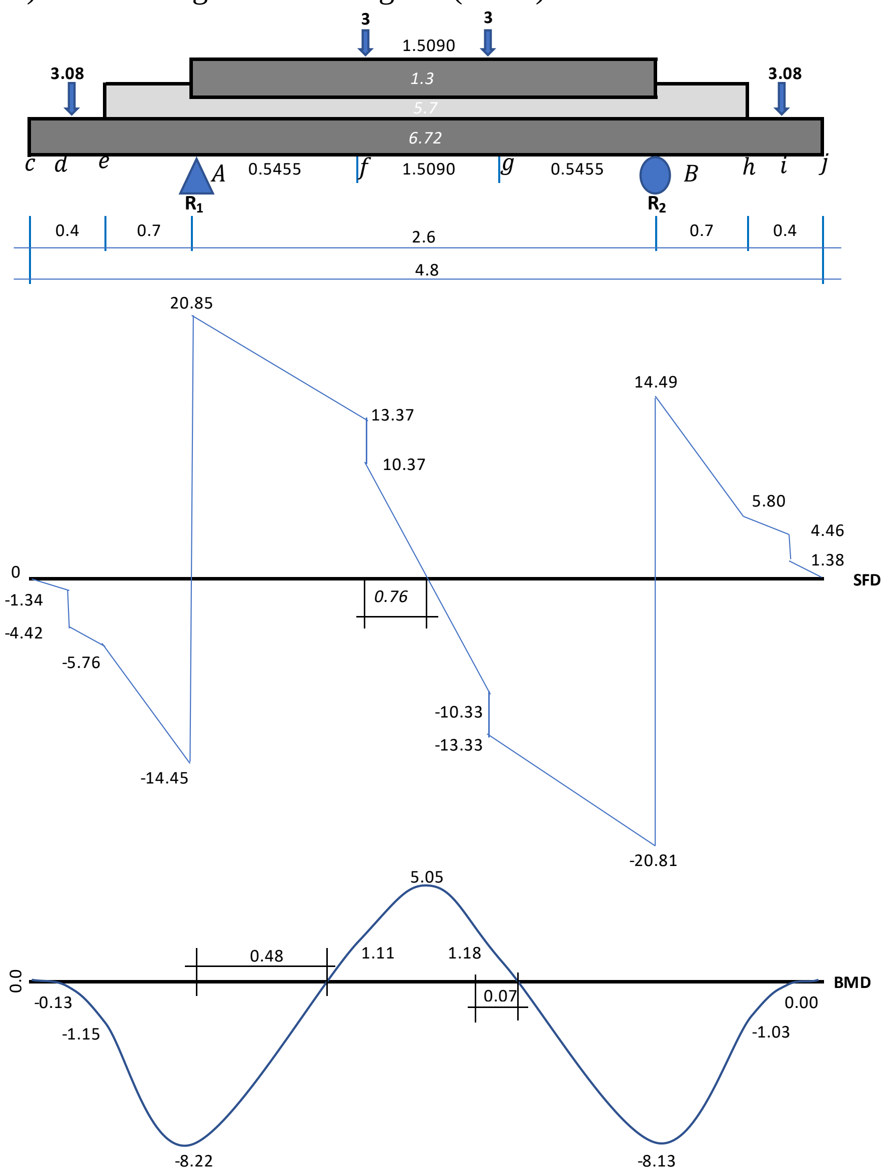

Fig. 4.3 Shear force and bending moment diagrams (NTS)

Points of Contraflexure/Inflection

In analysis and design, the point of contraflexure which can interchangeably be referred to as point of inflection, is that point at which the moment transitions from one state to another. In short, it is a transition from a negative to positive state or vice versa occurs.

$$X_{M=0} = \frac{M_{prev.}}{V_{next}} \qquad \text{Eqn 4-12}$$

$$X_{M=0_1} = \frac{M_{prev.}}{M_{next}} = \frac{8.22}{0.5 \times 34.22} = 0.48\ m$$

$$X_{M=0_2} = \frac{M_{prev.}}{M_{next}} = \frac{1.18}{0.5 \times 34.14} = 0.07\ m$$

4.1.4 Design of the Flange

Two scenarios are considered under the design of the slab.

1. Iterational perspective
2. Straight-forward

4.1.4.1 Assessing Flexure through iterations

Materials in this sub-chapter, though with significant literary and material omissions, are in accordance with [25] wherein a consideration of iterations in the quantities of almost all parameters involved is thematic. This allows for the establishment of several governing expressions when there is the need to adjust the capacity of the structure. These procedures all start with the effect of the load. The combination of loads on a structural member takes into account the most possible combination and their proper factors by which each load and or moment is multiplied.

Group	Item
I	1.4 (D + 5/3 (L + I) + CF + E + B + SF)
IA	1.8 (D + L + I + CF + E + B + SF)
II	1.4 (D + E + B + SF + W)
III	1.4 (D + L + I + CF + E + B + SF + 0.5W + WL + LF + F)
IV	1.4 (D + L + I + CF + E + B + SF + OF)
V	Group II + 1.4 (OF)
VI	Group III + 1.4 (OF)
VII	1.0 (D + E + B + EQ)
VIII	1.4 (D + L + I + E + B + SF + ICE)
IX	1.2 (D + E + B + SF + W + ICE)

Load combination	Equation	Primary load
$U = 1.4D$	(5.3.1a)	D
$U = 1.2D + 1.6L + 0.5(L_r \text{ or } S \text{ or } R)$	(5.3.1b)	L
$U = 1.2D + 1.6(L_r \text{ or } S \text{ or } R) + (1.0L \text{ or } 0.5W)$	(5.3.1c)	L_r or S or R
$U = 1.2D + 1.0W + 1.0L + 0.5(L_r \text{ or } S \text{ or } R)$	(5.3.1d)	W
$U = 1.2D + 1.0E + 1.0L + 0.2S$	(5.3.1e)	E
$U = 0.9D + 1.0W$	(5.3.1f)	W
$U = 0.9D + 1.0E$	(5.3.1g)	E

Table 4-3: Load combination table used by AREMA and ACI

The design shear or moment for the possible load combination in in this case is that of Group III as outlined in [2] Table 8-2-5.

$$M = 1.4\,(D + L + I + CF + E + B + SF + 0.5W + WL + LF + F) \qquad \text{Eqn 4-13}$$

The factored design moment for the dead load exclusively is obtained by limiting all other moments! This implies that only the dead load moment is considered.

$$Ø[1.4M_{DL}] \text{ where } Ø = 0.9$$

$M_{sd} = Ø[1.4M_{DL}] = 0.9[1.4(-8.22)]$ considering magnitude only, adopted dead load moment is $M_{sd} = 10.36\ kN.m = 10360\ N.m$

This is the maximum design moment caused by the application of all the calculated dead loads. It also includes effects of the cantilever section. It is then visualized that the maximum moment is at the supports instead of at midspan because of the arrangement of the sleepers/ties (girder to girder).

4.1.4.1.1 The effective depth of the slab

Though the difference between the bar size and its diameter might be minute, there might be some considerable difference in its area when using these figures. [26] provides the below chart for ease of computation.

$$d = t_f - (concrete\ cover + 0.5\ bar\ diameter) \quad \text{Eqn 4-14}$$

$d = 0.28 - (0.05 + 0.5 * 0.0254) \approx 0.22\ m \approx 220\ mm$

The gross area of concrete, ignoring the area occupied by steel, is a function of the dimensions of the section.

$$A_g = wt_f \quad \text{Eqn 4-15}$$

$A_{gross} = 1000\ mm\ (280\ mm) = 280000\ mm^2$

4.1.4.1.2 Steel Ratio

The steel ratio the expression representing the quantity of steel that constitutes a portion of the gross area of concrete of a section's area.

$$\rho_0 = \left[1 - \sqrt{1 - \left(\frac{2m_{sd}}{\emptyset\varphi f_c' bd^2}\right)}\right]\omega \quad \text{Eqn 4-16}$$

where,

$$\omega = \frac{0.85f_c'}{f_y} \quad \text{Eqn 4-17}$$

$\rho_0 \approx 0.0006 = 0.06\%$

Thus, *SoE 10-4* presents the procedure. This implies that a 0.06% area of the entire design strip is what makes up the steel area. In reality, this ratio is very minute for the applied load! [16] section 9.6.1.2 requires the minimum flexural reinforcement to be the larger of the two. But disregarding the area of the section and only considering the minimum reinforcement (ρ_{min}), the following shall apply for flexural member:

$$\rho_{min} = \frac{0.25f_c'}{\sqrt{f_y}} \quad \text{Eqn 4-18}$$

$\rho_{min} = \frac{0.25\sqrt{40}}{420} = 0.0038$

$$\rho_{min} = \frac{1.4}{f_y} \quad \text{Eqn 4-19}$$

$\rho_{min2} = \frac{1.4}{420} = 0.0033$

From Eqn 4-18 and Eqn 4-19, the larger value of ρ_{min} is selected as the adopted minimum steel ratio based on the provisions of the [16] . Thus, $\rho_{\text{min}} = \rho_{\text{min1}} = 0.0038$.

Additionally, [2] also limits minimum flexural reinforcement for brackets and corbels to:

$$\rho_{min3} = \frac{0.04f_c'}{f_y} \quad \text{Eqn 4-20}$$

$\rho_{min3} = \frac{0.04(40)}{420} = 0.0038$

Thus, ρ_{min} [16] vs. [2] is the larger of:

$$\rho_{min} = \begin{Bmatrix} ACI = \quad 0.0038 \\ \\ AREMA = 0.0038 \end{Bmatrix} = 0.0038\ (AREMA)$$

NB: It's always desirable and structurally required for ρ to be greater than ρ_{min}. The value of ρ adopted for the design is the larger of ρ and ρ_{min}. Since ρ_{min} is greater than $\rho_{0,}$

$$\rho = 0.0038$$

4.1.4.1.3 Adjusting the moment capacity of the Flange

Therefore, to find the maximum acceptable moment that would corroborate with the range of the minimum reinforcement ratio, the following table summarizes the range of the acceptable moment that the design moment should be in so as to satisfy the minimum reinforcement requirement. The table is applicable only when k_{mo} is less than c. Let's consider an arbitrary adjusting factor (k_{adj}) based on the total sample (i.e., S/N).

$$k_{adj} = \frac{k}{\left(\frac{S}{N}\right)} \qquad \text{Eqn 4-21}$$

$$k_{adj} = \frac{1}{51} = 0.0196$$

Balance Factor [k_b]	Adjusted m-term [k_{ma}]	ρ_o adjust. by k_{ma} [ρ_a]	Per. of k_b [%k_b]	Rel. accu. of K_{ma} to K_{mo} [$k_{ma\text{-}mo}$]
1.0000	0.9930	0.00057	0.00	100.00
0.9804	0.9736	0.00214	1.96	98.05
0.9608	0.9541	0.00372	3.92	96.08
0.9412	0.9347	0.00529	5.88	94.13
0.9216	0.9152	0.00687	7.84	92.17
0.9020	0.8957	0.00845	9.80	90.20
0.8824	0.8763	0.01002	11.76	88.25
0.8628	0.8568	0.01160	13.72	86.28
0.8432	0.8373	0.01318	15.68	84.32
0.8236	0.8179	0.01475	17.64	82.37
0.8040	0.7984	0.01633	19.60	80.40
0.7844	0.7790	0.01790	21.56	78.45
0.7648	0.7595	0.01948	23.52	76.49
0.7452	0.7400	0.02106	25.48	74.52
0.7256	0.7206	0.02263	27.44	72.57
0.7060	0.7011	0.02421	29.40	70.60
0.6864	0.6816	0.02579	31.36	68.64
0.6668	0.6622	0.02736	33.32	66.69
0.6472	0.6427	0.02894	35.28	64.72
0.6276	0.6233	0.03051	37.24	62.77
0.6080	0.6038	0.03209	39.20	60.81
0.5884	0.5843	0.03367	41.16	58.84
0.5688	0.5649	0.03524	43.12	56.89
0.5492	0.5454	0.03682	45.08	54.92
0.5296	0.5259	0.03840	47.04	52.96
0.5100	0.5065	0.03997	49.00	51.01
0.4904	0.4870	0.04155	50.96	49.04
0.4708	0.4676	0.04312	52.92	47.09
0.4512	0.4481	0.04470	54.88	45.13
0.4316	0.4286	0.04628	56.84	43.16
0.4120	0.4092	0.04785	58.80	41.21
0.3924	0.3897	0.04943	60.76	39.24
0.3728	0.3702	0.05101	62.72	37.28
0.3532	0.3508	0.05259	64.68	35.33
0.3336	0.3313	0.05416	66.64	33.36
0.3140	0.3119	0.05574	68.60	31.41
0.2944	0.2924	0.05732	70.56	29.45
0.2748	0.2729	0.05890	72.52	27.48
0.2552	0.2535	0.06047	74.48	25.53
0.2356	0.2340	0.06205	76.44	23.56

0.2160	0.2145	0.06363	78.40	21.60
0.1964	0.1951	0.06520	80.36	19.65
0.1768	0.1756	0.06678	82.32	17.68
0.1572	0.1561	0.06836	84.28	15.72
0.1376	0.1367	0.06993	86.24	13.77
0.1180	0.1172	0.07151	88.20	11.80
0.0984	0.0978	0.07308	90.16	9.85
0.0788	0.0783	0.07466	92.12	7.89
0.0592	0.0588	0.07624	94.08	5.92
0.0396	0.0394	0.07781	96.04	3.97
0.0200	0.0199	0.07939	98.00	2.00

Table 4-4: An iterating spreadsheet showing change in ρ with respect to change in moment capacity

Constant parameters excluded from Table 4-4 that are used against every line item are follows:

1. *S/N = range from 1 to 51*
2. *C = 1*
3. *Origin. m-term (k_{mo}) = 0.993*
4. *Stress Reduct. Factor [ω] = 0.081*
5. *Origin. steel ratio [ρ_o] = 0.038*

4.1.4.1.4 Discussion of the Abbreviations/Acronyms

Table 4-4 is developed to enable a rigorous iteration process that would aid designers in manipulating all terms within to suit a specified need**.** A review and explanation of each term follows, including those of the constant-figure type.

1. k_{adj} – An arbitrary adjusting factor by which a moment term is adjusted
2. S/N – Sequence number in line with the k_{adj}
3. $const\ (c)$ – The constant value (=1) in the ρ equation
4. $Origin.m - term\ (k_{mo})$ – The original moment term in the ρ equation
5. $Balance\ Factor\ [k_b]$ – A factor by which K_{adj} is accumulatedly subtracted from each moment term
6. $Adjusted\ m - term\ [k_{ma}]$ – The new moment term after the application of the balance factor
7. $kStress\ Reduct.Factor\ [\omega]$ – A stress reduction factor for flexural members
8. $\rho_0\ adjust.by\ k_{ma}[\rho_a]$ – The new actual ρ value after the application of the balance factor
9. $Origin.steel\ ratio\ [\rho_0]$ – The Original steel ratio value of the section obtained without any adjustment to dimensional and material properties
10. $\rho_{min}(Adopted\ \rho)\ [\rho]$ – The minimum code-required ρ value of the section adopted for the design because of the inadequacy of the calculated ρ
11. $Per.of\ k_b\ [\%k_b]$ – Percentage by which the arbitrary adjusting factor has caused the balance factor to be reduced

12. $Rel.accur.of\ k_{ma}\ to\ k_{mo}\ (\%k_{ma-mo})$ – The Relative Accuracy of $k_{ma}\ to\ k_{mo}$ is the ratio of the adjusted moment term to the original moment term, multiplied by 100.

The initial arrangement of this table considers an arbitrary number of steps the designer feels feasible working with. Being to the discretion of the designer, a more discrete arbitrary adjustment factor finely discretizes the equation to obtaining a somewhat more accurate value of each parameter under discussion.

4.1.4.2 Flexure: Traditional procedure

Here, a more direct procedure is used in designing the principal parameters of flexure, particularly the area of steel. Table A.13 of [3] provides that such (flexural) reinforcement ratio ranges from 0.33% to 1.81% of the gross area of the member. Hence, below is a tabulated value excerpted from the table from where a designer can choose:

ρ (%)	A_{gross} (mm^2)	A_{smin} (mm^2)	Remark
0.33	280000	924.0	Minimum
0.54	280000	1512.0	Intermediate
0.75	280000	2100.0	
0.96	280000	2688.0	
1.17	280000	3276.0	
1.38	280000	3864.0	
1.59	280000	4452.0	
1.80	280000	5040.0	Maximum

Table 4-5: The rho, concrete, and steel areas for main reinforcement flexural member table

4.1.4.2.1 The Unloaded Flange

In this case, the analysis first treats the railway bridge as an unloaded structure. That is, no imposed or live load is acting on it. When this is done, comparably with the application of the live load, a reasonable judgement can be drawn against the area of steel required of railway dead load and that of the live load. Loads are a key determinant of area of steel. As discussed above in the iteration process, the steel ratio depends on several parameters such as:

a. Applied/design moment (M_a or M_{sd})
b. Strength reduction factors ($\emptyset, \varphi$)
c. Base of the section (b)
d. Effective depth of the section (d)
e. The compressive strength of the concrete (f'_c)
f. The yield strength of the reinforcing steel (f_y)

It is represented as follows:

$$A_s = \rho bd \qquad \text{Eqn 4-22}$$

$$\Phi_{bar} = \frac{bar\ \#}{25} * 25.4 \qquad \text{Eqn 4-23}$$

Thus

$$\begin{cases} No.25 \ \rightarrow\rightarrow\rightarrow\rightarrow\rightarrow\rightarrow\rightarrow \ \Phi_{25} = 25.4\ mm \\ No.22 \ \rightarrow\rightarrow\rightarrow\rightarrow\rightarrow\rightarrow\rightarrow \ \Phi_{22} = 24.4\ mm \\ No.19 \ \rightarrow\rightarrow\rightarrow\rightarrow\rightarrow\rightarrow\rightarrow \ \Phi_{19} = 19.3\ mm \end{cases}$$

A simple mathematical expression relating the number (quantity) of bars, area of steel required and the area of a unit bar is given below

$$Q_{bar} = \frac{A_s}{A_{1\,bar}} \qquad \text{Eqn 4-24}$$

The area of a bar is calculated from that of a simple circular shape.

$$A_{1_{bar}} = \frac{\pi d^2}{4}, \qquad d = \Phi \qquad \text{Eqn 4-25}$$

The table below summarizes numerical data associated with a single bar and the quantity of bars required of the various areas of steel indicated.

4.1.4.2.1.1.1 Spacing

The spacing conforms to [2] Chapter 8-2.12. Where the calculated spacing exceeds the maximum allowable spacing as provided by the code, the code suffices. similarly, where less than the minimum specified requirement, the code also suffices.

$$s = \frac{b - Qd}{Q - 1}, \qquad b = 10000, d = \Phi \qquad \text{Eqn 4-26}$$

Thus, assuming only dead load (i.e., self-weight of the flange and structures above it), decision about the main reinforcement is then

$$\boldsymbol{Adopt}\ \#\mathbf{25@450}$$

4.1.4.2.1.2 Transverse Bars

Transverse reinforcement is reinforcement in the direction opposite to that of the main reinforcement. Amongst several functions, transverse reinforcement provides firmer connection to the main reinforcement. It serves the purpose of constraining the main reinforcement to avoid sudden movement away from the intended position. It also serves as a resistor against shear, torsion, etc. thus serving the functionality of a distributed bar. The rigorous analysis involved with the computation of main bar is less stringent for that of the transverse reinforcement.

4.1.4.2.1.2.1 Range of Transverse Reinforcement

In most structural design materials, tables and charts are effectively employed to obtaining the transverse reinforcement. For instance, Table A.13 [3] also provides that transverse and temperature reinforcement ratio ranges from 0.18% to 0.32% of the gross area of the member.

$\boldsymbol{\rho_t}$ (%)	$\boldsymbol{A_{gross}}\ (\boldsymbol{mm^2})$	$\boldsymbol{A_t}\ (\boldsymbol{mm^2})$
0.180	280000	504
0.192	280000	538
0.204	280000	571
0.216	280000	605
0.228	280000	638
0.240	280000	672
0.252	280000	706
0.264	280000	739
0.276	280000	773
0.288	280000	806
0.300	280000	840
0.312	280000	874
0.324	280000	907

Table 4-6: Table of rho, concrete area, and steel area for transverse & shrinkage reinforcement of flexural members

4.1.4.2.1.2.2 Transverse Area of steel

Several equations are employed for the area of steel of transverse reinforcement. However, it is normally a percentage of the gross area of the section as above or of the flexural area of steel. Thus, for the latter, the representative equation is as follows:

$$A_t = \left\{\left(\sqrt{\frac{1750}{\vartheta}}\right)\%\right\} A_s \qquad \text{Eqn 4-27}$$

$$A_t = \left\{\left(\sqrt{\frac{1750}{2.6}}\right)\%\right\} 836 = 217\ mm^2$$

As different versions/manipulations of the formula are available, one that is given in [26] considers the yield strength of the reinforcement bar as well.

$$A_{s,t} = \frac{1.3bh}{2(b+h)f_y} \qquad \text{Eqn 4-28}$$

$$A_{s,t} = \frac{1.3 * 2.6 * 0.28}{2(2.6+0.28)420} = 0.000391\ m^2 = 391\ mm^2$$

Yet, the difference in area between the two formulae is less than that of a single #25 bar. This implies that they would likely both yield the same quantity of bar required (i.e., when rounded). The transverse area of steel is based on that of the former equations.

4.1.4.2.1.2.3 Number of bars of Transverse Area

The equivalent "Number/quantity of bars" of transverse area of steel is practically obtained as in the traditional form and manner as above.

$$Q = \frac{A_{s,t}}{A_{1_{bar}}} \qquad \text{Eqn 4-29}$$

$$Q = \frac{217}{507} = 0.43 \approx 1$$

Area of steel and # of bar of transverse reinforcement								
By use of Formula	$A_t = \left\{\left(\sqrt{\frac{1750}{\vartheta}}\right)\%\right\} A_s$					$A_s = \frac{1.3bh}{2(b+h)f_y}$		**Remark Percentage by which $A_{t\%}$ is A_t and $A_{s,t}$:**
	ρ_t	**A_{gross} (mm^2)**	**A_s (mm^2)**	**A_t (mm^2)**	**Q**	**$A_{s,t}$ (mm^2)**	**Q**	
	-	**-**	**836**	**217**	**1**	**391**	**1**	**Calculated area (A_t)**
				$A_{t\%} = \rho_t A_g$				
By use of Percentage of A_{gross}	0.180	280000	-	504	1	-	-	232 of A_t, 129 of $A_{s,t}$
	0.192	280000	-	538	1	-	-	248 of A_t, 138 of $A_{s,t}$
	0.204	280000	-	571	1	-	-	263 of A_t, 146 of $A_{s,t}$
	0.216	280000	-	605	1	-	-	279 of A_t, 155 of $A_{s,t}$
	0.228	280000	-	638	1	-	-	294 of A_t, 163 of $A_{s,t}$
	0.240	280000	-	672	1	-	-	310 of A_t, 172 of $A_{s,t}$
	0.252	280000	-	706	1	-	-	325 of A_t, 181 of $A_{s,t}$
	0.264	280000	-	739	1	-	-	341 of A_t, 189 of $A_{s,t}$
	0.276	280000	-	773	2	-	-	356 of A_t, 198 of $A_{s,t}$
	0.288	280000	-	806	2	-	-	371 of A_t, 206 of $A_{s,t}$
	0.300	280000	-	840	2	-	-	387 of A_t, 215 of $A_{s,t}$
	0.312	280000	-	874	2	-	-	403 of A_t, 224 of $A_{s,t}$
	0.324	280000	-	907	2	-	-	418 of A_t, 232 of $A_{s,t}$

Table 4-7: Number of bars of transverse reinforcement

The data shows that transverse, temperature, and shrinkage bars are normally rounded up to obtain an adoptable quantity in structural design.

4.1.4.2.1.2.4 Spacing of temperature bars

Transverse bars spacings are calculated in the same fashion as that of flexural bars (Eqn 4-26). However, even flexural bars, practically, with a minimum of two bars,

$$s = \frac{1000 - 2(25.4)}{2 - 1} = 949\ mm$$

The table below summarizes the quantities of bars and spacing of all selected bars from the analysis. The row columns under the "Bar Designation represents"

1. #: Bar number
2. ϕ: Diameter of bar
3. A_b: Area of single bar

Further, the row contained below "# of bars and spacing yielded from each A_t, $A_{s,t}$, $A_{t\%}$" represents the various areas of steel. From Table 4-7,

Transverse Reinforcement Spacing table																	
Bar Designation			**# of bars and spacing yielded from each A_t, $A_{s,t}$, $A_{t\%}$**														
#	**Φ**	**A_b**	***217***	***391***	***504***	***538***	***571***	***605***	***638***	***672***	***706***	***739***	***773***	***806***	***840***	***874***	***907***
25	**25.4**	**507**	***1*** {949}	***1*** {949}	***1*** {949}	**1** {949}	**1** {949}	**1** {949}	**1** {949}	**1** {949}	**1** {949}	**1** {949}	2 {949}	2 {949}	2 {949}	2 {949}	2 {949}
22	**24.4**	**468**	***1*** {955}	***1*** {955}	2 {955}	2 {955}	2 {955}	2 {955}	2 {955}	2 {955}	2 {955}	2 {955}	2 {955}	3 {466}	3 {466}	3 {466}	3 {466}
19	**19.3**	**293**	***1*** {961}	2 {961}	2 {961}	2 {961}	2 {961}	3 {471}	3 {471}	3 {471}	3 {471}	3 {471}	3 {471}	3 {471}	3 {471}	3 {471}	4 {308}
16	**16.3**	**209**	2 {967}	2 {967}	3 {476}	3 {476}	3 {476}	3 {476}	4 {312}	4 {312}	4 {312}	4 {312}	4 {312}	4 {312}	5 {230}	5 {230}	5 {230}
12	**12.2**	**117**	2 {976}	4 {317}	5 {235}	5 {235}	5 {235}	6 {185}	6 {185}	6 {185}	7 {152}	7 {152}	7 {152}	7 {152}	8 {129}	8 {129}	8 {129}

Table 4-8: Transverse reinforcement quantity and spacing table

NB: 1 bar would regularly not fit into Eqn 4-26 to produce a structural result. Thus,

1. a 1-bar quantity that is **boldfaced** is increased by 1.
2. a 1-bar quantity that is ***boldfaced italic*** is one that does not produce a full one-bar quantity and also had to be increased by 1.

Therefore, with the effect of the self-weight only, the following is adopted:

1. $Main\ Bars: Adopt\ \#25\ @\ 450$
2. $Transverse\ Bars: Adopt\ \#25\ @\ 450$
3. $Temperature/shrinkage\ Bars: Adopt\ \#25\ @\ 450$

4.1.4.2.2 Design of the Loaded Flange

A key parameter to obtain in this design as in many other traffic engineering is the design speed. [2] section C-2.2.3(d.) adopts 160 km/h as the design speed. Meanwhile, as indicated in its Figure 8-2-1, the axle load of 360 kN (120 kN/m) is adopted as design live load using the Copper EM360 (E-80 loading) loading condition.

4.1.4.2.2.1 Configuration of Live Loads

Railway Copper E-80 live loads are extremely heavy. Even the unloaded vehicles may have weights equivalent to some loaded highway vehicles.

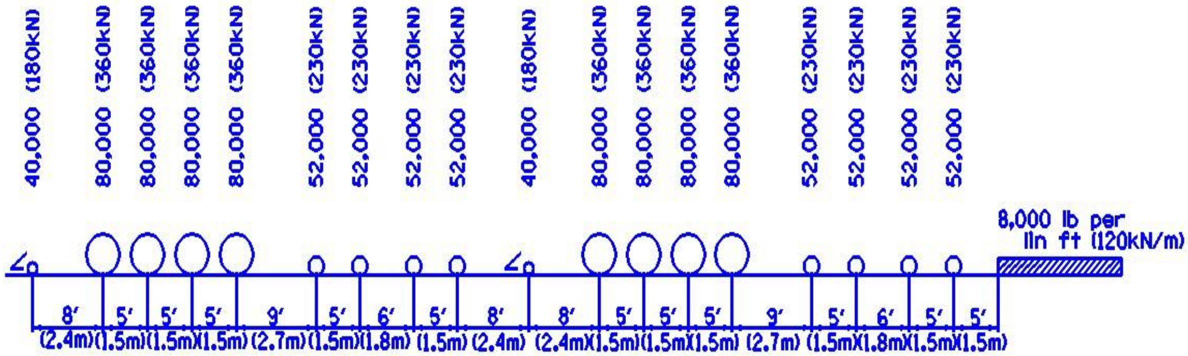

Fig. 4.4 Live Load arrangement of Cooper EM 360 Loading

From Fig. 4.4, the following is associated with Copper EM 360:

1. The uniformly distributed on the rail is 120 kN/m
2. The axle load on the track is 360 kN, and thus
3. The wheel load on a single track is 180 kN.

Here, the above loads are collectively referred to as the "Live Load" and are the primary live loads associated with the design of the superstructure. Their usage is distinct to a particular context [2]. Howbeit, due to their impacts, secondary live loads thus suffice in the design. From the axle load diagram, the arrangement of the axles according to [2]'s 8-2.2.3c(2), acts over a distance of 900 mm which is approximately equal to the one-meter design strip. This implies that a single axle load is adequate to be considered as the live load for the design of the 1-m strip flange. Wheel-Rail Contact properties provide very delicate considerations in the design of rail stresses however, wheel-rail contact stresses are not the thematic in this work. Notwithstanding, as the Rail Profile Radius (RPR) is the change in the cross-section of a rail shape to its perpendicular length, it controls the contact area that exists between the wheel and the rail. Contact area is technically referred to as contact patch in Wheel-rail analysis. A Transverse view of the wheel-rail contact length is presented in Fig. 4.4.

4.1.4.2.2.1.1 Secondary Live Loads

These loads, in the context of this design, include but not limited to the following:

1. Impact force
2. Wind Load on structure
3. Wind Load on Live Load
4. Longitudinal Force from Live Load

Notwithstanding other secondary loads applicable to the design of the superstructure, based on other factors like the orientation of the bridge, segmentation, span limitation, etc., may include: Longitudinal Force due to Friction or Shear Resistance at Expansion Bearings, Centrifugal force, Ice pressure, Rib shortening, Shrinkage, Temperature, Etc.

4.1.4.2.2.1.1.1 Impact force

As the name implies, the Impact forces is a secondary live load that is acted upon the rail in a 90-degree fashion that causes some agitation into the superstructure. Technically, it can be likened to that of resonance. Impact force is an estimated percentage of the axle load. The percentage of such force depends on the type of superstructure adopted in the design. Some superstructure types could be made of treated timbers, reinforced concrete, steel, or a combination of several of these materials and their decks may either the following: through deck, open-deck, ballasted, ballastless, slab, etc.

The throughness of the deck has a great numerical magnitude on the impact force. In other words, the complete throughness of the deck provides some level of damping to the deck. For instance, the impact force induced on a through reinforced concrete balllasted deck is up to 90% of that induced on an open-deck superstructure [27] section 38.3.1.7 and is represented in the US Customary units for normal rollingstock that do not adopt hammer blow system as

$$I = RE + 40 - \frac{3L^2}{1600} \qquad \text{Eqn 4-30}$$

for spans with a maximum length less than 80 feet, and

$$I = RE + 16 + \frac{600}{L - 30} \qquad \text{Eqn 4-31}$$

for spans with a minimum length of 80 feet. The following variables represent:

1. RE: 10% of the axle load or 20% of the wheel load. It should be noted that the wheel load is one-half of the axle load.
2. L: may be one of the following depending on the applicable case:
    a. The center-to-center dimension of the supports of the stringers
    b. Span of transverse floorbeams that are not constructed of stringers
    c. The span of the main longitudinal girder or truss
    d. The span of the main longitudinal girder or truss.

    The formula also applies to the span of

    e. the longer adjacent stringer under full support
    f. the longitudinally arranged beam
    g. specially built girder or truss that receives direct impact in the floorbeam
    h. the hangers of the floor-beam
    i. major trusses sub-diagonals
    j. transverse girders, and that of
    k. viaduct columns

Engineers using the formula must be cognizant of the design procedure which leads to the adoption of the specific line item to be used as L. The value of impacts is experimental; hence it is barred to a specific amount of the live load. This is one clue that helps the designer makes informed judgement as to which value of calculated impact, taking into consideration the multiple options of L, is adopted for the design. [27] guidelines for impact force is summarized in the table below. These impacts are associated with the provisions of [2] chapter 15 which is directly concerned with steel structures.

Load received from two tracks	
For L less than 175 ft	Full impact on two tracks
For L from 175 to 225 ft	Full impact on one track and a percentage of full impact on the other as given by the formula, 450 - 2L
For L greater than 225 ft	Full impact on one track and none on the other
Load received from more than two tracks	
For all values of L	Full impact on any two tracks

Fig. 4.5 WisDOT Bridge Manual Impact force table for various span limit and number of tracks

Note: WisDOT Bridge Manual is written in US Customary units.
The impact force adopted in this work is that of [2]. However, data obtained from this code is compared with those of other codes. [2] chapter 8-2.2.3 d(1) requires that, with the span adopted

herein being a 10-meter, the percentage of axle load serving as impact force for span ranging from 4 meters to 39 meters be computed as:

$$I = \frac{125}{\sqrt{l}} LL \qquad \text{Eqn 4-32}$$

$$I = \frac{125}{\sqrt{10}}(180) = 39.53(180)\% \approx 40\%(180) = 0.4(180) = 72.0\ kN.$$

Unlike [27], [2] stipulates limitations for impact load – ranging from 20% to 60% of the live load (Fig. 4.6). The deck span limit serves as the ideal regulator of the magnitude of the impact force.

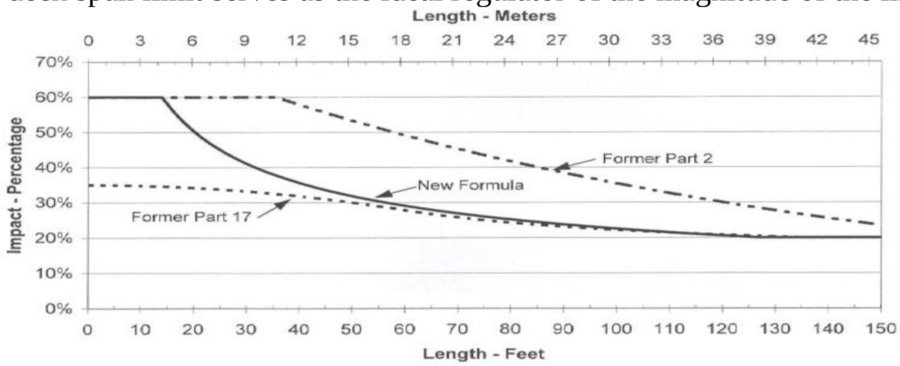

Fig. 4.6 AREMA Impact load graph for various impact formulae over the year

In most written Bridge texts, including [2], a key property of a bridge is the 6-meter minimum span attribute. Short span and medium span bridges are permitted to use the same equation in calculating the impact. This allows for the adoption of a 50% impact force for spans up to 39 meters. Impact for spans other than those of Eqn 4-32 is given as constant.
For spans of maximum length of 4 meter,

$$I = 60 \qquad \text{Eqn 4-33}$$

And for spans with minimum length of 39 meter,

$$I = 20 \qquad \text{Eqn 4-34}$$

Fig. 4.7 below graphically shows the trend by which impact force is affected with respect to the span of the structure. Vividly, there is a huge difference in the magnitude of impact force when using both manuals. Though [27] does not explicitly limit impact for spans with a maximum of 4-m length like [2], it also produces the same impact for all its spans up to 4 meters. For both manuals, the shape of impact is almost the same across the 100-meter sample. This shows some level of corroboration between each manual that the impact force would always take a downward turn with respect to an increase in the span.

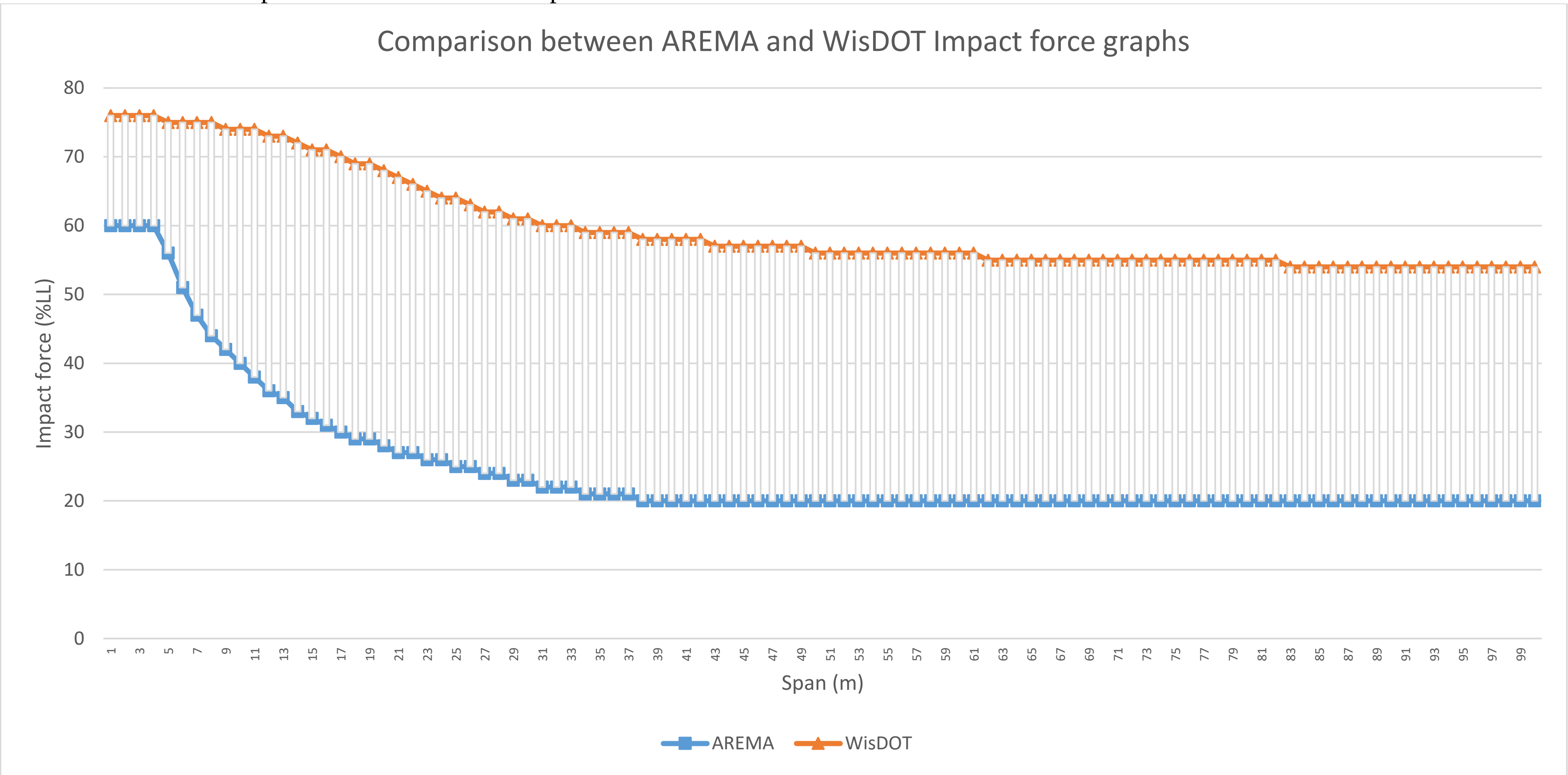

Fig. 4.7 Graphical Comparison between AREMA and WisDOT Impact force

In *Fig. 4.8*, the number of identical impact force obtained at each given span is given across a 2-meter interval. Because of the limit provided in the AREMA impact formula, the impact force in the range of the 20s dominates the chart with a whopping total sum of 82%.

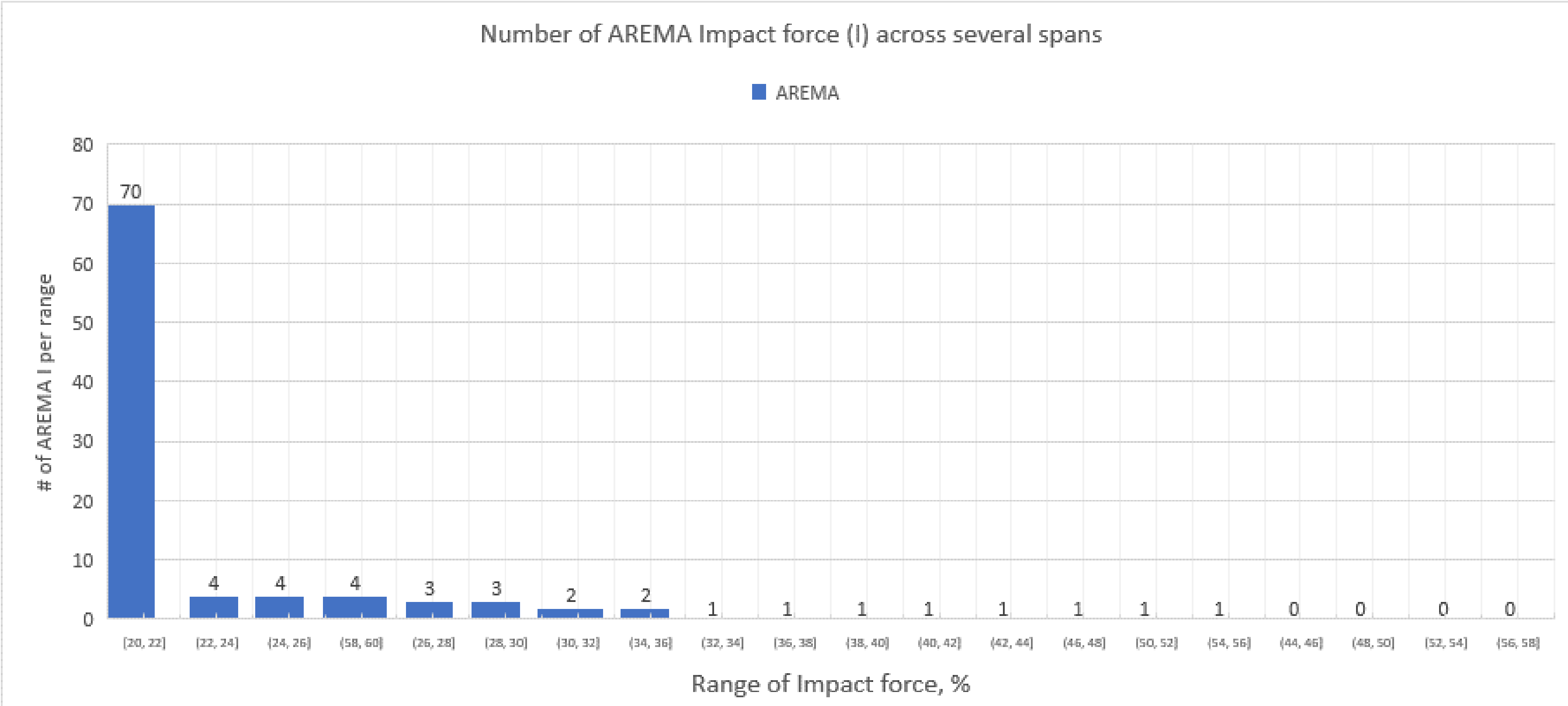

Fig. 4.8 Representation of the Number of AREMA Impact force (I_A) in a specified range across several spans

In the same 2-m band, the most dominant impact is in the range of the 50s with a total sum of 64%.

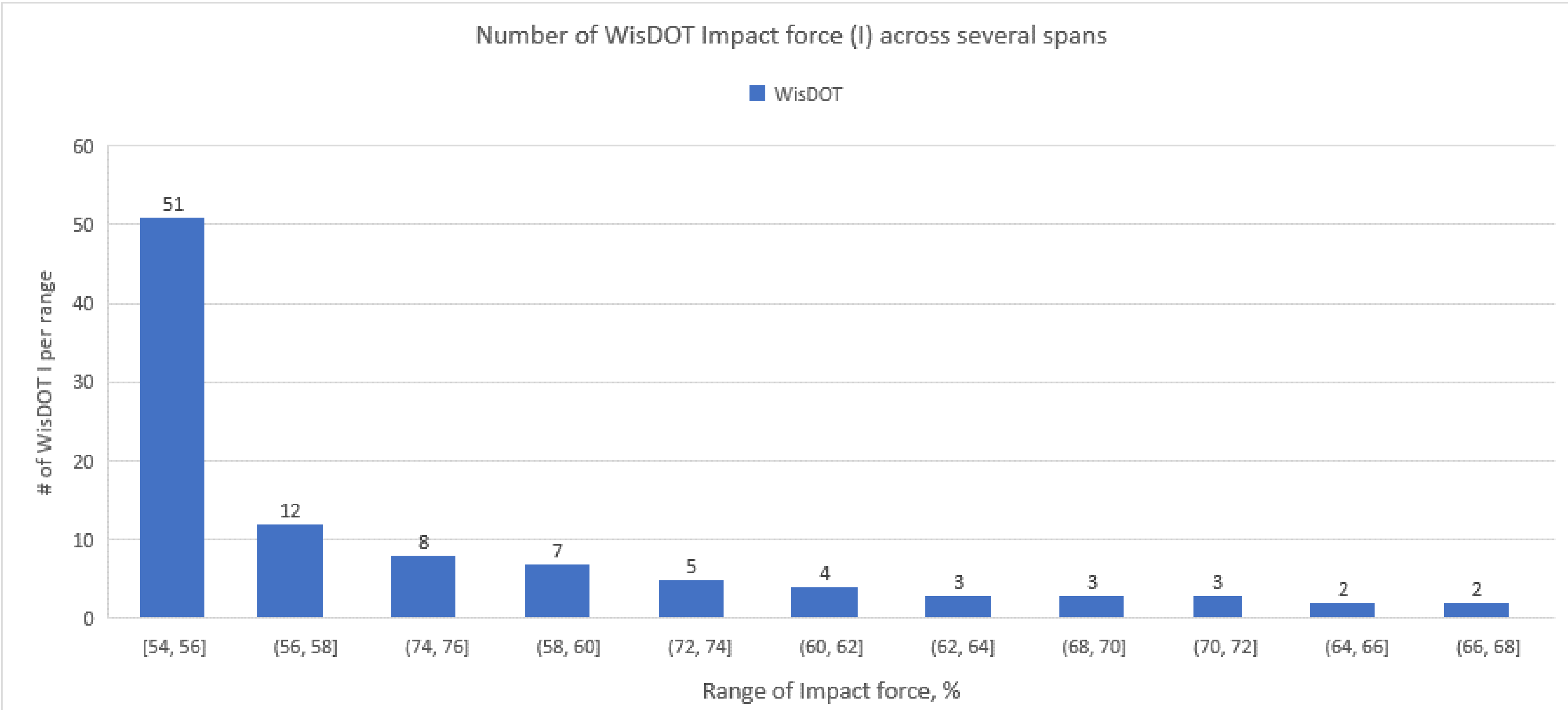

Fig. 4.9 Representation of the Number of WisDOT Impact force (I_W) in a specified range across several spans

4.1.4.2.2.1.1.2 Wind Load on structure

Wind loads are one of the most dynamic loads acting horizontally on the railway civil structure as well as the rolling stock itself. In this work, it is established that horizontal/transverse movement is restrained thus allowing wind-related effects to be considered as acting downward. These are some of the preconditions that have caused wind load determination and calculations to be very tedious and with a varying range of unpredictability. However, most experiments, even [2], have adopted to using a 100-mile-per-hour (mph) wind speed (i.e., 160 km/h) for most structural calculations, to be more conservative. Such speed, in real scenarios, is hardly experienced on structures in normal conditions.

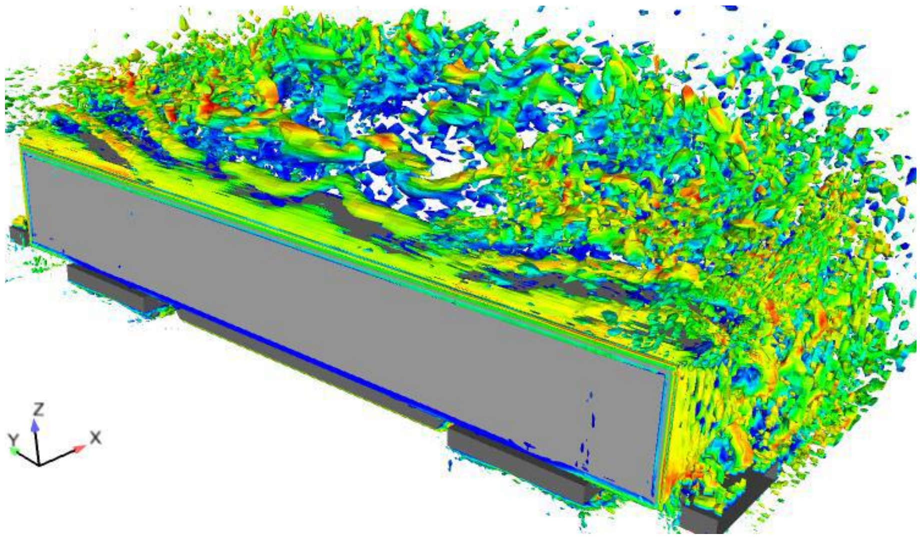

Fig. 4.10 Illustration of wind load on a vehicle body

The equivalent pressure exerted as a result of the wind speed is estimated in the procedure below:

1. Force is the product of the mass of the object and the acceleration due to gravity (a).

$$F = ma \qquad \text{Eqn 4-35}$$

The object under consideration is air. With gravitational acceleration being constant, the mass of the air (m_{air}) is configured from the unit area and the density of air (which is estimated at 1.225 kg/m^3).

$$m_{air} = A\rho_{air} \qquad \text{Eqn 4-36}$$

$$m_{air} = (1m * 1m)(1.225\frac{kg}{m^3}) = 1.2\frac{kg}{m}$$

2. Acceleration due to gravity is directly proportional to the square of the velocity of the of the wind.

$$F = mv^2 \qquad \text{Eqn 4-37}$$

As previously put, the velocity of the wind (i.e., the speed) is converted to consistent units.

$$v = 160\frac{km}{hr} * \frac{1\,hr}{1\,km} * \frac{1000\,m}{3600\,s} = 44.44\frac{m}{s} = 44\frac{m}{s}$$

3. Thus, the force as the result of the wind speed is

$$F = \left(1.2\frac{kg}{m}\right)\left(44\frac{m}{s}\right)^2 = 2323\ N = 2.323\ kN$$

4. And thus, the pressure acting on a 1-m^2 area thus become,

$$p = \frac{F}{A} \qquad \text{Eqn 4-38}$$

$$p = \frac{2323\ N}{1\ m * 1\ m} = 2323\frac{N}{m^2} = 2323\ Pa$$

2323 Pa is almost in the range of the 2160 Pa adopted by [2] and in this work. Wind load on a car body can be represented as illustrated below. Unlike wind load which application takes effect at the side of the structure and used for structural design, air resistance is applicable to the front or rear faces of the vehicle. The computation of air resistance is practically applicable in the geometry of the line and the required tractive efforts of the vehicle. The shape of the face of the vehicle is the main parameter associated with the magnitude of effort that the vehicle must be built with.

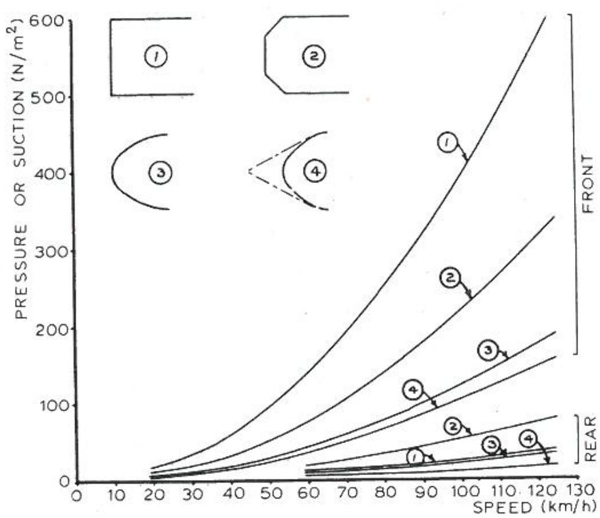

Fig. 4.11 The rolling stock face-pressure relationship

Thus, [2] section 2.2.3h requires that the Wind Load on Structure be computed as follows: "2160 Pa on the vertical projection of the structure applied at the center of gravity of the vertical projection in any horizontal direction". Since a 1-m strip of the section is considered in the metric system for design, and the combined height of the flange and the parapet wall/curb, as indicated, is 1.03 meters, this means that the center of gravity (c_g) for this surface is at the following coordinates:

$$c_g = 0.5(x, y) \qquad \text{Eqn 4-39}$$

$x = 0.5x = 0.5(1000\ mm) = 500\ mm = 0.5\ m$

$y = 0.5y = 0.5(1030\ mm) = 515\ mm = 0.515\ m$

Thus, the center of gravity is at (0.5, 0.515) meter and the magnitude of wind load acting at this coordinate (centroid) is obtained as the product of the base wind load and the area of the parapet.

$$WL_S = w_b A \qquad \text{Eqn 4-40}$$

[2] base wind load applies.

$$WL_S = 2160\frac{N}{m^2}(1\ m * 1.030\ m) = 2225\ N = 2.23\ kN$$

The equivalent moment caused by the wind load on the structure thus become

$$M_{WL} = WL(y) \qquad \text{Eqn 4-41}$$

$M_{WL_S} = 2.23\ kN(0.515\ m) = 1.133\ kN.m = 1.15\ kN.m$

4.1.4.2.2.1.1.3 Wind Load on Live Load

Wind load on live load is a secondary live load acting at a specified height of the car body. [2] chapter 8-2.2.3i specifies the wind load effect on the live load be taken at 2.45 meters above the rail with a distributed magnitude of 4.4 kN/m. The concentrated magnitude of the wind load on live load is obtained from the equation

$$WL_{LL} = WL_{LL}h_{WL_{LL}} \qquad \text{Eqn 4-42}$$

$WL_{LL} = 4.4\dfrac{kN}{m}(2.45\ m) = 10.78\ kN$

4.1.4.2.2.1.1.4 Longitudinal Force

[2] C-2.2.3j.(1) requires that Longitudinal force shall be the greater of:

$$LF = 200 + 17.5L \qquad \text{Eqn 4-43}$$

$LF_b = 200 + 17.5(1) = 200 + 17.5 = 217.5\ kN$

…due to braking, and

$$LF = 200\sqrt{L} \qquad \text{Eqn 4-44}$$

$LF_a = 200\sqrt{1} = 200\ kN$

…due to acceleration.

The higher of Eqn 4-43 and Eqn 4-44 is Eqn 4-43 based on a 1-m strip. Otherwise, for the entire span of the structure, Eqn 4-44 is higher. However, the magnitude of longitudinal force obtained from these equations is far larger than the wheel load, whereby it is a percentage of the live load. In such conditions, [2] 8-C-2.2.3(j)b allows for wheel-rail adhesion during braking, which yields higher magnitude than acceleration, to be 15%. This is directly proportional to the percentage of load. Similarly, [27] 38.3.1.10 also stipulates 15% of the live load to be taken as longitudinal force.

$$LF = 15\%LL \qquad \text{Eqn 4-45}$$

$LF = \dfrac{15}{100}(180\ kN) = 27.0\ kN$

Summary of all secondary live loads used in the analysis, with the primary live load equals:

1. **Live load …………………………………… 180.0 kN**
2. Impact force …………………...……………. 72.0 kN
3. Wind Load on structure …………………..… 2.23 kN
4. Wind Load on Live Load ………………...… 10.78 kN
5. Longitudinal force ………………………...... 27.0 kN

Total ……………..… 292.01 kN

4.1.4.2.2.2 Design of Main bars

As similar to the provisions of section 4.1.3 above, the following summary can be concluded about the shear and moment:

1. $R_1 = 292.01\ kN$

2. $R_2 = 292.01\ kN$
3. $V_A = 0\ kN$
4. $V_{R_1} = 292.01\ kN$
5. $V_f = -292.01\ kN$
6. $V_g = -292.01\ kN$
7. $V_{R_2} = 292.01\ kN$
8. $V_B = 0\ kN$
9. $M_f = 159.29\ kN.m$
10. $M_g = 159.29\ kN.m$

The total factored design live load moment as in [2]'s Table 8-2-5, but here, adjusted, is

$$M_{sd} = \emptyset[1.4M_{LL}]$$

$M_{sd} = 0.9[1.4(159.29\ kN.m)] \approx 200.71\ kN.m \approx 200710\ N.m$

4.1.4.2.2.2.1 Steel Ratio

Refer SoE 10-5.

$\rho_0 \approx 0.012 \approx 1.2\%$

Thus, a 1.2% area of the entire design strip makes up the steel area considering live load only. Referencing Eqn 4-18, Eqn 4-19 and Eqn 4-20, 1.2% is higher than all the minimums.

4.1.4.2.2.2.2 Area of steel

$A_s = \rho bd = 0.012(1000\ mm)(220\ mm) = 2640\dfrac{mm^2}{m}$

Using a minimal ρ value for flexure as contained in Table 4-5, the minimum area of steel is,

$$\begin{Bmatrix} A_{min,0.33} = 924.0\ mm^2/m\ = A_1 \\ A_{min,0.96} = 2688.0\ mm^2/m\ = A_2 \\ A_{min,1.8} = 5040.0\ mm^2/m = A_3 \end{Bmatrix}$$

4.1.4.2.2.2.3 Number of Bars

The number of for the loaded section is obtained in similar fashion as that of the unloaded section. Adopting the same diameter of tension bar, while considering other options as well, the following formulae and expressions apply:

1. $\phi_{bar} = \frac{bar\ \#}{25} * 25.4$
2. $\begin{cases} No.25\ \rightarrow\rightarrow\rightarrow\rightarrow\rightarrow\rightarrow\rightarrow\ \phi_{25} = 25.4\ mm \\ No.22\ \rightarrow\rightarrow\rightarrow\rightarrow\rightarrow\rightarrow\rightarrow\ \phi_{22} = 24.4\ mm \\ No.19\ \rightarrow\rightarrow\rightarrow\rightarrow\rightarrow\rightarrow\rightarrow\ \phi_{19} = 19.3\ mm \end{cases}$
3. $\#_{bar} = \frac{A_s}{A_{1\ bar}}$
4. $A_{1_{bar}} = \frac{\pi d^2}{4}, \qquad d = \phi$
5. $Q = \frac{A_s}{A_{1_{bar}}}$

And thus Table 4-9 summarizes the numerical data associated with a single bar and the quantity of bars required of the various areas of steel indicated in 4.1.4.2.2.2.2 above.

The number of bars table							
Bar Designation		**Number of Bars**					
#	**Φ (mm)**	**A_b (mm^2)**	**A_s**	**A_1**	**A_2**	**A_3**	**Remark***
25	25.4	507.0	5	2	5	10	A_2 corroborates with A_s while A_3 is 2x greater than A_s and A_2 but 5x > A_1
22	22.4	394.0	7	2	7	13	A_2 corroborates with A_s while A_3 is 2x greater than A_s and A_2 but 5x > A_1
19	19.3	293.0	9	3	9	17	A_2 corroborates with A_s while A_3 is 2x greater than A_s and A_2 but 5x > A_1
16	16.3	209.0	13	4	13	24	A_2 corroborates with A_s while A_3 is 2x greater than A_s and A_2 but 5x > A_1
12	12.2	117.0	23	8	23	43	A_2 corroborates with A_s while A_3 is 2x greater than A_s and A_2 but 5x > A_1

Table 4-9: The Area of steel – number of bar chart for loaded flange

* Rough estimation (the ratios indicated are NOT based on exact mathematical interpretation)

The #25 and #22 bars do not yield the same quantity in Table 4-9. #19 and #16 double the quantities obtained from #25 and #22 respectively. On another hand, #12 has the highest number of bars comparably three to four times than those of #25 whereby #25 is only twice the diameter of a #12.

4.1.4.2.2.2.4 Spacing

All the provision of 4.1.4.2.1.1.1 above also apply here.

The spacing table										
Bar Designation			**A_s**		**A_1**		**A_2**		**A_3**	
#	**Φ (mm)**	**A_b (mm^2)**	**Q**	**S (mm)**	**Q**	**S (mm)**	**Q**	**S (mm)**	**Q**	**S (mm)**
25	25.4	507.0	5	218	2	949	5	218	10	83
22	24.4	468.0	7	141	2	955	7	141	13	59
19	19.3	293.0	9	103	3	471	9	103	17	42
16	16.3	209.0	13	66	4	312	13	66	24	26
12	12.2	117.0	23	33	8	129	23	33	43	11

Table 4-10: Quantity of flexural rebar vs. spacing for loaded flange

In Table 4-10 above, and as in previous cases, #25 bar is adopted for the flexural design. Compared to the unloaded flange, the number of bars and spacing are all more and larger. The reinforcement (rounded up for uniformity) associated with the live load, is then

$$\boldsymbol{Adopt}\ \#\mathbf{25}\ @\ \mathbf{220}$$

4.1.4.2.2.3 Design of the Flange Transverse Reinforcement

The procedure for calculating the transverse parameters and literature follow that of 4.1.4.2.1.2 above.

4.1.4.2.2.3.1 Area of steel

Transverse area of steel is normally less than its flexural counterpart for 1-way members.

$$A_t = \left\{\left(\sqrt{\frac{1750}{2.6}}\right)\%\right\}2640 = 684.91\frac{mm^2}{m} \approx 685\frac{mm^2}{m}$$

From [26], the area of transverse reinforcement remains the same as that of 4.1.4.2.1.2.2 above because parameters needed are the same and constant for each case (loaded or unloaded).

$$A_{s,t} = \frac{1.3 * 2.6 * 0.28}{2(2.6 + 0.28)420} = 0.000391\ m^2 = 391\ mm^2$$

This same-area-of-steel points to one of the limitations of the ACI 350 equation (Eqn 4-28) for transverse reinforcement.

4.1.4.2.2.3.2 Number of bars

Using the same #25 bar,

$$\#_{bar} = \frac{685}{507} = 1.35\ \approx 2$$

Area of steel and # of bar of transverse reinforcement								
By use of Formula	$A_t = \left\{\left(\sqrt{\frac{1750}{\vartheta}}\right)\%\right\} A_s$					$A_s = \frac{1.3bh}{2(b+h)f_y}$		**Remark Percentage by which $A_{t\%}$ is of A_t:**
	ρ_t	**A_{gross} (mm^2)**	**A_s (mm^2)**	**A_t (mm^2)**	**Q**	**$A_{s,t}$ (mm^2)**	**Q**	
	-	**-**	**2640**	**685**	**2**	**391**	**1**	**Calculated transverse area (A_t)**
				$A_{t\%} = \rho_t A_g$				
By use of Percentage of A_{gross}	0.180	280000	-	504	1	-	-	74 of A_t, 129 of $A_{s,t}$
	0.192	280000	-	538	1	-	-	79 than A_t, 138 than $A_{s,t}$
	0.204	280000	-	571	1	-	-	83 than A_t, 146 than $A_{s,t}$
	0.216	280000	-	605	1	-	-	88 than A_t, 155 than $A_{s,t}$
	0.228	280000	-	638	1	-	-	93 than A_t, 163 than $A_{s,t}$
	0.240	280000	-	672	1	-	-	98 than A_t, 172 than $A_{s,t}$
	0.252	280000	-	706	1	-	-	103 than A_t, 181 than $A_{s,t}$
	0.264	280000	-	739	1	-	-	108 than A_t, 189 than $A_{s,t}$
	0.276	280000	-	773	2	-	-	113 than A_t, 198 than $A_{s,t}$
	0.288	280000	-	806	2	-	-	118 than A_t, 206 than $A_{s,t}$
	0.300	280000	-	840	2	-	-	123 than A_t, 215 than $A_{s,t}$
	0.312	280000	-	874	2	-	-	128 than A_t, 224 than $A_{s,t}$
	0.324	280000	-	907	2	-	-	132 than A_t, 232 than $A_{s,t}$

Table 4-11: Number of bars of transverse reinforcement for loaded flange

4.1.4.2.2.3.3 Spacing

$$s = \frac{1000 - 2(25.4)}{2 - 1} = 949\ mm; 949\ mm\ <\ 450\ mm \ldots NOT\ OK$$

Thus, use **#25@450** mm

4.1.4.2.2.4 Design for Shrinkage and Temperature Reinforcement

Section 7.12.1 of [26] ideally states that temperature reinforcement shall be applicable in one-way slab only – thus, this work is in conformity with the code. Concrete structural members are not as expansive as those of steel. Thermal loads, in their varying forms like those of wind loads, will usually not be as specifically and strategically applied at a specific point as those of dead and primary live loads. The effect of change in temperature as reported in [28] which focuses on a cable-stayed bridge, gives a clearer picture as to why temperature must be considered in structural design. Temperature loads which cause these temperature stresses which are also primarily accrued from radiation, the atmosphere and the surface of the water beneath the bridge, may in short be classified as short-wave and long-wave thermal loads.

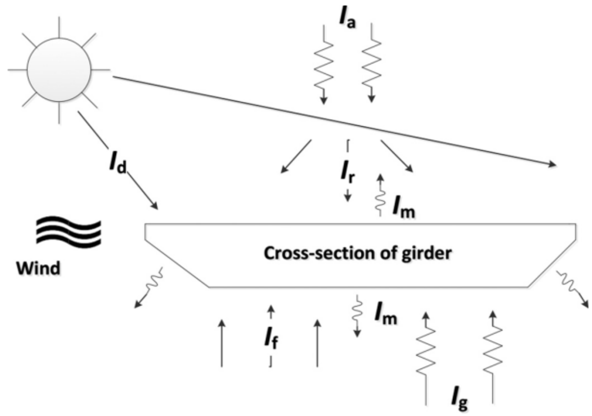

Fig. 4.12 Thermal load application format on a girder

From the diagram:

$$short - wave \begin{cases} I_d = direct\ radiation \\ I_r = diffusion\ radiation \\ I_f = reflected\ radiation \end{cases}$$

$$long - wave \begin{cases} I_a = atmospheric\ radiation \\ I_g = surface\ of\ ground\ water\ radiation \\ I_m = surface\ radiation \end{cases}$$

4.1.4.2.2.4.1 Area of Shrinkage and Temperature Reinforcement

For normal exposure conditions like for the condition specified herein, [2] considers that the area of temperature reinforcement for reinforced concrete structural members be empirically estimated as follows:

$$A_{tem} = \frac{0.75A_g}{f_y} \qquad \text{Eqn 4-46}$$

$$A_{tem} = \frac{0.75(1000\ mm)(280\ mm)}{420\dfrac{N}{mm^2}} = 500\frac{mm^2}{m}$$

However, [2]'s 8-2.12 provides that minimum area of temperature reinforcement shall be 530 mm^2.

4.1.4.2.2.4.2 Number of Shrinkage and Temperature bars

Number of bars designed for temperature are almost as those for shear, positioning (i.e., transverse reinforcement). Adopting a #14 bar, for [26] requires temperature bars range from #13 upwards,

$$Q = \frac{530}{158} = 3.4 \approx 4$$

4.1.4.2.2.4.3 Spacing of Shrinkage and Temperature bars

[2] specifies a 450-mm maximum spacing for temperature reinforcement applied on both surface faces. [26]'s7.12.2.2 does not allow the spacing for temperature reinforcement to exceed 300 mm.

$$s = \frac{bA_b}{A_t} \qquad \text{Eqn 4-47}$$

$$s = \frac{1000(158)}{530} = 298\ mm \approx 300\ mm$$

The above calculated spacing is less than both requirements. Hence it is acceptable.

4.1.4.2.2.5 Reinforcement summary for calculated transverse & shrinkage and temperature reinforcements

Transverse Reinforcement & Shrinkage and Temperature Reinforcement Details Table																		
Bar Desig.			**Number of bar and spacing yielded from each area of steel**															
			A_t	**$A_{s,t}$**	**$A_{t\%}$**													**A_{tem}**
#	**Φ**	**A_b**	***685***	***391***	***504***	***538***	***571***	***605***	***638***	***672***	***706***	***739***	***773***	***806***	***840***	***874***	***907***	***530***
25	25.4	507	1 {949}	*1* {949}	*1* {949}	1 {949}	1 {949}	1 {949}	1 {949}	1 {949}	1 {949}	1 {949}	2 {949}	2 {949}	2 {949}	2 {949}	2 {949}	1 {957}
22	24.4	468	1 {955}	*1* {955}	2 {955}	2 {955}	2 {955}	2 {955}	2 {955}	2 {955}	2 {955}	2 {955}	2 {955}	3 {466}	3 {466}	3 {466}	3 {466}	2 {743}
19	19.3	293	1 {961}	2 {961}	2 {961}	2 {961}	2 {961}	3 {471}	3 {471}	3 {471}	3 {471}	3 {471}	3 {471}	3 {471}	3 {471}	3 {471}	4 {308}	2 {553}
16	16.3	209	2 {967}	2 {967}	3 {476}	3 {476}	3 {476}	3 {476}	4 {312}	4 {312}	4 {312}	4 {312}	4 {312}	4 {312}	5 {230}	5 {230}	5 {230}	3 {394}
14	14.2	158	4 {314}	2 {972}	3 {479}	3 {479}	4 {314}	4 {314}	4 {314}	4 {314}	4 {314}	5 {232}	5 {232}	5 {232}	5 {232}	6 {183}	6 {183}	4 {298}
12	12.2	117	2 {976}	4 {317}	5 {235}	5 {235}	5 {235}	6 {185}	6 {185}	6 {185}	7 {152}	7 {152}	7 {152}	7 {152}	8 {129}	8 {129}	8 {129}	5 {221}

Table 4-12: Number of bar and spacing of transverse reinforcement & shrinkage and temperature reinforcement table

NB: As in Table 4-8, Error! Reference source not found. contains calculated number (quantity and s pacing) of bars ranging from one (1) to eight (8). 1 bar would regularly not fit into the spacing equation (Eqn 4-26) to produce a structural result. Thus,

1. a 1-bar quantity that is **boldfaced** is increased by 1 in Eqn 4-26 and,
2. a 1-bar quantity that is ***boldfaced italic*** is one that does not produce a full one-bar quantity thus had to be rounded up to one (1) and also had to be increased by 1 in Eqn 4-26

Therefore, considering the effect of live load only, the following specification is adopted for transverse reinforcement:

1. Transverse Bars: Adopt #25 @ 450
2. Shrinkage/Temperature Bars: Adopt #14 @ 298

4.1.4.2.3 Design of the Flange for both Dead Load and Live Load

The above designs considered loads, shears, and moments for dead load and all forms of live loads combined separate respectively. This is so done to enable a comparative analysis between the yield parameters of each load type. Now, a combination of all loads is performed to obtain generalized statements about the girder. A summary of all concentrated loads at the point of the rail is indicated below in the summary.

4.1.4.2.3.1 Summary of all loads

<u>Loads</u>

Rail load = 3.0 kN
Wheel load = 180.0 kN
Impact force = 72.0 kN
Wind Load on structure = 2.23 kN
Wind Load on Live Load = 10.78 kN
Longitudinal force = <u>27.00 kN</u>
292.01 KN

Now, the loaded girder for the combined instance would be represented as follows:

4.1.4.2.3.2 Reactions

NB: Because of the symmetry in the loading condition also, let both reactions be equal and the sign convention be "Clockwise is positive".

$$\sum M@R_1 = 0 \qquad \text{Eqn 4-48}$$

Refer *SoE 10-6* for the procedure.

$(2.6\ m)R_2 = 851.00\ kN.m$

$$R_2 = \frac{851.00\ kN.m}{2.6\ m}$$

$R_2 = 327.31\ kN$

4.1.4.2.3.3 General Shear and Bending moment diagrams

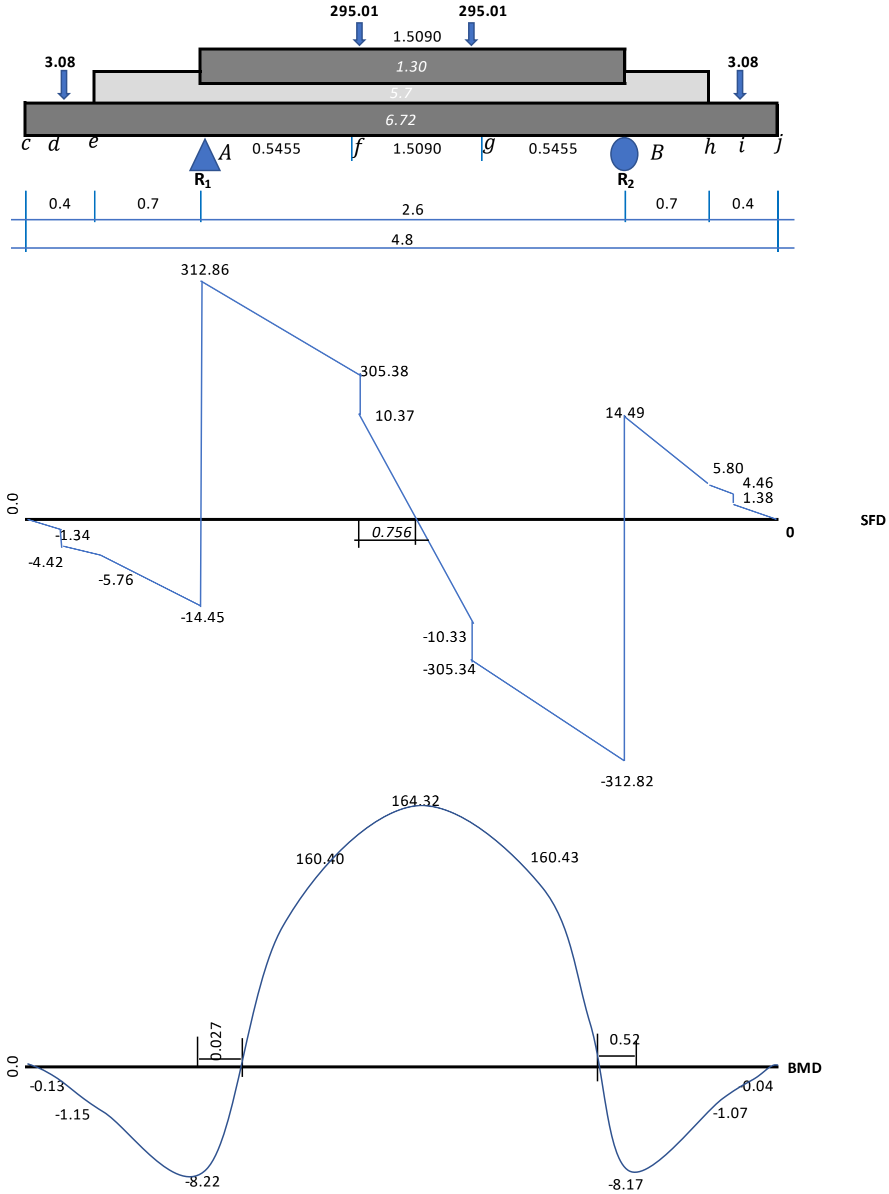

Fig. 4.13 Shear force and bending moment diagrams for dead and live loads combined

4.1.4.2.3.4 Shear

The maximum shear is $V_{R1} = -14.45\ kN + 327.31\ kN = 312.86\ kN$. For full procedure, refer *SoE 10-7*.

4.1.4.2.3.4.1 Point of Zero Shear

The point of zero shear occurs where the shear transitions from negative to positive shear or vice versa practically excluding those at the supports.

$$V_k = \frac{10.37\ kN}{13.72\,\frac{kN}{m}} = 0.756\ m$$

4.1.4.2.3.5 Bending moment

The Maximum moment is $M_k = 160.40\ kN.m + 0.5(0.756\ m)(10.37\ kN) = 164.32\ kN.m$. Refer *SoE 10-8* for details.

4.1.4.2.3.5.1 Point of Contraflexure/Inflection

$$x_1 = \frac{8.22\ kN.m}{0.5 * 618.24\ kN} = 0.027\ m$$

$$x_2 = \frac{160.43\ kN.m}{0.5 * 618.16\ kN} = 0.519\ m$$

4.1.4.2.3.6 Design for flexure

The following sub-chapters apply.

4.1.4.2.3.6.1 Design moment

From the superposition performed, the maximum design bending moment yields

$M_{sd} = \emptyset[1.4(M_{DL} + M_{LL})] = 0.9[1.4(164.32\ kN.m)] = 207.04\ kN.m$

However, comparatively, the design moment obtained by the individual operation is:

$$M_{sd} = M_{sdDL} + M_{sdLL} \qquad \text{Eqn 4-49}$$

$M_{sd} = 10.39\ kN.m + 200.71\ kN.m = 211.07\ kN.m$

From the two alternatives with the design moment being 207.04 kN.m and 211.07 KN.m, the larger value is obtained from the individual procedure. This is so because the maximum moment obtained from the procedure containing dead load only is at the support rather than at the middle of the deck. But with the application of the live load, the maximum moment shifted to the middle of the deck. Notwithstanding, by considering the dead load moment and the live load moment at the middle of the deck, the same moment as that obtained in the superposition method is obtained. Thus, the adopted moment is that of the 207.04 kN.m obtained from the superposition method!

$$\boldsymbol{M = 207040\ N.m}$$

4.1.4.2.3.6.2 Steel ratio

This is the total ratio of steel that is present in the section for the effect of dead load and live load.

$\rho_0 \approx 0.012 = 1.2\%$

4.1.4.2.3.6.3 Area of flexural reinforcement

$A_s = \rho bd = 0.012(1000)(220) = 2640\ mm^2/m$

The minimum area of flexural reinforcement would be, according to Table 4-5 $\rho_{min} = 0.0033$ (0.33% A_g) and the equivalent area of flexural reinforcement is

$$A_{s_{min}} = 924\ mm^2/m$$

4.1.4.2.3.6.4 Number of flexural bar

$$Q = \frac{A_s}{A_b} = \frac{2640}{507} = 5.2 = 5$$

4.1.4.2.3.6.5 Spacing of flexural bar

With these 5 bars in a 1-m band, there would be a total of 50 bars in this 10-m span railway bridge. This is so done to effectively distribute the spacing on centers. To better and accurately obtain the spacing, adopt the following procedure:

1. For in-to-in spacing,

$$S = \frac{Total\ width - 2(side\ cover + 0.5\phi))}{Total\ void\ spaces\ between\ bars} \qquad \text{Eqn } 4\text{-}50$$

$$S = \frac{10000 - 2(50 + 0.5 * 25.4) - (50 - 2 * 0.5)25.4}{50 - 1} = 176\ mm\ O/c$$

2. For center-to-center spacing along the entire span of the girder

$$S = \frac{Total\ width - 2(side\ cover + 0.5\phi)}{Total\ void\ spaces\ between\ bars} \qquad \text{Eqn } 4\text{-}51$$

$$S = \frac{10000 - 2(50 + 0.5 * 25.4)}{50 - 1} = \ 202\ mm\ O/c$$

Flexural bars arrangement for the 176-mm in-to-in spacing adjusted to 175-mm (Eqn 4-50)

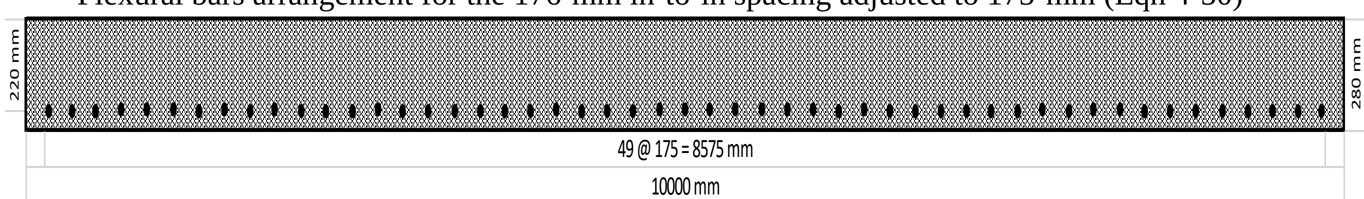

Fig. 4.14 Main bar arrangement of 175-mm in-to-in spacing for the entire 10-m span bridge

Flexural bars arrangement for the center-to-center spacing of 202-mm spacing adjusted to 200-mm (Eqn 4-51)

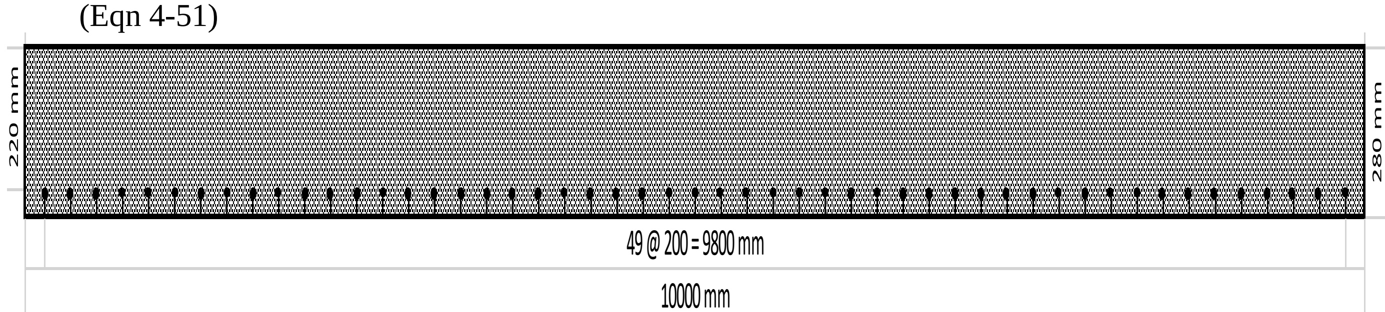

Fig. 4.15 Main bar arrangement of 200-mm on-centers spacing for the entire 10-m span bridge

4.1.4.2.3.7 Final Design of the Flange Transverse Bars for all loads

Because this slab is a one-way element, transverse reinforcement in the slab runs parallel to traffic.

4.1.4.2.3.7.1 Area of steel

$$A_t = \left\{\left(\sqrt{\frac{1750}{2.6}}\right)\%\right\}2640 = 685\ mm^2/m$$

4.1.4.2.3.7.2 Number of bars

$$Q_{bar} = \frac{685}{507} = 1.4 \approx 2$$

Therefore, the total number of bars in the 2.6-m width is,

$$Q_{tot} = Qw \qquad \text{Eqn } 4\text{-}52$$

$$Q_{tot} = 2\frac{bars}{m}(2.6\ m) = 5.2\ bars \approx 6\ bars$$

4.1.4.2.3.7.3 Spacing

$$S = \frac{Total\ width - 2(side\ cover + 0.5\phi))}{Total\ void\ spaces\ between\ bars} \qquad \text{Eqn } 4\text{-}53$$

$$S = \frac{2600 - 2(50 + 0.5 * 25.4)}{6 - 1} = 495\ mm$$

Since 495 mm is greater than 450 mm, adopting the 450-mm maximum value is allowed. However, for achieving the objective of a more consistent spacing, adopt 350 mm which would produce seven bars (blue bars). The shrinkage/temperature reinforcement is the same for the final design (red bars)

4.1.4.2.3.7.4 Final Diagrams

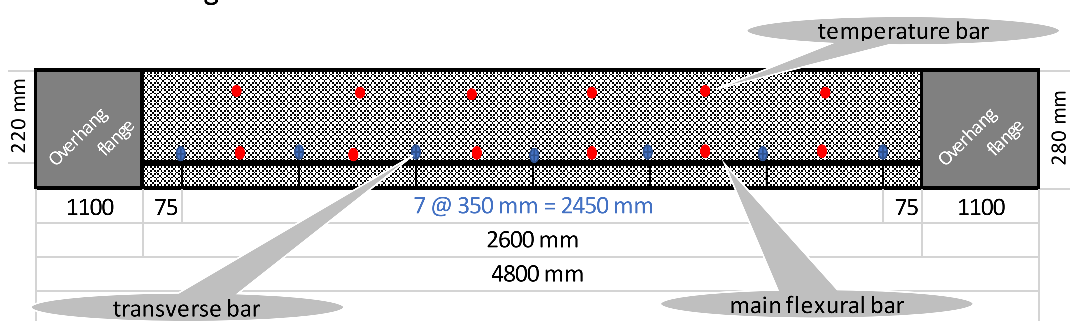

Fig. 4.16 Transverse view: Transverse bars (blue) (on-centers) and Shrinkage and temperature bars (red) (in-to-in) in the flange

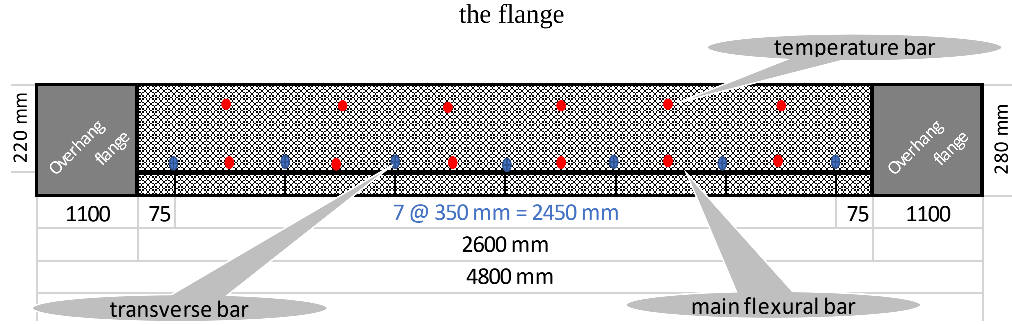

Fig. 4.17: Longitudinal view: Main bars (black), transverse bars (blue), and temperature bars (red) in the fully reinforced flange

4.1.4.2.3.8 Design for Flange Shear

The basis of the computation of shear relies on [2] section 8-2.10. The code permits that it is needless to design for shear stress in slab and footing, etc. This is primarily due to the application of reinforcement in both directions (main and transverse) usually adopted due to the large area as compared to beams, columns, etc.

4.1.4.2.3.8.1 Design Shear

The total shear is the maximum shear calculated and obtained for the combined effect of all loads. That is:

$$V_{max} = highest\ shear\ from\ the\ combined\ loads \qquad \text{Eqn } 4\text{-}54$$

$V_{max} = V_{R_1} = 312.86\ kN$

The factored shear, being ultimate shear, used to obtain the design shear and furthermore the design shear stress is the maximum theoretical shear multiplied by the amplification factor of 1.4.

$$V_u = 1.4V_{max} \qquad \text{Eqn 4-55}$$

$V_u = 1.4(312.86\ kN) = 438.004\ kN = 438004\ N$

Safety is at the core of design. This is one of the primary reasons why these coefficients are adopted. For shear is increased for uncertainties, at the same time it is decreased to a factor less than unity to also account for further safety against unforeseeable circumstances. Thus, the design shear is one that adopts the shear strength reduction factor of 0.85 against the ultimate shear.

$$V_{sd} = \varphi V_u \qquad \text{Eqn 4-56}$$

$V_{sd} = 0.85(438.004\ kN) = 372.3034\ kN \approx 372.3\ kN = 372300\ N$

On the overall, the goal is to design in that contingency is addressed. The percentage of increment/decrement in the design shear to that of the initial calculated shear is

$$\aleph_{\left(\frac{V_{sd}}{V_{max}}\right)} = \frac{V_{sd}}{V_{max}} \qquad \text{Eqn 4-57}$$

$$\aleph_{\left(\frac{V_{sd}}{V_{max}}\right)} = \frac{V_{sd}}{V_{\max}} = \frac{372.3\ kN}{312.86\ kN} = 1.1899 \approx 1.19 = 19\%$$

A 19% increment from the original shear is enough to serve as contingency.

4.1.4.2.3.8.2 Design Shear stress

Shear is a force that cuts across a member. For concentrated load, it remains constant between any two points until it is acted upon by another force. Thus, it's shape has a zero slope. On the other hand, the shape of shear force changes with distance if the applied load is other than that of a concentrated load. There are several stresses that occur in a member once an external force is applied, yet even if an external force is not applied, body force exists. Thus, the design shear stress.

$$v_{sd} = \frac{V_u}{\varphi bd} \qquad \textit{Eqn 4-58}$$

$$v_{sd} = \frac{438.004\ kN}{0.85(1.0\ m)(0.22\ m)} = 2342.273\frac{kN}{m^2} \approx 2.34\ MPa$$

4.1.4.2.3.8.2.1 Limiting (permissible) Shear stresses

Recall, concrete even if reinforced, fails under self-weight or external load. This leads to the adoption of permissible (allowed, regulatory, or governing stresses that concrete should undergo). Permissible stresses are set/stipulated for either non-reinforced or reinforced sections.

4.1.4.2.3.8.2.1.1 Minimum (Considering concrete compressive strength only under service load)

$$v = 0.079\sqrt{f_c'} \qquad \text{Eqn 4-59}$$

$v = 0.079\sqrt{40}\,MPa = 0.50\,MPa$

4.1.4.2.3.8.2.1.2 Lower (Considering concrete compressive strength only under ultimate load)

Limiting the value of $\sqrt{f_c^{'}}$ to 69 MPa as dictated by [2] chapter 8-2.35.2,

$$v = 0.17\sqrt{f_c'} \qquad \text{Eqn } \textit{4-60}$$

$v = 0.17\sqrt{40} = 1.08\,MPa = 1080\,kPa$

4.1.4.2.3.8.2.1.3 Minimum (Considering concrete compressive strength only under service load)

$$v = 0.16\sqrt{f_c'} + 17\rho_w\left(\frac{V_u d}{M_u}\right) \qquad \text{Eqn } \textit{4-61}$$

Where ρ_w is the steel ratio equating to,

$$\rho_w = \frac{A_s}{b_w d} \qquad \text{Eqn } \textit{4-62}$$

In Eqn 4-62, bw is the width of the web but in the case of the flange, here, it is considered as the width of the design strip.

$$v = 0.16\sqrt{40} + 17\left(\frac{0.002640\,m^2}{1.0\,m * 0.22\,m}\right)\left(\frac{438.004\,kN(0.22\,m)}{207.040\,kN.m}\right) = 1.012 + 0.095 = 1.107\,MPa$$

However, using Eqn 4-61 above, AREMA limits the upper value to

$$v = 0.29\sqrt{f_c'} \qquad \text{Eqn } \textit{4-63}$$

$v = 0.29\sqrt{40} = \ 1.834\,MPa$

Therefore, from the three limiting stresses, it would be logically prudent to limit the shear strength to the least so as to provide room for more safety. Thus,

$$\boldsymbol{v = 1.08\,MPa}$$

However, $v_{sd}$is greater than all the limiting stresses. This means that the slab requires shear reinforcement. But since shear is not necessarily designed for in slabs and footings, as required by [2], the tension reinforcement is sufficient! In the case of one-way slab, like this being designed for, transverse reinforcement serves the purpose of shear reinforcement as well for this is one reason why transverse reinforcement is provided for. In two-way construction, it is even more rigid. In the case of flexural, and axial compression members, stirrups serve the purpose of taking on shear.

4.1.4.2.4 Investigating the adequacy of the overhanging flange (the cantilever section)

In structural design, there are several different magnitudes of moment, shear, torsion, deflection along the span of any member. Logically, an individual design for each output could be cumbersome and impractical. This allows for the adoption of, in practical terms, the highest value of said data to account for all. In this light, the effects of the overhanging flanges are considered in the design above to ascertain the adequacy of the structure (section 4.1.4.2.3.6). Considering the cantilever section loads only, the total theoretical moment at the support is statically obtained from the equation below

$$M_{OF} = wL + PL \qquad \text{Eqn 4-64}$$

…where w and P are the distribute and concentrated loads respectively, and L is the length upon which the load acts. From the procedure calculations of Eqn 4-48, the sum of the moments of all cantilever loads is

$Deck{:}\ -6.72\frac{kN}{m}(1.1\ m)(0.5x1.1\ m) \qquad = -4.07\ kN.m$

$Curb{:}\ -3.08\ \text{kN (0.9 m)} \qquad = -2.77\ kN.m$

$Ballast{:}\ -5.7\frac{kN}{m}(0.7\ m)(0.5x0.7\ m) \qquad = -1.40\ kN.m$

$$\boldsymbol{M_{OF} = -8.240\ kN.m}$$

The moment obtained from Eqn 4-64, is comparably infinitesimal to that of (4.1.4.2.3.6.1 above: Design moment) and is numerically given as:

$$\aleph_{\left(\frac{M_{OF}}{M_{sd}}\right)} = \frac{M_{OF}}{M_{sd}} \qquad \text{Eqn 4-65}$$

$$\aleph_{\left(\frac{M_{OF}}{M_{sd}}\right)} = \frac{8.24\ kN.m}{207.04\ kN.m} = 0.0398 \approx 0.04 \approx 4\%$$

It can be concluded that the design (4.1.4.2.3.7 Final Design of the Flange Transverse Bars for all loads) be applicable to the entire transverse width of the deck.

4.1.5 Design of the Girder

The figure below is a representation of a typical T-section: containing a girder/beam and a flange and the applied forces thereto.

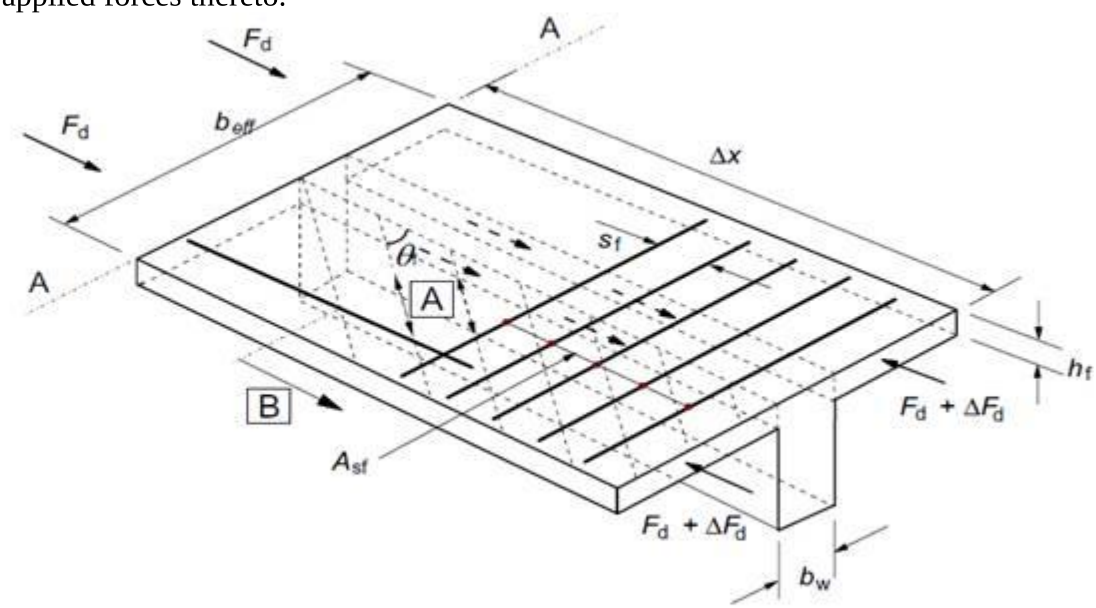

Fig. 4.18 Label, force, and typical reinforcement of a typical T-section

4.1.5.1 Sizing the Girder

The analysis involved herein is almost all static. However, a couple of dynamic theories, applications are mentioned in the latter portion of the design. [2] includes impact based on the effects of static, moving, and dynamic characteristics of Copper-E80 loads that is adopted in the design of railway structures. Impact force increases on a structure if the speed of the acting body increases but proportionally with a rather short span. All of these inputs factored have led to the development of several empirical equations adopted. In the absence of rigorous structural analysis and design to determine the dimensions of reinforced concrete members, [2] developed satisfactory formulas that can be adopted. Referencing [2]'s Table 8-2-10, the minimum depth of the girder can be obtained.

$$t = \frac{clear\ span + 2.75}{15} \qquad \text{Eqn 4-66}$$

Here, the clear span as stipulated in Table 4-1 is 10 meters.

$$t_{gir} = \frac{s + 2.75}{15} = \frac{10\ m + 2.75}{15} = 0.85\ m$$

For serviceability requirements, as recommended for by every structural design, like the wearing course of highway pavement, a one-hundred-fifty-millimeter serviceability thickness is added to Eqn 4-66 to obtain the total sectional thickness of the girder (web plus flange). Thus,

$$t_{gir} = t + t_{ser} \qquad \text{Eqn 4-67}$$

$$t_{gir} = 0.85 + 0.15 = 1.0\ m$$

The width is configured from the rule of thumb that the base is a percentage of the height.

$$w_{gir} = kt_{ser} \qquad \text{Eqn 4-68}$$

Taking the more practical 50%-value,

$$w_{gir} = \left(\frac{50}{100}\right)(1.0\ m) = 0.5\ m$$

However, [2] and some railway texts also use the below formula for sizing the width of the girder

$$w = \frac{center - to - center\ span\ of\ girder\ + 3}{15} \qquad \text{Eqn 4-69}$$

$$w = \frac{s_g\ + 3}{15} = \frac{2.6\ m + 3}{15} = 0.37\ m$$

However, the 0.5-m width is adopted in this design.

4.1.5.2 Verification of the acceptance of the girder dimensions

The basic/preliminary dimensions provided in Table 4-1 are to be crosschecked in order to structurally satisfy the conditions of [2] 8-2.23.10 b(1). It should be noted that the conditions (linguistics) stated in the requirement differ a little from those of normal structures (i.e., buildings, frames, etc.).

> *"The effective slab width acting as a T-girder flange shall not exceed one-fourth of the span length of the girder, and its overhanging width on either side of the girder shall not exceed six times the thickness of the slab or one-half the clear distance to the next girder."*

The following equations interpret the requirements contained above and also further above in section 4.1.1 above.

1. The effective flange width (b_{eff}) shall not exceed one-fourth the span length,

$$b_{eff} \ngtr \left(\frac{1}{4}\right) s \qquad \text{Eqn 4-70}$$

$b_{eff} \ngtr \left(\frac{1}{4}\right)(10\ m) \ngtr 2.5\ m$

The b_{eff} obtained from the dimensions of the T-section is thus,

$$b_{eff} = s_{cant} + \frac{s_g}{2} \qquad \text{Eqn 4-71}$$

…where s_{cant} is the length of the cantilever section from the center of the width of the girder.

$b_{eff} = (0.4 + 0.7)m + \frac{2.6}{2} m = 2.4\ m$

2. …and an overhanging width (w_{oh}) not exceed six times slab/flange thickness

$$w_{oh} \ngtr 6t_{slab} \qquad \text{Eqn 4-72}$$

$w_{oh} \ngtr 6(0.28\ m) \ngtr 1.68\ m$

Thus, for the exterior/outer overhanging width (w_{oho}),

$w_{oh_o} = 0.4\ m + \left(0.7\ m - \left(\frac{0.5}{2}\right) m\right) = 0.85\ m$

Thus, for the interior/inner overhanging width (w_{ohi}),

$$w_{oh_i} = \frac{s_g - w_{gir}}{2} \qquad \text{Eqn 4-73}$$

$w_{oh_i} = \frac{2.6 - 0.5}{2} = 1.05$

Both w_{oh_o} and w_{oh_i} are all less than 1.68 m thus satisfying the condition.

3. …or one-half the clear distance to the next girder.

$$w_{oh} \ngtr \frac{1}{2} s_{g_o} \qquad \text{Eqn 4-74}$$

The clear distance to the girder is s_g minus two halves of the width of the girder/web. The condition stipulated herein is the same as that of Eqn 4-73 thus indicating that the condition is also fully met. Finally, it can therefore be concluded that the dimensions meet all the requirements of a flanged setion as stipulated by [2]. Thus the calculations involving the loads transmitted to the girder can commence.

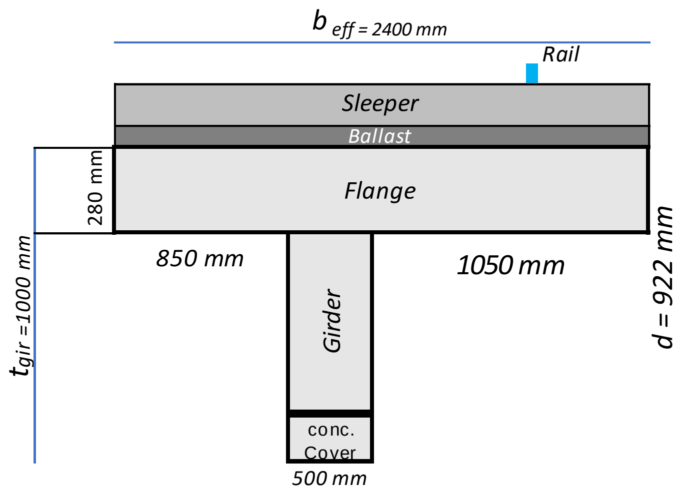

Fig. 4.19 Transverse view of the flanged section for analysis

4.1.5.3 Dead Load configuration

The weights contained in the table are the total calculated dead loads (self-weight) of the flange section. The performance of any structure can logically start with the investigation of the ability to contain its own weight. Unlike the flange, calculations involving the net dead load transferred to the flange-girder interface requires some resolutions that would enable all dead loads act at said interface. This involves moment effects as well.

Girder dead loads configuration table									
	Dimensions			**Properties**		**Output: Moment and Forces**			
Member	***l* (m)**	***W* (m)**	**t (m)**	**Ut. Wt. (kN/m)**	**wt. den. (ρ) (kN/m)**	**Moment @ girder (kN.m)**	**PL on girder (kN)**	**UDL on girder (kN/m)**	**Total Load (kN/m)**
1	2	3	4	5	6	7	8	9	10
Web	10	0.50	0.72		24	0.00	8.64	8.64	**8.64**
$Deck_{int.}$	10	1.30	0.28		24	5.68	11.36	11.36	**11.36**
$Deck_{ext}$	10	1.10	0.28		24	4.07	8.14	8.14	**8.14**
Curb	10	0.40	0.75		24	6.48	12.96	12.96	**12.96**
$Ball._{int}$	10	1.30	0.30		19	4.82	9.64	9.64	**9.64**
$Ball._{ext}$	10	0.70	0.30		19	1.4	2.8	2.8	**2.80**
Rail	10	0.5455		3.00		1.64	3.28	3.28	**3.28**
$Ties_{ext,\ out}$	0.85	0.3 0.5	0.234	1.30		0.47	0.94	**1.13**	**1.13**
$Ties_{ext,\ in}$	1.05	0.3 0.5	0.234	1.30		0.72	1.44	1.73	**1.73**
$Ties_{int.\ out}$	0.85	0.3 0.9	0.234	1.30		0.72	1.44	0.96	**0.96**
$Ties_{int.\ in}$	1.05	0.3 0.9	0.234	1.30		0.47	0.94	0.63	**0.63**
									61.27

Table 4-13: Tabular representation of dead load acting on the girder

4.1.5.3.1 Dissecting Table 4-13

Table 4-13 is a consolidated table representing synchronized sections, dimensions, unit weights, material properties, and the calculated forces induced on the girder labelled ① to ⑩.
① is the column representing all the sections at which a possible moment or force can be calculated from.
② represents the length of the member with respect to the asxis of interest. For longgitudinal members, it is the span of the girder. For transverse members like sleepers, it is the effecticve width along the span of the girder.
③ provides the width dimensions perpendicular to the longitudinal axis of the girder for longitudinal members. For the sleepers, w is the effective width divided by the tributry width. Further, for a more detailed calculation, the sleepers are divided into exterior and interior sleepers. The exterior sleepers are those at the edges of the span while the interior sleepers are those in between the exteriors.
④ specifies the thickness t of each member. For the rail, the nonrectangular/irregular shapes cause it to simply be assigned a unit weight per length (in ⑤) as compared to other shapes.
⑤ is a material property associated with elements normally in one dimension or with irregularity. For this calculation, the rail and sleepers are assigned unit weights (Ut. Wt).
⑥ is the weight density of the material. It is used for materials with the three dimensions.
⑦ provides information about the moment each element contributes to the girder. Farther elements, in constant condition, produce higher moment. The moment associated with each element containing properties in ⑥ is calculated from the formula

$$M = wt\boldsymbol{\rho} \qquad \text{Eqn 4-75}$$

Whereas, moment containing properties in ⑤ is calculated from

$$M = 0.5l^2\boldsymbol{\rho} \qquad \text{Eqn 4-76}$$

In ⑧, the moment obgtained from ⑦ is divided by the width of the girder thus causing a theoretical concentrated load at the middle of the girder.
⑨ yields the uniformly distributed load (UDL) along the 1-m design width span, applicable over the entire span of the girder. It is ⑧ divided 1.0 meter.
⑩ is the same as ⑨, indicated for emphasis.

Note: the weight table (Table 4-13) does not contain effects of foundation movements, concrete shrinkage and creep, wearing course and future wearing course.

4.1.5.3.1.1 Special note about sleeper adopted

Usually, sleepers are provided to the structure as a readymade component. They are mostly precast, pre-tensioned components installed to enhance the general performance of the track. Their convenience of application is one of some key factors attributed to their worldwide adaptation into the railway industry. High-speed lines also adopt concrete sleepers for they withstand external pressure appreciable well (due to their effective area). There are several kinds and types of standard sleepers on the market for railway usage. However, certain design parameters and ties characteristics would dictate which one to be suitably adopted. The speed adopted on the line under consideration, dimensions between girders, are factors that necessitated the selection of this German B70 sleeper. Its length fits directly from center-to-center of the girders.

Fig. 4.20 Illustration of railed sleepers

Summary of the dimensions is given below:

height = 234 mm
width = 300 mm
spacing = 600 mm
Length = 2600 mm
A_{eff} = 680000 mm^2 *
Weight = 280 kg

Weight = 350 kg rounded for add-ons like pad, fasteners, stiffeners, clips, etc.
Weight = 3.5 kN
Weight = 1.3 kN/m

* The effective area of the sleeper (A_{eff}) is that beneath the sleeper which makes contact with the ballast. Here, it is not simply the product of the length and base width but with some calibrations due to the indentions along the length of the sleeper. The directory to the sleeper is attached https://www.railone.com/.../downloads/broschueren/en/ConcreteSleepers_2014_EN.pdf.

Parameters	Unit
Permissible axle loads	25 t
Maximum speed	250 km/h
Concrete grade	C 50/60
Concrete volume	114 l
Weight (without fastenings)	280 kg
Length (L)	2600 mm
Width (W)	300 mm
Sleeper height (H)	234 mm
Height of centre of rail base (h_1)	214 mm
Height of sleeper centre (h_2)	175 mm
Support surface (total)	6800 cm^2
Standard application	Main track sleeper

Fig. 4.21 Germany B70 ballasted track sleeper details

4.1.5.3.1.2 Number of sleepers

The number of sleepers is a function of the total span of the girder, the depth of ballast layer, as well as sleeper-to-sleeper spacing. In the basic layout of a conventional ballasted track, sleepers are the primary carrier of the rail. Their distribution is so arranged in that rail deflection at spacing is set to the minimum allowable spacing of the rail. The quantity of sleeper (q_s) is estimated as

$$q_s = \frac{s - 2s_{s_0}}{w_{s_{eff}}} + 1 \qquad \text{Eqn 4-77}$$

From Eqn 4-77,

1. s is the span of the girder,
2. s_{s_0} is half the sleeper spacing (assumed to be the overhanging distance from the beginning of the span to the first sleeper. Same applies for the last sleeper),
3. $w_{s_{eff,i}}$ is the effective sleeper spacing, defined here as the dimension over which the sleeper distributes the applied load.

Where, $w_{s_{eff,i}}$ can be represented as,

$$w_{s_{eff,i}} = 0.5s_s + w_s + 0.5s_s \qquad \text{Eqn 4-78}$$

$w_{s_{eff,i}} = 0.5(600) + 300 + 0.5(600) = 900\ mm = 0.9\ m$

$q_s = \frac{10000-2\left(\frac{600}{2}\right)}{900} + 1 = 10.44 + 1 = 11.44 \approx 12$

The number of interior sleeper (q_{s_i}) is

$$q_{s_i} = q_s - 2 \qquad \text{Eqn 4-79}$$

$q_{s_i} = 12 - 2 = 10$

For the exterior/edge sleepers, the equation becomes

$$w_{s_{eff,e}} = \frac{s - q_{s_i}\left(w_{s_{eff,i}}\right)}{2} \qquad \text{Eqn 4-80}$$

$w_{s_{eff,e}} = \frac{10000\ mm - 10(900\ mm)}{2} = 500\ mm = 0.5\ m$

This implies that a 100-mm space is on each side of the exterior sleeper. And this is so because of the adjustment (up rounding) made in the total adopted number of sleepers.

4.1.5.4 Live load configuration

Here, only the effects of live load is considered on the girder.

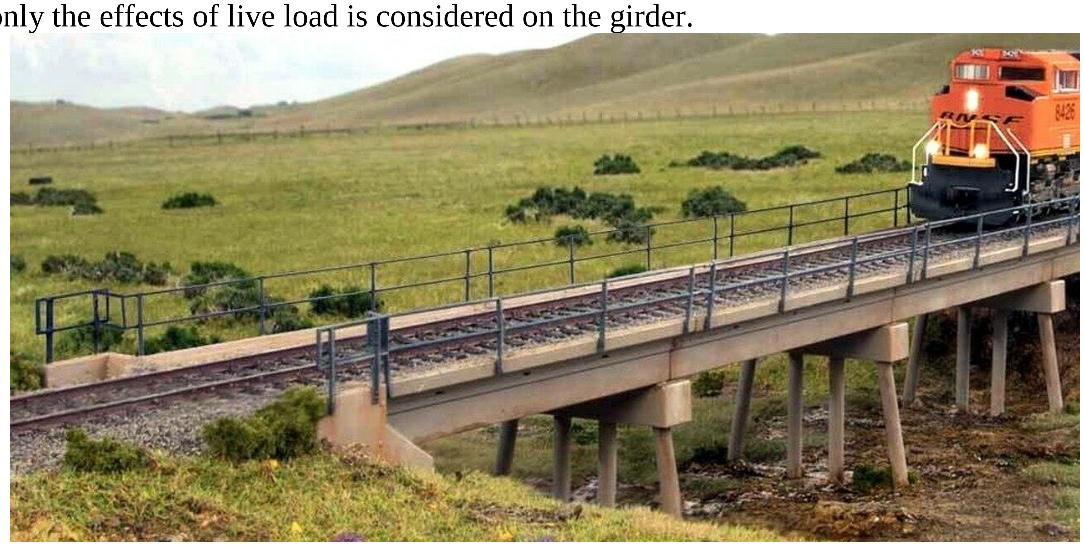

Fig. 4.22 Pictorial view of a being loaded railway bridge

To calculate the rolling stock live load, the maximum moments, shears, and pier (or floor-beam) reactions for Cooper EM 360 live load can be obtained from Figure 8-2-1 (same as Figure 15-1-2) or alternate live load Figure 15-1-3 of [2]. The maximum shall apply.

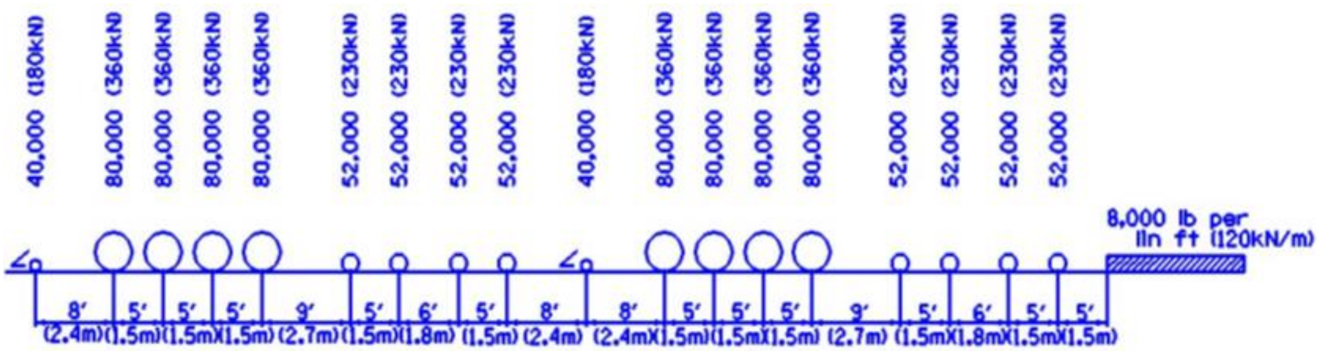

Fig. 4.23: Live Load arrangement of Cooper EM 360 Loading [[2]]

All the primary and secondary live loads calculated in 4.1.4.2.2.1 are applicable hereto but with the only difference in load application format. Here, the concentrated wheel load of 180 kN is changed to the 120 kN/m as indicated in the diagram above (Fig. 4.23).

1. **Live load ……………………………………. 120.0 kN**
2. Impact force …………………………..…….. 48.0 kN
3. Wind Load on structure ……………………..… 2.23 kN
4. Wind Load on Live Load ……………..….… 4.4 kN
5. Longitudinal force ……………………..…..... 18 kN

Total ………….… 192.63 kN/m

4.1.5.4.1 The Non-momented and momented effects

Due to the location arrangement of the applied load, a live load-distance chart/table is formulated to establish a relationship between non-momented and momented effects of the loads. Thus, the reactions, shears, and moment due to live load can then be drawn up.

Category of live load	**Unit Load**		**Moment Effect**		**Concentrated Load**		**Momented live load**
	Longit. (kN/m)	**Trans. (kN/m)**	**Dist. to center of girder (m)**	**Moment at center of girder (kN.m)**	**W_{gir} (m)**	**Point load on girder (kN)**	**Longit. UDL on girder (kN/m)**
❶	❷	❸	❹	❺	❻	❼	❽
Wheel Load	120.00	120.00	0.5455	65.46	0.50	130.92	130.92
Impact Load	48.00	48.00	0.5455	26.18	0.50	52.36	52.36
Wind Load	2.23	2.23	0.900	2.01	0.50	4.02	4.02
Wind load on live load	4.40	4.40	0.5455	2.40	0.50	4.80	4.80
Longitudinal force	18.00	18.00	0.5455	9.82	0.50	19.64	19.64
	192.63						**211.74**

Table 4-14: Tabular representation of live non-momented and momented load acting on the girder

Hence, 211.74 kN/m is Uniformly Distributed Load momented effect on the surface of the girder. However, using this load to design the girder would imply a structural double-dipping. These loads are directly carried by the slab and the loaded slab is then being carried by the girders. Therefore, it's logical to use the non-momented effect of these loads to design the girder.

1. Columns ❶, ❷, ❸, ❹, and ❻ provide the raw data as the name of each column indicates.
2. Column ❸ is the main data against which momented effect is calculated. In this transverse analogy, it is taken as concentrated load because of the adoption of the 1-m width.
3. ❺ is the product of ❸ and ❹. Note that, the rail is longitudinally fastened and so the wheel load as well. This theoretical moment obtained, is acted directly at the middle of the girder.
4. ❼ is the quotient of ❺ by ❻. Dividing the moment by the width of the girder changes the moment to a concentrated load.
5. ❽ again converts the ❼ into a UDL in the longitudinal direction as it is divided by the 1-m strip design width.

4.1.5.4.2 Reactions, shears and moment due to live load

$$R_{LL} = \frac{(192.63\ kN/m)(10\ m)}{2} = 963.15\ kN$$

$$M_{LL} = \frac{\left(192.63\frac{kN}{m}\right)(10\ m)^2}{8} = 2407.88\ kN.m$$

However, a new equation is formulated from the two original equations to obtain a new moment equation once the reaction is already calculated.

$$\begin{cases} R = \dfrac{ws}{2} \\ M = \dfrac{ws^2}{8} \end{cases} \qquad \text{Eqn 4-81}$$

Where

$$s = \frac{2R}{w} \qquad \text{Eqn 4-82}$$

By substituting Eqn 4-82 in Eqn 4-81 for M,

$$M = \frac{w\left(\frac{2R}{w}\right)^2}{8} = \frac{\left(\frac{4R^2}{w}\right)}{8} = \frac{4R^2}{w} * \frac{1}{8} = \frac{R^2}{2w}$$

Thus, the new equation for the moment,

$$M = \frac{R^2}{2w} \qquad \text{Eqn 4-83}$$

$$M = \frac{(963.15\ kN)^2}{2(192.63\frac{kN}{m})} = 2407.875\ \approx 2407.88\ kN.m \dots\dots\dots\dots\dots\dots\dots ok$$

From the above procedures, a Reaction-Moment (R-M) iteration table for a UDL on a simply supported short span beam is developed. In said table, coefficients that relate all items are derived. These coefficients are then used as direct multipliers to obtain the next desired quantity. The key controlling item in the table is the Dead-Load-to-Live-Load-ratio ($\aleph_w$). From background comparisons done, the range works perfectly between 1 and 100%.

$$(\aleph_w) = \frac{DL}{LL} \qquad \text{Eqn 4-84}$$

The R-M table adopted here is for a 32% $\aleph_w$which is that for the dead and live loads used in this design. The columns in the table are obtained as follow:
② is the reaction
③ equals ②
④ is the maximum moment
⑤ is the reactions of ② divided by the respective values of ② as demonstarted below:

a. Cells ⑤❶, ⑤❷, and ⑤❸ respectively, equal ②❶ divided ②❶, ②❷, and ②❸ respectively.

$$\aleph_{⑤❶} = \frac{⑤❶}{⑤❶, ⑤❷, ⑤❸}$$ Eqn 4-85

…and said pattern also applies to columns ⑥ and ⑦ but making ②❷ and ②❸ numerator respectively. The procedure contained above is repeated in similar fashions for columns ⑥ to ⑦, columns ⑧ to ⑩, columns ⑪ to ⑬, and columns ⑭ to ⑯. The procedure in Table 4-15 and Table 4-16 forms a 3 x 3 square matrix.

Reaction-Moment iteration table																
Column reference	DL = 61.27 kN/m							LL = 192.63 kN/m					s = 10 m			
	$\aleph_w$ = 0.32															
	Loading category	React.	shear	Moment	Reaction to Reaction			Reaction to Moment			Moment to Reaction			Moment to Moment		
					② ❶ to ②	② ❷ to ②	② ❸ to ②	② ❶ to ④	② ❷ to ④	② ❸ to ④	④ ❶ to ②	④ ❷ to ②	④ ❸ to ②	④ ❶ to ④	④ ❷ to ④	④ ❸ to ④
	①	②	③	④	⑤	⑥	⑦	⑧	⑨	⑩	⑪	⑫	⑬	⑭	⑮	⑯
❶	DL	306.35	306.35	765.88	1.00	3.14	4.14	0.40	1.26	1.66	2.50	7.86	10.36	1.00	3.14	4.14
❷	LL	963.15	963.15	2407.88	0.32	1.00	1.32	0.13	0.40	0.53	0.80	2.50	3.30	0.32	1.00	1.32
❸	DL + LL	1269.50	1269.50	3173.75	0.24	0.76	1.00	0.10	0.30	0.40	0.60	1.90	2.50	0.24	0.76	1.00

Table 4-15: Reaction-Moment iteration table for a 32%-DL/LL ratio and a 10-m span

Reaction-Moment iteration table																
Column reference	DL = 31.81 kN/m							LL = 100.00 kN/m					s = 10 m			
	$\aleph_w$ = 0.32															
	Loading category	React.	shear	Moment	Reaction to Reaction			Reaction to Moment			Moment to Reaction			Moment to Moment		
					② ❶ to ②	② ❷ to ②	② ❸ to ②	② ❶ to ④	② ❷ to ④	② ❸ to ④	④ ❶ to ②	④ ❷ to ②	④ ❸ to ②	④ ❶ to ④	④ ❷ to ④	④ ❸ to ④
	①	②	③	④	⑤	⑥	⑦	⑧	⑨	⑩	⑪	⑫	⑬	⑭	⑮	⑯
❶	DL	159.05	159.05	397.63	1.00	3.14	4.14	0.40	1.26	1.66	2.50	7.86	10.36	1.00	3.14	4.14
❷	LL	500.00	500.00	1250	0.32	1.00	1.32	0.13	0.40	0.53	0.80	2.50	3.30	0.32	1.00	1.32
❸	DL + LL	659.05	659.05	1647.63	0.24	0.76	1.00	0.10	0.30	0.40	0.60	1.90	2.50	0.24	0.76	1.00

Table 4-16: Reaction-Moment iteration table for a 32% DL/LL ratio (reduced load) and the same 10-m span

4.1.5.5 Total Design Moment

The total design moment accounts for the sum of both dead and live load moments combined and factored against a coefficient and a strength reduction factor. The procedure is same 4.1.4.2.3.6.1.
$M_{sd} = \emptyset[1.4(M_{DL} + M_{LL})] = 3998940\ N.m$

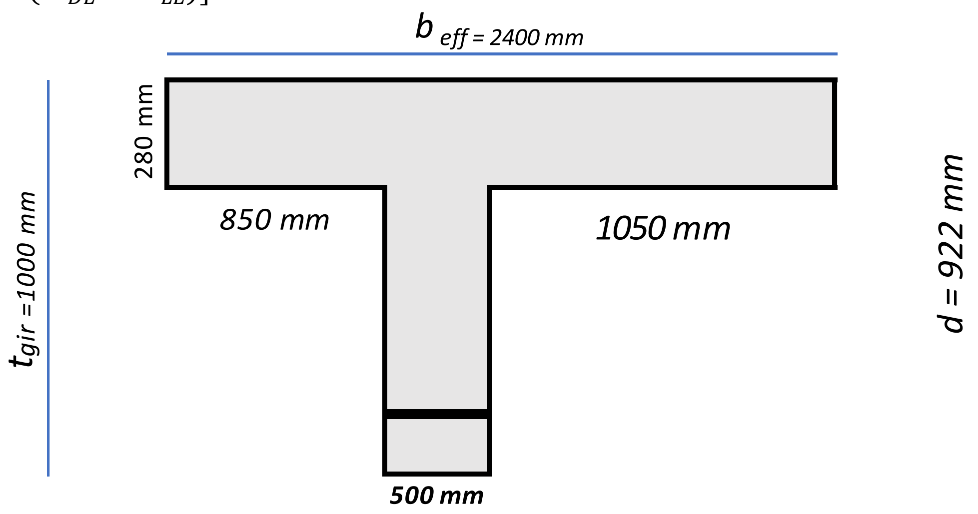

Fig. 4.24: Effective dimensions of the flanged section

4.1.5.6 Effective depth, d

The stirrups used on the main reinforcement conforms to 8-2.11.2b(1) of [2]. Thus, it is safe to adopt #12 bar as ties and the cover requirement conforms to [2] Table 8-2-7.

Longitudinal (main) Bar dia.	=	32.5 mm
Concrete cover	=	50 mm
Ties	=	12 mm
Main bars spacing	=	32.5 mm (minimum permissible spacing)

$$d = t_{gir} - (cc + \phi_s + 0.5\phi_d) \qquad \text{Eqn 4-86}$$

…where ϕ_s is the diameter of the stirrup, and ϕ_d is the diameter of the flexural (main) bar. Thus,
$d = 1000 - (50 + 12.2 + 0.5(32.5)) \approx 0.922\ m$
Now, with the effective depth computed, the adequacy of the reinforcements in the member can be computed.

4.1.5.7 Steel Ratio

$$\rho_0 = \left[1 - \sqrt{1 - \left(\frac{2 * 3998940.0}{0.9 * 0.85 * \left(40 * 10^6\right) * 0.5 * 0.922^2}\right)}\right]\frac{0.85(40 * 10^6)}{420 * 10^6} = 0.031 = 3.1\%$$

$$\rho_{min} = 0.04\frac{f_c'}{f_y} = 0.04\frac{40}{420} = 0.0038$$

$$\rho_0 > \rho_{min}\ therefore\ adopt\ \rho_0$$

4.1.5.8 Balanced steel ratio

The balanced steel ratio is the ratio of steel necessary to cause the section fail in tension, that is for the failure to occur as the concrete starts to crush.

$$\rho_b = \left(\frac{0.85\beta_1 f_c'}{f_y}\right)\left(\frac{600}{600 + f_y}\right) \qquad \text{Eqn 4-87}$$

$$\rho_b = \left(\frac{0.85(0.77)(40\ MPa)}{420\ MPa}\right)\left(\frac{600\ MPa}{600\ MPa + 420\ MPa}\right) = 0.037 = 3.7\%$$

With a 3.7% balanced steel ratio, the required steel ratio is 84% of ρ_b. [2] and some previous codes subjected ρ_0 to 75% of ρ_b. However, with improvement in concrete strength, advancement in theories, the penalty is not as strict as earlier versions [3]. Hence, it is applicable.

4.1.5.9 Longitudinal area of steel

$$A_s = 0.031(0.5\ m)(0.922\ m) = 0.014291\frac{m^2}{m}$$

4.1.5.10 Number of Longitudinal bars

With the main bar being a #32, the diameter is 32.5 mm, and the area is 830 mm^2

$$Q_{bar} = \frac{14291\ mm^2}{830\ mm^2} = 17.22 \approx 18$$

4.1.5.10.1 Arrangement of bottom longitudinal bars

To satisfy the spacing requirement, the analysis invokes [16] chapter 25.2 and [2] with the below table. Considering 6 bars laid in the bottom (at the designer's discretion), at most there would be 3 layers of side bars in the tension zone.

Spacing Check for bottom bars									
Sectional properties of this 10-m girder					General Requirements				
					ACI 319-19 Chpt. 25.2			AREMA 8-2.5	
$W_{gir.}$ (mm)	Sc (mm)	$\boldsymbol{\phi_d}$ (mm)	$\boldsymbol{Q_{b_b}}$	void	Min. Req.			Max. Req.	
500	40	32.5	6	5	$\boldsymbol{\phi_d}$	4/3 Agg_{max}	25	$0.5t_{slab}$	450
The spacing is calculated from Eqn 4-88 below					32.5	Agg_{max} = 20	25	0.5(280)	450
					32.5	27	25	140	450

Table 4-17: Spacing parameters table for bottom bars

From the table, s_b is the bottom bar spacing, sc represents width of side cover, Q_{b_b} is quantity of bottom bars. Note, [29] defines coarse aggregate as aggregate ranging from 90 mm to 1.18 mm.

$$s_b = \frac{w_{gir} - (2sc + \phi_d + \phi_s)}{voids} \qquad \text{Eqn 4-88}$$

$$s_b = \frac{500 - (2(40) + 32.5 + 12.2)}{6 - 1} = 40\ mm$$

The spacing conform to all minima and maxima specified by [2] thus indicating design conformity.

4.1.5.10.2 Arrangement of side bars

The spacing requirements for bottom and side bars are practically the same. However, the minimum spacing for side bars as required for by [16] is higher than that for the bottom bars. Bottom bar or side bar, they are all flexural bars but with the only difference being the direction into which their spacing goes. The number of layers of flexural bars, Q_{s_b} can be estimated at

$$Q_{s_b} = \frac{Q_{bar}}{Q_{b_b}} \qquad \text{Eqn 4-89}$$

$$Q_{s_b} = \frac{18}{6} = 3$$

Thus, the full side spacing arrangement parameters table.

Spacing Check for side bars									
Sectional properties of this 10-m girder					**General Requirements**				
					ACI 319-19 Chpt. 25.2			AREMA 8-2.5	
d (mm)	**c (mm)**	**ϕ_d (mm)**	**# of layers**	**void**	**Min. Req.**			**Max. Req.**	
922	100	32.5	3	2	**$1.5\phi_d$**	**4/3 Agg_{max}**	**40**	**$0.5t_{slab}$**	**450**
The spacing is calculated from Eqn 4-90 below					48.75	$Agg_{max} = 20$	40	0.5(280)	450
					≈ 49	27	40	140	450

Table 4-18: Side tension steel spacing requirement table

From Table 4-18, c is the depth of neutral axis. This is a pre-calculated value which shows that all reinforcements are tension reinforcements. For estimating a more accurate spacing, Q_{s_b} is to be half bar less because that is the location of the effective depth under consideration.

$$s_s = \frac{d - (c + Q_{s_b}\phi_d)}{voids} \qquad \text{Eqn 4-90}$$

$$s_s = \frac{922 - (100 + (3 - 0.5)(32.5))}{2} = 370\ mm$$

Eqn 4-90 conforms to the all minima and maxima requirements hence its is satisfactory. However, engineer's judgement has to be employed in adopting the final arrangement considering the outcome from both Table 4-8 and Eqn 4-90. Therefore, these bars can be laid at a 50-mm.

With these adopted conditions, this means that the area of steel is modified (due to the adjustment made in the quantity of steel obtained from section 4.1.5.10) to:

$$A_{sd} = Q_{bar}A_{bar} \qquad \text{Eqn 4-91}$$

$$A_{sd} = 18(830\ mm^2) = 14940\ mm^2 = 0.01494\ m^2$$

Thus, the adjusted steel also become,

$$\rho_{sd} = \frac{A_{sd}}{bd} \qquad \text{Eqn 4-92}$$

$$\rho_{sd} = \frac{0.01494\ mm^2}{(0.5\ m)(0.922\ m)} = 0.0324 \approx 3.2\%$$

Finally, the most suited arrangement is:

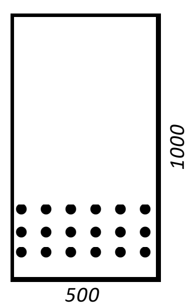

Fig. 4.25: Schematic arrangement of longitudinal bars in the girder

4.1.5.11 Skin Reinforcement

Because skin reinforcement is practically applicable to deep elements, yet it is always structurally sound to be checked for. Put in the bottom half area, it helps in restraining the sides of the element. The basic requirement for skin reinforcement is met as provided in Eqn 4-93.

$$t > 900\ mm \qquad \text{Eqn 4-93}$$

The area of skin reinforcement, A_{sk}, is given in Eqn 4-94 below:

$$A_{sk} = 0.3(d - 750) \qquad \text{Eqn 4-94}$$

$A_{sk} = 0.3(1000 - 750) = 75.0\ mm^2$

$Q_{sk} = \frac{75\ mm^2}{117} = 0.64 \approx 1$

NB: The area of skin reinforcement and the equivalent number of bars are so minute that it might technically be negligible for adoption. The least probable diameter of bar that may be decidedly used for skin reinforce would only require one bar. However, considering the effects of environmental impacts, [26] chapter C.10.6.6, the requirement is more flexible and is reduced to:

$$A_{sk} = 1.0(d - 750) \qquad \text{Eqn 4-95}$$

$A_{sk} = 1.0(1000 - 750) = 250\ mm^2$

$Q_{sk} = \frac{250}{117} = 2.1 \approx 2$

It should be noted that different texts offer somehow slight difference in the formulae involving skin reinforcement. For instance, [3] proposes that for a member to utilize skin reinforcement, its effective depth should be greater than 1000 mm. However, structurally these differences would not likely lead to the omission of (i.e., a difference in) more than two bars at most. Spacing requirement for skin reinforcement [3] shall not exceed the following:

$$s_{max} \ngtr \begin{cases} \frac{d}{6} = \\ 300\ mm \\ \frac{1000A_b}{d - 750} \end{cases} \qquad \text{Eqn 4-96}$$

$$s_{max}\ is\ the\ least\ of \begin{cases} \frac{d}{6} = \frac{922}{6} = 154\ mm \\ 300\ mm \\ \frac{1000A_b}{d - 750} = \frac{1000(117\ mm^2)}{(922 - 750)mm} = 680\ mm \end{cases}$$

Hence, $s_{max} = 154\ mm$ but is technically inactive because the number of skin reinforcement cannot form a layer (because only one bar is on each side). Thus, it can be placed immediately above the last flexural bars since they are spaced at least 50 mm apart.

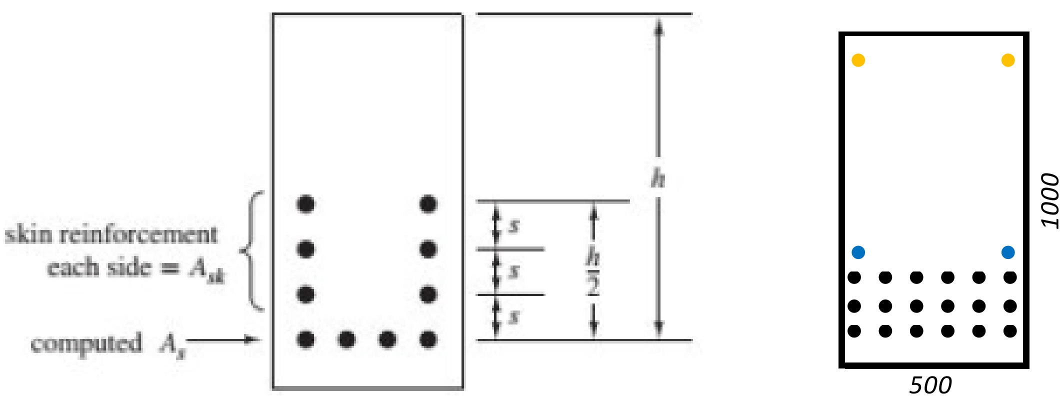

Fig. 4.26: Schematic arrangement of the probable placement of bars obtained as skin reinforcement [(a): general example, (b): specific to this design)

With this, 1 bar is placed in each side face of the girder or may be used as hangers since there is no compression steel on which stirrups may be supported (this latter suggestion is only applicable for field/on-site judgement: blue for use as skin reinforcement, and orange for use as hangers).

4.1.5.12 Verification of the minimum area of steel

Section 9.6.1.2 of [16] requires that the minimum flexural reinforcement shall be the larger of:

$$A_{s_{min}} = \left(\frac{0.25 f_c^{'}}{f_y}\right) b_w d \qquad \text{Eqn 4-97}$$

$$A_{s_{min}} = \left(\frac{1.4 b_w d}{f_y}\right) \qquad \text{Eqn 4-98}$$

From the above equations, b_w is the smaller of:

$$smaller\ of \begin{cases} b_w = b_{eff} \\ b_w = 2b_w \end{cases} \qquad \text{Eqn 4-99}$$

$$smaller\ of \begin{cases} b_w = 2.4\ m \\ b_w = 2(0.5\ m) = 1.0\ m \end{cases}$$

$$1.0\ m < 2.4\ m, thus\ b_w = 1.0\ m$$

Thus,

$$Larger\ of \begin{cases} A_{s_{min}} = \left(\frac{0.25 f_c'}{f_y}\right) b_w d = \left(\frac{0.25(40\ MPa)}{420\ Mpa}\right)(1.0\ m)(0.922\ m) = 3471 \frac{mm^2}{m} \\ A_{s_{min}} = \left(\frac{1.4 b_w d}{f_y}\right) = \left(\frac{1.4(1.0\ m)(0.922\ m)}{420\ MPa}\right) = 3073 \frac{mm^2}{m} \end{cases} A_{s_{min}} = 3471 \frac{mm^2}{m}$$

Since $A_{s_{min}}$ is less than the design area of steel A_{sd}, the section steel requirement is met. Thus, the tensile force, which is also equivalent to the compressive force is

$$T = A_{sd} f_y \qquad \text{Eqn 4-100}$$

$$T = 0.01494\ m^2 \left(420 \frac{MN}{m^2}\right) = 6.275\ MN = 6275\ kN = 6{,}275{,}000\ N$$

4.1.5.13 Neutral Axis

The location of the Neutral Axis (NA) (interchangeably represented as c) depicts whether the member is to be designed as a T- (flanged section) or a rectangular (non-flanged member) member.

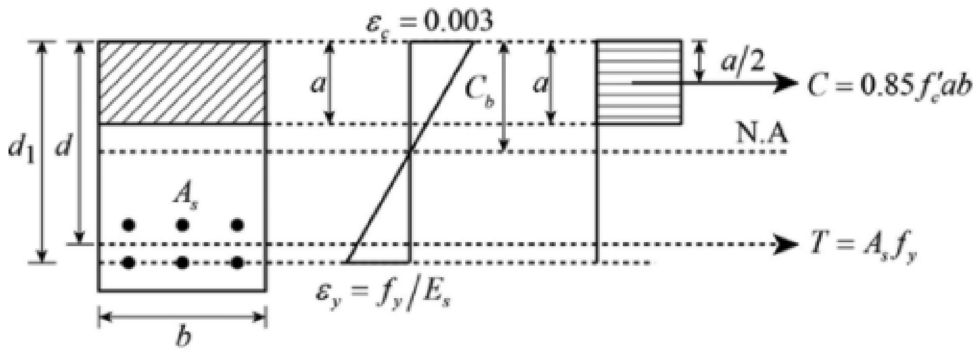

Courtesy: Chegg

Fig. 4.27: Schematic arrangement of the structural properties of a reinforced concrete beam

Technically, every design methodology with constant properties would provide some distinct characteristics about the neutral axis. For instance, for a rectangular section composed of no reinforcement, the neutral axis is at the mid-height. For an uncracked reinforced rectangular section, the neutral axis may be a little deeper, whereas for the cracked elastic version, the neural axis (kd) would somehow be located at a one-fourth distance from the top of the section. Finally, for an inelastic design, the neutral axis would be as low as an eighth. During the determination of the steel ratio of the section (4.1.5.7), the section was subjected to the design criteria of a rectangular section. To prove or disprove this earlier assumption, the area of concrete under compression would indicate where does the compression stress block lie. if it lies in the flange, then it's actually a rectangular member but otherwise, it's a T-section. Yet then still, there are other preconditions that should be considered. In the design of a T-beam, there are three conditions to consider as exemplified in https://limitstatelessons.blogspot.com/ considering the provisions of [30].

1. When the compressive stress block falls within the flange
2. When the compressive stress block equals the flange thickness
3. When the compressive stress block falls within the web

…and the area of concrete (A_c) supposedly in compression is

$$A_c = \frac{T}{0.85 f'_c} \qquad \text{Eqn 4-101}$$

$$A_c = \frac{6.275}{0.85(40)} = 0.184559\ m^2 = 184559\ mm^2$$

The area of concrete contained in the flange and in the web respectively is given as follows:

$$\begin{cases} A_f = b_{eff}(t_f) \\ A_w = b_{eff}(t_{gir} - t_f) \end{cases} \qquad \text{Eqn 4-102}$$

$$\begin{cases} A_f = (2400\ mm)(280\ mm) = 672000\ mm^2 \\ A_w = (500\ mm)(1000\ mm - 280\ mm) = 360000\ mm^2 \end{cases}$$

Comparably, the area of concrete in compression is far less than the area of the compression flange concrete. This means that the stress block is wholly submerged into the flange. The depth of the compression stress block a, which gives a clearer as to where the neutral axis lies is thus given as:

$$a = \frac{A_c}{b_{eff}} \qquad \text{Eqn 4-103}$$

$$a = \frac{184559\ mm^2}{2400\ mm} = 76.897\ mm = 77\ mm$$

The Whitney stress block limits the restraining factor to maximum of 0.85 and a minimum of 0.65.

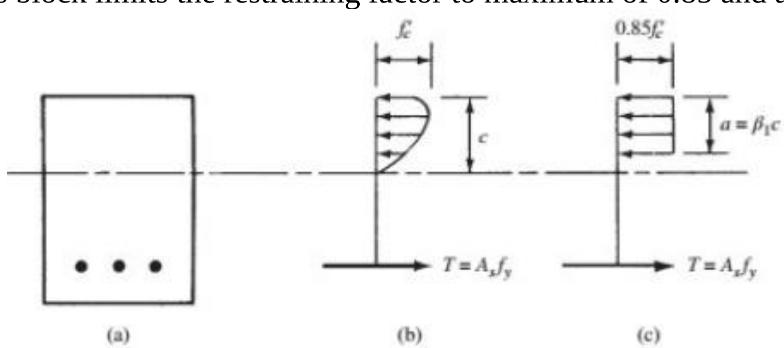

Fig. 4.28: Relationship between neutral axis and depth of stress block using the Whitney theory

$$\beta_1 = 0.85 - 0.008(f'_c - 30) \qquad \text{Eqn 4-104}$$

$$\beta_1 = 0.85 - 0.008(40 - 30) = 0.77$$

This implies that the concrete strength has an inverse relationship on the depth of the neutral axis, meaning, a high strength concrete would only need a comparably little depth of compression stress block. The magnitude of this impact is established from the relationship:

$$\aleph_{\beta_1} = 1 - \frac{\beta_{1_{min}}}{\beta_{1_{max}}} \qquad \text{Eqn 4-105}$$

$$\aleph_{\beta_1} = 1 - \frac{0.65}{0.85} = 1 - 0.76 = 0.24 = 24\%$$

The implication is that the maximum compressive strength that would cause the factor reach the minimum 0.65 would rather reduce the depth of compression stress block by 24% and that such stress is determined from the relationship described below.

$$\beta_1 = \beta_{1_{min}} \qquad \text{Eqn 4-106}$$

$$0.85 - 0.008(f_c' - 30) = 0.65$$

$$f_c' = 55\ MPa$$

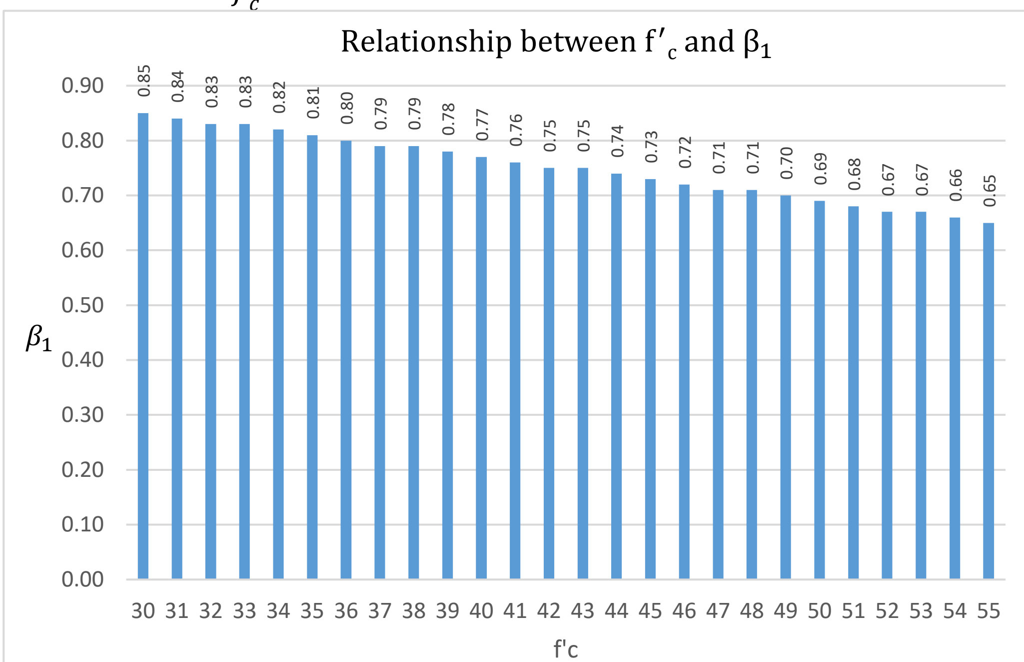

Fig. 4.29: Graphical relationship between compressive strength and β_1

The depth of the neutral axis (c), then becomes

$$c = \frac{a}{\beta_1} \qquad \text{Eqn 4-107}$$

$$c = \frac{a}{\beta_1} = \frac{77\ mm}{0.77} = 100\ mm$$

Since the depth of neutral axis is less than the thickness of the flange (100 mm < 280 mm), the neutral axis falls within the flange of the girder. This implies that the section is to be designed as a rectangular T-Girder rather than a true T-girder.

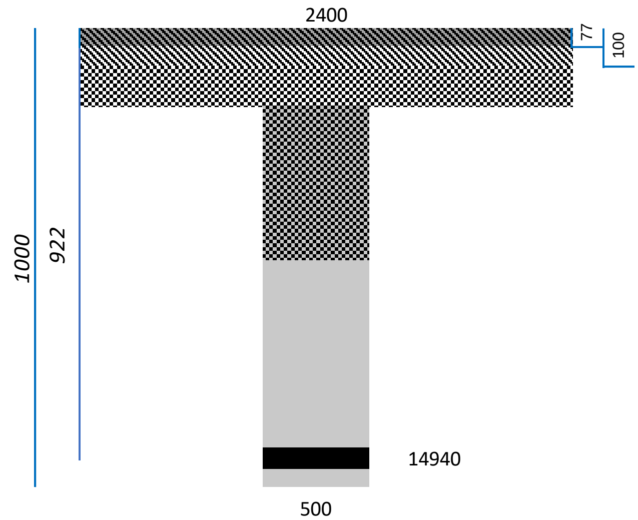

Fig. 4.30: Transverse section through the RC girder

4.1.5.14 Strain compatibility requirement

Strain is associated with movement in a body. Tensile strain (ε_{t_0}) associated with the RC members sets the basis for brittleness or ductility. The steel strain (ε_{ty}) associated with any ASTM 615 steel of Grade 420 is

$$\varepsilon_{ty} = \frac{f_y}{E_s} \qquad \text{Eqn 4-108}$$

$$\varepsilon_{ty} = \frac{420\ MPa}{2x10^5 MPa} = 0.002$$

From *Fig. 4.27*, concrete compressive strain is

$$\varepsilon_{cu} = 0.003 \qquad \text{Eqn 4-109}$$

Steel experiences less strain than concrete. ε_{t_0} does not consider but the scalar quantity only.

$$\varepsilon_{t_0} = \varepsilon_{ty} + \varepsilon_{cu} \qquad \text{Eqn 4-110}$$

$$\varepsilon_{t_0} = 0.002 + 0.003 = 0.005$$

The section's net tensile strain (ε_t) considers $d, c,$ and ε_{cu}. ε_t is then compared with $\varepsilon_{t_0}$to classify the section as brittle or ductile. The appropriate strength reduction factor (∅) for achieving ε_t above ε_{t_0}according to several design codes including [2] and [16]'s Table 21.2.2, etc. put ∅ at 0.9 meaning that the section is tension-controlled [3].

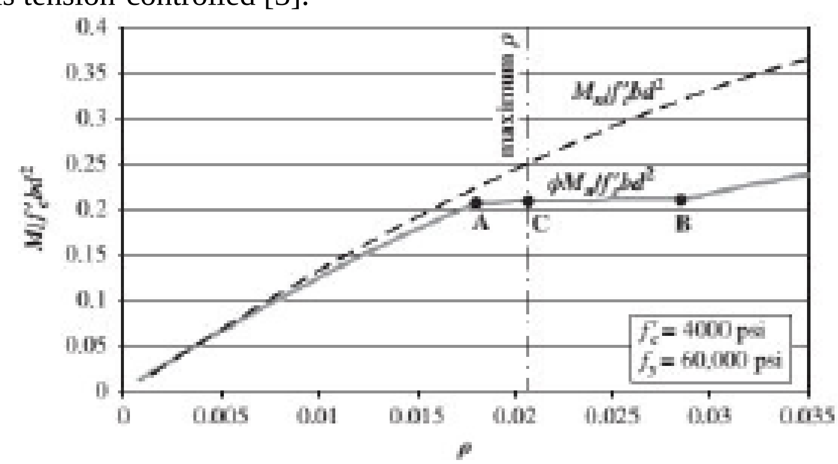

Fig. 4.31:: Moment capacity−ρ diagram

Further, it implies that the net tensile strain is far above that of the 0.003 for concrete. When this condition is met, it represents a brittle condition state of failure of the section: the concrete will well fail before the steel yields. Thus, the Net Tensile strain with respect to the section's dimensional properties can be computed as:

$$\varepsilon_t = \frac{d-c}{c}\varepsilon_{cu} \qquad \text{Eqn 4-111}$$

$$\varepsilon_t = \frac{922-100}{100}0.003 = 0.02466 = 0.025$$

A 0.025 ε_t provides a high leverage of movement in the section before it finally fails. This is due to the high depth of tension stress bock $(d-c)$ associated with the cross-section; and comparably the maximum net tensile strain ratio to that of the concrete is formulated and illustrated below

$$\aleph_{\frac{\varepsilon_t}{cu}} = \frac{\varepsilon_t}{\varepsilon_{cu}} \qquad \text{Eqn 4-112}$$

$$\aleph_{\frac{\varepsilon_t}{cu}} = \frac{0.025}{0.003} = 8.33 \approx 833\%$$

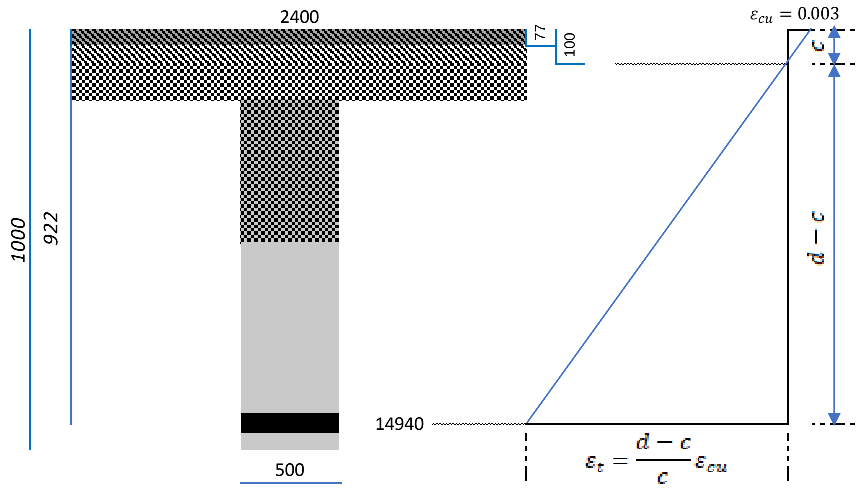

Fig. 4.32: Section and strain diagram

4.1.5.15 Sectional Resistance Capability

A section designed should be able to withstand all probable forces to ensure structural safety. If tension reinforcement alone is not sufficient, the need for compression reinforcement has to be considered and other parameters to consider also include those of [25]. Thus, resisting moment (M_r) capacity is a function of the internal moment arm (z) of the section, and tension which should also equal to compression. With the application of such analogy, the structure is stabilized in sway.

$$z = d - \frac{a}{2} \qquad \text{Eqn 4-113}$$

$$z = 922 - \frac{77}{2} = 883.5 \approx 884\, mm$$

It can be seen that the effective depth is a somewhat independent variable in this procedure [30]. The nominal resisting moment capacity (M_{r_n}) of the web section becomes

$$M_{r_n} = Tz \qquad \text{Eqn 4-114}$$

$$M_{r_n} = Tz = (6.275\, MN)(0.884\, m) = 5.547 \approx 5.55\, MN.m$$

…and thus, the ultimate resisting moment capacity is a function of $\emptyset$ and M_{r_n}.

$$M_{r_u} = \emptyset M_{r_n} \qquad \text{Eqn 4-115}$$

$$M_{ru} = \emptyset M_{rn} = 0.9(5.55) = 4.995\, MN.m = 4995\, kN.m$$

The design moment, the resisting moment, and the cracking moment are three cardinal moments that are needed to be satisfied to obtaining a safe, crack-controlled section. The relationship between the design moment and the resisting moment informs the designer of the mode of failure (immediate or time-dependent) of said section. If the resisting moment capacity of the structure is greater than the design moment by certain margin, the structure is safe. Otherwise, immediate failure is imminent.

$$\text{Is } \mathrm{M_{ru}}(4995\ \mathrm{kN.m}) > \mathrm{M_{sd}}\ (3998.94\ \mathrm{kN.m})?\ \textbf{True}$$

$$\text{Therefore the section can withstand the moment}$$

The Factor of Safety (FOS) for the section thus becomes

$$FOS = \frac{M_{ru}}{M_{sd}} \qquad \text{Eqn 4-116}$$

$$\mathrm{FOS} = \frac{4995}{3998.94} = 1.25 > 1.0 \ldots \mathrm{OK}$$

Otherwise, the extra moment should be structurally considered as a doubly RC member.

$$M_{sd}^{'} = M_{sd} - M_{ru} \qquad \text{Eqn 4-117}$$

$$M_{sd}^{'} = 3998.94\ kN.m - 4995\ kN.m = -996.06\ kN.m < M_{sd} \ldots\ldots OK$$

Thus, the resisting moment capacity verification stops here. Therefore, for longitudinal flexural reinforcement, consider

<u>18–#32 @ 40 Maximum spacing (ADOPTED)</u>

4.2 Preliminary synthesis of crack

Section loss as used in this work is synonymous to deterioration, specifically flexural crack.

When a fully well-designed member (i.e., in the case of reinforced concrete) separates from itself either in a complete or partial fashion, then such instance is what is termed as crack [31]. Structurally, cracks are classified into different forms and their design follow distinct patterns.

4.2.1 Overview of Cracks

In structural analysis and design, cracks is one of the most unpredictable structural failures a section/member faces. Mostly, in structural design crack-control reinforcement in the form of shrinkage, temperature, and skin reinforcements are accounted for yet cracks develop later. For substructures, settlement is also considered. Some of these are merely craze cracks (nonstructural, or cosmetic, etc.). Quality Control Engineers (QCE), Infrastructural Assessment Engineers (IAE) should adequately distinguish between these cracks to avoid misinformation about the structural adequacy of the section/member as well as misrepresentation.

4.2.2 Types of cracks

In occurrence, cracks may be complete or incomplete. Complete cracks will normally put the member in a failure mode meaning that the section no longer connects. An incompletely cracked section is still offered some level of resistance by the concrete. Relative to the load producing the crack, the location of crack on the member and the pattern of crack formation, [3], [32] cracks may be classified into flexural, inclined, splitting, bonding, torsional cracks, etc.

4.2.2.1 Flexural Cracks

In flexural members like beams, cracks patterned from the soffit of the beam towards the neutral axis and then to the top are the characteristics of the flexural cracks. These cracks are notably present around the middle of the span, thus increasing the deflection in the member, increasing the stress on the remaining intact member area, etc.

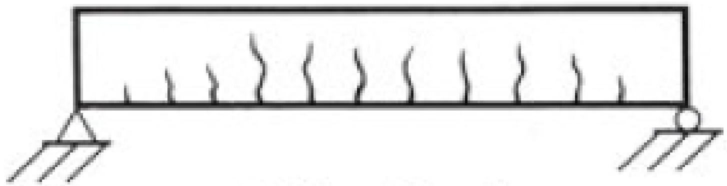

Fig. 4.33: General outlook (non-strategic) view of flexural cracks on a simply supported reinforced concrete beam

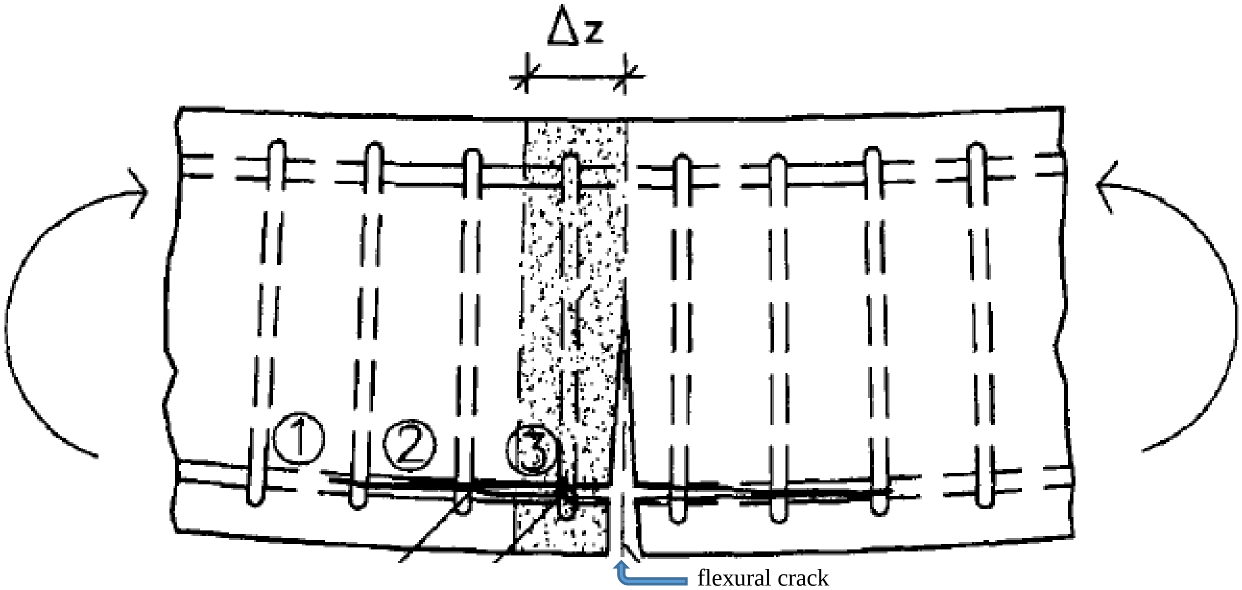

Fig. 4.34: Strategic (closer) view of flexural cracks on beam [32]

Flexural cracks may also result from hogging: an upward deflection. When a structural member contains cantilevered end(s) or upward loads applied between the supports, such types of deflection and cracks (i.e., hogging) occur.

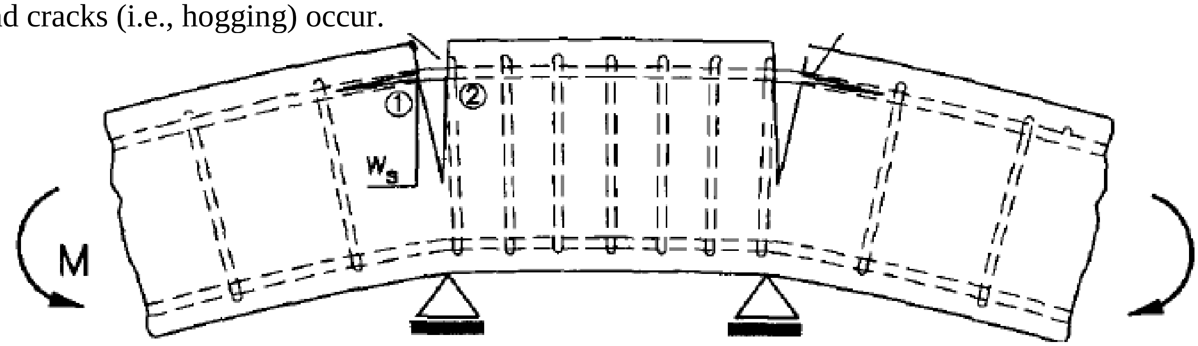

Fig. 4.35: Flexural cracks caused from hogging on member

4.2.2.2 Inclined Cracks

Web-shear cracks and flexure-shear cracks are the two most predominant inclined shear cracks in a flexural member. Shear force along the member is the primary load effect that is considered when designing for shear cracks. However, it is not the design shear (V_{sd}). Design shear requires subjecting the maximum shear to a strength reduction factor.

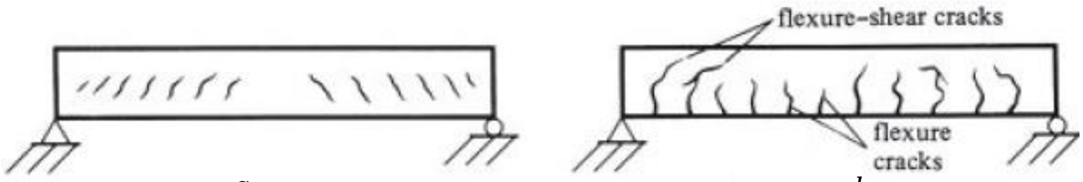

Fig. 4.36: Inclined cracks: [a: web-shear cracks, b: flexure-shear crack].

Web-shear independently develop from within the web usually around the area of negative moment towards mid-span. On the other hand, flexure-shear cracks combine those of flexure and web-shear and may reach as far as the compression zone. With such patterns, flexure-shear cracks pose severe danger to the performance of the section than that of the web-shear.

4.2.2.3 Splitting Cracks

Anchorages and splices give a great deal of rise to the formation of splitting cracks in the vicinity of flexural cracks [32]. The effects of radial pressure that reinforcement bars experience also contribute to the formation of splitting cracks.

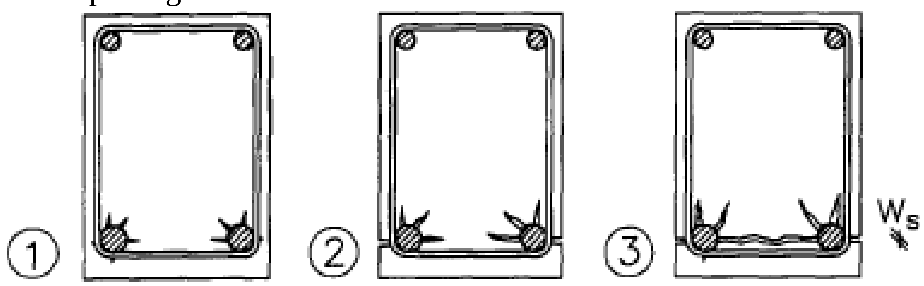

Fig. 4.37: Stages of formation of splitting cracks.

The formation trend of Fig. 4.37 shows that bottom stirrup-enclosed flexural bars start to build up the radial pressure within the confines of the stirrups and the splitting crack is exposed on the side surfaces of each side cover parallel to the longitudinal axis of the span. During this period, the radial pressure build-up rapidly expands in all directions and then finally intersect above the stirrup. At the completion of this stage, the structural defect is spalling. Spalling then accelerates corrosion related defects including rebar diameter reduction and structural concrete weakening.

4.2.2.4 Bonding Cracks

Bonds build up pressure at the bonding periphery. These cracks start to occur when tension is applied (especially on the reinforcing bar). Bond cracks are somehow similar to splitting cracks.

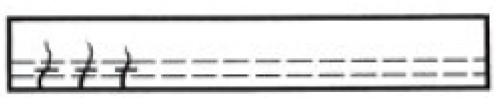

Fig. 4.38: Illustration of bond cracks

4.2.2.5 Torsional Cracks

Generally, when a member is subjected to twisting, torsion is applied. Torsional force and moment take effect across the entire volume of the member by means of a complete spiral.

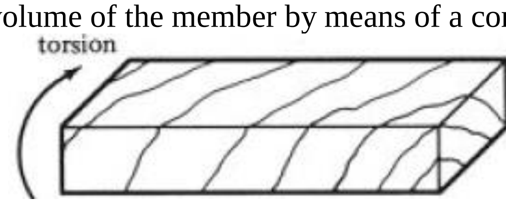

Fig. 4.39: Illustration of torsional cracks

4.2.3 Design for Inclined (shear) cracks

The design for shear basically considers the capacity and arrangement of stirrups to adequately resist shear force. Thus, the reactive force (which has been considered the maximum shear because of its high magnitude) due to the dead load and live load is computed as in section 4.1.5.4.2 as well. Thus,

$$V_{DL} = 306.35\ kN$$
$$V_{LL} = 963.15\ kN$$

…and ultimate shear capacity magnifies the combined shear to:

$$V_u = 1.4(V_{DL} + V_{LL}) \qquad \text{Eqn 4-118}$$

$V_u = 1.4(306.35\ kN + 963.15\ KN) = 1777.30\ kN$

Thus, for shear analysis, using the strength reduction factor of 0.85 in accordance with [2] chapter 8-2.30.2b, the combined shear (Dead + live) yields the following design shear (V_{sd}):

$$V_{sd} = \emptyset V_u \qquad \text{Eqn 4-119}$$

$V_{sd} = 0.85(1777.30\ kN) = 1510.71\ kN$

$1510.71\ kN$ is the shear that is going to be used to design for shear cracks. The procedure above can be structurally represented as outlined and factored by [2]'s 2.29.1b.

$$w_{sd} = 1.4\emptyset(w_{DL} + w_{LL}) \qquad \text{Eqn 4-120}$$

$$w_{sd} = 1.4(0.85)(61.27\frac{kN}{m} + 192.63\frac{kN}{m}) = 302.14\frac{kN}{m}$$

$$R_{sd} = \frac{302.14(10)}{2} = 1510.70\ kN$$

$$M_{sd} = \frac{302.14(10)^2}{8} = 3776.75\ kN.m$$

4.2.3.1 Critical shear

Critical shear is the difference between ultimate maximum shear and shear at a distance equal to the depth of the member. The rule has exceptions [16] if concentrated load(s) is/are placed in the vicinity of the distance under consideration. For a simply supported UDL beam, support shear/reaction gives a fair idea about the length over which the ties can be effectively placed. In this case, the critical shear can be used to design the shear reinforcement.

$$R - w_u d = V_{cri} \qquad \text{Eqn 4-121}$$

$$V_{cri} = 1777.30\ kN - 355.46\frac{kN}{m}(0.922\ m) = 1449.56\ kN$$

When the critical shear is greater than 50% of the section concrete capacity, shear reinforcement must be provided for. The concrete capacity for the section from which the 50% can be obtained is tabulated in Table 4-20.

$$V_{sd} = 1510.71\ kN$$

4.2.3.2 Shear stress

In engineering, stress is always associated with area. Several limiting values of shear stress unto which a section is subjected as contained in section 4.1.4.2.3.8.2.1 are contained herein. When does the design shear force require a design for shear reinforcement? If it is less than what the concrete can safely carry, then there is no need to design for shear. Otherwise, shear reinforcement design is mandatory. The permissible concrete shear stress (v_c) to be used as required by [2] chapter 8-2.35.2 include:

$$v_c = 0.17\sqrt{f_c^{'}}$$

The compressive strength of concrete being 40 MPa. Thus,

$v_{c_1} = 0.17\sqrt{40} = 1.075\ MPa = 1075\ kPa$

In lieu of both the effects of shear and flexure occurring simultaneously in the girder, v_c, referencing [2]'s 8-2.35.2b., is limited to…

$$v_c = 0.16\sqrt{f_c^{'}} + 17\rho_w\left(\frac{V_u d}{M_u}\right)$$

$v_{c_2} = 0.16\sqrt{40} + 17\left(\frac{0.01494}{(0.5)(0.922)}\right)\left(\frac{1.51071(0.922)}{3.99894}\right) = 1204\ kPa = 1.204\ MPa$

With this limitation, the code also requires that $V_u d/M_u$ shall not exceed 1.0. Hence,

$\frac{V_u d}{M_u} = \frac{1.51071(0.922)}{3.99894} = 0.35 < 1.0 \ldots.OK$

Yet, the code also permits the maximum permissible value of v_c at:

$v_{c_3} = 0.29\sqrt{f_c^{'}} = 0.29\sqrt{40} = 1.834\ MPa = 1834\ kPa$

In summary, the shear stresses are indicated below:

$\boldsymbol{v_{c_1} = 1075\ kPa}$

$\boldsymbol{v_{c_3} = 1204\ kPa}$

$\boldsymbol{v_{c_3} = 1834\ kPa}$

In furtherance of the requirements, the maximum permissible shear stress value carried by the ties/stirrups (v_s) is set at:

$$v_s = 0.33\sqrt{f_c^{'}}$$

$v_s = 0.33\sqrt{40} = 2.087\ MPa = 2087\ kPa$

The three requirements listed above set a basis from where the design shear can be compared. Hence, the nominal stress carried by both concrete and steel accounting for the condition of both flexure and shear is:

$$v_n = v_c + v_s \qquad \text{Eqn 4-122}$$

Here, assumptions are made concerning which of the above limiting stress should the design be subjected to. In engineering judgement, it is always necessary to leave room for safety and uncertainty. In this case it's logically appropriate to assume that the stress that this section can ably carry is the least amongst the rest. Thus, adopt $v_c = v_{c_1}$ for now. Henceforth,

$v_n = v_c + v_s = 1075 + 2087 = 3162\ kPa = 3.162\ MPa$

This means we are subjecting the section to the least stress that it can safely carry.

The ultimate shear capacity of this section is then

$v_u = \emptyset v_n = 0.85(3.162) = 2687.7\ kPa = 2.688\ MPa$

With these limitations given, notwithstanding the average shearing stress (design stress) of this girder is computed from [2] chapter 8-2.30.2b for the adoption of the required strength reduction factor and 8-2.35.1a. for the selection of the most appropriate equation.

$$v_u = \frac{V_{sd}}{\emptyset b_w d} \qquad \text{Eqn 4-123}$$

$v_{u_a} = \frac{1.51071}{0.85(0.5)(0.922)} = 3855.33\ kPa = 3.86\ MPa$

Note:

1. v_{ua} is greater than all the permissible shearing stresses

$$v_{ua} = 3860 > (v_{c_3} = 1834) > (v_{c_2} = 1204) > (v_{c_1} = 1075)$$

2. Even the critical shear is greater than the shears of Table 4-20.

Thus, the design for shear reinforcement is imminent. Thus, the nominal shear stress:

$$v_n = \frac{v_u}{\emptyset} \qquad \text{Eqn 4-124}$$

$$v_{n_a} = \frac{v_{ua}}{\emptyset} = \frac{3.86\ MPa}{0.85} = 4.541\ MPa$$

Hence, the nominal average shear stress carried by the ties becomes:

$$v_{s_a} = \frac{v_{ua} - \emptyset v_{c1}}{\emptyset} \qquad \text{Eqn 4-125}$$

$$v_{s_a} = \frac{v_{ua} - \emptyset v_{c1}}{\emptyset} = \frac{3.86\ MPa - 0.85(1.075\ MPa)}{0.85} = 3.47\ MPa$$

The following table summarizes all shear stresses calculated above.

Permissible and actual shear stresses for each equation (MPa)					
Shear stress category		v_c	v_s	v_n	v_u
Permissible	v_{c_1}	1.075	2.087	3.16	2.686
	v_{c_2}	1.196	2.087	3.29	2.7965
	v_{c_3}	1.834	2.087	3.92	3.3320
Actual		1.07500	3.466	4.54	3.86
		1.19600	3.337	4.54	3.86
		1.83400	2.707	4.54	3.86

Table 4-19: Shear stress arrangement table

Table 4-19 is formulated by first categorizing the shear stresses into permissible and actual (i.e., applied). From this arrangement, all the possible shear stresses that need to be calculated are columned as v_c, v_s, v_n, and v_u and corresponding stresses are rowed thereof. The chart is computed as follows:

1. For permissible stresses
   a. All v_c are entered as they are calculated from the limiting conditions
   b. Unlike v_c which has several permissibles, v_s has only one permissible condition which in turn cuts across all v_c
   c. v_n is the sum of v_c and v_s (see Eqn 4-122)
   d. v_u is the product of the strength reduction factor and v_n (see Eqn 4-124 rearranged)

2. There is a little difference with the case of the actual shear
   a. $v_c$is entered just as above
   b. $v_u$is constant for all rows because it was subjected to the cross-section of the member at the location under consideration (see Eqn 4-123).
   c. $v_n$is also constant for it is dependent on v_u and the strength reduction factor. Thus, everything must now be borne by the stirrups
   d. v_s is calculated from Eqn 4-125

The corresponding shear strength to each shear stress tabulated above can be configured from [2] 8-2.35. The general equation yielding each shear strength associated with each stress is presented as follows:

$$V = \emptyset v b_w d \qquad \text{Eqn 4-126}$$

Permissible and actual shear strength for each from Table 4-19 (MN)					
	b = 0.5 m		**d = 0.922 m**		**∅ = 0.85**
Shear strength category		v_c	v_s	v_n	v_u
Permissible	v_{c1}	0.496	0.961	1.457	0.571
	v_{c2}	0.555	0.962	1.517	0.594
	v_{c3}	0.845	0.962	1.807	0.708
Actual		0.496	1.597	2.093	1.513
		0.555	1.538	2.093	1.513
		0.845	1.248	2.093	1.513

Table 4-20: Section minimum shear strength arrangement table

In this context, the design that accounts for shear reinforcement particularly deals with the properties of bar used and the required spacing. As an emphasis, shear reinforcement helps to reduce the length of (diagonal) crack in a beam. However, the mode of placement of these stirrups also plays a very important role in further serving its intended purpose. When nonflexural reinforcement bars are used as stirrups, they could be placed either vertically or inclined. Here, the shears are designed with reference to [2] chapters 8-2.10.3, 8-2.35.3 etc. Adopting #12 bars as stirrups/ties, [2] 8-2.10.3 requires that "Where shear reinforcement is required and is placed perpendicular to axis of member, it shall be spaced not further apart than 0.50d, but not more than 24 inches (600 mm)…". Mathematically interpreting the expression with respect to this section,

$$S \leq 0.5d \leq S_{max} \qquad \text{Eqn 4-127}$$

$S \leq 0.5(0.922\, m) \leq 600\, mm$

$$S \leq 461\, mm \leq 600\, mm \ldots\ldots OK$$

4.2.3.2.1 Mode of stirrup Placement

There are two modes of stirrup placement adopted herein.

4.2.3.2.1.1 Vertical placement (perpendicular to the flexural reinforcement)

The spacing requirement is solely dependent on the diameter of stirrup/ties adopted with an additional dependence on the shape of the stirrup. Thus, the vertical area of a U–shape stirrup reinforcement (A_{vp}) can be represented as:

$$A_{vp} = \frac{(v_u - v_c) b_w s}{f_y} \qquad \text{Eqn 4-128}$$

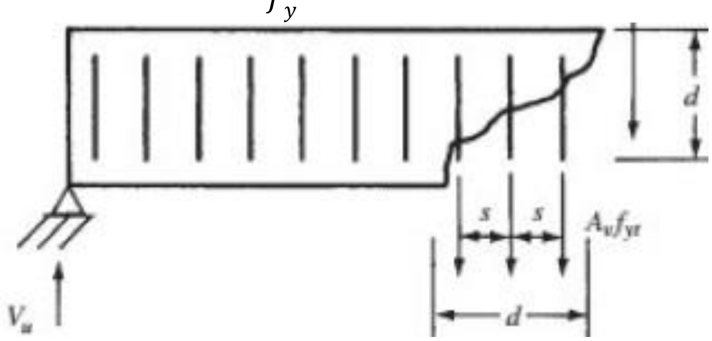

courtesy: [3]

Fig. 4.40: Illustration of the relationship between vertical stirrups, d, A_v, f_y and s

Because it is perpendicularly placed, the area can be calculated as indicated.

$$A_{vp} = 2A_b \qquad \text{Eqn 4-129}$$

$A_{vp} = 2(117\ mm^2) = 234\ mm^2$

Hence, rearranging the equation, the required spacing and the number of perpendicular stirrups that can be obtained are as follows:

$$s_p = \frac{A_v f_y}{(v_u - v_c)b_w} \qquad \text{Eqn 4-130}$$

For validation of the assumptions made earlier concerning which stress shall be adopted, all the stresses are considered and the case that produces the least spacing shall prevail.

$$Q_{ties} = \frac{d}{s_v} \qquad \text{Eqn 4-131}$$

4.2.3.2.1.1.1 Considering v_{c_1}

$$s_{vc_1} = \frac{0.000234(420)}{(3.86 - 1.075)0.5} = 71 \approx 70\ mm$$

$$Q_{tie} = \frac{d}{s_{vc1}} = \frac{922}{70} = 12.3 = 12$$

4.2.3.2.1.1.2 Considering v_{c_2}

$$s_{vc_2} = \frac{0.000234(420)}{(3.86 - 1.204)0.5} = 74 \approx 75\ mm$$

$$Q_{tie} = \frac{d}{s_{vc2}} = \frac{922}{75} = 12.2 \approx 12$$

4.2.3.2.1.1.3 Considering v_{c_2}

$$s_{vc_3} = \frac{0.000234(420)}{(3.86 - 1.834)0.5} = 97 \approx 100\ mm$$

$$Q_{tie} = \frac{d}{s_{vc3}} = \frac{922}{100} = 9.22 \approx 9$$

All the spacings satisfy the spacing requirement of Eqn 4-127 and the minimum area of shear reinforcement [2] 8-2.10.1b required. An expression which further validates all of the above is

$$A_{vmin} = \frac{0.42 b_w S}{f_y} \qquad \text{Eqn 4-132}$$

$$A_{vmin} = \frac{0.42(500)(70)}{420} = 35\ mm^2$$

Minimum area of shear reinforcement, like any other minimum value, are set as regulatory values for which a section must satisfy in order to meet structural integrity regulations.

$$\text{Thus, for vertical stirrups, adopt \#12 ties @ 75 mm}$$

NB: The distance from mid-span (which technically implies zero shear because of the UDL loading condition) to point along the span where stirrups would technically not be required (s'_d) (i.e., at $0.5V_c$), is obtained from the expression

$$s'_d = \frac{0.5V_c}{w_u} \qquad \text{Eqn } \textit{4-133}$$

$$s'_d = \frac{0.5(496\ kN)}{355.46 \frac{kN}{m}} = 0.7\ m$$

Now, the distance from the face of the support to s'_d (s_d) is

$$s_d = 0.5s - s'_d \quad \text{Eqn } 4\text{-}134$$

$s_d = 0.5(10\ m) - 0.7m = 4.3\ m$

Theoretically, during the installation of stirrups, s'_d is not required to be stirrupped. However, field work (practical) would always have it covered up in full to allow for rigidity in the flexural bars [32]. Thus, the adopted spacing runs over the entire 10-m span of the girder.

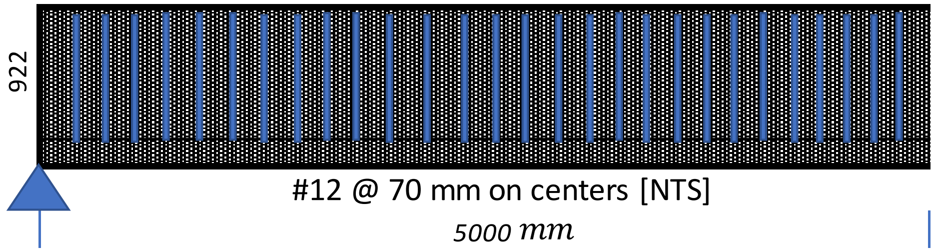

Fig. 4.41: Placement of vertical stirrups through to mid-span of the girder.

NB: Assuming a double-U stirrup, the bar area would double thus meaning that the spacing would proportionately increase whereas the number of bars would proportionately decrease.

Relatively, the mode of placing the stirrups vertically can also be explained by adopting the truss analogy. In this design, though it is structurally needless for a compression steel, shear reinforcement has to be anchored (as proposed in Section 4.1.5.11 Skin Reinforcement). Hence the truss analogy works ideally in this instance as well wherein it is assumed that because of the placement of the stirrups, an initiated crack causes the in-tight concrete to provide the needed resistance at an approximate shearing angle of 45°.

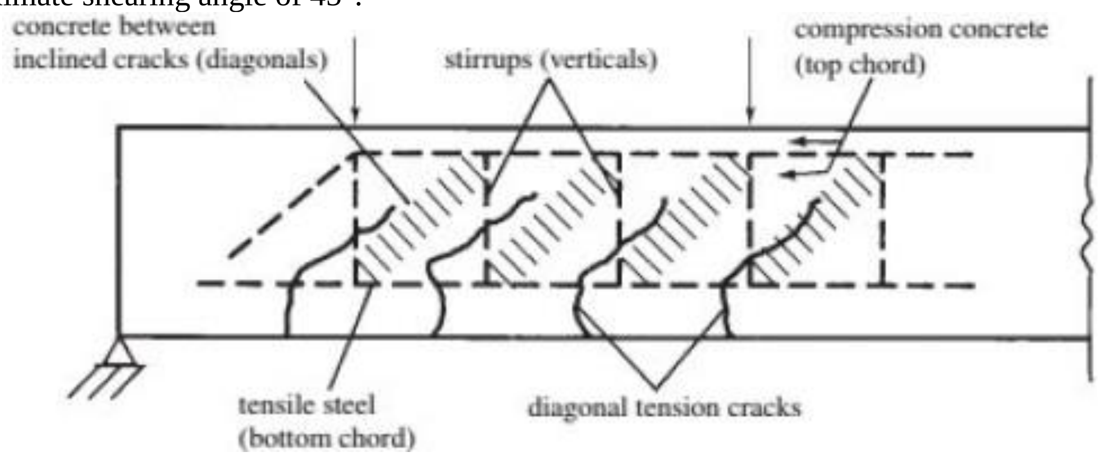

courtesy: [3]

Fig. 4.42: Illustration of the truss analogy

4.2.3.2.1.2 Diagonal placement (diagonal/angular to the flexural reinforcement)

Unlike the vertical placement, diagonal placement involves angular consideration but with all other parameters and procedures remaining the same. Normally, because of the truss analogy, the 45° is practically adopted in calculating diagonal reinforcement.

$$A_{vd} = \frac{(v_u - v_c)b_w s}{f_y(sin\alpha + cos\alpha)} \quad \text{Eqn 4-135}$$

The expression for the diagonal area of stirrups can then be rewritten as

$$A_{vd} = A_p(sin45° + cos45°) \quad \text{Eqn 4-136}$$

$A_{vd} = 234(sin45° + cos45°) = 331\ mm^2$

Hence, the various spacings and quantities.

4.2.3.2.1.2.1 Considering v_{c_1}

$$s_{vc1} = \frac{0.000331(420)}{(3.86 - 1.075)0.5} = 0.072\ m = 72\ \approx 70mm$$

$$Q_{tie} = \frac{d}{s_{vc1}} = \frac{922}{70} = 13.2 = 13$$

4.2.3.2.1.2.2 Considering v_{c_2}

$$s_{vc2} = \frac{0.000331(420)}{(3.86 - 1.204)0.5} = 0.105\ m = 105\ mm$$

$$Q_{tie} = \frac{d}{s_{vc2}} = \frac{922}{105} = 8.8 \approx 9$$

4.2.3.2.1.2.3 Considering v_{c_2}

$$s_{vc3} = \frac{0.000331(420)}{(3.86 - 1.834)0.5} = 0.137\ m \approx 140\ mm$$

$$Q_{tie} = \frac{d}{s_{vc3}} = \frac{922}{140} = 6.6 \approx 7$$

With the same minimum spacing, therefore A_{vmin} is the same that of Eqn 4-132 and the arrangement is as follows:

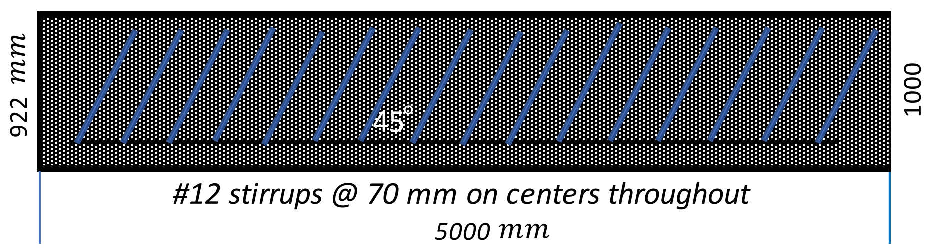

Fig. 4.43: Placement of diagonal stirrups through to mid-span of the girder.

Fig. 4.44 is the complete half-figure representing the total layout of the girder, the imposed load, all symmetrical shears, and their various distance away from the support over which reinforcement is required. The green 0.7-m distance is the distance which may not require stirrup reinforcement. However, the design covers it up with reinforcement for flexural rigidity and additional safety.

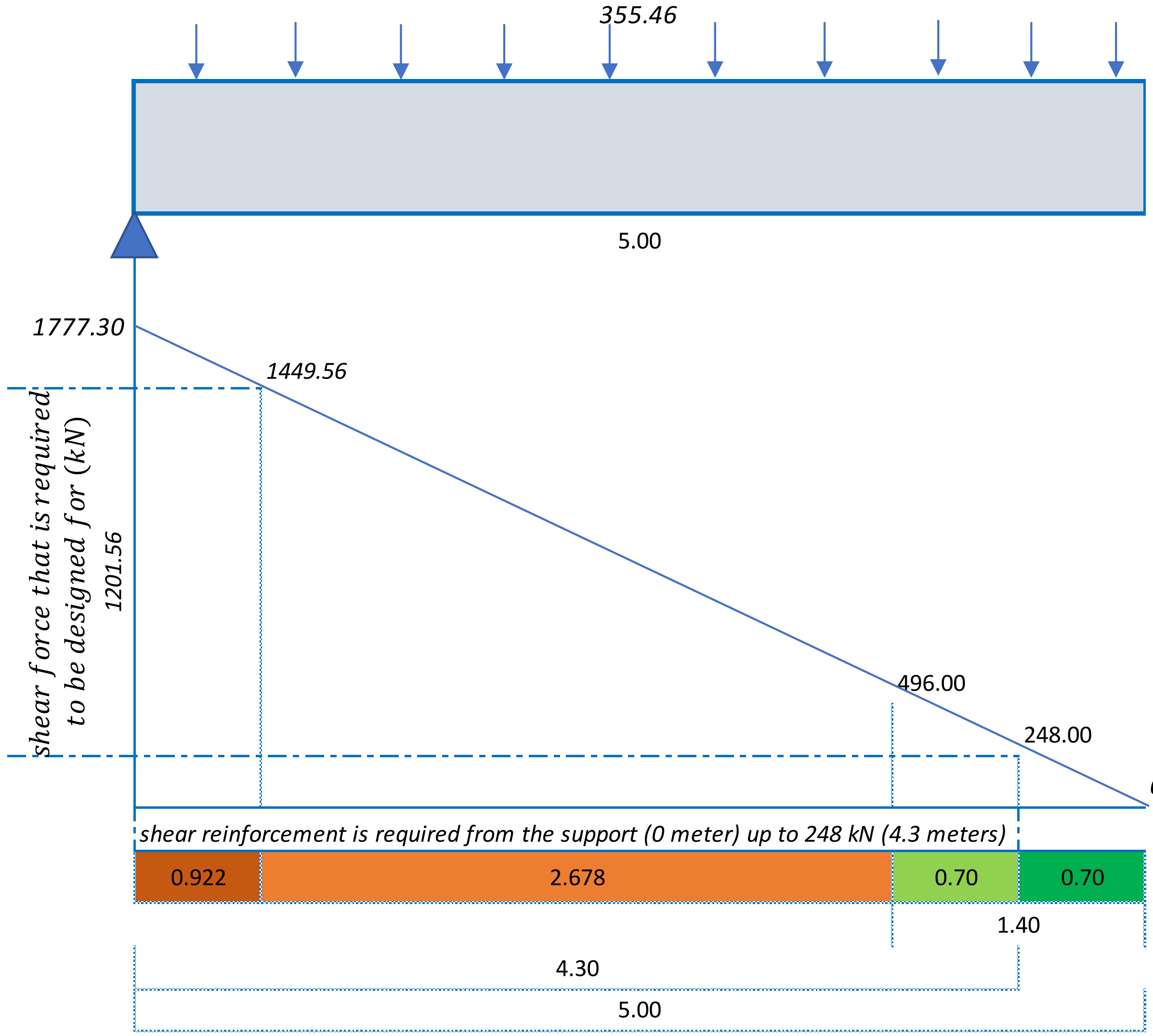

Fig. 4.44: General shear reinforcement formulation diagram of the girder

4.2.3.2.1.3 Graphical analogy

This section considers graphically comparing all the outputs from the two methods of stirrup installation.

Stirrup spacing and quantity table for perpendicular and diagonal placement				
v_c	Spacing		Quantity	
	s_p	s_d	$\#_p$	$\#_d$
v_{c_1}	70	70	12	13
v_{c_2}	75	105	12	9
v_{c_3}	100	140	9	7

Table 4-21: The spacing–number of bars summary table for both perpendicular and diagonal placements

From Fig. 4.45 and Fig. 4.46, it is portrayed that data involving perpendicular placement of stirrups show more inconsistencies than those of diagonal placement.

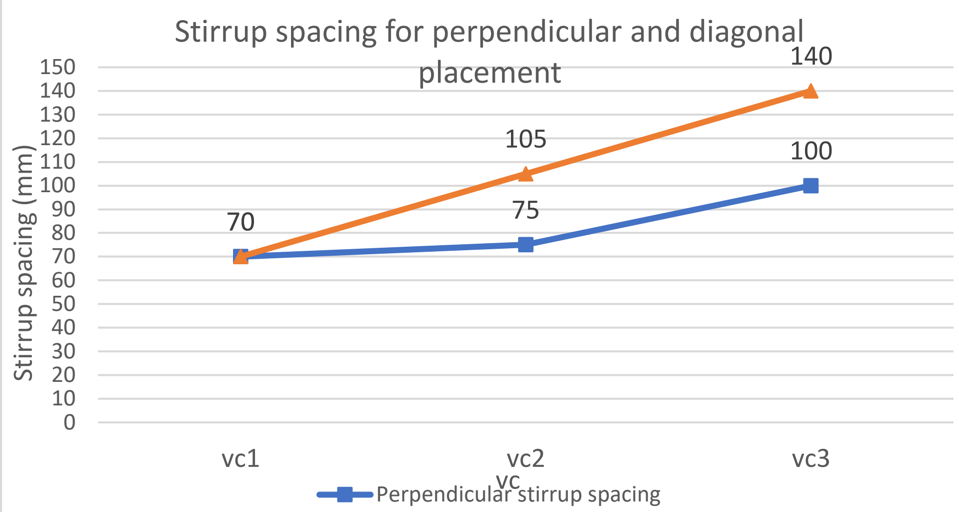

Fig. 4.45: Graphical representation of the difference in stirrup spacings

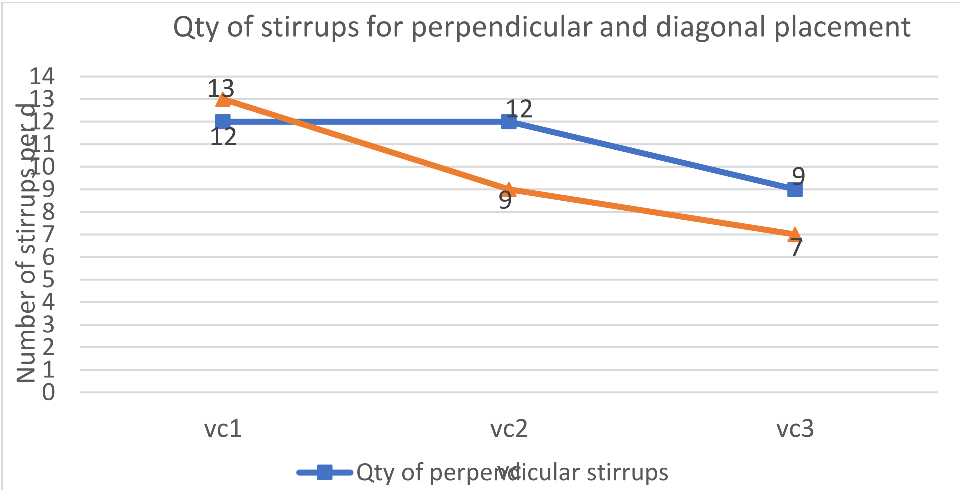

Fig. 4.46: Graphical representation of the difference in the number of stirrups

4.2.4 Design for Flexural Cracks

Fig. 4.47: A typical girder under crack

Serviceability Requirements in structural design dictates structures to follow minimum requirements that would keep them in safe state. Cracks, according to [3], go through three main stages, namely the uncracked stage, the cracked-elastic stress stage, and the failure stage. These stages are all associated with some distinct characteristics with respect to the depth of crack emanating from the tension face of the concrete towards its compression face. In a practical sense involving simply supported beam loaded atop, tension reinforcement would normally be placed in the bottom/soffit of the beam. However, it should be keenly considered that the concrete beneath the tension reinforcement is normally not considered in flexural calculations leading to the determination of the moment capacity of the beam. Yet it is from this face that failure is normally calculated. This can be attributed to the thousands of laboratory tests that back the theory that concrete somehow makes insignificant contribution to tension about 8 to 15% f'_c

4.2.4.1 Modulus of rupture

Pure bending, one of the theories upon which deflection is calculated, utilizes the application of the theory of modulus of rupture of concrete (f_r). This theory utilizes the size effect of a member which can thus be put that before the maximum fracturing load is applied to the beam, micro-cracking occurs over the boundary layer length and slips that are associated with strain softening would be ideally reached [33]. The relationship between the modulus of rupture of a specific section, its cracking moment and the compressive strength of the concrete greatly depends on its overall depth. This has led [16] to estimate the modulus of rupture based on concrete strength as:

$$f_r = 0.62\lambda\sqrt{f_c^{'}} \qquad \text{Eqn 4-137}$$

In Eqn 4-137, λ is a modification factor representing the relationship between the equilibrium density of lightweight concrete and normal weight concrete. Eqn 4-137 is the same as that used in [2] except that it drops the λ because the design philosophy is based on that of a normal weight concrete. For lightweight concrete, the factor is estimated at 75% of that of normal weight concrete.

$$\lambda_{lw} = \frac{75}{100}\lambda_{nw} \qquad \text{Eqn 4-138}$$

Wherein considering all the section parameters and the load magnitude required by the [34], the modulus of rupture, which is synonymous to the section's flexural stress, can be represented by the equation:

$$f_r = \frac{Mc}{I} \qquad \text{Eqn 4-139}$$

Though the case under consideration is a UDL, a similar case for concentrated loads is also applicable when applied at the one-third locations, the formula is then reduced to:

$$f_r = \frac{PL}{bh^2} \qquad \text{Eqn 4-140}$$

$$f_r = \frac{Mc}{I} = \frac{M\left(\frac{h}{2}\right)}{\left(\frac{1}{12}\right)bh^3} = \frac{Mh}{2} * \frac{12}{bh^3} = \frac{6Mh}{bh^3} = \frac{6M}{bh^2} = \frac{6\left(\frac{PL}{6}\right)}{bh^2} = \frac{PL}{bh^2}$$

4.2.4.2 Determination of the cracking moment of the T - girder shown

Cracking moment is a very delicate feature in the design of any structure. It gives the magnitude of applied moment under which the section would start to crack. It is calculated by the formula:

$$M_{cr} = \frac{f_r I_g}{y_t} \qquad \text{Eqn 4-141}$$

A series of formulae is presented below that lead to the determination of the cracking moment of this girder. As a recap of the major dimensions indicated on the section, note the following:
b_{eff} = 2400 mm
a = 77 mm
c = 100 mm
h_f = 280 mm
d = 922 mm
t = 1000 mm
b_w = 500 mm
A_s = 14940 mm^2
M_{sd} = 3998.94 KN.m

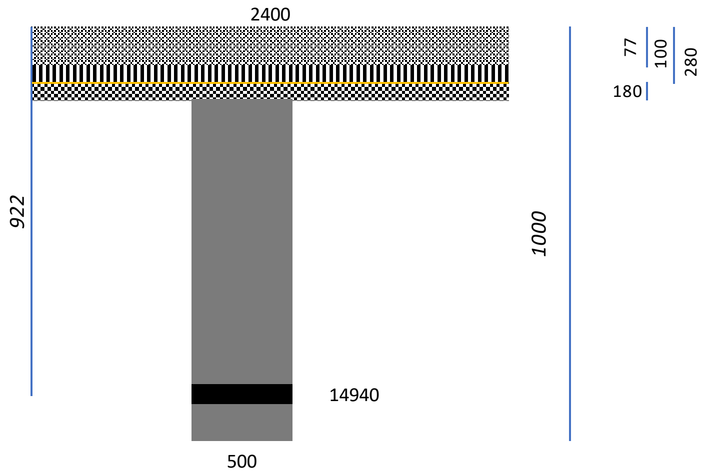

Fig. 4.48: Dimensions associated with the T-girder

4.2.4.2.1 Section Modulus

Section modulus (S) is a geometric property of any shape. Depending on the analysis type, different formulas are used. In the flexural design, the elastic section modulus is adopted for it considers the effect of force, moment etc. The centroidal distance of a section from the top (y_t) can be obtained as follows:

$$y_t = \frac{b_{eff}h_f\left(\frac{h_f}{2}\right) + b_w(t-h_f)(h_f + \frac{t-h_f}{2})}{b_{eff}h_{hf} + b_w(t-h_f)} \qquad \text{Eqn 4-142}$$

$$y_t = \frac{(2.4\,m)(0.28\,m)\left(\frac{0.28\,m}{2}\right) + (0.5\,m)(1\,m - 0.28\,m)\left(0.28\,m + \frac{1\,m - 0.28\,m}{2}\right)}{(2.4\,m)(0.28\,m) + (0.5\,m)(1\,m - 0.28\,m)} = 314\,mm$$

This means that the centroidal axis falls a little below the flange. This is so because the concrete contained in the flange is as twice as that in the web (Eqn 4-102) wherein considering that the web section is also uncracked. Notwithstanding, because of the high depth of the web section, its section modulus would be far greater than that of the flange. And from the bottom, the centroidal bottom distance (y_b) is the difference between the total sectional depth and the top centroidal distance.

$$y_b = t_{gir} - y_t \qquad \text{Eqn 4-143}$$

$y_b = 1000\,mm - 314\,mm = 686\,mm$

From the above analysis, the section modulus in relation to the compression stress block (S_a), can also be calculated.

$$S_a = A_a y_a \quad \text{Eqn 4-144}$$

$$S_a = 2.4 \times 0.077 \left(\frac{0.077}{2}\right) = 0.1848(0.0385) = 0.0071148\ m^3$$

For the compression flange thickness is greater than the compression stress block, the remaining depth equivalent section modulus ($S_{(f-a)}$) is

$$S_{(f-a)} = (Ay)_{(f-a)} \quad \text{Eqn 4-145}$$

$$S_{(f-a)} = 2.4(0.28 - 0.077)\left(0.077 + \frac{0.28 - 0.077}{2}\right) = 0.4872(0.1785) = 0.0869652\ m^3$$

For the web,

$$S_w = (Ay)_w \quad \text{Eqn 4-146}$$

$$S_{(w)} = 0.5(1.0 - 0.28)\left(0.28 + \frac{1.0 - 0.28}{2}\right) = 0.36(0.64) = 0.2304\ m^3 = 230400000\ mm^3$$

The total section modulus is the sum of all the section moduli calculated above

$$S_{tot} = S_a + S_{(f-a)} + S_w \quad \text{Eqn 4-147}$$

$$S_{tot} = 0.0071148 + 0.0869652 + 0.2304 = 0.32448\ m^3 = 324480000\ mm^3$$

4.2.4.3 Deflection

Deflection is an elastic property of a flexural member defined by [31] as "movement of a point on a structure or structural element, usually measured as a linear displacement or as succession displacements transverse to a reference line or axis". With this definition, this work concentrates on deflection in the direction of the applied load. However, to derive at the said deflection, several intermediate parameters including the different types of moment of inertia, flexural stresses, cracking moment etc. are calculated in connection with general procedures. The cracking and applied moments are then compared to ascertain the magnitude at which the cracks are differed.

4.2.4.3.1 Considering a T-Section

T-sections are flanged sections whose neutral axis fall within the web of the section but technically those with their compression stress block in the flange can also be T-section.

4.2.4.3.1.1 Gross moment of inertia

Structural cracks, fracture etc. would normally follow a deflection. The gross (uncracked) moment of inertia of the entire section (I_g) and normally used in the calculation of deflection, being the sum of the moment of inertia for each constituent element (the flange and the web), based on the location of the neutral axis, can also be calculated as follows:

$$I_g = \frac{1}{12} b_{eff} h_f^3 + b_{eff} h_f \left(y_t - \frac{h_f}{2}\right)^2 + \frac{b_w (t - h_f)^3}{12} + b_w (t - h_f)\left(y_t - \left(h_f + \frac{t - h_f}{2}\right)\right)^2 \quad \text{Eqn 4-148}$$

$$I_g = \frac{1}{12}(2.4\ m)(0.28\ m)^3 + (2.4\ m)(0.28\ m)\left(0.314\ m - \frac{0.28\ m}{2}\right)^2 + \frac{(0.5\ m)(0.314\ m - 0.28\ m)^3}{12} + (0.5\ m)(0.314\ m - 0.28\ m)\left(0.314\ m - \left(0.28\ m + \frac{0.314\ m - 0.28\ m}{2}\right)\right)^2$$

$$I_g = 4390400000 + 20345472000 + 15552000000 + 38259360000 = 78547232000\ mm^4$$

4.2.4.3.1.2 Sectional stresses

The cracked moment of inertia (I_{cr}) of a T-section, because of the inclusion of the effect of steel, yields a rather higher moment of inertia than that of the gross moment of inertia. This will be seen later. Now, the flexural stress that exists in the tension face of the girder (f_{rt}) due to the induced moment can be calculated as:

$$f_{rt} = \frac{M_{sd} y_b}{I_g} \qquad \text{Eqn 4-149}$$

$$f_{rt} = \frac{(3998.94\ kN.m)(0.686\ m)}{0.078547232\ m^4} = 34925.14\ kPa \approx 34.93\ MPa$$

On the other hand, for the compression section, it becomes:

$$f_{rt} = \frac{M_{sd} y_t}{I_g} \qquad \text{Eqn 4-150}$$

$$f_{rc} = \frac{(3998.94\ kN.m)(0.314\ m)}{0.078547232} = 15986.14\ kPa \approx 16.0\ MPa$$

NB: Because of the centroidal distance being adjacent the flange area, the stress in tension is as twice as that in compression. These are cracking stresses that are induced on the section and are needed to be compared with the minimum stresses allowable to the section. The limiting value of flexural stress as provided for by both the [16] and [2] in Eqn 4-137 shows that the induced stresses (Eqn 4-149 and Eqn 4-150) are all far higher. This implies that the section is cracked.

To cause this rupture, the proportionate cracking moment is then obtained from:

$$M_{cr} = \frac{f_r I_g}{y_b} \qquad \text{Eqn 4-151}$$

$$M_{cr} = \frac{\left(3.92 \frac{MN}{m^2}\right)(0.078547232\ m^4)}{0.686\ m} = 0.45\ MN.m = 450\ kN.m$$

This 450 kN.m moment is that which should be induced on the girder before the modulus of rupture can be matched or reached. It should be noted here that this moment is comparably far less than the design moment.

4.2.4.3.1.3 Effective moment of Inertia

Referencing [16]'s Table 24.2.3.5, the ideal type of effective moment of inertia to be applied in deflection calculations (i.e., either the gross moment of inertia or the effective moment of inertia (I_e)) can be determined based on the difference in magnitude of the service (applied) moment and the cracked moment. When:

Service moment	Effective moment of inertia, I_e, mm^4	
$M_a \le (2/3)M_{cr}$	I_g	(a)
$M_a > (2/3)M_{cr}$	$\dfrac{I_{cr}}{1-\left(\dfrac{(2/3)M_{cr}}{M_a}\right)^2\left(1-\dfrac{I_{cr}}{I_g}\right)}$	(b)

Table 4-22: The effective moment or inertia requirement table

$$\left(\frac{2}{3}\right) M_{cr} = \left(\frac{2}{3}\right)(450\ kN.m) = 300.0\ kN.m = 0.30\ MN.m < 3.99894\ MN.m$$

Now, since M_a (= M_{sd}) is far greater than the (2/3)M_{cr}, adopt eq. (b). Yet, another requirement as stipulated by [3] allows for the design moment to be substituted in the place of the cracking moment if the dead load moment is less than the cracking moment. It also furthers that in such case, the effective moment of inertia shall be considered as the gross moment of inertia. Thus,

$$M_{DL} = 765.88\ kN.m > 450\ kN.m$$

Since this latter condition is not met, the former condition shall be adopted in the calculation of the effective moment of inertia as well as the deflection. The percentage of cracking moment to design moment, which expresses the gap between these two moments is calculated as below:

$$\frac{M_{cr}}{M_{sd}} = \frac{0.45}{3.99894} = 0.112 = 11.2 \approx 11\%$$

The also implies that the design moment is about nine times higher than the cracking moment. Further, the load to be induced on the girder to cause it reach its optimum rupture stage [cracking load (w_{cr})] is obtained as follows:

$$w_{cr} = \frac{8M_{cr}}{s^2} \qquad \text{Eqn 4-152}$$

$$w_{cr} = \frac{8(450\ kN.m)}{(10\ m)^2} = 36\ kN/m$$

This load is very low compared to the total applied load. However, for the loads and moments would be carried by the steel [2] 8-2.27C, design moment may exceed cracking moment, but the design has to consider such case! The cracked moment of inertia for a T-section structurally designed as a Rectangular T-section that does not contain compression reinforcement is calculated from the series of parameters that follow. The cracked moment of inertia is the gross moment of inertia plus the moment of inertia offered by the reinforcement element. Thus, the moment of inertia of the cracked section is equivalent to the following expression:

$$I_{cr} = I_g + nA_s(d - kd)^2 \qquad \text{Eqn 4-153}$$

…where k is a directly proportionate coefficient relating to the effective depth thus yielding the depth of neutral axis of the cracked section.

$$k = \sqrt{(\rho n)^2 + 2(\rho n)} - (\rho n) \qquad \text{Eqn 4-154}$$

Further, the modular ratio (n) is a quantity that relates the elastic modulus of steel to that of the elastic modulus of concrete. It presents the magnitude by which the two moduli differ, and is normally rounded to the nearest whole number, structurally. ρ is the steel ratio as obtained from 4.1.5.7 above.

$$n = \frac{E_s}{E_c} \qquad \text{Eqn 4-155}$$

$$n = \frac{210\ GPa}{30\ GPa} = 7$$

This means, the reinforcing steel can be seven times as stressed as the concrete. Thus,

$$k = \sqrt{(0.031 \times 7)^2 + 2(0.031 \times 7)} - (0.031 \times 7) = 0.4766057958 \approx 0.477$$

The cracked neutral axis (c_{cr}) is thus,

$$c_{cr} = kd \qquad \text{Eqn 4-156}$$

$$c_{cr} = 0.4766057958(0.922\ m) = 0.4394305437\ m$$

$$I_{cr} = 0.078547232\ m^4 + 7(0.01494\ m^2)(0.922\ m - 0.4394305437\ m)^2$$
$$I_{cr} = 0.078547232\ m^4 + 0.02435388764\ m^4 = 0.1029011196\ m^4 = 102901119600\ mm^4$$

The cracked moment of inertia (I_{cr}) of a T-section, because of the inclusion of the effect of steel, yields a rather higher moment of inertia than that of the gross moment of inertia. This will be seen later. Now, the flexural stress that exists in the tension face of the girder (f_{rt}) due to the induced moment can be calculated as:

$$f_{rt} = \frac{M_{sd}y_b}{I_g} \qquad \text{Eqn 4-157}$$

$$f_{rt} = \frac{(3998.94\ kN.m)(0.686\ m)}{0.078547232\ m^4} = 34925.14\ kPa \approx 34.93\ MPa$$

On the other hand, for the compression section, it becomes:

$$f_{rt} = \frac{M_{sd}y_t}{I_g} \qquad \text{Eqn 4-158}$$

$$f_{rc} = \frac{(3998.94\ kN.m)(0.314\ m)}{0.078547232} = 15986.14\ kPa \approx 16.0\ MPa$$

[2] 8-2.23.7 like many other reinforced concrete texts, considers the usage of the effective moment of inertia where dictated by according to the preliminary inputs such as the cracking moment, applied moment and the cracked moment of inertia [35].

$$I_e = \left(\frac{M_{cr}}{M_a}\right)^3 I_g + \left[1 - \left(\frac{M_{cr}}{M_a}\right)^3\right] I_{cr} \qquad \text{Eqn 4-159}$$

$$I_e = \left(\frac{0.45\ kN.m}{3.99894\ kN.m}\right)^3 0.078547232\ m^4 + \left[1 - \left(\frac{0.45\ kN.m}{3998.94\ kN.m}\right)^3\right] 0.1029011196\ m^4$$

$$I_e = 0.1028664163\ m^4 = 102866416300\ mm^4$$

4.2.4.3.1.4 Effective Young Modulus of Elasticity of concrete

In deflection calculations, one parameter that is normally worked around/adjusted to suit a given condition is the second moment of area which is normally referred to as the moment of inertia. As have been deliberated on earlier, this is due to the difference in cracking and design moments. On the other hand, the modulus of elasticity of concrete is generally considered as the modulus of elasticity of the section thus excluding the contributions of that of the reinforcement element. However, [36] takes into consideration the effect of the contributions of the steel as well. Thus, the Effective Young Modulus of Elasticity of Concrete ($E_{c,eff}$) can be adopted as well.

$$A_sE_s\varepsilon_s = 0.5bd_c\varepsilon_cE_{c,eff} \qquad \text{Eqn 4-160}$$

Rearranging the equation, Effective Young Modulus of Elasticity of Concrete ($E_{c,eff}$)

$$E_{c,eff} = \frac{A_sE_s\varepsilon_t}{0.5bd_c\varepsilon_c} = \frac{(0.01494\ m^2)\left(2.0x10^{11}\frac{N}{m^2}\right)(0.025)}{0.5(0.5\ \ m)(0.1\ m)(0.003)} = 996\ GPa$$

4.2.4.3.1.5 Deflection tables and graphs

Every possible paramater discussed above would be used in the investigation. In this vein, a comparative analysis of the behavoir of each parameter and its effects on the overall performance is captured. Now, it should be emphasized that although the section, according to Eqn 4-103 and Eqn 4-107 is designed as a rectangular section, under all loads and stresses the flange provides additional stiffness to the entire section. Hence, a T-sectioned girder and a rectangular section girder are analyzed respectively. Deflection is generally represented for a UDL as

$$\Delta = \left(\frac{5}{384}\right)\left(\frac{wL^4}{EI}\right) \qquad \text{Eqn 4-161}$$

Under the T-construction, as would also be in the rectangular, four generic tables are constructed in order to clearly present key considerations relative to a specific deflection types, section properties, etc. [37]'s work on deflection literarily recognizes immediate and time-dependent deflection in which of course the later comprises of the immediate and long-term elastic deflections, cracking, shrinkage, and creep deflection. These categories of deflections primarily involve the load regime and time.

The tables are structured as followed:

Unfactored Dead Load to both E and I								
#	***w*n (N/m)**	***l* (m)**	**E_c (N/m^2)**	**$E_{c,eff}$ (N/m^2)**	**I_g (m^4)**	**I_e (m^4)**	**Δ (m)**	**Δ (mm)**
1	61270	10	30000000000		0.078547232		0.0034	3.40
2	61270	10	30000000000			0.1028664163	0.0026	2.60
3	61270	10		996000000000	0.078547232		0.0001	0.10
4	61270	10		996000000000		0.1028664163	0.0001	0.10

Table 4-23: Unfactored dead load deflection table

Table 4-23 matches the formulation of deflection characteristics of what is described as initial elastic deflection in [37]. Here, dead loads as they are in their original state are considered to initiate deflection after the removal of the falsework.

Unfactored Live Load to both E and I								
#	***w*n (N/m)**	***l* (m)**	**E_c (N/m^2)**	**$E_{c,eff}$ (N/m^2)**	**I_g (m^4)**	**I_e (m^4)**	**Δ (m)**	**Δ (mm)**
1	192630	10	30000000000		0.078547232		0.0106	10.60
2	192630	10	30000000000			0.1028664163	0.0081	8.10
3	192630	10		996000000000	0.078547232		0.0003	0.30
4	192630	10		996000000000		0.1028664163	0.0002	0.20

Table 4-24: Unfactored live load deflection table

Table 4-24 considers all other parameters of Table 4-23 except that it covers live loads only. Live load, as in [37], is considered long-term load and is thus used in long-term deflection.

Unfactored Loads: Dead Load + Live Load to both E and I								
#	***w*n (N/m)**	***l* (m)**	**E_c (N/m^2)**	**$E_{c,eff}$ (N/m^2)**	**I_g (m^4)**	**I_e (m^4)**	**Δ (m)**	**Δ (mm)**
1	253900	10	30000000000		0.07854723		0.014	14.00
2	253900	10	30000000000			0.1028664163	0.0107	10.70
3	253900	10		996000000000	0.07854723		0.0004	0.40
4	253900	10		996000000000		0.1028664163	0.0003	0.30

Table 4-25: Unfactored dead and live loads deflection table

Table 4-25 combines the dead load of Table 4-23 and the live load of Table 4-24.

Factored Loads: Dead Load + Live Load to both E and I								
#	***w*n (N/m)**	***l* (m)**	**E_c (N/m^2)**	**$E_{c,eff}$ (N/m^2)**	**I_g (m^4)**	**I_e (m^4)**	**Δ (m)**	**Δ (mm)**
1	355460.0	10	30000000000		0.07854723		0.0196	19.60
2	355460.0	10	30000000000			0.1028664163	0.0150	15.00
3	355460.0	10		996000000000	0.07854723		0.0006	0.60
4	355460.0	10		996000000000		0.1028664163	0.0005	0.50

Table 4-26: Factored dead and live loads deflection table

In some texts, deflection is calculated based on unfactored loads, however, here, all categories are considered. Table 4-26 is factored from Table 4-25 thus the factor is the only difference.

The following detailed tables in the appendicular table (Tablapp) present a more in-depth parametric consideration about the deflection. In each table, column 1 provides a consecutively incremental percentage of live load that is added to the dead load in column 2. At 0.0% live load, the implication is that the girder is completely under the condition of initial elastic deflection. By adding any live load, this leads to stepping the load thus allowing a visual representation of the deflection trend. Column 3 through column 7 each provides the data used in the deflection calculation while column 8 to column 11 gives details about the calculated deflection to include:

1. **% Incre. in Δ (%↑Δ)** – which means percentage of increment in deflection is the percentage by which an increment in the live leads to an increment in deflection. In other words, with the 2.5% increment in live load, what would be the equivalent increment in deflection?
2. **%↑Δ_{acc}** – is the accumulated percentage of the increment in deflection at a specified increment in live load.

The mathematical experession for % Incre. in Δ (%↑Δ) is given as

$$\%\Delta = \left(\frac{\Delta_{now}}{\Delta_{prev}} - 1\right) * 100 \qquad \text{Eqn 4-162}$$

Note that at 0.0% increment of live load, %↑Δ is zero because only dead load is acting hence there is no change. The sharp increment in the graph of %↑ΔEcIg depicits the magnitude of the effect that a live load would have on the structure.

NB: All deflections are limited to a four-decimal place displacement magnitude!

Further, %↑Δ_{acc} is

$$\% \uparrow \Delta_{acc} = \left(\Delta_{now} + \Delta_{prev}\right) \qquad \text{Eqn 4-163}$$

4.2.4.3.1.5.1 Deflection calculation using E_cI_g stiffness

Reference is made to Tablapp 10-1 for the detailed deflection table at every stage of load increment. FigApp 10-1 also provides clarity on the increment in deflection due to the 2.5% increment of live load imposed on the dead load. An increment in the load definitely leads to an increment in the magnitude of the deflection. Up to the maximum value of the load, the percentage in increment from one deflection to the other does not follow suit as that of the deflection whereby it follows a downward increment. The pattern is not linear but is characteristically constant in shape. The below chart clearly presents the clearer representation From the chart, it can be hypothesized that as the increment in the loading approaches maximum, the percentage of increment in deflection due to the combined load decreases gradually from one deflection to the other.

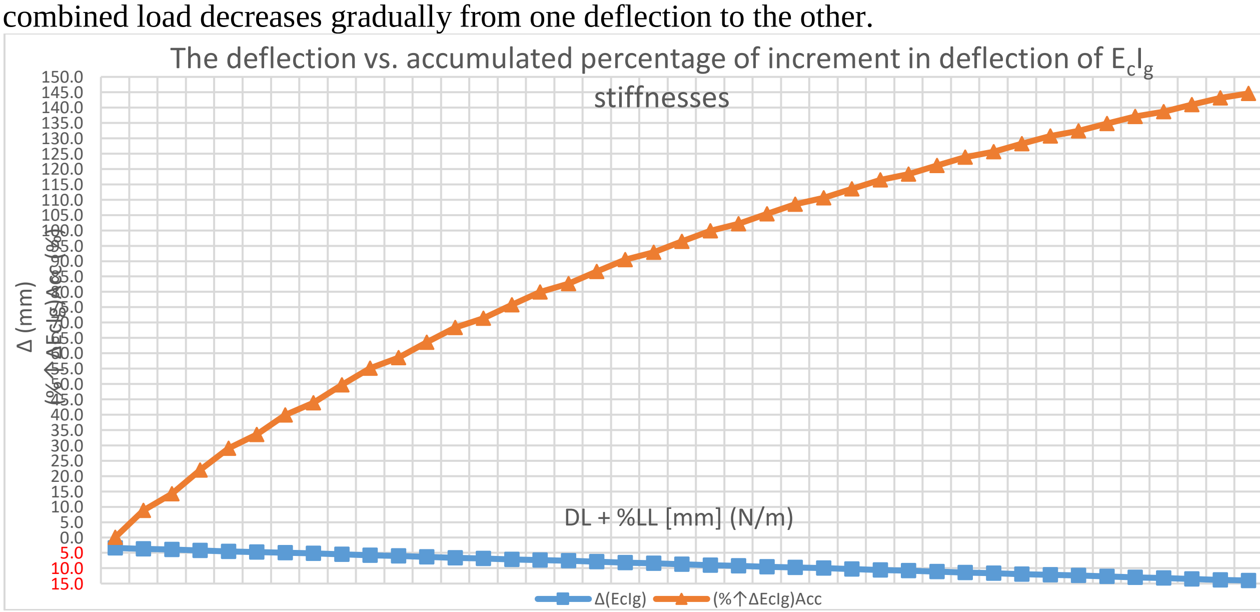

Fig. 4.49: Deflection vs. accumulated percentage of increment in deflection of E_cI_g stiffness

On a keen note, the chart represents a deflection characteristic in which the stiffness constant E_cI_g brings about a reasonable intepretation that could be adopted for this case as follows:

1. as the increment in the loading approaches maximum, deflection approaches maximum whereas,
2. the percentage of increment in deflection due to the combined effects of the loads decreases in a gorgy W-m-like shape with a top slanted then indented line.
3. More interestingly, at an approximate 1/10 of this total increment, the shape of the graph repeats itself.

On the overall, the accumulated percentage of increment in deflection shows a clearer trend on how deflection changes towards midspan. As deflection moves toward midspan, $\%\uparrow\Delta_{acc}$ changes concomitantly. For this E_cI_g stiffness, after the full 100% application of the live load, the $\%\uparrow\Delta_{acc}$ reached a total of approximately 150%.

4.2.4.3.1.5.2 Deflection calculation using E_cI_e stiffness

Tablapp 10-2 gives the detailed table with its graph being similar to that of FigApp 10-1 except that there is a characteristically strange sharp increment around the region of the 50% live load increment thus causing the graph a distortion in its consistency in shape. Reference FigApp 10-2. In a detailed description, it can also be said that as the increment in the loading approaches maximum, the percentage of increment in deflection due to the combined load decreases gradually up to around 50% the increment in the live load. Then a sharp wedged increase is experienced at said point up to the next 2.5 % (at 52.5%) and then drops in the similar slope as it previously increased. At this point of sharp increment, the structure would experience a sharp magnitude of deflection. By the utilization of E_cI_e, the stiffness of the structure becomes higher while the deflection becomes lower and even lower than that of the E_cI_g stiffness. As in Fig. 4.49, the E_cI_e stiffness of Fig. 4.50 also takes the same shape in increment but notably with both lower deflection and accumulated percentage. This is due to the increase from gross moment of inertia to effective moment of inertia.

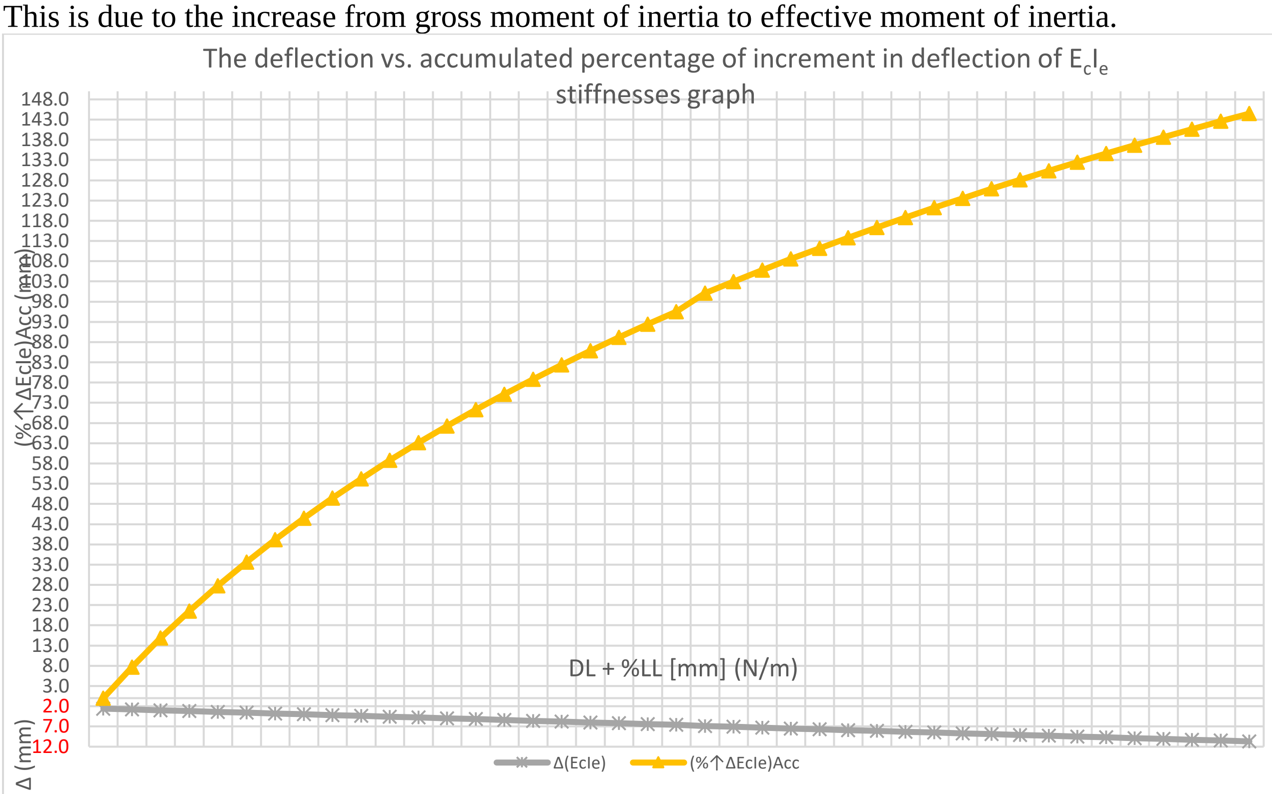

Fig. 4.50: Deflection vs. accumulated percentage of increment in deflection of E_cI_e stiffness

4.2.4.3.1.5.3 Deflection calculation using $E_{c,eff}I_g$ stiffness

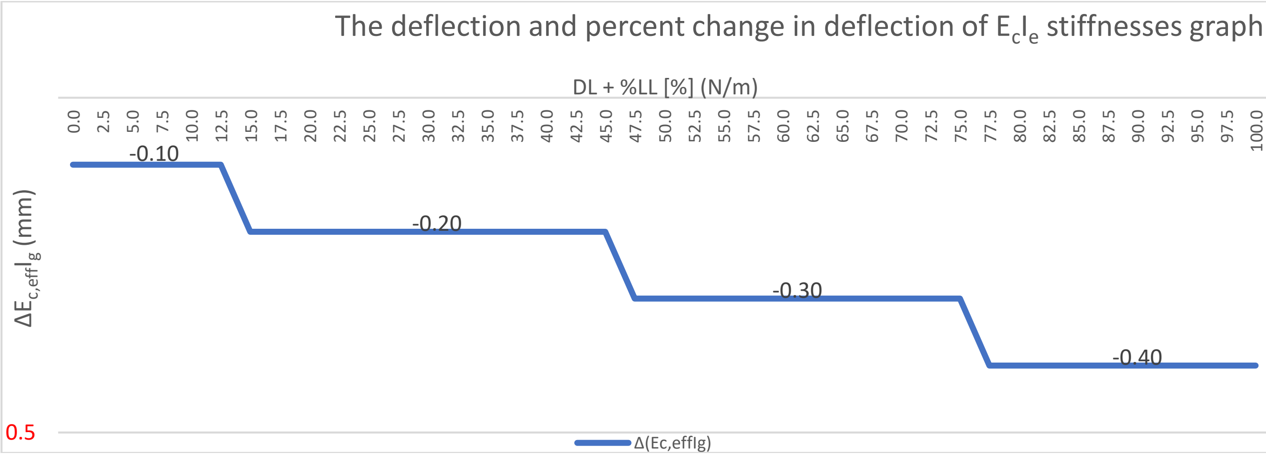

Fig. 4.51: Graphical representation of deflection for Tablapp 10-3

Fig. 4.51 shows a technically steady-then-sharp pattern of deflection. For an $E_{c,eff}I_g$ stiffness, the deflection magnitude is an infintesimal value to that of the increment in the load. It is estimated that a bay width is technically as twice as its preceeding bay up to the event of the application of 50% of the live load. Past this limit, the bay ratio takes the otherwise pattern. Unlike stiffnesses that contain the E_c parameter, those that contain the $E_{c,eff}$ parameter like in this case, which when greater ($E_{c,eff} > E_c$), definitely lead to an infinitesimal increment in the magnitude of the deflection. Up to the maximum value of the load, the percentage of increment in both deflection and its increment is effectuted at varying duration and distances from the point of initial inelastic deflection. As the deflection increases in a steady-then-sharp pattern so does the percentage of increment but rather in a diminishing/downward increment trend. FigApp 10-3 clearly presents the percent increment in deflection.

Another key trend that is being observed in the $(\%\uparrow\Delta E_{c,eff}I_g)_{Acc}$ graphs is that members that undergo a very little deflection show higher $(\%\uparrow\Delta E_{c,eff}I_g)_{Acc}$.

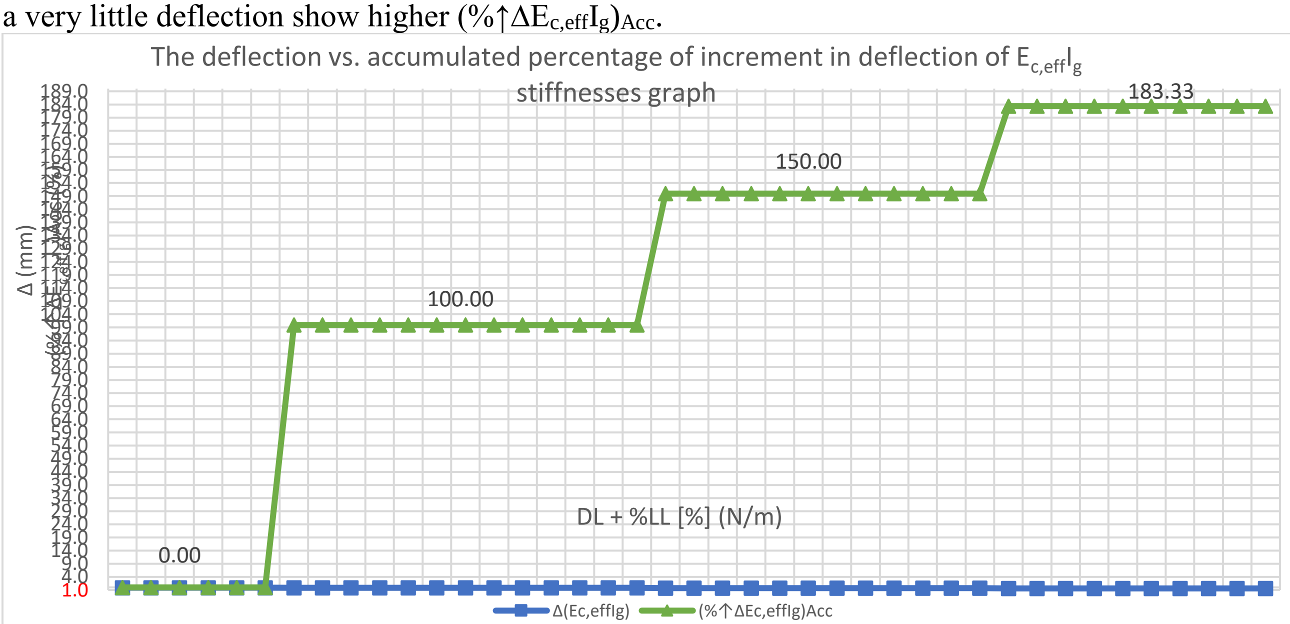

Fig. 4.52: Deflection vs. accumulated percentage of increment in deflection of $E_{c,eff}I_g$ stiffness

4.2.4.3.1.5.4 Deflection calculation using $E_{c,eff}I_e$ stiffness

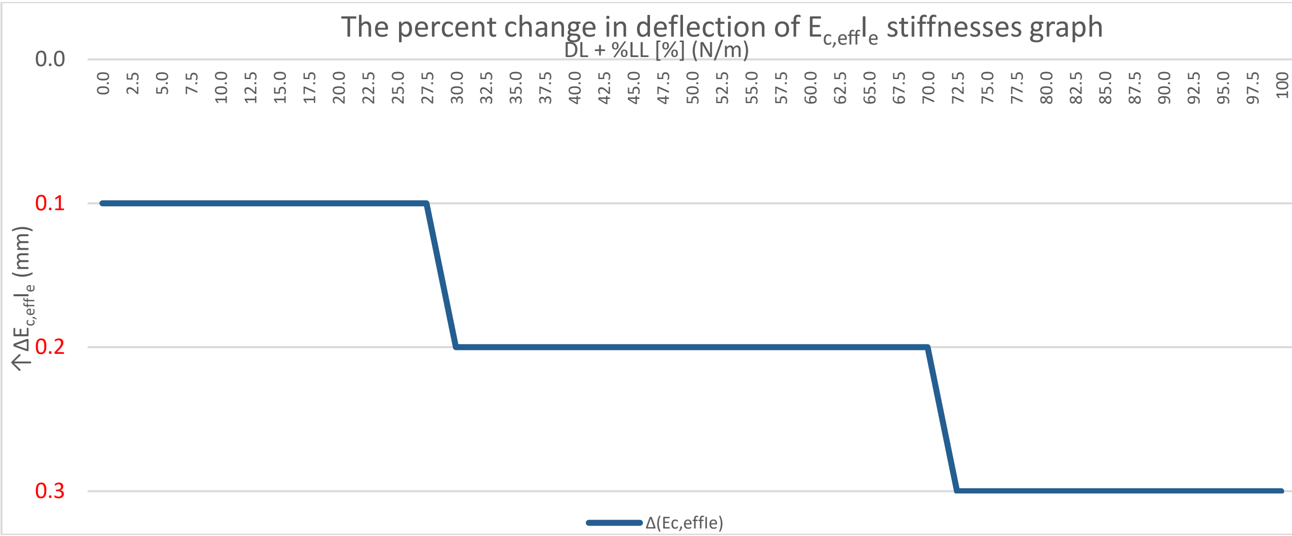

Fig. 4.53: Graphical representation of deflection for Tablapp 10-4

Like the $E_{c,eff}I_g$ stiffness, the deflection magnitude due to the $E_{c,eff}I_e$ stiffness is pretty close the same. All other previous characteris are almost identical but the most notable difference is the number of bays into which the graph is shaped – three for $E_{ceff}I_e$ while there are four for $E_{c,eff}I_g$. The increments in the graph is one less than the number of bays in the deflection graph.

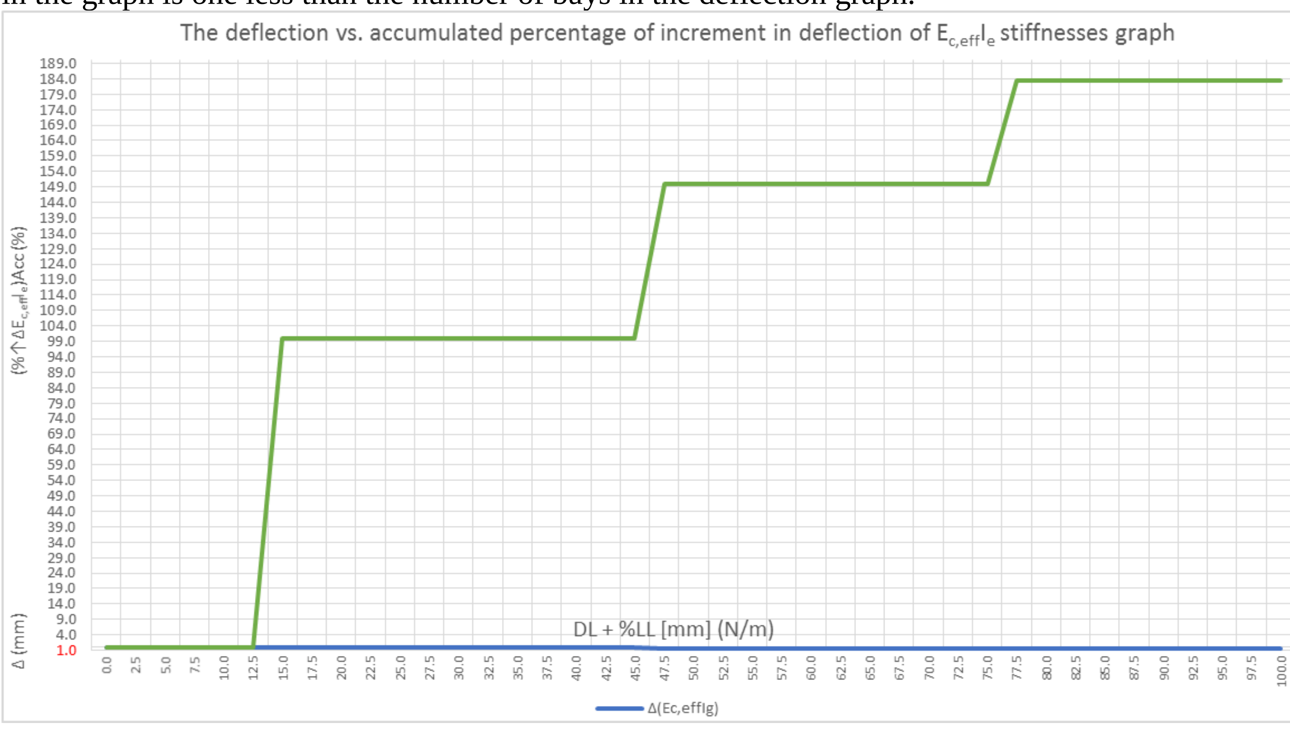

Fig. 4.54: Deflection vs. accumulated percentage of increment in deflection of $E_{c,eff}I_e$ stiffness

Tablapp 10-6 summarizes the findings from the four cases described above. Note that these cases strictly apply to the condition wherein it is only the unfactored loads are used. Because of the wide range of weight associated with each deflection, a simple statistics is performed to ascertain the magnitude of such difference. Fig. 4.55 *combines the paramount graphs generated above to show the trajectory that each category takes relative to their individual stiffness. All conditions follow the unique patterns discussed above.*

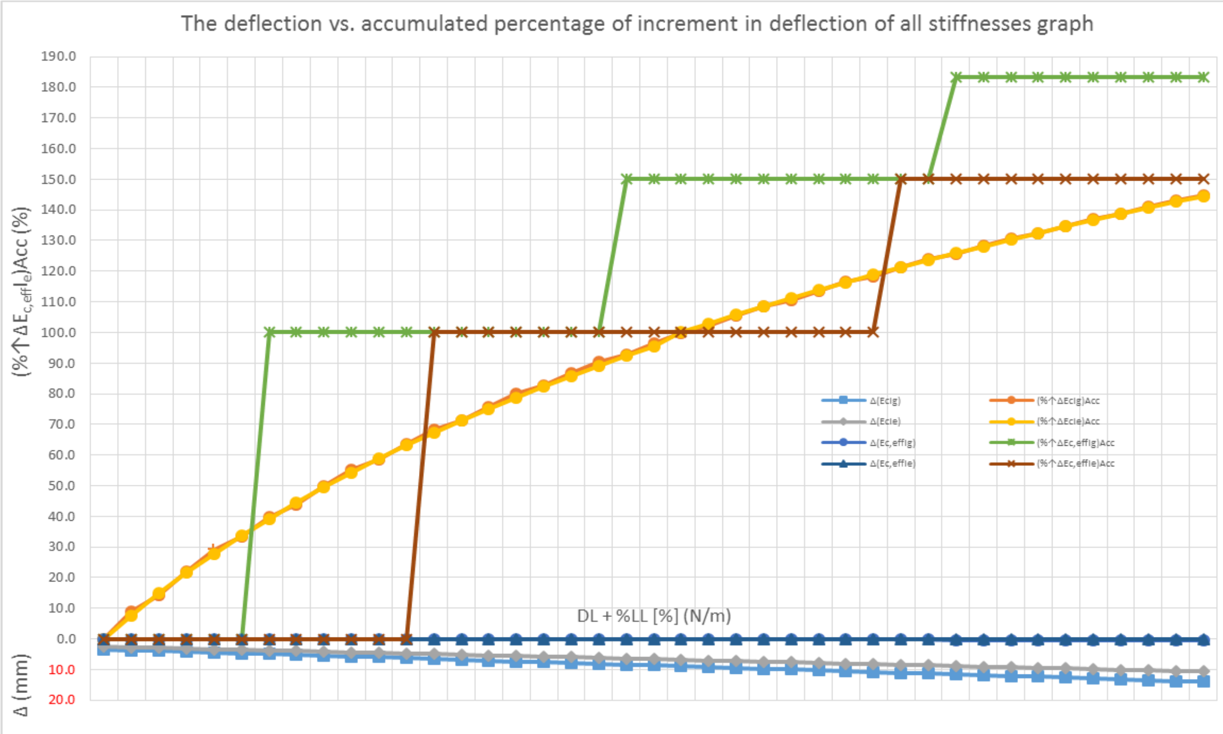

Fig. 4.55: Deflections vs. accumulated percentage of increment in deflection of all stiffnesses

4.2.4.3.1.5.5 Deflection summary and statistics table

Refere Tablapp 10-6 for the detailed table. Due to the high difference in the stiffness, which also culminated in the large difference in deflection, the carryover effect is proportionately evident in the statistical components. Variance, standard deviation, and coefficient of variation (c_v) calculated for deflections show significant difference. Each graph is thus a visual representation of the data contained in Tablapp 10-6. It is evident that deflections due to stiffness containing Effective Young modulus of elasticity of concrete ($E_{c,eff}$) yield deflection magnitudes that might appear to be technically negligible relative to the permissible deflection. On the other hand, those containing the normalized Young modulus of Elasticity of concrete (E_c) which solely excludes the effects of the reinforcement, the deflection magnitude increases by a very high factor. The percentage of increment relative to each modulus can be expressed as follows:

$$\aleph_{\Delta} = \frac{\Delta_{E_c I_g}}{\Delta_{EI}} \qquad \text{Eqn 4-164}$$

Deflection comparison matrix		
Variable	**Numerical**	**Result**
$\frac{\Delta_{E_c I_g}}{\Delta_{E_c I_g}}$	$\frac{14.0}{14.0}$	$1\ time$
$\frac{\Delta_{E_c I_g}}{\Delta_{E_c I_e}}$	$\frac{14.0}{10.7}$	$1.3\ times$
$\frac{\Delta_{E_c I_g}}{\Delta_{E_{c,eff} I_g}}$	$\frac{14.0}{0.4}$	$35\ times$
$\frac{\Delta_{E_c I_g}}{\Delta_{E_{c,eff} I_e}}$	$\frac{14.0}{0.3}$	$47\ times$
$\frac{\Delta_{E_c I_g}}{\Delta_{Ave}}$	$\frac{14.0}{6.35}$	$2.2\ times$

Table 4-27: Rational comparison of deflections against the normalized deflection ($\Delta_{E_c I_g}$)

The data shows a wide range of variation in the deflection magnitude using various stiffnesses. It is also worth noting that all deflections calculated are for the case in which the member is treated as a T-section. To get a further comprehension of how this section would behave under the applied load thus leading to possible cracking, the same analysis is run for the member as rectangular section. This stance is considered because up to some point in the analysis, it was computed that because of the location of the compression stress block, the section may be designed as that of a rectangular section. However, this does not negate the fact that the flanges cannot contribute to the overall stiffness of the section. For the rectangular section, the difference from its T-section counterpart is that its second moment of area and its cracked moment of area are all less than that of the T-section.

4.2.4.3.2 Considering a Rectangular section

The process is somehow same for the rectangular section as that of the T-section.

4.2.4.3.2.1 Gross moment of inertia

The gross moment of inertia for rectangular (having tension reinforcement only) is

$$I_g = \frac{1}{12} b d^3 \qquad \text{Eqn 4-165}$$

$$I_g = \frac{1}{12}(0.5\ m)(1.0\ m)^3 = 0.041666667\ m^4$$

4.2.4.3.2.2 Stress

The stresses acting at the top and bottom of the centroidal axis are definitely equal.

$$y_t = \frac{w_{gir} t_{gir} \left(\frac{t_{gir}}{2}\right)}{w_{gir} t_{gir}} \qquad \text{Eqn 4-166}$$

$$y_t = \frac{(0.5\ m)(1.0\ m)\left(\frac{1.0\ m}{2}\right)}{(0.5\ m)(1.0\ m)} = 0.5\ m$$

$$y_b = t_{gir} - y_t = 1.0\ m - 0.5\ m = 0.5\ m$$

$$f_{rt} = f_{rc} = \frac{(3998.94\ kN.m)(0.5\ m)}{0.041666667\ m^4} = 47987.27962\ kPa \approx 48.0\ MPa$$

And the cracking moment,

$$M_{cr} = \frac{\left(3.92 \frac{MN}{m^2}\right)(0.041666667\ m^4)}{0.5\ m} = 0.33\ MN.m = 330\ kN.m$$

Consideration is made to Eqn 4-101 which provides the total area in compression. From Eqn 4-103, The neutral axis would therefore change considering the change in section and the equation for the compression stress block would then be rewritten as

$$a = \frac{A_c}{b_w} \qquad \text{Eqn 4-167}$$

$$a = \frac{184559\ mm^2}{500\ mm} = 369.118\ mm \approx 369\ mm$$

Thus, the neutral axis and the net tensile strain become,

$$c = \frac{369\ mm}{0.77} = 479.22\ mm \approx 479\ mm$$

$$\varepsilon_t = \frac{922 - 479}{479} 0.003 = 0.003$$

With a net tensile strain of 0.003, the section is brittle. Eqn 4-167 would then cause a significant change in the depth of compression stress block.

$$E_{c,eff} = \frac{A_s E_s \varepsilon_s}{0.5bd_c\varepsilon_c} E_{c,eff} = \frac{(0.01494\ m^2)\left(2.0x10^{11}\ \frac{N}{m^2}\right)(0.003)}{0.5(0.5\ \ m)(0.479\ m)(0.003)}$$

$$E_{c,eff} = 24951983299\ Pa \approx 25000000000\ Pa$$

The moment of inertia of the cracked section is equivalent to the following expression for a rectangular section:

$$I_{cr} = \frac{b(kd)^3}{3} + nA_s(d-kd)^2 \quad \text{Eqn 4-168}$$

But, kd which is technically the cracked neutral axis, equals

$$kd = \frac{\sqrt{2dB+1}-1}{B} \quad \text{Eqn 4-169}$$

Furthermore, relating the base of the section to the reinforcement transformed to concrete (B), is

$$B = \frac{b}{nA_s} \quad \text{Eqn 4-170}$$

$$B = \frac{0.5\ m}{7(0.01494\ m^2)} = 4.781028877/m$$

Finally, *kd* is determined as

$$kd = \frac{\sqrt{2(0.922\ m)(4.781028877)+1}-1}{4.781028877} = 0.4461559128\ m = 446 < 479\ mm$$

c and kd should be literally equal. Hence, the cracked moment of inertia for the procedural formula (Eqn 4-170) becomes:

$$I_{cr} = \frac{(0.5\ m)(0.4461559128\ m)^3}{3} + 7(0.01494\ m^2)(0.922\ m - 0.4461559128)^2$$

$$I_{cr} = 0.01480160153 + 0.023679797972 = 0.03848139945\ m^4 = 38481399450\ mm^4$$

The cases of I_e shall be in twofold: when the expression $\left(\frac{M_{cr}}{M_a}\right)$ is equal to 1, and when it is not equal to 1. If it is equal to 1, then the cracking moment and the design moment are equal thus the procedure yields

$$I_e = I_g \quad \text{Eqn 4-171}$$

On the other hand, the actual value of I_e is computed as provided for by [35] and other codes (section 4.2.4.3.1.3 above):

$$I_e = \left(\frac{M_{cr}}{M_a}\right)^3 I_g + \left[1 - \left(\frac{M_{cr}}{M_a}\right)^3\right] I_{cr}$$

$$I_e = \left(\frac{0.33}{3.99894}\right)^3 0.041666667 + \left[1 - \left(\frac{0.33}{3.99894}\right)^3\right] 0.03848139945$$

$$I_e = 0.03848318945\ m^4 = 38483189450\ mm^4 I_e = 38483189450\ mm^4$$

4.2.4.3.2.3 Tables and graphs of deflection

The tables of section 10.2.2 below provide, as in section 4.2.4.3.1.5, the trend a deflection takes relative to iterating the loading condition, the various types of Young Modulus of elaticity of concrete, as well as that of moment of inertia. Consider the following tables for the different magnitudes of deflection.

Unfactored Dead Load to both E and I								
#	w_n (N/m)	l (m)	E_c (N/m^2)	$E_{c,eff}$ (N/m^2)	I_g (m^4)	I_e (m^4)	Δ (m)	Δ (mm)
1	61270	10	30000000000		0.041666667		0.0064	6.40
2	61270	10	30000000000			0.038481401205	0.0069	6.90
3	61270	10		25000000000	0.041666667		0.0077	7.70
4	61270	10		25000000000		0.038481401205	0.0083	8.30

Table 4-28: Unfactored dead load deflection table

Unfactored Live Load to both E and I								
#	w_n (N/m)	l (m)	E_c (N/m^2)	$E_{c,eff}$ (N/m^2)	I_g (m^4)	I_e (m^4)	Δ (m)	Δ (mm)
1	192630	10	30000000000		0.041666667		0.0201	20.10
2	192630	10	30000000000			0.0384814012	0.0217	21.70
3	192630	10		25000000000	0.041666667		0.0241	24.10
4	192630	10		25000000000		0.0384814012	0.0261	26.10

Table 4-29: Unfactored live load deflection table

Unfactored Loads: Dead Load + Live Load to both E and I								
#	w_n (N/m)	l (m)	E_c (N/m^2)	$E_{c,eff}$ (N/m^2)	I_g (m^4)	I_e (m^4)	Δ (m)	Δ (mm)
1	253900	10	30000000000		0.041666667		0.0264	26.40
2	253900	10	30000000000			0.038481401205	0.0286	28.60
3	253900	10		25000000000	0.041666667		0.0317	31.70
4	253900	10		25000000000		0.038481401205	0.0344	34.40

Table 4-30: Unfactored dead and live loads deflection table

Factored Loads: Dead Load + Live Load to both E and I								
#	w_n (N/m)	l (m)	E_c (N/m^2)	$E_{c,eff}$ (N/m^2)	I_g (m^4)	I_e (m^4)	Δ (m)	Δ (mm)
1	355460	10	30000000000		0.041666667		0.037	37.00
2	355460	10	30000000000			0.038481401205	0.0401	40.10
3	355460	10		25000000000	0.041666667		0.0444	44.40
4	355460	10		25000000000		0.038481401205	0.0481	48.10

Table 4-31: Factored dead and live loads deflection table

4.2.4.3.2.3.1 E_cI_g stiffness

Refer Tablapp 10-7 for the detailed table and FigApp 10-5 for the graph. Here, gorge(s) are not found in %↑ΔE_cI_g.

4.2.4.3.2.3.2 Combined stiffnesses

To summarize, the data of section 10.2.2 below are graphically represented Fig. 4.56 as in Fig. 4.55. There are several characteristics observed from Fig. 4.56:

1. Every similar property has the same shape
2. An increase in the load leads to an increase in deflection
3. All percentages of increment in deflection have been diminishing
4. All accumulated percentages of increment in deflection are approximately equal

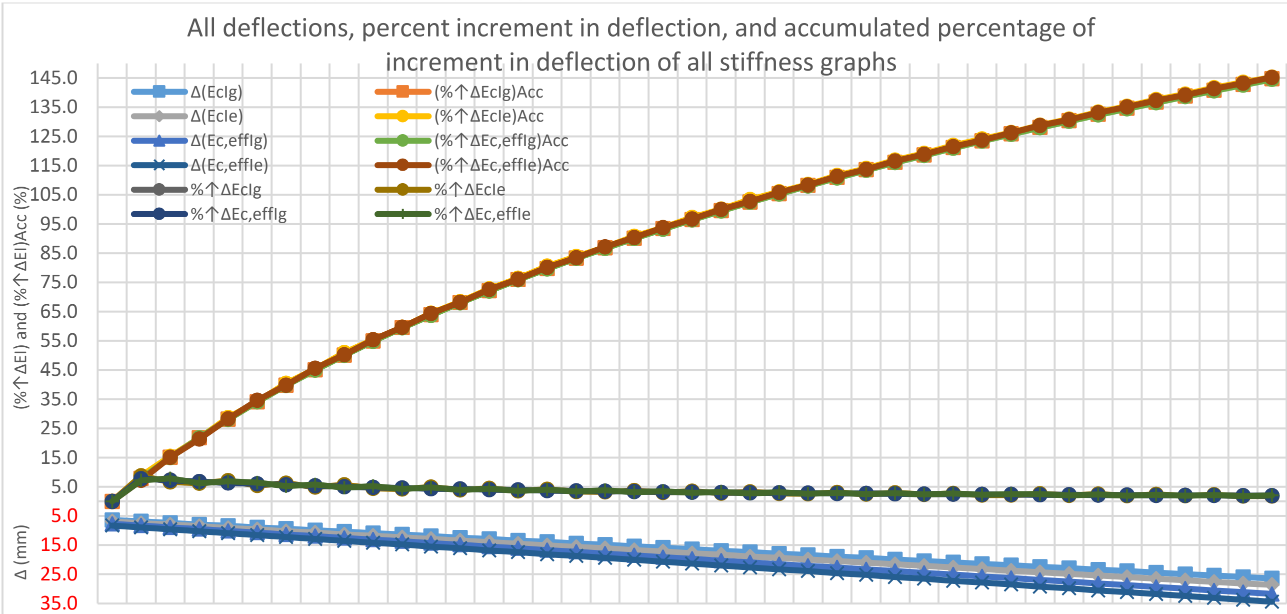

Fig. 4.56: Deflections, percent increment in deflection, and accumulated percentage of increment in deflection of all stiffnesses for rectangular section

4.2.4.3.2.3.3 Summary

Like the above case for the T-section, Tablapp 10-11 presents the detailed table. The relative magnitude of deflection data is calculated in the same fashion as that of Eqn 4-164.

$$\aleph_{\Delta} = \frac{\Delta_{E_cI}}{\Delta_{E_{c,eff}I}}$$

Thus, the table summarizes the percentage of increment amongst the four deflections calculated. The benchmark deflection against which all other deflections are critiqued is the deflection due to the E_cI_g stiffness. This is so because this expression normally gives the deflection value that does not directly count on the contributions of the steel Young modulus of elasticity (E_s).

Multiplier effect in deflection of rectangular section due to varying E and I		
Variable	**Numerical**	**Result**
$\frac{\Delta_{E_cI_g}}{\Delta_{E_cI_g}}$	$\frac{26.4}{26.4}$	$1\ time$
$\frac{\Delta_{E_cI_g}}{\Delta_{E_cI_e}}$	$\frac{26.4}{28.6}$	$0.92\ times$
$\frac{\Delta_{E_cI_g}}{\Delta_{E_{c,eff}I_g}}$	$\frac{26.4}{31.7}$	$0.83\ times$
$\frac{\Delta_{E_cI_g}}{\Delta_{E_{c,eff}I_e}}$	$\frac{26.4}{34.4}$	$0.77\ times$
$\frac{\Delta_{E_cI_g}}{\Delta_{Ave}}$	$\frac{26.4}{30.28}$	$0.87\ times$

Table 4-32: Rational comparison of deflections against the normalized deflection ($\Delta_{E_cI_g}$) for the rectangular section

Here, the data shows only a little variation in the deflection magnitude using various stiffnesses. Data for the two conditions, when compared shall provide key information as to the behavior of the deflection pattern and would assist in selecting the adopted deflection based on the various stiffness conditions. With the above data provided, it is also compelling to mention the effect that factored load would have on a structure. What would be the logic of designing a structure based on factored load but deflection is calculated against service loads and not factored loads? The point being stressed allows live load to be fully factored while maintaining the dead load unfactored! Such hypothetical instance also depends on the likelihood of major maintenance work that is to be undertaken. The results produced can also appreciably inform the study on formulating revised equations that can predict the most likely displacement magnitude in the section rather than obtaining an over-or under-exaggerated magnitude. In the table below, parenthesized deflections subscripted with a T are those for the T-section while those subscripted with an R are those for the rectangular section. Their averages are also indicated and the average of average also computed. The equation is generated as follows,

$$\Delta_\eta = \frac{(\Delta_{Ave})_T + (\Delta_{Ave})_R}{n} \qquad \text{Eqn 4-172}$$

Deflection summarization table												
Loads		**Deflections from T- analysis and rectangular analysis**								**Average Deflection**		
%LL	**DL + %LL (N/m)**	**$(\Delta E_cI_g)_T$ (mm)**	**$(\Delta E_cI_g)_R$ (mm)**	**$(\Delta E_cI_e)_T$ (mm)**	**$(\Delta E_cI_e)_R$ (mm)**	**$(\Delta E_{c,eff}I_g)_T$ (mm)**	**$(\Delta E_{c,eff}I_g)_R$ (mm)**	**$(\Delta E_{c,eff}I_e)_T$ (mm)**	**$(\Delta E_{c,eff}I_e)_R$ (mm)**	**$(\Delta_{Ave})_T$ (mm)**	**$(\Delta_{Ave})_R$ (mm)**	**Δ_η (mm)**
0.0	61270.00	3.4	6.4	2.6	6.9	0.1	7.7	0.1	8.3	**1.55**	**7.33**	***4.44***
2.5	66085.75	3.7	6.9	2.8	7.5	0.1	8.3	0.1	8.9	**1.68**	**7.90**	***4.79***
5.0	70901.50	3.9	7.4	3.0	8.0	0.1	8.9	0.1	9.6	**1.78**	**8.48**	***5.13***
7.5	75717.25	4.2	7.9	3.2	8.5	0.1	9.5	0.1	10.2	**1.90**	**9.03**	***5.47***
10.0	80533.00	4.5	8.4	3.4	9.1	0.1	10.1	0.1	10.9	**2.03**	**9.63**	***5.83***
12.5	85348.75	4.7	8.9	3.6	9.6	0.1	10.7	0.1	11.6	**2.13**	**10.20**	***6.17***
15.0	90164.50	5.0	9.4	3.8	10.2	0.2	11.3	0.1	12.2	**2.28**	**10.78**	***6.53***
17.5	94980.25	5.2	9.9	4.0	10.7	0.2	11.9	0.1	12.9	**2.38**	**11.35**	***6.87***
20.0	99796.00	5.5	10.4	4.2	11.3	0.2	12.5	0.1	13.5	**2.50**	**11.93**	***7.22***
22.5	104611.75	5.8	10.9	4.4	11.8	0.2	13.1	0.1	14.2	**2.63**	**12.50**	***7.57***
25.0	109427.50	6.0	11.4	4.6	12.3	0.2	13.7	0.1	14.8	**2.73**	**13.05**	***7.89***
27.5	114243.25	6.3	11.9	4.8	12.9	0.2	14.3	0.1	15.5	**2.85**	**13.65**	***8.25***
30.0	119059.00	6.6	12.4	5.0	13.4	0.2	14.9	0.2	16.1	**3.00**	**14.20**	***8.60***
32.5	123874.75	6.8	12.9	5.2	14.0	0.2	15.5	0.2	16.8	**3.10**	**14.80**	***8.95***
35.0	128690.50	7.1	13.4	5.4	14.5	0.2	16.1	0.2	17.4	**3.23**	**15.35**	***9.29***
37.5	133506.25	7.4	13.9	5.6	15.1	0.2	16.7	0.2	18.1	**3.35**	**15.95**	***9.65***
40.0	138322.00	7.6	14.4	5.8	15.6	0.2	17.3	0.2	18.7	**3.45**	**16.50**	***9.98***
42.5	143137.75	7.9	14.9	6.0	16.1	0.2	17.9	0.2	19.4	**3.58**	**17.08**	***10.33***
45.0	147953.50	8.2	15.4	6.2	16.7	0.2	18.5	0.2	20.0	**3.70**	**17.65**	***10.68***
47.5	152769.25	8.4	15.9	6.4	17.2	0.3	19.1	0.2	20.7	**3.83**	**18.23**	***11.03***
50.0	157585.00	8.7	16.4	6.6	17.8	0.3	19.7	0.2	21.3	**3.95**	**18.80**	***11.38***
52.5	162400.75	9.0	16.9	6.9	18.3	0.3	20.3	0.2	22.0	**4.10**	**19.38**	***11.74***
55.0	167216.50	9.2	17.4	7.1	18.9	0.3	20.9	0.2	22.6	**4.20**	**19.95**	***12.08***
57.5	172032.25	9.5	17.9	7.3	19.4	0.3	21.5	0.2	23.3	**4.33**	**20.53**	***12.43***
60.0	176848.00	9.8	18.4	7.5	19.9	0.3	22.1	0.2	23.9	**4.45**	**21.08**	***12.77***
62.5	181663.75	10.0	18.9	7.7	20.5	0.3	22.7	0.2	24.6	**4.55**	**21.68**	***13.12***
65.0	186479.50	10.3	19.4	7.9	21.0	0.3	23.3	0.2	25.2	**4.68**	**22.23**	***13.46***
67.5	191295.25	10.6	19.9	8.1	21.6	0.3	23.9	0.2	25.9	**4.80**	**22.83**	***13.82***
70.0	196111.00	10.8	20.4	8.3	22.1	0.3	24.5	0.2	26.5	**4.90**	**23.38**	***14.14***
72.5	200926.75	11.1	20.9	8.5	22.7	0.3	25.1	0.3	27.2	**5.05**	**23.98**	***14.52***
75.0	205742.50	11.4	21.4	8.7	23.2	0.3	25.7	0.3	27.8	**5.18**	**24.53**	***14.86***
77.5	210558.25	11.6	21.9	8.9	23.7	0.4	26.3	0.3	28.5	**5.30**	**25.10**	***15.20***
80.0	215374.00	11.9	22.4	9.1	24.3	0.4	26.9	0.3	29.2	**5.43**	**25.70**	***15.57***
82.5	220189.75	12.2	22.9	9.3	24.8	0.4	27.5	0.3	29.8	**5.55**	**26.25**	***15.90***
85.0	225005.50	12.4	23.4	9.5	25.4	0.4	28.1	0.3	30.5	**5.65**	**26.85**	***16.25***
87.5	229821.25	12.7	23.9	9.7	25.9	0.4	28.7	0.3	31.1	**5.78**	**27.40**	***16.59***
90.0	234637.00	13.0	24.4	9.9	26.5	0.4	29.3	0.3	31.8	**5.90**	**28.00**	***16.95***
92.5	239452.75	13.2	24.9	10.1	27.0	0.4	29.9	0.3	32.4	**6.00**	**28.55**	***17.28***
95.0	244268.50	13.5	25.4	10.3	27.6	0.4	30.5	0.3	33.1	**6.13**	**29.15**	***17.64***
97.5	249084.25	13.8	25.9	10.5	28.1	0.4	31.1	0.3	33.7	**6.25**	**29.70**	***17.98***
100.0	253900.00	14.0	26.4	10.7	28.6	0.4	31.7	0.3	34.4	**6.35**	**30.28**	***18.32***

Table 4-33: Rational comparison of deflections against the normalized deflection ($\Delta_{E_cI_g}$) for the rectangular section

From Table 4-33, the average deflection that could be associated with the section considering both cases of design, when final deflections associated with the section is yet unknown, can be formulated as follows:

$$\Delta_\eta = \frac{(\Delta_{Ave})_T + (\Delta_{Ave})_R}{n}$$

$$\Delta_\eta = \frac{\left(\Delta_{E_cI_g} + \Delta_{E_cI_e} + \Delta_{E_c,effI_g} + \Delta_{E_{c,eff}I_e}\right)_T + \left(\Delta_{E_cI_g} + \Delta_{E_cI_e} + \Delta_{E_c,effI_g} + \Delta_{E_{c,eff}I_e}\right)_R}{n}$$

Since there are possibly eight cases of deflection given the conditions being satisfied, n could be substituted by 8.

$$\Delta_\eta = \frac{\left(\Delta_{E_cI_g} + \Delta_{E_cI_e} + \Delta_{E_c,effI_g} + \Delta_{E_{c,eff}I_e}\right)_T + \left(\Delta_{E_cI_g} + \Delta_{E_cI_e} + \Delta_{E_c,effI_g} + \Delta_{E_{c,eff}I_e}\right)_R}{8}$$

$$\Delta_\eta = \frac{\left(\frac{5wl^4}{384E_cI_g} + \frac{5wl^4}{384E_cI_e} + \frac{5wl^4}{384E_{c,eff}I_g} + \frac{5wl^4}{384E_{c,eff}I_e}\right)_T + \left(\frac{5wl^4}{384E_cI_g} + \frac{5wl^4}{384E_cI_e} + \frac{5wl^4}{384E_{c,eff}I_g} + \frac{5wl^4}{384E_{c,eff}I_e}\right)_R}{8}$$

$$\Delta_\eta = \frac{\left(\frac{5wl^4}{384}\right)\left(\frac{1}{E_cI_g} + \frac{1}{E_cI_e} + \frac{1}{E_{c,eff}I_g} + \frac{1}{E_{c,eff}I_e}\right)_T + \left(\frac{5wl^4}{384}\right)\left(\frac{1}{E_cI_g} + \frac{1}{E_cI_e} + \frac{1}{E_{c,eff}I_g} + \frac{1}{E_{c,eff}I_e}\right)_R}{8}$$

Thus, the final equation can be written as,

$$\Delta_\eta = \frac{\left\{\left\{\frac{5wl^4}{384}\right\}\left[\left(\frac{1}{E_cI_g} + \frac{1}{E_cI_e} + \frac{1}{E_{c,eff}I_g} + \frac{1}{E_{c,eff}I_e}\right)_T + \left(\frac{1}{E_cI_g} + \frac{1}{E_cI_e} + \frac{1}{E_{c,eff}I_g} + \frac{1}{E_{c,eff}I_e}\right)_R\right]\right\}}{8} \qquad \textit{Eqn 4-173}$$

Fig. 4.57 shows close agreement between/amongst:

1. Deflection due to E_cI_g stiffness of the T- section to the averaged section
2. Deflection due to all stiffnesses of the rectangular section are less than 20% apart.

Findings here are further discussed in further sections.

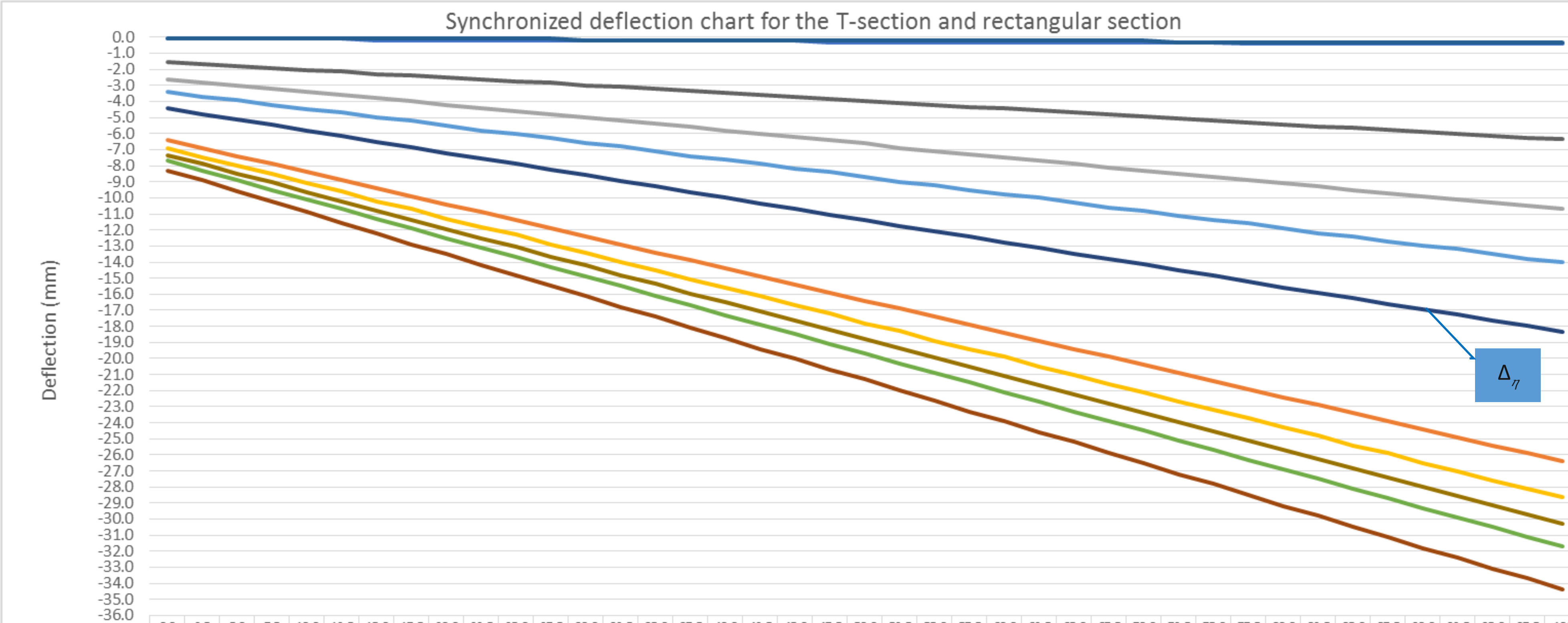

	0.0	2.5	5.0	7.5	10.0	12.5	15.0	17.5	20.0	22.5	25.0	27.5	30.0	32.5	35.0	37.5	40.0	42.5	45.0	47.5
(ΔEclg)T	-3.4	-3.7	-3.9	-4.2	-4.5	-4.7	-5.0	-5.2	-5.5	-5.8	-6.0	-6.3	-6.6	-6.8	-7.1	-7.4	-7.6	-7.9	-8.2	-8.4
(ΔEclg)R	-6.4	-6.9	-7.4	-7.9	-8.4	-8.9	-9.4	-9.9	-10.4	-10.9	-11.4	-11.9	-12.4	-12.9	-13.4	-13.9	-14.4	-14.9	-15.4	-15.9
(TΔEcle)T	-2.6	-2.8	-3.0	-3.2	-3.4	-3.6	-3.8	-4.0	-4.2	-4.4	-4.6	-4.8	-5.0	-5.2	-5.4	-5.6	-5.8	-6.0	-6.2	-6.4
(ΔEcle)R	-6.9	-7.5	-8.0	-8.5	-9.1	-9.6	-10.2	-10.7	-11.3	-11.8	-12.3	-12.9	-13.4	-14.0	-14.5	-15.1	-15.6	-16.1	-16.7	-17.2
(ΔEc,efflg)T	-0.1	-0.1	-0.1	-0.1	-0.1	-0.1	-0.2	-0.2	-0.2	-0.2	-0.2	-0.2	-0.2	-0.2	-0.2	-0.2	-0.2	-0.2	-0.2	-0.3
(ΔEc,efflg)R	-7.7	-8.3	-8.9	-9.5	-10.1	-10.7	-11.3	-11.9	-12.5	-13.1	-13.7	-14.3	-14.9	-15.5	-16.1	-16.7	-17.3	-17.9	-18.5	-19.1
(ΔEc,effle)T	-0.1	-0.1	-0.1	-0.1	-0.1	-0.1	-0.1	-0.1	-0.1	-0.1	-0.1	-0.1	-0.2	-0.2	-0.2	-0.2	-0.2	-0.2	-0.2	-0.2
(ΔEc,effle)R	-8.3	-8.9	-9.6	-10.2	-10.9	-11.6	-12.2	-12.9	-13.5	-14.2	-14.8	-15.5	-16.1	-16.8	-17.4	-18.1	-18.7	-19.4	-20.0	-20.7
(ΔAve)T	-1.55	-1.68	-1.78	-1.90	-2.03	-2.13	-2.28	-2.38	-2.50	-2.63	-2.73	-2.85	-3.00	-3.10	-3.23	-3.35	-3.45	-3.58	-3.70	-3.83
(ΔAve)R	-7.33	-7.90	-8.48	-9.03	-9.63	-10.2	-10.7	-11.3	-11.9	-12.5	-13.0	-13.6	-14.2	-14.8	-15.3	-15.9	-16.5	-17.0	-17.6	-18.2
Δ	-4.44	-4.79	-5.13	-5.47	-5.83	-6.17	-6.53	-6.87	-7.22	-7.57	-7.89	-8.25	-8.60	-8.95	-9.29	-9.65	-9.98	-10.3	-10.6	-11.0

	50.0	52.5	55.0	57.5	60.0	62.5	65.0	67.5	70.0	72.5	75.0	77.5	80.0	82.5	85.0	87.5	90.0	92.5	95.0	97.5	100
(ΔEclg)T	-8.7	-9.0	-9.2	-9.5	-9.8	-10.0	-10.3	-10.6	-10.8	-11.1	-11.4	-11.6	-11.9	-12.2	-12.4	-12.7	-13.0	-13.2	-13.5	-13.8	-14.0
(ΔEclg)R	-16.4	-16.9	-17.4	-17.9	-18.4	-18.9	-19.4	-19.9	-20.4	-20.9	-21.4	-21.9	-22.4	-22.9	-23.4	-23.9	-24.4	-24.9	-25.4	-25.9	-26.4
(TΔEcle)T	-6.6	-6.9	-7.1	-7.3	-7.5	-7.7	-7.9	-8.1	-8.3	-8.5	-8.7	-8.9	-9.1	-9.3	-9.5	-9.7	-9.9	-10.1	-10.3	-10.5	-10.7
(ΔEcle)R	-17.8	-18.3	-18.9	-19.4	-19.9	-20.5	-21.0	-21.6	-22.1	-22.7	-23.2	-23.7	-24.3	-24.8	-25.4	-25.9	-26.5	-27.0	-27.6	-28.1	-28.6
(ΔEc,efflg)T	-0.3	-0.3	-0.3	-0.3	-0.3	-0.3	-0.3	-0.3	-0.3	-0.3	-0.3	-0.4	-0.4	-0.4	-0.4	-0.4	-0.4	-0.4	-0.4	-0.4	-0.4
(ΔEc,efflg)R	-19.7	-20.3	-20.9	-21.5	-22.1	-22.7	-23.3	-23.9	-24.5	-25.1	-25.7	-26.3	-26.9	-27.5	-28.1	-28.7	-29.3	-29.9	-30.5	-31.1	-31.7
(ΔEc,effle)T	-0.2	-0.2	-0.2	-0.2	-0.2	-0.2	-0.2	-0.2	-0.2	-0.3	-0.3	-0.3	-0.3	-0.3	-0.3	-0.3	-0.3	-0.3	-0.3	-0.3	-0.3
(ΔEc,effle)R	-21.3	-22.0	-22.6	-23.3	-23.9	-24.6	-25.2	-25.9	-26.5	-27.2	-27.8	-28.5	-29.2	-29.8	-30.5	-31.1	-31.8	-32.4	-33.1	-33.7	-34.4
(ΔAve)T	-3.95	-4.10	-4.20	-4.33	-4.45	-4.55	-4.68	-4.80	-4.90	-5.05	-5.18	-5.30	-5.43	-5.55	-5.65	-5.78	-5.90	-6.00	-6.13	-6.25	-6.35
(ΔAve)R	-18.8	-19.3	-19.9	-20.5	-21.0	-21.6	-22.2	-22.8	-23.3	-23.9	-24.5	-25.1	-25.7	-26.2	-26.8	-27.4	-28.0	-28.5	-29.1	-29.7	-30.2
Δ	-11.3	-11.7	-12.0	-12.4	-12.7	-13.1	-13.4	-13.8	-14.1	-14.5	-14.8	-15.2	-15.5	-15.9	-16.2	-16.5	-16.9	-17.2	-17.6	-17.9	-18.3

DL + %LL [%] (N/m)

(ΔEclg)T (ΔEclg)R (TΔEcle)T (ΔEcle)R (ΔEc,efflg)T (ΔEc,efflg)R (ΔEc,effle)T (ΔEc,effle)R (ΔAve)T (ΔAve)R Δ

Fig. 4.57: Comparative representative line graph of all T- and rectangular deflections calculated (Table 4-33)

4.2.4.4 Profile of vertical crack

When a beam is loaded, it reacts in several ways depending on the composition of the section. Theories, experiments and practice have all reported that due to the non-linerity of the stress-strain curve of concrete and the change in moment of inertia from the gross to transformed and then to cracked, the beam also follows such non-linearity pattern in its response to the effects of the applied load. Cracks reduce the strength of a section. As cracks begin to propagate, they force the Neutal Axis upward to the compression face proportionally to the form and manner by which the load increment occurs. This happens till the tension concrete can no longer hold stresses in tension. Logical implications thus correlate that the maximum height of crack is the cracked neutral axis. A recently published article [38] which studied many bridges across the United States, discusses some key aspects that lead to cracking. For cracks do not only depend on the effects of load, the article studied concrete paste, concrete strength, the temperature during placement, the method of concrete placement, environmental factors, and slump requirements etc. In most common structural designs for cracks, the arrangement of the tension steel has a varying impact on the estimated magnitude of the imminent cracks. When tension bars are layered rather than being in a single row, the area of crack increases. Thus, the area of concrete in tension (A_{ten}) equals

$$A_{ten} = yb \qquad \text{Eqn 4-174}$$

4.2.4.4.1 Vertical cracks

Vertical cracks are those that run parallel (but which is practically rare) to the depth of the beam. Cracks in general are very unpredictable because the dimension of cracks vary from the concrete surface to the concrete-steel periphery. [20] finds out that these cracks are wider on the surface than at the bonding area. It further stresses that some of the several irregularities associated with cracks are due to the improper considerations given the bond-slip relationship that exists between the principal elements around the area under consideration (i.e., the tensile concrete and the reinforcing bar), theories relating to the behavior of the nonlinearity of the fracture mechanics of the tensile reinforced concrete, and the bonding mechanisms associated with the aggregates. When these conditions are appreciably satisfied, theoretical crack profiles would normally agree with experimental crack profiles.

4.2.4.4.1.1 Bar spacing, tension area, and area of crack relationship

Considering a few probable arrangements of the area in tension as contained in Fig. 4.25, let

- y = equal distance to d on both sides (bottom and top) of the longitudinal reinforcement.
- $b = b_w$

$$y = 2cc + \phi_s + 3\phi_d + 2S \qquad \text{Eqn 4-175}$$

The term "equal distance to d" means the same distance from the surface of the concrete cover to the point where the d stops should also be applicable to the upper last tension steel within the girder.

- 2cc = 2(50 mm) = 100 mm
- ϕ_s = 12.2 mm = 12.2 mm
- $3\phi_d$ = 3(32.5 mm) = 97.5 mm
- 2S = 2(50 mm) = <u>100 mm</u>

y = 309.7 mm = 310 mm

A ratio of the most likely possible spacing to that of the adopted spacing ($\aleph_s$) gives the magnitude by which the most possible incremental factor for the spacing may be adjusted. The most possible spacing is calculated from Eqn 4-90. The factor is the judgement of the designer.

$$\aleph_s = \frac{S_{poss}}{S} \qquad \text{Eqn 4-176}$$

$$\aleph_s = \frac{370\ mm}{50\ mm} = 7.4$$

Henceforth, the most possible spacing is almost seven-and-half times larger than the adopted spacing. So, arbitrarily dividing this 7.4 equally, yields a constant by which the spacing is adjusted ($\aleph_{s_k}$) to reach/match that which is calculated.

$$\aleph_{s_k} = \frac{\aleph_s}{k} \qquad \text{Eqn 4-177}$$

In this case, dividing by an arbitrary constant (k), say 15 (chosen at the design conscience of the designer, but should be reasonable enough), the following constant is obtained.

$$\aleph_{s_k} = \frac{7.4}{15} = 0.49\ or\ 49\%$$

The table below summarizes the inputs with respect to the height of probable tension area and the area of crack. Thus, the increment in spacing leading up to the maximum spacing (S_{s_k}) is a function $\aleph_{s_k}$.

$$S_{s_k} = S + S\#\aleph_{s_k} \qquad \text{Eqn 4-178}$$

In Eqn 4-178, S is the adopted side bar spacing (i.e., between layers of longitudinal reinforcing bars) while # is the sequence along which $\aleph_{s_k}$ changes. The equation is further simplified to:

$$S_{s_k} = S(S + \#\aleph_{s_k})$$

Hence, with the three layers of tension bar, at the adopted spacing, the area under tension susceptible to immediate cracking is given as

$$A_{ten} = (310\ mm)(500\ mm) = 155000\ mm^2$$

As the spacing increases, the neutral axis is approached until it is covered in cracks (see Table 4-34). However, the instance under which the neutral axis is covered (i.e., it falls within the spacing between two bars) is not covered into this research.

#	2cc (mm)	ϕ_t (mm)	ϕ_s (mm)	s (mm)	y (mm)	b_w (mm)	A_{ten} (mm^2)	A_{cr} (mm^2)	s/y	$\aleph\Delta_{(s/y)}$ (%)	$\aleph_A$ (%)
0	100	12	98	50	310	500	155000	8611	*0.1613*	-	-
1	100	12	98	75	360	500	180000	10000	*0.2083*	*4.70*	*86*
2	100	12	98	99	408	500	204000	11333	*0.2426*	*3.43*	*88*
3	100	12	98	124	458	500	229000	12722	*0.2707*	*2.81*	*89*
4	100	12	98	148	506	500	253000	14056	*0.2925*	*2.18*	*91*
5	100	12	98	173	556	500	278000	15444	*0.3112*	*1.87*	*91*
6	100	12	98	197	604	500	302000	16778	*0.3262*	*1.50*	*92*
7	100	12	98	222	654	500	327000	18167	*0.3394*	*1.32*	*92*
8	100	12	98	246	702	500	351000	19500	*0.3504*	*1.10*	*93*
9	100	12	98	271	752	500	376000	20889	*0.3604*	*1.00*	*93*
10	100	12	98	295	800	500	400000	22222	*0.3688*	*0.84*	*94*
11	100	12	98	320	850	500	425000	23611	*0.3765*	*0.77*	*94*
12	100	12	98	344	898	500	449000	24944	*0.3831*	*0.66*	*95*
13	100	12	98	369	948	500	474000	26333	*0.3892*	*0.61*	*95*

Table 4-34: The Spacing-Heigh-Area (S-H-A) adjustment table

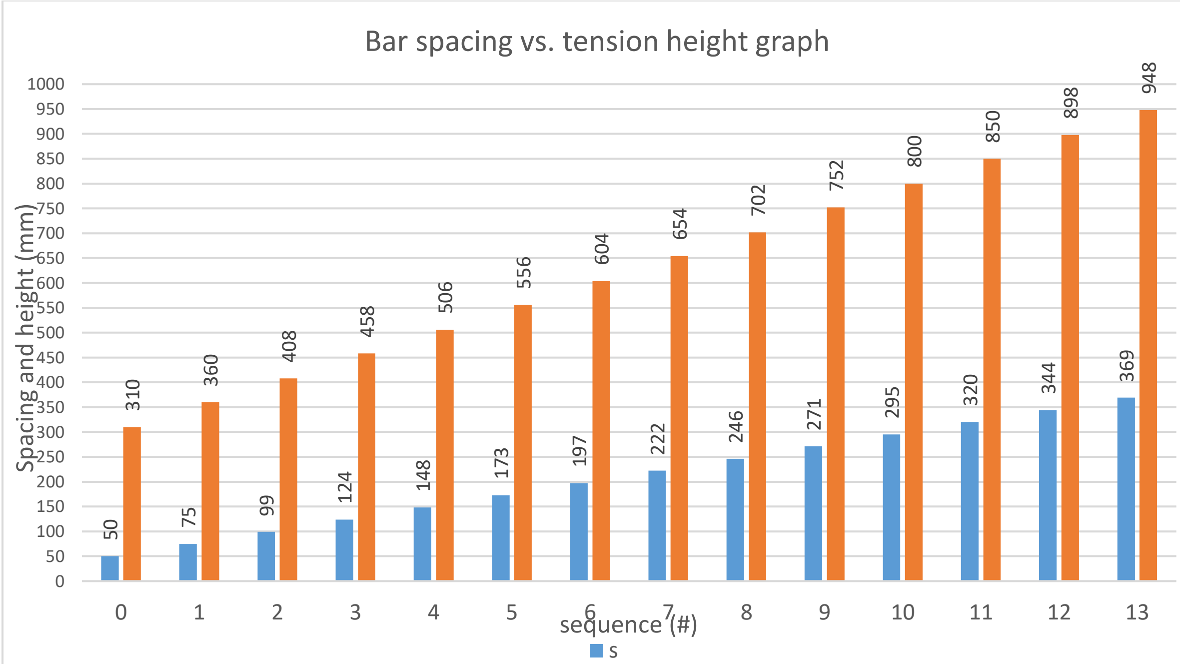

Fig. 4.58: Graphical representation of the Spacing-Height (S-H) relationship from Table 4-34

The relative change that occurs in the tension height due to the change in spacing (s/y) is on a downward trajectory. The magnitude, in percentage, is represented by column $\Delta_{(s/y)}$.

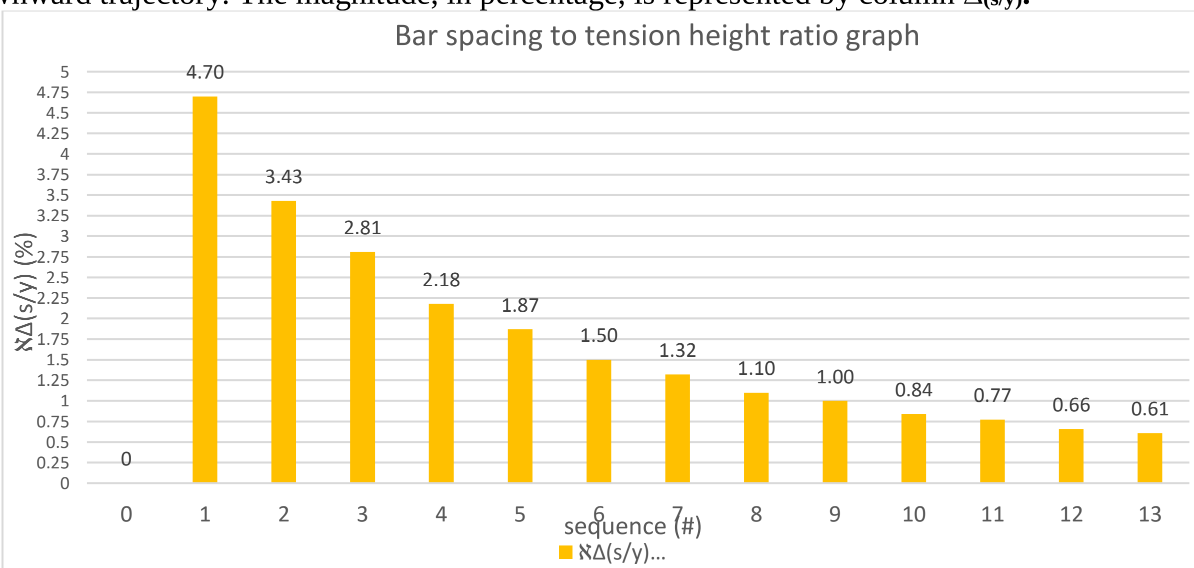

Fig. 4.59: Graphical representation of the diminishing trend of percent increment in Spacing-Height (S-H) relationship

The nominal area (A_0) is the original tension area as based on the calculations contained herein. Other areas (A_1 to A_{13}) are based on the iterations wherein A_0 is consecutively multiplied by the 0.49 incremental factor. This is so done to vividly compare how the area of crack responds to change in the tension area. Hence, the area of the section under consideration susceptible to cracking is given as the quotient of the susceptible cracking area to the total number of tensile bars.

$$A_{cr} = \frac{A_{ten}}{N} \qquad \text{Eqn 4-179}$$

$$A_{cr} = \frac{155500\ mm^2}{18} = 8611\ mm^2$$

From Table 4-34, the following notations represent:

#: the sequence of adjusting the spacing
2cc: twice the concrete to d on both top and bottom of the longitudinal reinforcement (mm)
Φ_t: diameter of the longitudinal reinforcement (mm)
Φ_s: diameter of the lateral/stirrup reinforcement (mm)
s: vertical spacing between longitudinal spacing in-to-in (mm)
y: height of concrete in tension due to the current spacing adopted (mm)
b_w: width of girder (mm)
A: area of concrete in tension (mm^2)
A_{cr}: area of crack (mm^2)

It is established that as the spacing increases, the height and area in tension also increase. Hence, the percentage of increase in the area ($\aleph_A$) corresponding to the increment in spacing can be represented as follows:

$$\aleph_A = \frac{A_1}{A_0} - 1 \qquad \text{Eqn 4-180}$$

$$\aleph_A = \frac{180000\,mm^2}{155000\,mm^2} - 1 = 16\%$$

The impact an increment in spacing has on increment in the tension area ($\aleph_{s_k,A}$) informs the research of the cross-over magnitudinal effect an increment in spacing has against the tension area. It can be represented as:

$$\aleph_{s_k,A} = \frac{\aleph_{s_k}}{\aleph_A} \qquad \text{Eqn 4-181}$$

$$\aleph_{s_k,A} = \frac{49}{16} = 3.06$$

Thus, an impact factor of 3.06 exists between spacing and tension area. However, following the same procedure above, but with a more compact spacing increment of 1% till the maximum possible spacing is achieved, the graph takes the same shape but with some modifications and can be represented as illustrated in the following graphs (Fig. 4.60, and Fig. 4.61) below. This smoothing gives a more exact picture of the trend. An increment in the spacing definitely leads to an increment in the tension height but the percentage by which the increment takes place is in twofold: a somewhat slight steady pattern and then a constantly increase-decrease fashion at the end of the graph.

The two graphs below depict the steady then increase-decrease relationship in the ratio of spacing to height when a compact ratio is used.

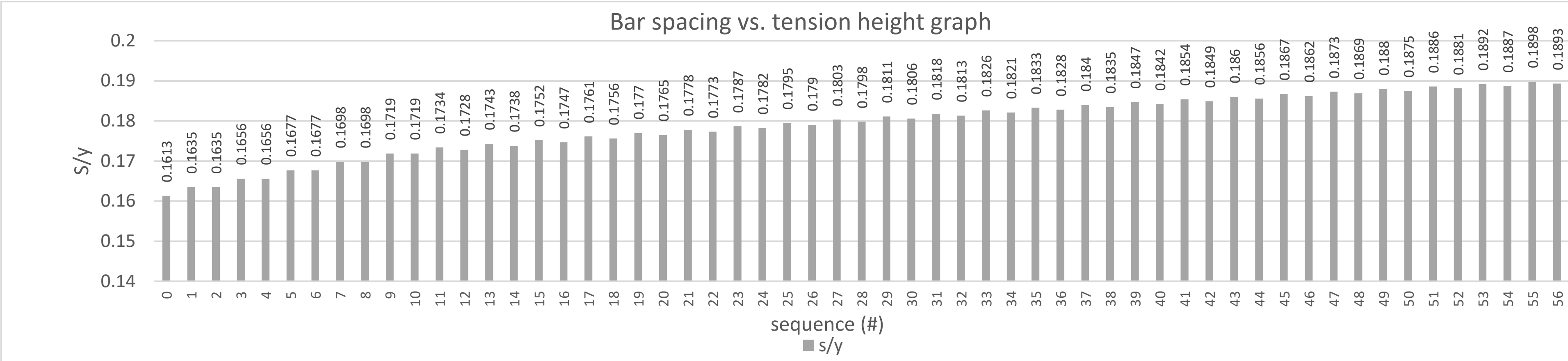

Fig. 4.60: Portion of the more compact spacing to height relationship showing steadiness

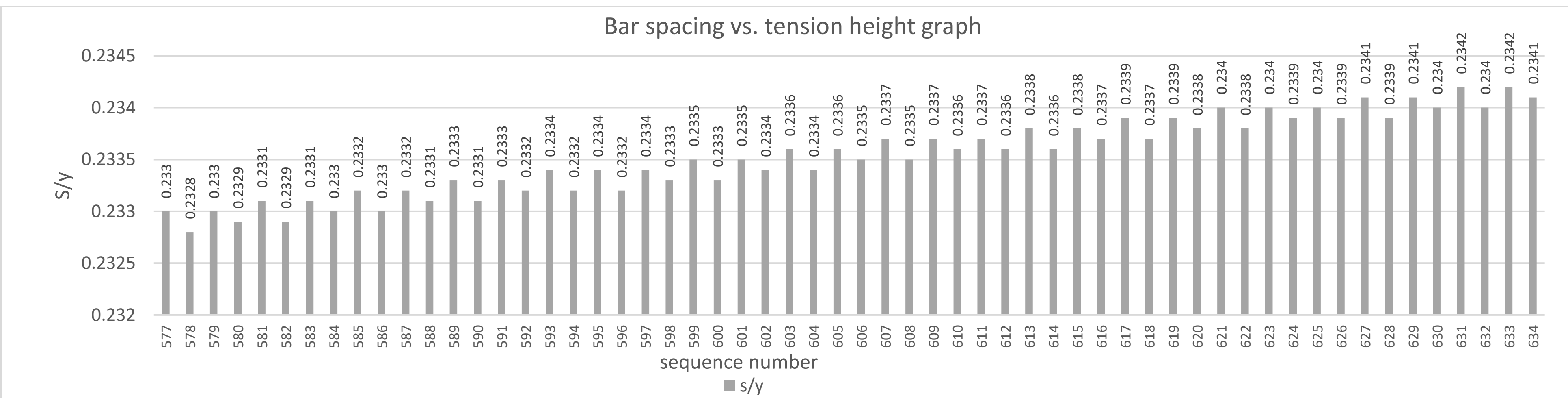

Fig. 4.61: Portion of the more compact spacing to height relationship showing the increase-decrease phenomenon

4.2.4.4.1.2 Width of vertical crack

The width of vertical crack is a function of force and distance. This is due to the interaction that exists between the concerned concrete area and the steel stress. Several codes and experimental works have produced equations for cracks parameters. Yet there is no definite equation that exactly quantifies these parameters. One of the most notable equations, The Gergely-Lutz equation [39] is widely adopted in estimating cracks profile. It is also worthwhile noting that analysis involving other composites also follow these procedures but with add-ons. Hence, [40] compiled and compared several equations of several codes on cracks and then compared them against experimental results and concluded on a couple of findings to include statements in the form of:

a. that polymers enhance the width of cracks,
b. some codes need to investigate their equations governing cracks,
c. that the strain in the steel contributes immensely to the properties of the cracks, etc.

Hence, the basic equations for calculating crack profile in different codes are discussed below.

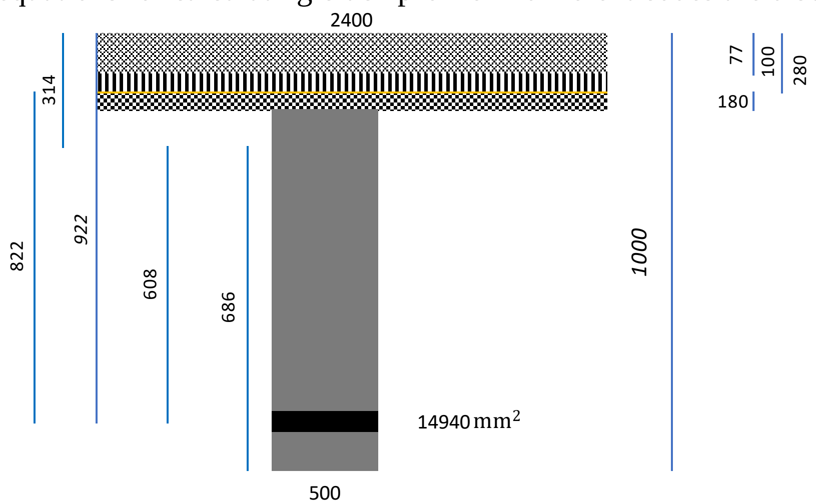

Fig. 4.62 (for easier reference): Detailed dimensions associated with the T-girder

4.2.4.4.1.2.1 ACI and AREMA approaches

[41], [2], and [16] have all stressed the need that the stress in the reinforcing steel shall not exceed certain limit in order to attain a more reasonable crack width. [2]'s eq. 2-60 states that the stress in the steel be represented as

$$f_s = \frac{Z}{\sqrt[3]{d_c A_{cr}}} \qquad \text{Eqn 4-182}$$

…where f_s is the reinforcement steel tensile stress when considering an instance of service loads but barred from exceeding fifty percent of that of the yield strength of the steel ($\leq 0.5f_y$), in MPa. Other codes also limit f_s to $0.6f_y$, Z covers the manner and form by which flexural reinforcement is limited (kN/mm), d_c is the depth of concrete cover up to the effective depth (mm), but not greater than $d_{c_{max}}$, A_{cr} equals the area of crack (mm^2), $d_{c_{max}}$ is the maximum allowable thickness of concrete cover in the calculation of concrete crack width.

$$d_{c_{max}} = 50\ mm + 0.5\phi_s \qquad \text{Eqn 4-183}$$

$d_{c_{max}} = 50\ mm + 0.5(32.5\ mm) = 66.25\ mm \approx 66\ mm$

The expression for the most probable maximum crack width (w_{max}) in mm, as contained in [42] is

$$w_{max} = 0.001(0.011)\beta f_s \sqrt[3]{d_c A_{cr}}) \times 10^{-3} \qquad \text{Eqn 4-184}$$

Section 2.39b of the code [2] permits the value of Z to 30 kN/mm when the structure is to be constructed in a moderate exposure condition and also 23 kN/mm if in a severe exposure condition. By far, almost all parameters being used from the onset are based on moderate exposure condition.

$$Z = f_s \sqrt[3]{d_c A_{cr}}$$

The design crack width can then be computed as

$$w_{max} = 0.001(0.011\beta Z)$$

The value of β though normally taken at 1.2, [2] [16] [40] concord that it can be calculated as:

$$\beta = \frac{t_{gir} - c}{d - c} \quad \text{Eqn 4-185}$$

$$\beta = \frac{1000 - 100}{922 - 100} = 1.1$$

Hence,

$$w_{max} = 0.001[0.011(1.1)30] = 0.0004\,mm$$

From the equation, the equivalent tensile stress in the steel as a result of Z has to be verified in order to substantiate the result of the crack width obtained.

$$d_c = cc + \phi_t + 0.5\phi_s \quad \text{Eqn 4-186}$$

$d_c = 50\,mm + 12.2\,mm + 0.5(32.5\,mm) = 78.45 = 78\,mm > 66\,mm,$ thus

$$d_c = d_{c_{max}} = 66\,mm$$

$$f_s = \frac{30\frac{KN}{mm}}{\sqrt[3]{(66\,mm)(8611\,mm^2)}} = 0.362\frac{kN}{mm^2} = 362\frac{N}{mm^2} = 362 \times 10^6\frac{N}{m^2} = 362\,MPa$$

As seen from the value of f_s, it is apparent that the stress in the steel is astronomically higher than the limiting value of $0.5f_y$ as well as $0.6f_y$ even if it is adopted.

$f_s = 343 > 0.6(420) > 252\,MPa > 0.5(420) > 210\,MPa \ldots\ldots..Not\ satisfactory$!

Because f_s is greater than $0.5f_y$, the percent of unacceptability of stress in the steel ($\aleph_{fs}$) expression can then be formulated as

$$\aleph_{fs} = \frac{f_s}{0.5f_y} - 1 \quad \text{Eqn 4-187}$$

$$\aleph = \frac{362}{210} - 1 = 0.72381 = 72\%$$

The stress calculated based on the maximum Z value is 72% higher than the allowable. [43] provides that the stress in the steel has a direct relationship with the modulus of rupture.

$$f_s = \left(\left(\frac{1}{\rho}\right) - 1 + n\right) f_t \quad \text{Eqn 4-188}$$

Substituting the reinforcement ratio (section 4.1.5.7 above), the modular ratio (Eqn 4-155), and the tensile strength of concrete which has been equated to that of the modulus of rupture (Eqn 4-137), the stress in the steel can be estimated as:

$$f_s = \left(\left(\frac{1}{0.031}\right) - 1 + 7\right)(3.92\,MPa) = 150\,MPa$$

Note, this value is much accurately placed as required by the limit of which according to [2] f_s shall not exceed, i.e., $0.5f_y$.

$f_s = 150\,MPa < 0.5(420\,MPa) = 150\,MPa < 210\,MPa \ldots\ldots..satisfactory$!

Thus, resubstituting in the crack width equation,

$$w_{max} = 0.001 \left[0.011(1.1)\left(150 \frac{MN}{m^2}\right) \sqrt[3]{(66\ mm)(8611\ mm^2)}\right] \times 10^{-3} = 0.00015\ m = 0.15\ mm$$

The relation between the crack width and the mean crack spacing is represented as follows:

$$w_{max} = \beta s_{rm} \xi \epsilon_2, \qquad \text{Eqn 4-189}$$

…wherein the mean crack width to the maximum crack width coefficient β is equal to 1.7. It is of great importance to discuss a little further on the tension stiffening parameter included in this equation. Tension stiffening mechanisms can simply be put as a serviceability technique that enhances the effectiveness of concrete in tension especially when considering deformation and crack analyses. [44] outlines several cardinal tension stiffening mechanisms which have proven exceptionally well against experimental results involving crack and deflection investigations. A simple and very widely used and effective tension stiffening method is the use of tensile stress block. Several authors and codes have their take on the relationship between the tensile strain and tensile stress as indicated below [44].

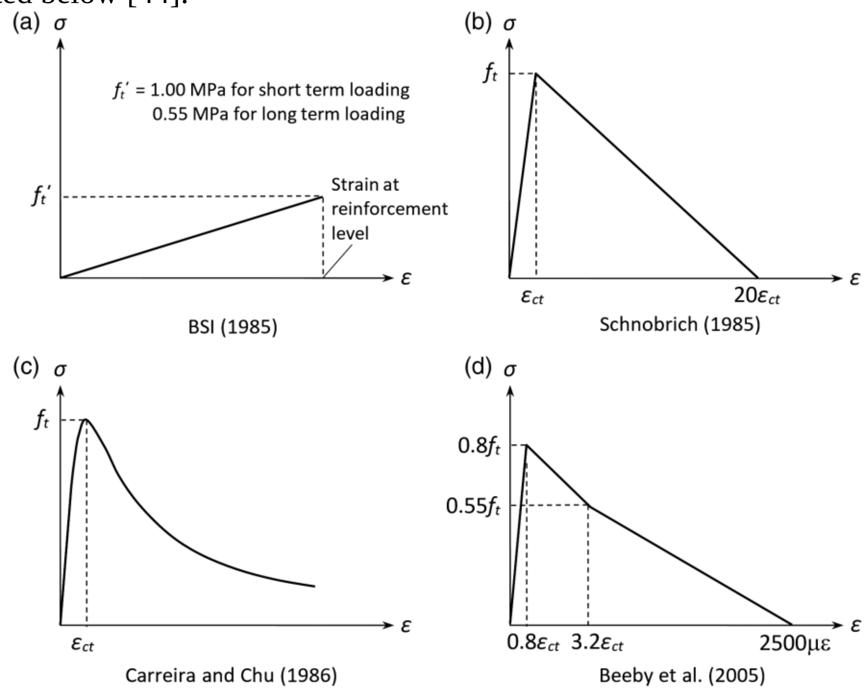

Fig. 4.63 Tensile stress block from different authors

High-strength concrete, increased allowable steel stress, etc. perfect tension stiffener. Tension stiffening enhances the width of crack. The codes provide coefficients for tension stiffening in the absence of detailed calculations wherein the tension-stiffening coefficient ξ can be represented as follows:

$$\xi = \begin{Bmatrix} 0 & M_k < M_{cr} \\ 1 - \beta_1 \beta_2 \left(\frac{M_{cr}}{M_k}\right)^2 & M_k > M_{cr} \end{Bmatrix} \qquad \text{Eqn 4-190}$$

As earlier calculated, because the design moment is greater than the cracking moment, the lower equation of (Eqn 4-190) is adopted. This equation proved effective in (Crack Width Prediction for Concrete Beams Strengthened with Carbon FRP Composites).

$\xi = 1 - 1(1)\left(\frac{450}{3998.94}\right)^2 = 0.987$ considering short-term loading condition.

$\xi = 1 - 1(0.5)\left(\frac{450}{3998.94}\right)^2 = 0.994$ considering cyclic/long-term loading condition.

Furthermore, considering the deformation that occurs in a cracked section, there must be a strain associated with the section ($\boldsymbol{\epsilon_2}$) that has undergone such crack. Said strain can be calculated as

$$\epsilon_2 = \frac{T_R + E_f A_f \varepsilon_0}{E_s A_s + E_f A_f} \quad \text{Eqn 4-191}$$

Eliminating the nonapplicable parameters and substituting the value of T_R, the cracked reinforcement strain is obtained. Comparably, the gross, uncracked reinforcement strain of Eqn 4-108 and the cracked reinforcement strain do not extensively differ.

$$T_R = \frac{M_k}{z_e} \quad \text{Eqn 4-192}$$

$$\epsilon_2 = \frac{\frac{3998940\ N.m}{0.884\ m}}{(2x10^{11}\frac{N}{m^2})(0.01494\ mm^2)} = 0.001514$$

In the above equation, z_e is the moment arm (the distance over which the tensile force acts towards the compressive force). To obtain the cracked strain, the acting moment on the section is utilized in the equation. Thus, the mean spacing between the cracks (i.e., the mean crack spacing), s_{rm} is a function of four parameters, to include the mean tensile strength of concrete, the effective area of the concrete in tension, bond stress associated with the steel in the present condition, and the bond perimeter associated with the reinforcement present.

$$s_{rm} = \frac{2f_{ctm}A_{c,eff}}{\tau_{sm}u_s} \quad \text{Eqn 4-193}$$

The mean tensile strain of concrete (f_{ctm}) is,

$$f_{ctm} = 0.3\sqrt[3]{(f_c')^2} \quad \text{Eqn 4-194}$$

$$f_{ctm} = 0.3\sqrt[3]{\left(f_c'\right)^2} = 0.3\sqrt[3]{(40)^2} = 3.5\ MPa$$

The effective area in tension ($A_{c,eff}$) is the lesser of the two equations.

$$A_{c,eff} = lesser\ of \begin{Bmatrix} 2.5w_{gir}\left(t_{gir} - d_s\right) \\ \frac{b\left(t_{gir} - c\right)}{3} \end{Bmatrix} \quad \text{Eqn 4-195}$$

$$A_{c,eff} = lesser\ of \begin{Bmatrix} 2.5(0.5\ m)(1.0\ m - 0.922\ m) = 0.0975 \\ \frac{0.5(1.0\ m - 0.1\ m)}{3} = 0.15 \end{Bmatrix} = 0.0975\ m^2$$

The mean bond stress (τ_{sm}) contributed by the bonding of concrete and rebars can be estimated as

$$\tau_{sm} = 1.8f_{ctm} \quad \text{Eqn 4-196}$$

$$\tau_{sm} = 1.8f_{ctm} = 1.8(3.5\ MPa) = 6.3\ MPa$$

The mean bond perimeter (u_s) is a function of the total reinforcement bars and its diameter.

$$u_s = Q_s\pi\phi_s \quad \text{Eqn 4-197}$$

$$u_s = 18(3.14)(32.5\ mm) = 1836.9\ mm = 1.8369\ m$$

Thus,

$$s_{rm} = \frac{2(3.5MPa)(0.0975\ m^2)}{(6.3\ MPa)(1.8369\ m)} = 0.059\ m = 59\ mm$$

Also, the maximum length over which the bar slips thus causing a crack, ($l_{s,max}$). It is synonymous to the length over which the crack occurs.

$$l_{s,max} = \frac{\emptyset_s}{3.6\rho_{s,eq}} \quad \text{Eqn 4-198}$$

$$l_{s,max} = \frac{\emptyset_s}{3.6(A_s/A_{c,eff})} = \frac{32.5\ mm}{(3.6)\left(\frac{0.01494\ mm^2}{0.0975\ mm^2}\right)} = 58.92\ mm \approx 59\ mm$$

The both equations have yielded the same result thus proving correlation. However, the maximum crack spacing is a half greater than the the adopted spacing.

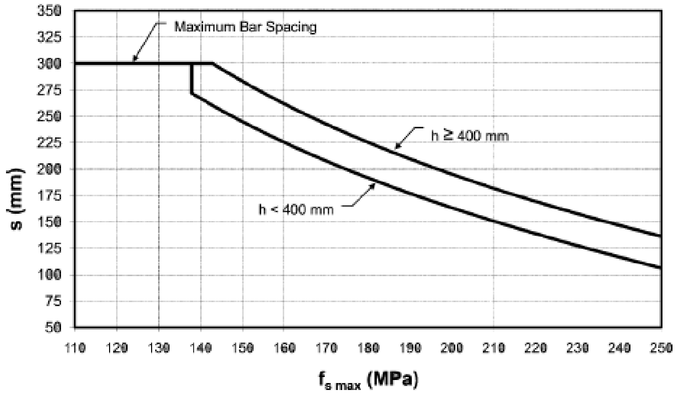

Fig. 4.64: Graphical Relationship between steel stress and spacing for normal exposure of one-way elements. [26]

The calculated bar spacing of 40 mm in the bottom face (for flexural crack) is well below the maximum stipulated value associated with flexural crack to sustainably minimize the cracks.

$w_{max} = \beta s_{rm}\xi\epsilon_2 = 1.7(59\ mm)(0.994)(0.001514) = 0.15\ mm$

The most probable crack width is analytically the most unlikely dimension of the crack width associated with the steel stress of a particular section. It is somehow rarely achievable. Table 4-35 when compared with the design crack width (Eqn 4-184 and Eqn 4-189), proves to be greater.

Exposure condition	Crack width	
	in.	mm
Dry air or protective membrane	0.016	0.41
Humidity, moist air, soil	0.012	0.30
Deicing chemicals	0.007	0.18
Seawater and seawater spray, wetting and drying	0.006	0.15
Water-retaining structures†	0.004	0.10

Table 4-35: ACI 224R-01 Recommened crack width table

However, with time, actual crack width may exceed design and maxima crack widths. Like the spacing, the calculated crack width is also well below the maximum stipulated value also.

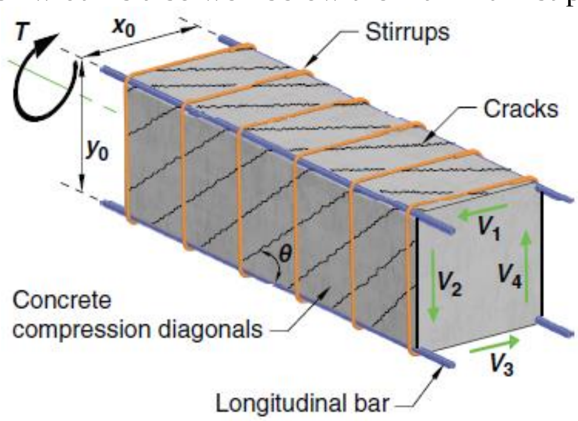

Courtesy: [16]

Fig. 4.65: Representation of diagonal flexural cracks, stirrups, longitudinal bars and shear in a beam

As unpredictable cracks may be, consider a hypothetical case wherein a vertical crack intercepts the diagonal crack (Fig. 4.65). A huge volume of cracked concrete would fall off. Now, the relationship between cracks, flexural stiffness and deflection associated with a member is cardinal in establishing the parameters of section loss. Section loss, as contained in this work is not merely the calculation of crack widths due to flexure. It also considers losses due to environmental factors, time dependency, etc. The above numerical analysis is based on the provisions of [41] and also [45] as contained in [40]. Although this work does not contain FRP composites, it is recognized in all of the equations in [40] that each original equation has a section attached for FRP element.

4.2.4.4.1.2.2 EUROCODE 2 approach

As an emphasis, even [41] section 4.2.3.2 references [45]. As such, most of the crack equations adopted by [40] and [46] are considered herein. The maximum value of crack width is a function of its spacing and strain and is represented for normalized beams as

$$w_{max} = s_{r,max}(\varepsilon_{sm} - \varepsilon_{cm}) \qquad \text{Eqn 4-199}$$

It can be seen that a section with a higher crack spacing as well as tensile strain would allow for wider crack width. The maximum crack spacing therefore depends on the parameters of

Eqn 4-200.

$$s_{r,max} = \begin{cases} 3.4cc + 0.425k_b k_l \left(\dfrac{d_b}{\rho_{p,eff}}\right) & \ldots\ldots\ldots when\ spacing\ (s) \leq 5\left(cc + \dfrac{d_b}{2}\right) \\ 1.3(h - x) & \ldots\ldots\ldots\ldots\ldots\ldots\ldots\ldots\ldots\ldots when\ spacing\ (s) \geq 5\left(cc + \dfrac{d_b}{2}\right) \end{cases} \qquad \text{Eqn 4-200}$$

Comparing the spacing magnitude of $5\left(cc + \frac{d_b}{2}\right)$ against Eqn 4-88 determines which of the equations of

Eqn 4-200 is to be adopted.

$$s = 40\ mm\ \text{(Eqn 4-88)} \leq 5\left(cc + \frac{d_b}{2}\right) \leq 5\left(50\ mm + \frac{32.5\ mm}{2}\right) \leq 331.25 mm. Correct$$

Here, the bonding properties between reinforcing bar and concrete as well as loading condition are captured when calculating the maximum crack spacing. Cover plays a key role in crack design. k_b and k_l are the constants covering these effects respectively. k_b is taken at 0.8 for ribbed bar and 1.6 for plain bars, where k_l is taken at 0.5 for flexure and 1.0 for tension. Though not applicable herein, h and x in the second equation represent the total height of the section and the neutral axis, respectively. Furthermore, the effective steel ratio ($\rho_{p,eff}$) considers the ratios of the steel and any other materials/composites used in the design and is represented as follows. Since there is no composite used herein, terms relating to composites cancel out and the equation for flexural crack, substituting for $A_{c,eff}$ as in Eqn 4-96 and Eqn 4-198, and for ribbed bar and for long term-term loading, is then reduced to,

$$s_{r,max} = 3.4cc + 0.425k_b k_l \left(\frac{d_b}{A_s/A_{c,eff}}\right) = 3.4(50\ mm) + 0.425(0.8)(0.5)\left(\frac{32.5\ mm}{\frac{0.01494}{0.0975}}\right) = 206\ mm$$

Repeating the procedure for pure tension, the maximum crack width becomes $s_{r,max} = 242\ mm$

The average differential reinforced concrete strain ($\varepsilon_{sm} - \varepsilon_{cm}$) denotes the difference in average strain of the reinforcing bar and that of the cracked concrete.

$$(\varepsilon_{sm} - \varepsilon_{cm}) = \frac{f_s - k_t\left(\frac{f_{ctm}}{\rho_{p,eff}}\right)\left(1 + n\rho_{p,eff}\right)}{E_s} \qquad \text{Eqn 4-201}$$

Time effect in RC member causes deterioration. Here, k_t is a coefficient that accounts for the duration of the existence of the load on the structure. The section being designed for cyclic/long-term loading, it is set at 0.4 while for short-term it 0.6. f_s is the steel stress (see Eqn 4-188). However, Eqn 4-201 is at least equal to the average minimum reinforced concrete strain (ε_{scmin}).

$$(\varepsilon_{sm} - \varepsilon_{cm}) = \frac{150\ MPa - 0.4\left(\frac{3.5\ MPa}{\frac{0.01494}{0.0975}}\right)\left(1 + 7\left(\frac{0.01494}{0.0975}\right)\right)}{2x10^5\ MPa} = 0.00066$$

The minimum average strain (ε_{scmin}) equals,

$$\varepsilon_{scmin} = \frac{0.6 f_s}{E_s} \qquad \text{Eqn 4-202}$$

$$\varepsilon_{scmin} = \frac{0.6(150)}{2x10^5} = 0.00045$$

$$\boldsymbol{(\varepsilon_{sm} - \varepsilon_{cm}) > \varepsilon_{scmin} \dots \dots ok}$$

Finally, the maximum crack width (Eqn 4-199):

a. $w_{max} = (206\ mm)(0.00066) = 0.13596\ mm \approx 0.14\ mm \dots \dots \dots \dots for\ flexure$
b. $w_{max} = (242\ mm)(0.00066) = 0.15972\ mm \approx 0.16\ mm\ \dots \dots \dots \dots for\ tension$

The crack width of section 4.2.4.4.1.2.1 and section 4.2.4.4.1.2.2 perfectly agree.

4.2.4.4.1.2.3 Canadian Standard approach

The crack width analysis contained herein are in reference to the Canadian Highway Bridge Design Code as contained in [40]. Most of the parameters are almost as same as those of the previous codes.

$$w_{max} = k_c \beta_c s_{rm} \varepsilon_{sm} \qquad \text{Eqn 4-203}$$

Where k_c accounts for the coating condition of the rebar (1.0 for uncoated bars and 1.2 for epoxy-coated bars), β_c is a constant that considers the dominant agent/mechanism that responsible for the crack (if due to load then $\beta_c = 1.7$, but rather 1.7 for sections with minimum dimension greater than 0.8 m and 1.3 for sections with minimum less than or equal to 0.3 m if the main agent of crack is deformation. Interpolation is allowed for section for β_c when the minimum dimension is less than 0.3 m). A key difference between the average crack spacing (s_{rm}) of the Canadian Standard and the maximum crack spacing of the Eurocode ($s_{r,max}$) is the magnifying coefficient of the concrete cover.

$$s_{rm} = 50 + 0.25 k_l \left(\frac{d_b}{\rho_{p,eff}}\right) \qquad \text{Eqn 4-204}$$

$$s_{rm} = 50\ mm + 0.25(0.5)\left(\frac{32.5\ mm}{\frac{0.01494}{0.0975}}\right) = 76.51 \approx 77\ mm\ for\ flexure/bending$$

For tension, $s_{rm} = 103\ mm$.

The average strain for the reinforcement (ε_{sm}) under which the maximum crack occurs is as follows. f_{sr} is synonymous to f_r of Eqn 4-137.

$$\varepsilon_{sm} = \frac{f_s}{E_s}\left[1 - \left(\frac{f_{sr}}{f_s}\right)^2\right] \qquad \text{Eqn 4-205}$$

$\varepsilon_{sm} = \frac{150\ MPa}{2x10^5\ MPa}\left[1 - \left(\frac{3.92\ MPa}{150\ MPa}\right)^2\right] = 0.00075$

Here, the average strain (
Eqn 4-201) is higher than the differential strain adopted by [45]. Hence the maximum width of crack is

$w_{max} = 1.0(1.7)(77\ mm)(0.00075) = 0.098\ mm \approx 0.1\ mm\ for\ flexure/bending$

For tension, $w_{max} = 0.13\ mm$

4.2.4.4.1.2.4 Japanese Standard approach

Crack width for normal conventional members is estimated from [47] using

$$w_{max} = 1.1\alpha_1\alpha_2\alpha_3[4cc + 0.7(c_s - d_b)]\left(\frac{f_{se}}{E_s} + \varepsilon'_{csd}\right) \quad \text{Eqn 4-206}$$

The constant $\alpha_1$describes the condition of the bar surface (1.0 deformed bars and 1.3 for plain bars), α_2 considers the concrete quality, where

$$\alpha_2 = \frac{15}{f'_c + 20} + 0.7 \quad \text{Eqn 4-207}$$

$\alpha_2 = \frac{15}{40 + 20} + 0.7 = 0.95$

…whereas α_3 addresses issue with the number of layers of the reinforcing bars in the beam.

$$\alpha_3 = \frac{5(n_l + 2)}{7n_l + 8} \quad \text{Eqn 4-208}$$

$\alpha_3 = \frac{5(3 + 2)}{7(3) + 8} = 0.862$

Substituting the center–to–center distance between rebars (c_s), diameter of the bar (d_b), the amount of increase in reinforcing stress (f_{se}), and the effect that shrinkage and creep of concrete has on crack width (ε'_{csd}) into Eqn 4-206, the crack width is determined. [47] (table C8.3.1 and Section 8.3.3 respectively) recommends values of f_{se} and ε'_{csd} in the absence of experimental data. Thus,

$w_{max} = 1.1(1.0)(0.95)(0.862)[4(50\ mm) + 0.7(40\ mm)]\left(\frac{120\ MPa}{2x10^5\ MPa} + 0.0015\right) = 0.43\ mm$

The crack width obtained herein is almost three times greater than those of the previous codes.

4.2.4.4.1.2.5 Indian Standard approach

Calculation of crack width as provided for by [30] limits the steel reinforcement strain to

$$\varepsilon_s \leq \frac{0.8f_y}{E_s} \quad \text{Eqn 4-209}$$

$\varepsilon_s \leq \frac{0.8(420\ MPa)}{2x10^6\ MPa} = 0.00168$

Subjecting the average strain to this strain would constrain the crack width to its maximum value. Crack width, which is limited to a maximum of 0.3 mm ([30] section 35.3.2) is then calculated from

$$w_{cr} = \frac{3a_{cr}\varepsilon_m}{1 + \frac{2(a_{cr} - C_{min})}{h - x}} \quad \text{Eqn 4-210}$$

a_{cr} is the distance from the soffit of the beam to the nearest longitudinal reinforcement, ε_m denotes the average steel strain, C_{min} represents the minimum concrete cover for the longitudinal rebars, h is the total depth of the girder, x is the depth of the neutral axis

$$w_{cr} = \frac{3(62.2\, mm)(0.00168)}{1 + \dfrac{2(62.2 - 50)\, mm}{(1000 - 100)\, mm}} = 0.31\, mm$$

The crack width obtained is as twice as those of ACI/AREMA and the Eurocode.

5 Experimentation

Experimentation is a physical, hands-on process leading to the determination of practical parameters of concern to the investigation. Experimentation usually conducted in the field of civil engineering with emphasis in reinforced concrete structures seeks to determine several parameters. One such key parameter is the flexural rigidity of the element or structure. Constituent materials, concrete, beams/girders, columns, etc. are normally experimented (tested) in the laboratory or on-site. Here in this context, flexural rigidity covers the following but not limited to: stiffness, deflection, cracks, etc. The experimentation regime requires a comprehensive understanding of the procedures and setup of any test. Improper setup might just lead to a worse result. Theories, as well as tests, all use some level of assumptions that may not always be very accurate: we design based on specific values, however, in reality it is technically unachievable; reinforced concrete beams are highly likely to be tested as simply supported beams whereby these elements are always framed in a building. Nonetheless, there is always room for percentage of error and, hence tests properly conducted would in some degree of variance read in line with theory [48].

Reference is made to [49] in relating experimental data obtained to the theoretical design done in this work. As an emphasis, five T-beams were tested in that experimental program for fatigue. Due to the limited data available about the analysis and design of the beams concerned, this work performs a countercheck on the data of the experiment to validate their accuracy by adjusting the dimensions contained in this research to that of the published article. With the consistencies in both works, deflections and cracking magnitudes and patterns are measured against those of the experiment.

The below diagrams were used in experiment.

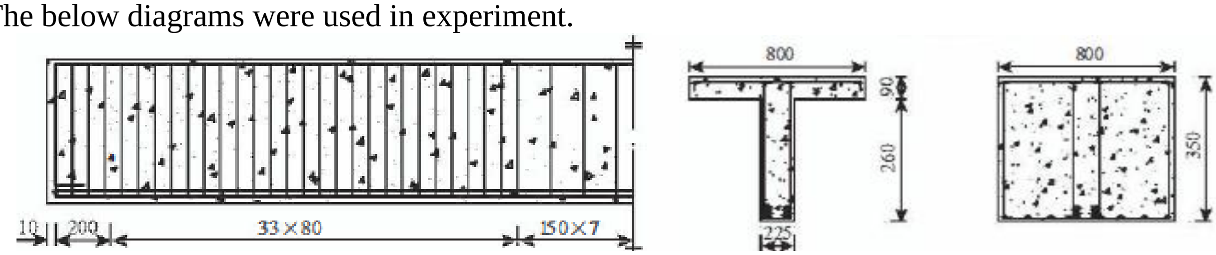

(a) (b)

Fig. 5.1: Sectional views of girder [49] [(a): longitudinal span, (b): transverse view]

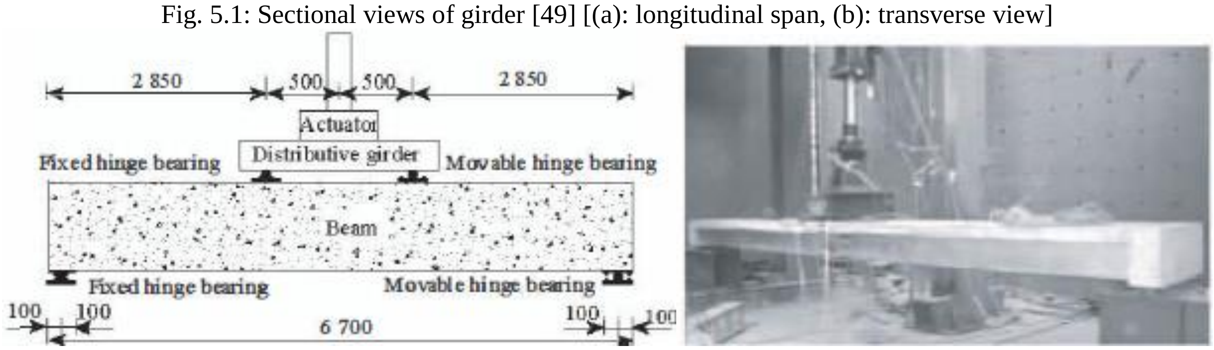

(a) (b)

Fig. 5.2: Experimentation setup used in [(a): structural longitudinal view, (b): photographic view]

5.1 T- Section: Load, shear, and moment recheck

This section seeks to calculate and verify the loads, shear, and moment used in the experiment against data used in the publication and then to compare results of the paper to this research that would in turn seek to substantiate the findings herein. This is technically what is referred to as virtual laboratory. Thus, from the section the dead load for the flange and the web is computed.

1. $DL_w = (0.255\, m)(0.26\, m)(24kN/m^3) = 1.5912 \approx 1.6 \frac{kN}{m}$
2. $DL_f = (0.80\, m)(0.09\, m)(24\, kN/m^3) = 1.728 \approx 1.73 \frac{kN}{m}$

$$\boldsymbol{w_{DL} = 3.33 \frac{kN}{m}}$$

$$R_{DL} = \frac{w_{DL}S}{2} = \frac{\left(3.33 \frac{kN}{m}\right)(6.5\, m)}{2} = 10.8225 \approx 10.83\, kN$$

$$M_{DL} = \frac{w_{DL}S^2}{8} = \frac{\left(3.33 \frac{kN}{m}\right)(6.5\, m)^2}{8} = 17.587 \approx 17.59\, kN.m$$

For primary live load, a 133-kN is considered for fatigue. Considering some of the secondary live loads are applicable to the experimental setup, as in section 4.1.4.2.2.1.1, the live load yields:

$$w_{LL} = \frac{133}{6.5} = 20.46\, kN/m$$

$$I = \frac{125}{\sqrt{6.5}}(20.46\, kN/m) = 10.03\, kN/m$$

$$LF = 0.15(20.46\, kN/m) = 3.07\, kN/m$$

$$\boldsymbol{w_{LL} = 33.56 \frac{kN}{m}}$$

$$R_{LL} = \frac{\left(33.56 \frac{kN}{m}\right)(6.5\, m)}{2} = 109.07\, kN$$

$$M_{LL} = \frac{\left(33.56 \frac{kN}{m}\right)(6.5\, m)^2}{8} = 177.24\, kN.m$$

Henceforth, with the total unfactored load, $\boldsymbol{w_n = 36.89 \frac{kN}{m}}$

$$R_n = \frac{\left(36.89 \frac{kN}{m}\right)(6.5\, m)}{2} = 119.8925 \approx 119.89\, kN$$

$$M_n = \frac{\left(36.89 \frac{kN}{m}\right)(6.5\, m)^2}{8} = 194.8253 \approx 194.83\, kN.m$$

$$M_{sd} = 0.9[1.4(194.83\, kN.m)] = 245.4858 \approx 245.49\, kN.m = 245490\, N.m$$

The effective depth is also calculated on the basis of the experimentation. Here, note that the concrete cover is almost four times lower than what is used in the research.

$$d = 350\, mm - (18 + 8.1 + 0.5 * 25.4)mm = 311.2 \approx 311\, mm$$

Here also, the assumption is made that the section can be designed as a rectangular section,

$$\rho_0 = \left[1 - \sqrt{1 - \left(\frac{2(245490)}{0.9(0.85)(29.7x10^6(0.225)(0.311^2)}\right)}\right]\frac{0.85(29.7)}{426.7} = 0.054 = 5.4\%$$

From calculation, it is noted that these dimensions are minimum that could possibly lead to an iterating process to obtaining a suitable steel ratio.

$A_s = 0.054(225\,mm)(311\,mm) = 3778.65\ \approx 3779\,mm^2$

$$Q_b = \frac{3779}{507} = 7.45 \approx 8$$

The balanced steel ratio is then calculated as

$$\rho_b = \frac{0.85\beta_1 f_c^{'}}{f_y}\left(\frac{600}{600 + f_y}\right) = \frac{0.85(0.85)(29.7\,MPa)}{426.7\,MPa}\left(\frac{600}{600 + 426.7}\right) = 0.029 = 2.9\% < 5.4\%$$

With the adjustments above, the design area of steel becomes

$A_s = 8(507\,mm^2) = 4056\,mm^2$

The centroidal distance from the top of the flange for the gross uncracked section,

$$y_t = \frac{800(90)\left(\frac{90}{2}\right) + 225(260)\left(90 + \left(\frac{90}{2}\right)\right)}{800(90) + 225(260)} = 123.45 \approx 123\,mm$$

And from the bottom, $y_b = 227\,mm$

The net tensile force,

$$T = 0.004056\ \ m^2\left(426.7\frac{MN}{m^2}\right) = 1.731\,MN = 1731\ \ kN = 1731000\,N$$

The area in compression

$$A_c = \frac{1.731}{0.85(29.7)} = 0.0685680\,m^2 = 68568\,mm^2$$

$$a = \frac{68568}{800} = 85.71\,mm \approx 86\,mm$$

NB: Since the compression stress block is less than the thickness of the compression flange, the assumption made that the section can be designed as a rectangular section, is also valid for determining the moment capacity of the section as required for by [2] chapter 8-2.32. Thus,

$\beta_1\ = \ 0.85 - \ 0.008(29.7 - \ 30) = 0.8524 \approx 0.85$

$$c\ = \frac{a}{\beta_1} = \frac{86}{0.85} = 101.2 \approx 101\,mm$$

$$z = 311 - \frac{86}{2} = 268\,mm$$

$M_{r_n} = Tz = (1.731)(0.268) = 0.463908 \approx 464\,kN.m$

$M_{r_u} = \emptyset M_{r_n} = 0.9(464) = 417.6 \approx 418\,kN.m > 245.49\,kN.m \ldots\ldots\ldots\ldots\ldots\ldots\ OK!!!$

Following the procedures of section 4.1.5.14, all other strains (steel, concrete, and tensile) are identical. However, the net tensile strain is

$$\varepsilon_t = \frac{311 - 101}{101}0.003 = 0.006 > 0.005 \ldots\ldots\ldots\ldots OK!!!$$

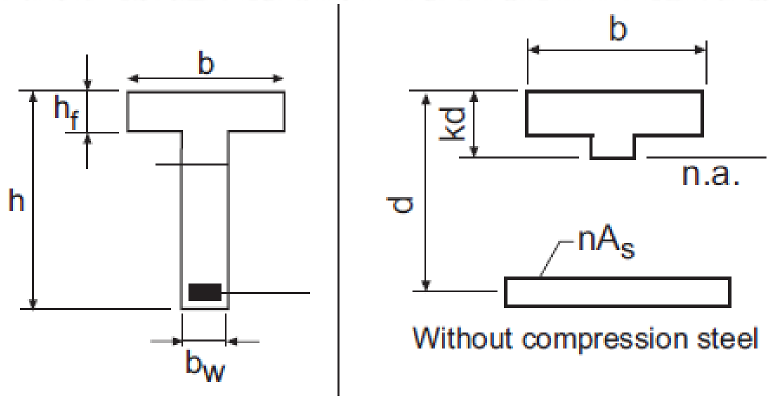

Fig. 5.3: representation of the section for gross and cracked moment of inertia

For a T-section whose neutral axis falls in the web, the gross and cracked moment of inertia can be obtained a little different from the previous case. Consider Fig. 5.3.

The gross moment of inertia

$$I_g = \frac{1}{12}(b - b_w)h_f^3 + \frac{1}{12}b_w h^3 + h_f(b - b_w)\left(h - \frac{1}{2}h_f - y_b\right)^2 + b_w h\left(y_b - \frac{1}{2}h\right)^2 \quad \text{Eqn 5-1}$$

$$I_g = \frac{1}{12}(575)(90)^3 + \frac{1}{12}(225)(350)^3 + 90(575)\left(350 - \frac{1}{2}90 - 227\right)^2 + 225(350)\left(227 - \frac{1}{2}350\right)^2$$

$$I_g = 1366624500\ mm^4 = 0.0013666245\ m^4$$

The following initial quantities may be calculated or substituted directly into the equations for cracked moment of inertia:

$$C_k = \frac{b_w}{nA_s} \quad \text{Eqn 5-2}$$

$$n = \frac{E_s}{E_c} = \frac{200}{26} = 7.7 \approx 8$$

$$C_k = \frac{225\ mm}{8(4056\ mm^2)} = \frac{75}{10816\ mm}$$

$$f_k = \frac{h_f(b - b_w)}{nA_s} \quad \text{Eqn 5-3}$$

$$f_k = \frac{(90)(800 - 225)}{8(4056)} = \frac{8625}{5408}$$

$$kd = \frac{\left[\sqrt{C_k(2d + h_f f_k) + (1 + f_k)^2} - (1 + f_k)\right]}{C_k} \quad \text{Eqn 5-4}$$

$$kd = \frac{\left[\sqrt{\frac{75}{10816}\left(2 * 311 + 90 * \frac{8625}{5408}\right) + \left(1 + \frac{8625}{5408}\right)^2} - \left(1 + \frac{8625}{5408}\right)\right]}{\frac{75}{10816}} = 126\ mm$$

…and the cracked moment of inertia

$$I_{cr} = \frac{1}{12}(b - b_w)h_f^3 + \frac{1}{3}b_w kd^3 + h_f(b - b_w)\left(kd - \frac{1}{2}h_f\right)^2 + nA_s(d - kd)^2 \quad \text{Eqn 5-5}$$

$$I_{cr} = \frac{1}{12}(575)(90)^3 + \frac{1}{3}(225)(126)^3 + 90(575)\left(126 - \frac{1}{2}90\right)^2 + 8(4056)(311 - 126)^2$$

$$I_{cr} = 34931250 + 150028200 + 339531750 + 1110532800$$

$$I_{cr} = 1635024000\ mm^4 = 0.001635024\ m^4$$

$$M_{cr} = \frac{3.38(0.0013666245)}{0.227} = 0.02\ MN.m$$

$$I_e = \left(\frac{0.02}{245.49}\right)^3 0.0013666245 + \left[1 - \left(\frac{0.02}{245.49}\right)^3\right] 0.001635024 = 0.001635024\ m^4$$

Because of an infinitesimal M_{cr}, cracking moment and effective moment are relatively equal. The effective E_c becomes,

$$E_{c,eff} = \frac{A_s E_s \varepsilon_s}{0.5 b d_c \varepsilon_c} = \frac{(0.004056)(200)(0.006)}{0.5(0.225)(0.101)(0.003)} = 142.785\ \approx 143\ GPa > 26\ GPa$$

Unfactored Loads: Dead Load + Live Load to both E and I								
#	w_n (N/m)	l (m)	E_c (N/m^2)	$E_{c,eff}$ (N/m^2)	I_g (m^4)	I_e (m^4)	Δ (m)	Δ (mm)
1	36890.0	6.5	26000000000		0.001366625		0.0241	24.10
2	36890.0	6.5	26000000000			0.001635024	0.0202	20.20
3	36890.0	6.5		143000000000	0.001366625		0.0044	4.40
4	36890.0	6.5		143000000000		0.001635024	0.0037	3.70

Table 5-1: Deflection summary table for T-section

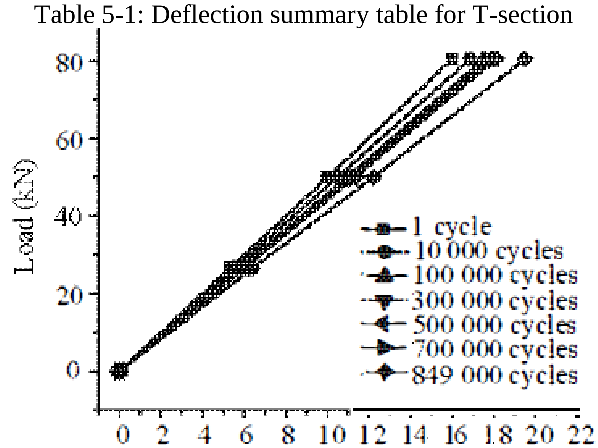

Fig. 5.4: Deflections obtained over different cycles in [49]

60% of the fatigue load was utilized in [49] to calculate the deflection over various cycles whereas the full fatigue load, dead load, and presumable secondary live load is utilized in this research. With only 1 cycle, deflection is 16 mm whereas with a total of approximately 0.85 million cycles (repeated load), the maximum deflection measured is 19.5 mm. These values are in close proximity to those of Table 5-1 that utilize the E_c modulus and more specifically the I_g. It shows a 6% difference between the actual experimental data to that of the crosscheck performed in this research – thus depicting a perfect agreement in the exercise!

Crosschecked experimental deflection	**Relative experimental deflection to its crosschecked deflection at each cycle**					**Remarks**
Δ (mm)	**16 mm**	**17 mm**	**18 mm**	**19 mm**	**20 mm**	
24.10	66%	71%	75%	79%	83%	Ratio in better proximity
20.20	79%	84%	89%	94%	99%	Ratio in good proximity
4.40	364%	386%	409%	432%	455%	Ratio is extremely far apart
3.70	432%	459%	486%	514%	541%	Ratio is extremely farther apart

Table 5-2: Relative deflection check table for T-section

5.2 Rectangular section: Load, shear, and moment recheck

$$I_g = \frac{1}{12}bd^3 = \frac{1}{12}(0.225)(0.35)^3 = 0.000803906\ m^4$$

$$y_t = y_b = \frac{0.35}{2} = 0.175\ m$$

$$f_{rt} = f_{rc} = \frac{(245.49)(0.175)}{0.000803906} = 53440\ kPa \approx 53.44\ \approx 54.0\ MPa$$

$$M_{cr} = \frac{(3.38)(0.000803906)}{0.175} = 0.16\ MN.m = 160\ kN.m$$

$$a = \frac{68568}{225} = 304.75\ mm \approx 305\ mm$$

Thus, the neutral axis and the net tensile strain become,

$$c = \frac{305}{0.85} = 358.82\ mm \approx 359\ mm > (d = 311\ mm), NOT\ APPLICABLE!!!$$

This means that that the depth of compression flange is even larger than the effective depth.

$$\varepsilon_t = \frac{311 - 359}{359}0.003 = -0.0004$$

$$E_{c,eff} = \frac{(0.004056)(200)(-0.0004)}{0.5(0.225)(0.359)(0.003)} = -2678056329 \approx -2.7\ GPa$$

The above NA yielded is unrealistic! Try the method of moment of inertia of the cracked section,

$$B = \frac{225}{8(4056)} = \frac{75}{10816}$$

$$kd = \frac{\sqrt{2(311)\left(\frac{75}{10816}\right) + 1} - 1}{\frac{75}{10816}} = 188 = 0.188\ m$$

$$\varepsilon_t = \frac{311 - 188}{188}0.003 = 0.002 < 0.005\ (compression\ controlled)$$

With a net tensile strain of 0.002, the section is brittle!

$$E_{c,eff} = \frac{(0.004056)(200)(0.002)}{0.5(0.225)(0.188)(0.003)} = 25.6 \approx 26\ GPa = E_c$$

Thus, the cracked moment and effective moments of inertia become:

$$I_{cr} = \frac{(0.225)(0.188\ m)^3}{3} + 8(0.004056)(0.311 - 0.188)^2 = 0.000989256\ m^4 = 989256000\ mm^4$$

$$I_e = \left(\frac{0.16}{0.24549}\right)^3 0.000803906 + \left[1 - \left(\frac{0.16}{0.24549}\right)^3\right] 0.000989256 = 0.00093794\ m^4$$

$$I_e = 937940000\ mm^4$$

Unfactored Loads: Dead Load + Live Load to both E and I								
#	w_n (N/m)	l (m)	E_c (N/m^2)	$E_{c,eff}$ (N/m^2)	I_g (m^4)	I_e (m^4)	Δ (m)	Δ (mm)
1	36890	6.5	26000000000		0.000803906		0.0410	41.00
2	36890	6.5	26000000000			0.00093794	0.0352	35.20
3	36890	6.5		26000000000	0.000803906		0.0410	41.00
4	36890	6.5		26000000000		0.00093794	0.0352	35.20

Table 5-3: Unfactored dead and live loads deflection table from the experiment

Except for the static load test, the percentage of the constant-amplitude fatigue load test to that of the static load for the five beams range from 59% to 74% in Table 1 of [49]. These loads were terminated when a failure was noticed in the beam relative to the number of cycles. Various beams were subjected to different magnitude of loads and cycles as well as thus yielding different deflection magnitudes. Again, the static load of 133 kN was fully utilized with the effect of secondary live loads. The percentaged values of Table 5-4 indicate the relative deflection magnitude obtained in the experiment to that of the crosscheck/verification conducted herein. Consider the deflection graph for all constant fatigue cases from the experiment [49]:

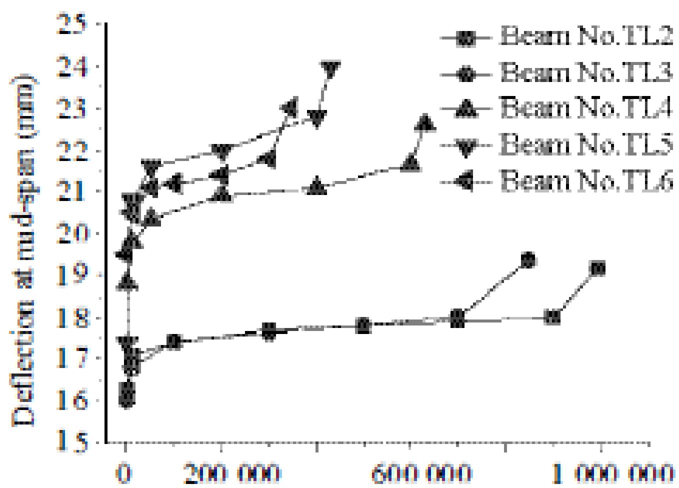

Fig. 5.5: Deflection as function of load repetition

Crossch'd experim. Defl.	Relative experimental deflection to its crosschecked deflection at different cycles										Remarks
	TL-2		TL-2 & TL-3		TL-3 & TL-4		TL-4 & TL-5		TL-5 & TL-6		
Δ (mm)	16 mm	17 mm	18 mm	19 mm	20 mm	21 mm	22 mm	23 mm	24 mm	25 mm	
41.00	39%	41%	44%	46%	49%	51%	54%	56%	59%	61%	see NOTE
35.20	45%	48%	51%	54%	57%	60%	63%	65%	68%	71%	see NOTE
41.00	39%	41%	44%	46%	49%	51%	54%	56%	59%	61%	see NOTE
35.20	45%	48%	51%	54%	57%	60%	63%	65%	68%	71%	see NOTE

Table 5-4: Relative deflection check table for Rectangular section

NOTE: The deflection is well in line to meet the calculated (Table 5-3). The maximum applied load was (100 – 74 = 26)% less than the fatigue load (133 kN) and it produced a deflection of 23 mm. Relative to the varying moment of inertia, the said deflection (i.e., 23 mm) is 100% – 56% = 44% and 100% – 65% = 35% less than what is crosschecked herein for gross and effective moment of inertia respectively. However, to put it more Explicitly, assuming all the fatigue load was applied and the deflection followed the same trajectory, the percentage of difference between the experiment and this verification would be ±(74 – 56 = 18)% and ±(74 – 65 = 9)% for the I_g and I_e respectively assuming the beam was built as a rectangular section.

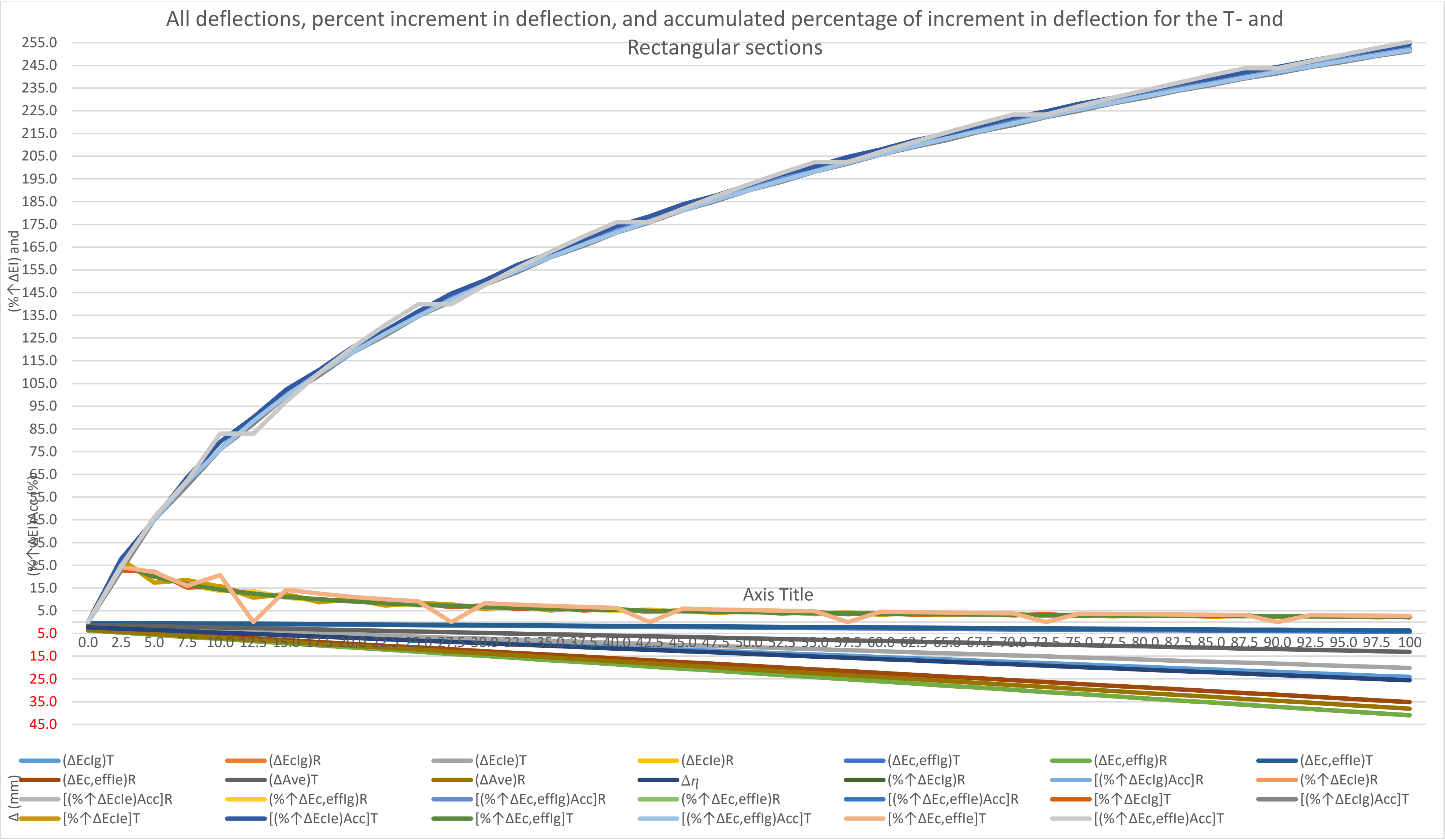

Fig. 5.6: Deflections, percent increment in deflection, and accumulated percentage of increment in deflection of all stiffnesses the experimented rectangular section

6 Validation of Analytical results

Nowadays, software contributes a lot to every research! Regardless of the power (ability to perform several hardcore tasks) of individual software, their specific objective functions matter a whole lot to the user/executor. Software speed up design, especially the provision of output data which thus become almost the most single-handed data audience need yet there are series of steps involved in any procedure. Here, because of the nature of what is being assessed/studied, LISA Finite Element Analysis Software published in 2013 versioned 8.0.0 is used to configure the stresses and deflections under several conditions. By the way, by the utilization of the representation of elements like rods, plates, blocks, etc., a numerical technique is applied to obtaining an approximate solution to a problem – the finite method philosophy. The response matrix, which enables the presentation of the data in tables and graphs, is represented as follows:

$$[Node\ matrix\ of\ constraints\ (N)] \times [Response\ (R)] = [Applied\ 'force'\ (F)] \qquad \text{Eqn 6-1}$$

The basic steps in almost all finite element method analysis include but not limited to building the model, solving the model, displaying the model.

6.1 Simulating the data from the research and experiment

Here, LISA FEA software is used to verify/validate all deflections obtained in the analysis and then also be used to estimate the effects of capacity reduction when defect such as cracks initiate at the section. By far, LISA is not a program specifically designed to simulate cracks! However, the crack profile calculated in section 4.2.4.4 above would be painstakingly modeled into the member to obtain the section loss (i.e., the magnitudinal impacts cracks have on deflection).

6.1.1 T-section

T-sections are modelled as Line Element in LISA. Line elements are one-dimensional and are the building-block elements so cracks won't be modelled herein but in the rectangular section. Here, the deflection for each young modulus of concrete is considered. From Fig. 6.1, the deflection from the analysis for E_cI_g stiffness, and of the software (Fig. 6.1) are exactly the same (14.00 and 14.12 mm). This depicts that a LISA-based deflection analysis is purely carried out on the basis of E_cI_g stiffness.

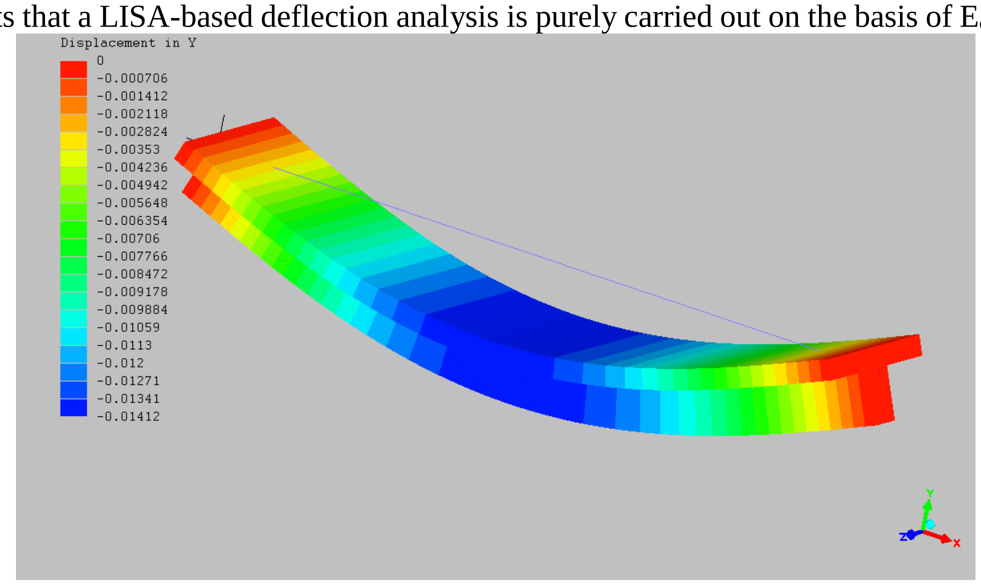

Fig. 6.1: Deflected shape of the T-girder

Computing the simulated values of the maximum shear and maximum moment of Fig. 6.2 and Fig. 6.3 respectively to that of the calculated, refer column 3 and column 4 of Table 4-15.

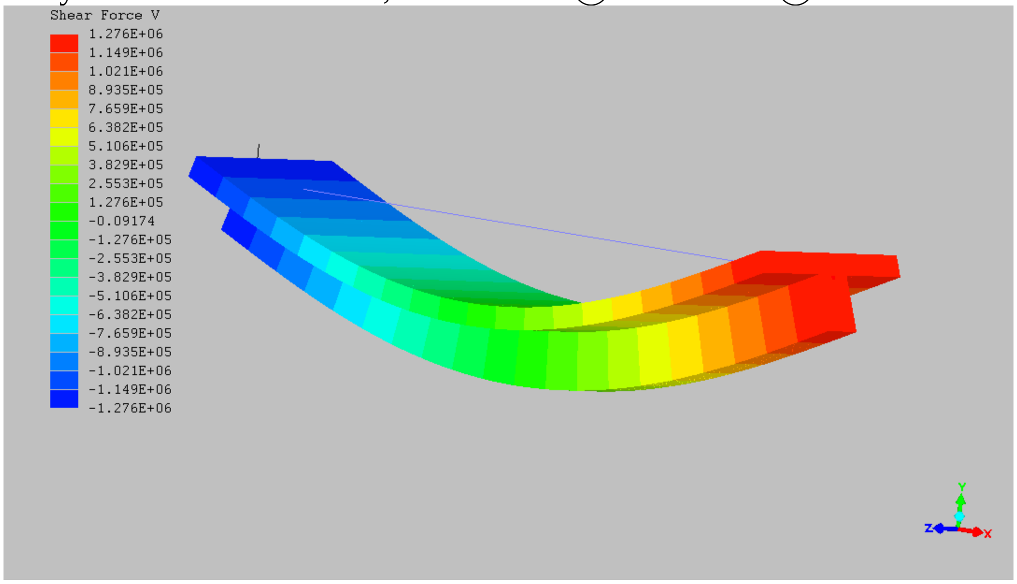

Fig. 6.2: Shear magnitude under the displaced shape

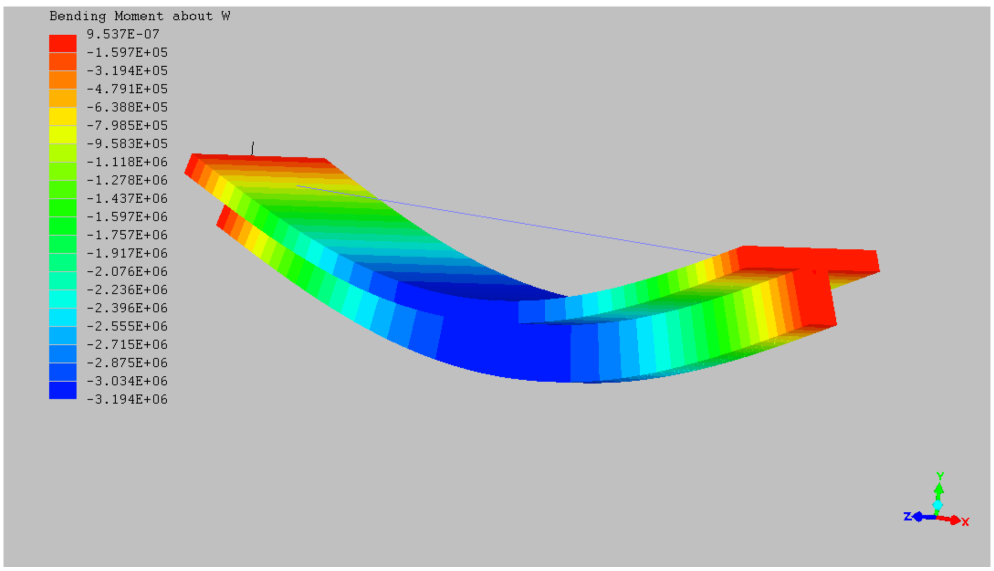

Fig. 6.3: Moment magnitude along the span

Estimating the deflection due to a specific flexural crack width (Δ_{cr}), a formula is developed from a conglomeration of previous ones. The crack width–deflection formula being proposed here considers steel stress, concrete strength, modulus of rupture, modular ratio, as well as section modulus. The formulation is made possible by first computing the steel ratio and then correlating it to the allowable steel stress. Thus, an equation formulated (a so-called Fallah's equation) for calculating deflection due to crack width for a rectangular section is given as

$$\Delta_{cr} = \frac{25l^2}{672E_cI_g}\psi f'_c bd^2 \left\{1 - \left[1 - \left(\frac{f_t f_y}{0.85f'_c\left\{\frac{w_{cr}}{10^{-6}(0.011)\beta\sqrt[3]{d_cA_{cr}}} + f_t(1-n)\right\}}\right)\right]^2\right\} \qquad \text{Eqn 6-2}$$

Substituting for the T-section, the 0.15 mm crack width of section 4.2.4.4.1.2.1 above would therefore cause a 14.0 mm additional deflection ($\Delta_{cr}= 14.0\ mm$).

$$\Delta_{cr}= \frac{25(10)^2}{672\left(30x10^3\right)(0.078547232)}(0.85)(40)(0.5)(0.922)^2\left\{1 - \left[1-\left(\frac{3.92(420)}{0.85(40)\left\{\frac{0.00015}{10^{-6}(0.011)(1.1)\sqrt[3]{66(8611)}}+3.92(1-7)\right\}}\right)\right]^2\right\}$$

$\Delta_{cr}= 14.0\ mm$

Hence, the total deflection:

$\Delta_{tot}= 14.0 + 14.0 = 28\ mm$

6.1.2 Rectangular section

Four conditions are considered relative to the point of application of the load, that is:

a. If the dead load is assumed to act at the soffit of the web
b. If that live load is assumed to act at the top surface of the beam
c. Both (a) and (b)
d. All loads act at the soffit

A fifth condition, which may not technically be applicable, could be that all loads act at the surface of the beam. This condition is ideally used in schematics.

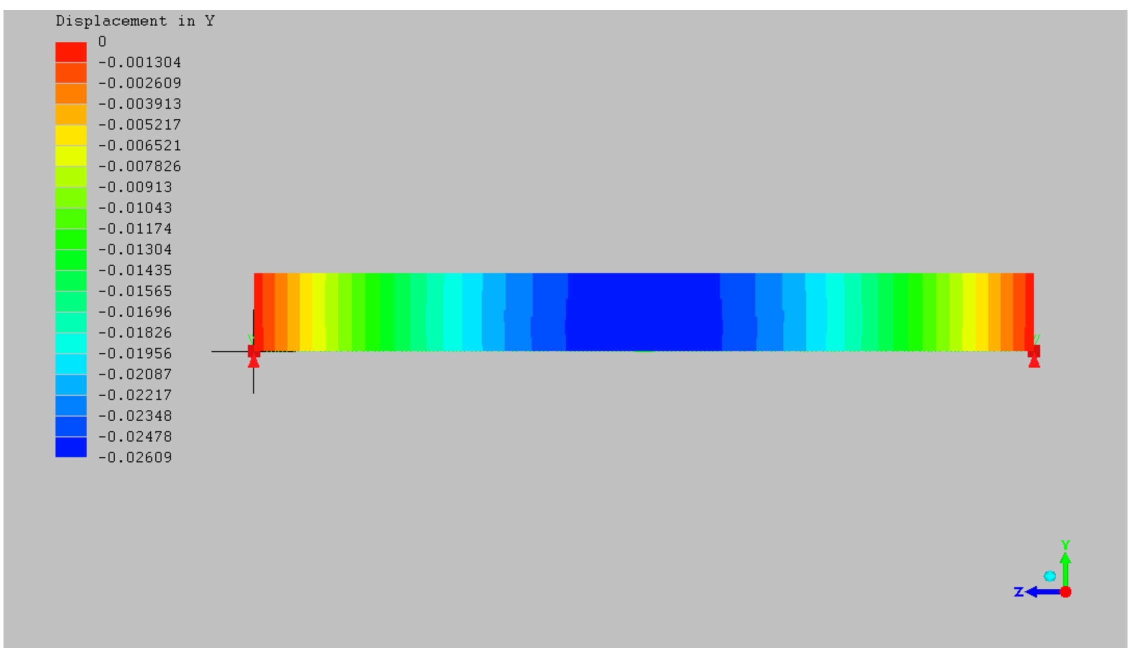

Fig. 6.4: Deflection magnitude along the rectangular girder for condition ©

With the indicative deflections, theoretical crack width of 4.2.4.4.1.2.1 above is then modelled into the section in twofold at the main flexural point to predict the performance of the section. Said approach is taken to observe the trend deflection takes during cracking.

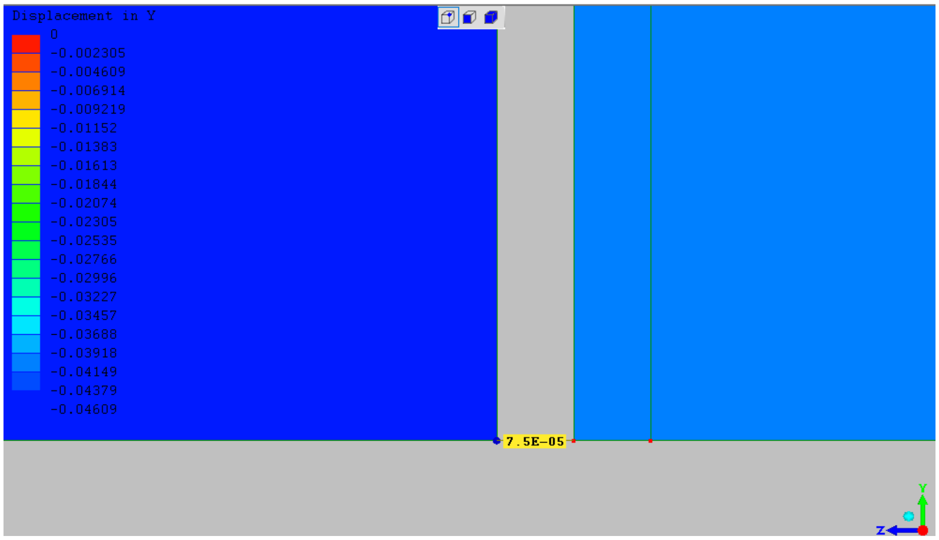

Fig. 6.5: Illustration of crack width at 50% and deflection magnitude for the rectangular girder for condition (c)

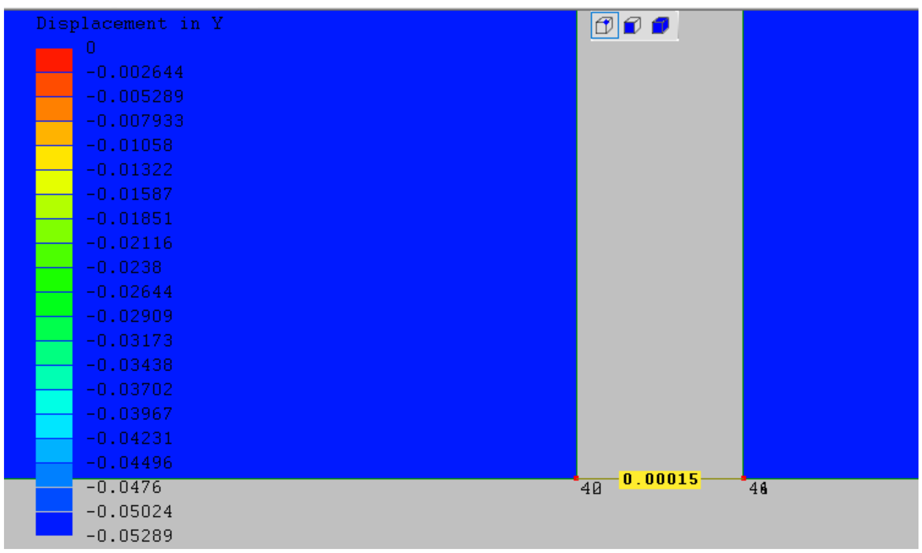

Fig. 6.6: Illustration of full crack width and deflection magnitude for the rectangular girder for condition (c)

In these models, deflection seems to increase rapidly from the inception of the first crack but takes a steady trend when approaching full crack width. Such findings perfectly corroborate with what's reported in [49]. The same relaxation pattern is identical to crack width caused by corrosion [50].

$$\Delta_{cr}=\frac{25(10)^2}{672\left(30x10^3\right)(0.041666667)}(0.85)(40)(0.5)(0.922)^2\left\{1-\left[1-\left(\frac{3.92(420)}{0.85(40)\left\{\frac{0.00015}{10^{-6}(0.011)(1.2)\sqrt[3]{66(8611)}}+3.92(1-7)\right\}}\right)\right]^2\right\}$$

$\Delta_{cr}= 0.0288 = 28.8\ mm$

$\Delta_{cr}= 26.4 + 28.8 = 55.2\ mm$

The two formulae perfectly agree, with a 4% (i.e., 52.89/55.2) differential value only.

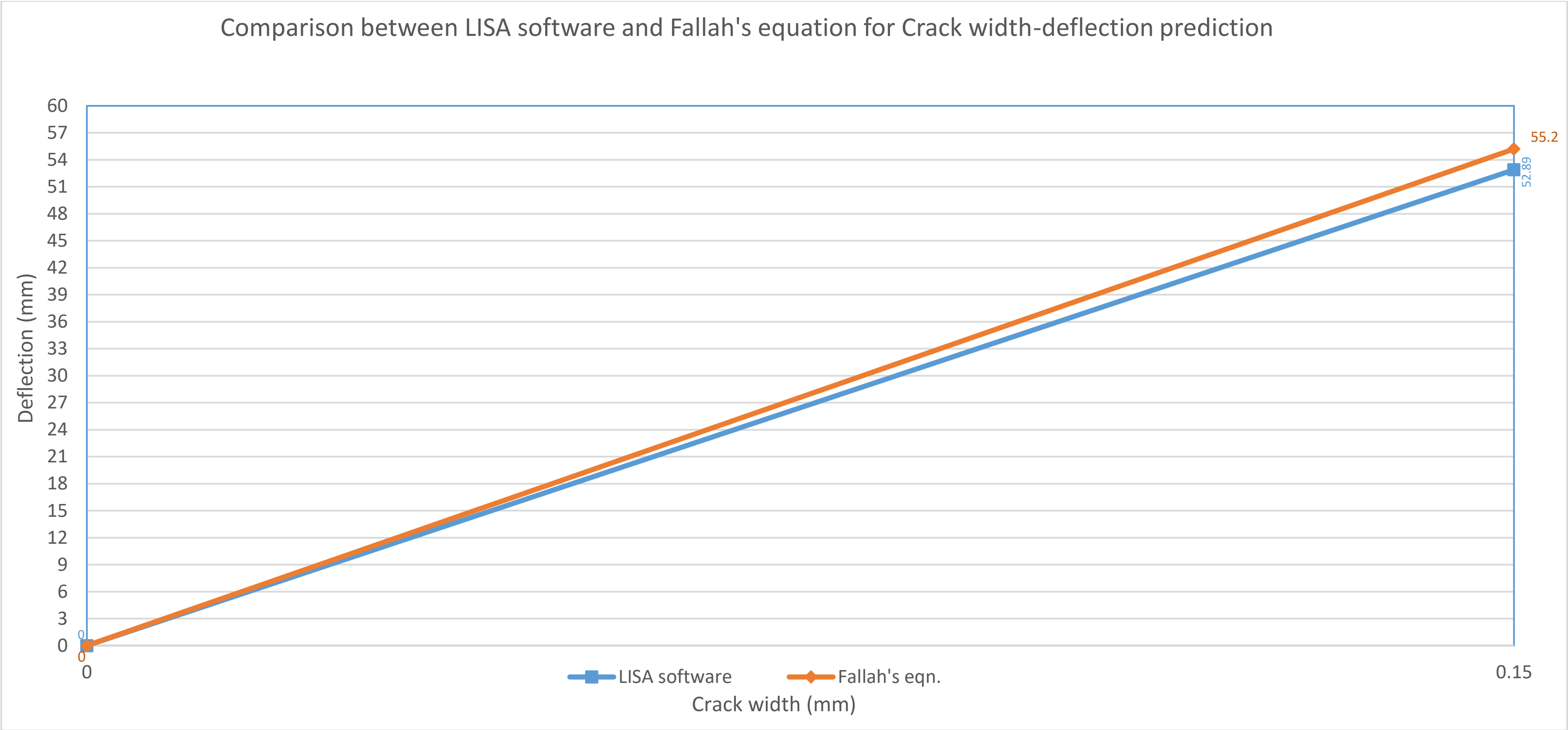

Fig. 6.7: Validation of the relationship between Crack width and deflection for the rectangular section using LISA software and Fallah's equation

7 Summary of discussion on research findings

This section summarizes key findings that have been concluded on in the work. It provides insights of backstage analyses that influence the design once some parameters are iterated.

7.1 General discussion of key research findings

The thematic of this project was to get a comprehensive understanding as to how a crack would influence the performance of a section. However, achieving this goal a section must be well designed considering assumptions that suit the reality. Almost all analyses were performed with reference to [2]. The size requirement of the members which is normally a span-dependent criterion was met. Concrete compressive strength plays a key role in the reinforcement requirements of a section. Generally, Higher strength would normally lead to the adoption of less reinforcement. However, the statement may not always be true in yielding some definite results due to the magnitude of the applied moment and the principal sectional dimensions of the particular section. The graph below summarizes different concrete strengths to their proportionate steel ratio, and area of steel. With the dimensions associated with the section and the magnitude of the applied load, the minimum compressive strength needed is 25 MPa. Below this, the expression for the original moment indicated in count 4 of 4.1.4.1.4 would be negative. Reference to the iteration enables such manipulation [25].

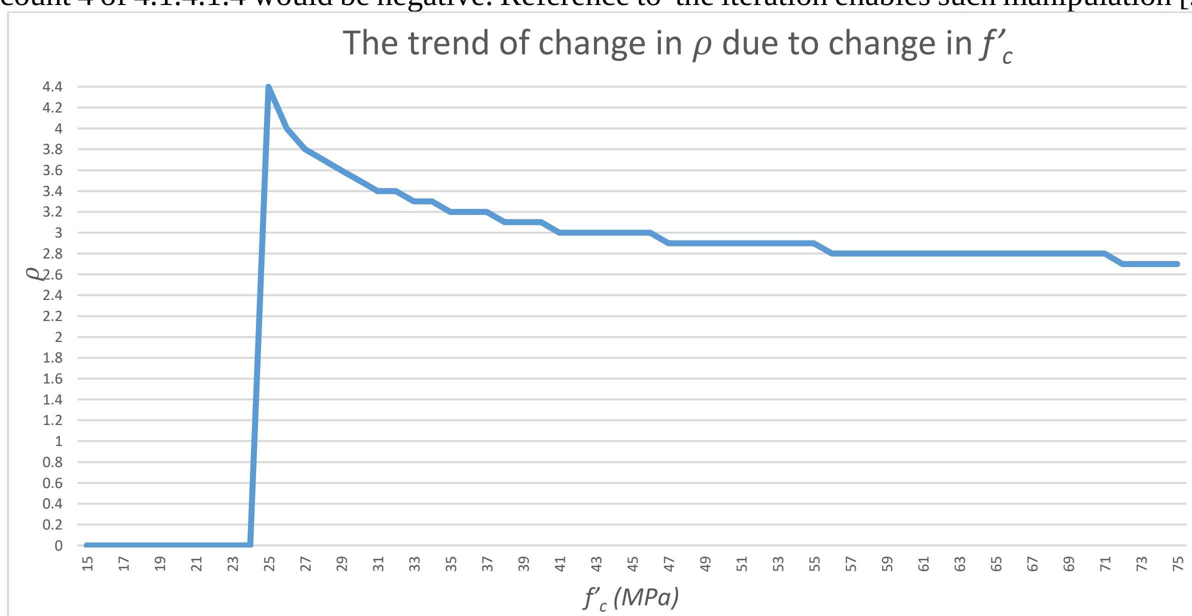

Fig. 7.1: The trend of change in the reinforcement ratio due to change in f'_c

From Fig. 7.1, the area of steel thus having direct proportionality with ρ, would follow the same pattern. Furthermore, the number of bars would follow suit assuming that the same diameter is used. The stress in the section was also calculated and the steel ratio came up to 84% of the balanced steel ratio (4.1.5.7 and 4.1.5.8) which was a little over the 75% stipulated by [2] for the rectangular section requirement. This result is technically still valid for use in practicality. The maximum load the section can resist is the load beyond which the section would fail (Eqn 4-100).

$$w_{fail} = \frac{T}{l} \qquad \text{Eqn 7-1}$$

$$w_{fail} = \frac{6275000\ N}{10\ m} = 627500\ N/m$$

S/N	Load (N/m)	T-sect. Displ. (mm)	Rect. Sect. Displ. (mm)	Displacement notation & remark
1	0	0	0	Δ_0 – beam soffit fully supported/jacked or no load at all
2	36000	2	4	Δ_{cr} – when the first theoretical crack initiates
3	253900	14	26	Δ_{wn} – due to unfactored loads
4	355460	20	37	Δ_{wu} – due to factored loads
5	627500	35	65	Δ_{wR} – when the maximum resisting load is induced
6	>627500	>35	>65	Failure – any point beyond Δ_{wR}

Table 7-1: Load-displacement table

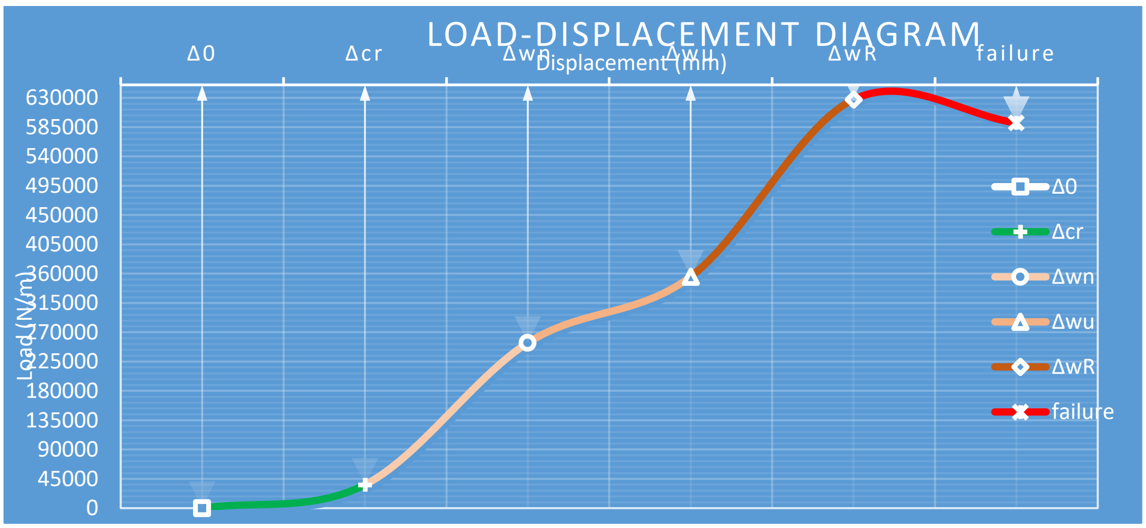

Fig. 7.2: Shape of Load-displacement diagram for the T- and rectangular sections under consideration

All deflections calculated are based on w_n (Unfactored dead and live loads). The deflection caused by the presence of cracks falls between w_u and w_R (factored load and resisting load). This implies that with the 0.15-mm crack width, the section may only be able to appreciably perform further if the concrete strength is almost doubled (i.e., to the maximum allowable of 70 to 75 MPa). This would allow an increase in the modulus of rupture which further in turn increases the allowable stress in the steel. Consequently, an increase in the steel stress leads to an increase in the maximum allowable crack width.

7.1.1 Long-term deflection

Because of fatigue, every structural element has room for Long-term deflection. This happens due to the constant application of load that then weakens the stiffness of the member. [2] 8-2.23.7 provides an alternative equation for long-term deflection. A factor which also incorporates the effects of reinforcement (ב) is utilized.

$$\text{ב} = \left(2 - \frac{1.2A'_s}{A_s}\right) \qquad \text{Eqn 7-2}$$

Thus, [2] long-term deflection is thus

$$\Delta_{lt} = \Delta\text{ב} \qquad \text{Eqn 7-3}$$

However, [2] version of long-term deflection taking into effect of compression reinforcement is represented as below. ρ' is the steel ratio obtained from the compression steel.

$$\Delta_{lt} = \Delta\left(\frac{\xi}{1 + 50\rho'}\right) \quad \text{Eqn 7-4}$$

However, with no compression steel designed for in the entire analysis, the long-term factor in both Eqn 7-2 and Eqn 7-4 are equal based on the value of ξ provided above. With this, the implication is that the said elastic modulus is going to be reduced by one-half.

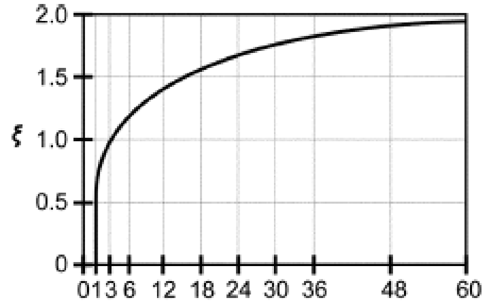

Fig. 7.3: Value of ξused as long-term deflection multiplier over specific period in months

T-section unfactored Loads: Dead Load + Live Load to both E and I									
#	w_n (N/m)	l (m)	E_c (N/m^2)	$E_{c,eff}$ (N/m^2)	I_g (m^4)	I_e (m^4)	Δ (m)	Δ (mm)	Δ_{lt} (mm)
1	253900	10	30000000000		0.07854723		0.014	14.00	28.0
2	253900	10	30000000000			0.1028664163	0.0107	10.70	21.4
3	253900	10		996000000000	0.07854723		0.0004	0.40	0.8
4	253900	10		996000000000		0.1028664163	0.0003	0.30	0.6

Table 7-2: Long-term deflection for the T-section

Rectangular section unfactored Loads: Dead Load + Live Load to both E and I									
#	w_n (N/m)	l (m)	E_c (N/m^2)	$E_{c,eff}$ (N/m^2)	I_g (m^4)	I_e (m^4)	Δ (m)	Δ (mm)	Δ_{lt} (mm)
1	253900	10	30000000000		0.041666667		0.0264	26.40	52.8
2	253900	10	30000000000			0.038481401205	0.0286	28.60	57.2
3	253900	10		25000000000	0.041666667		0.0317	31.70	63.4
4	253900	10		25000000000		0.038481401205	0.0344	34.40	68.8

Table 7-3: Long-term deflection for the rectangular section

[51] reports a comprehensive work on cracks in reinforced concrete bridges. The work discusses aspects of cracking in terms of causes, types, constituent RC member elements effects on cracks, construction effects, reinforcement effects, time-dependence effect, etc. This leads to the formulation of the statement that values obtained in this research and the several other researches been conducted still do not perfectly exactly calculate crack width nor deflection. Every force acting on a bridge structure has an adverse effect on cracking. However, of more importance to the discussion is structural crack (relating to crack profile). Yet, those that do not reach into the effective depth also affect performance in that they provide the channel for corrosion [42] [51] [7] [52]. [53] performed an academic interpretation of what it takes to deflect a member. In it, which is also used in parts as virtual lab for this research project, comparison is made so as to validate the findings herein. Normally, in deflection calculation as this, the elastic modulus of concrete is used rather than that of the reinforcing bars. Why? Technically, tracing the equations leading to the deflection, the stress in concrete and steel are adopted in the crack analysis and design which too is further used in the determination of the deflection of the cracked section.

8 Conclusion and Recommendation

This chapter is a synopsis of what has been researched and what needs to be researched further.

8.1 Conclusion

The specific objective of this work has been met: the adequacy of the performance of a railway girder against loads was determined. With this, the following statements are drawn up:

1. The derived equation perfectly agrees with theoretical, virtual experimentation, and laboratory works
2. Structural integrity is possibly achievable beyond the design crack width
3. Displacement due to crack width and the deflection have similar magnitude
4. Flexural cracks and tensile cracks yielded similar magnitude.
5. Accumulated magnitude of displacement/deflection and percent increment in deflection from one step of load application to the next show and indirect properties respectively.
6. It is possible to attain a reasonable displacement magnitude (of a rectangular section) by superimposing those of analytical calculations to that of the experimentation.

8.2 Recommendation

1. Beyond design crack width, proper structural health monitoring should be conducted
2. Robotics would do better in estimating crack parameters.
3. On-site investigations of railway bridge girder with actual freight/passenger vehicles needs to be conducted to obtain more appreciable results
4. Box girder construction would exhibit better structural integrity than T-gider.

9 References

[1] "TCRP Report 155," 2012.

[2] AREMA, "Manual for Railway Engineering Volume 2," AREMA, MD 20706 USA., 2010.

[3] J. C. McCormac and R. H. Brown, "Design of Reinforced Concrete, 10th Ed.," John Wiley & Sons, Inc., New Jersey, 2016.

[4] D. R. Sahoo, A. Solanki and A. Kumar, "Influence of Steel and Polypropylene Fibers on Flexural Behavior of RC Beams," *J. Mater. Civ. Eng.,* pp. 04014232-1 to 04014232-9, 2014.

[5] M. Theriaule and B. Benmokrane, "Effects Of FRP Reinforcement Ratio And Concrete Strength On Flexural Behavior Of Concrete Beams," *J. Compos. Constr. ,* pp. 2:7-16., 1998.

[6] [Online]. Available: Fiber-reinforced concrete - Wikipedia..

[7] P. KOTEŠ, J. VIČAN, M. BRODNAN and R. NIKOLIČ, *Reliability of existing concrete bridges from the aspect of the reinforcement corrosion,* ResearchGate, 2016.

[8] M. Pimentel, E. Bruhwiler and J. Figueiras, "Fatigue life of short-span reinforced concrete rail bridges," *Structural Concrete Journal of the fib,* pp. 216 - 223, 2008.

[9] J. Li, M. Su and L. Fan, "Natural Frequency of Railway Girder Bridges Under Vehicle Loads," *ASCE J. Bridge Eng. ,* pp. 8:199-203., 2003.

[10] E. O. L. Lantsoght, R. T. Koekkoek, C. v. d. Veen and D. A. Hordijk, "Pilot Proof-Load Test on Viaduct De Beek: Case Study," *J. Bridge Eng.,* pp. 22(12): 05017014-1 to 05017014-15, 2017.

[11] S. Alampalli, D. M. Frangopol and e. al., "Bridge Load Testing: State-of-the-Practice," *J. Bridge Eng.,* pp. 26(3): 03120002-1 to 03120002-17, 2021.

[12] Z. Guo, Y. Ma, L. Wang, X. Zhang, J. Zhang, C. Hutchinson and I. E. Harik, "Crack Propagation-Based Fatigue Life Prediction of Corroded RC Beams Considering Bond Degradation," *J. Bridge Eng.,* pp. 25(8): 04020048 1-13, 2020.

[13] R. S. RAVINDRARAJAH and R. N. SWAMY, "Load effects on fracture of concrete," *Materials and Structures/Mat&iaux et Constructions,* pp. 15-22, 1989.

[14] S. J. Pantazopoulou and K. D. Papoulia, "Modeling Cover-Cracking Due To Reinforcement Corrosion In RC Structures," *JOURNAL OF ENGINEERING MECHANICS,* pp. 342 - 351, 2001.

[15] R. Ravindrarajah and K. Ong, "Corrosion of steel in concrete in relation to Bar Diameter and Cover Thickness," Sri Lanka.

[16] Committee-318, "Building Code Requirements for Structural Concrete (ACI 318-19) / Commentry on Building Code Requirements for Structural Concrete (ACI 318R-19) /," American Concrete Institute, Farmington Hills, MI 48331, 2019.

[17] V. IVICA, "The rate of corrosion of concrete reinforcement and possibilities of," *Bull. Mater. Sci,* pp. 115-124, 1995.

[18] M. Brodòan, P. Kotes and e. al, "CORROSION DETERMINATION OF REINFORCEMENT USING THE ELECTRICAL RESISTANCE METHOD," *MATERIALS AND TECHNOLOGY,* pp. 1, 85–93, 2017.

[19] Y. J. LAFTA and K. YE, "STRUCTURAL BEHAVIOR OF DEEP REINFORCED CONCRETE BEAMS UNDER INDIRECT LOADING CONDITION," *International Journal of Civil, Structural, Environmental and Infrastructure Engineering, Research and Development (IJCSEIERD),* pp. 53-72, 2015.

[20] A. P. Fantilli, H. Mihashi and P. Vallini, "Crack profile in RC, R/FRCC and R/HPFRCC members in tension," *Materials and Structures,* p. 40:1099–1114, 2007.

[21] B. Chiaia, A. P. Fantilli and P. Vallini, "Crack Patterns in Reinforced and Fiber Reinforced Concrete Structures," *The Open Construction and Building Technology Journal,* pp. 2, 146-155, 2008.

[22] R. Clark and M. e. Shubaili, "Time Dependent Strength and Stiffness of Shear Controlled Reinforced Concrete Beams under High Sustained Stresses," in *Structure Congress 2020*, 2020.

[23] A. Ebrahimkhanlou, A. Athanasiou, T. D. Hrynyk, O. Bayrak and S. Salamone, "Fractal and Multifractal Analysis of Crack Patterns in Prestressed Concrete Girders," *J. Bridge Eng.,* pp. 24(7): 04019059 (1-13), 2019.

[24] M. Maguire, C. Roberts-Wollmann and T. and Cousins, "Live-Load Testing and Long-Term Monitoring of the Varina-Enon Bridge: Investigating Thermal Distress," *J. Bridge Eng.,* pp. 23(3): 04018003 1-14, 2018.

[25] J. Fallah, "Development of an Iterative Modular Expression to Accurately Adjust the Moment Capacity of a Reinforced Concrete Member," *IJASR,* pp. 32 - 47, 2021.

[26] Committee-350, "CODE REQUIREMENTS FOR ENVIRONMENTAL ENGINEERING CONCRETE STRUCTURES (ACI 350M-06) AND COMMENTRY," American Concrete Institute, 2006.

[27] WisDOT, "WisDOT Bridge Manual," WisDOT, 2020.

[28] J. Zhu and Q. Meng, "Effective and Fine Analysis for Temperature Effect of Bridges in Natural Environments," *J. Bridge Eng.,* pp. 04017017 (1-19), 2017.

[29] Subcommittee-C09.20, "Standard Specification for Concrete Aggregates," ASTM, PA, USA, 2016.

[30] IS-456, "PLAIN AND REINFORCED CONCRETE - CODE OF PRACTICE," Indian Standards, New Delhi, 2000.

[31] ACI-CT, "ACI CT - 18," ACI, MI, USA, 2018.

[32] E. Giuriani and G. A. Plizzari, "Interrelation of Splitting And Flexural Cracks In RC Beams," *JOURNAL OF STRUCTURAL ENGINEERING,* pp. 124:1032-1049, 1998.

[33] Z. P. Bazant and Z. Li, "Modulus of Rupture: Size Effect Due to Fracture Initiation In Boundary Layer," *JOURNAL OF STRUCTURAL ENGINEERING,* pp. 739 - 746, 1995.

[34] ASTM, "ASTM C78/C78M," ASTM International, 2021.

[35] D. E. Branson, "Instantaneous and Time-Dependent Deflections on Simple and Continuous Reinforced Concrete Beams," Alabama Highway Department, Bureau of Public Roads, Alabama, 1965.

[36] R. S. N. A. W. BEEBY, DESIGNERS' GUIDE TO EUROCODE 2: DESIGN OF CONCRETE STRUCTURES, London E14 4JD.: Thomas Telford, 2009.

[37] Himat and Sabnis, "Long-term Deflections of Reinforced Concrete Structures," *INDIAN CONCRETE JOURNAL,* pp. 107 - 110, 1987.

[38] R. Khajehdehi, D. Darwin and M. Feng, "Dominant Role of Cement Paste Content on Bridge Deck Cracking," *Journal of Bridge EngineeringJuly,* 2021.

[39] P. Gergely and L. A. Lutz, "Maximum Crack Width in Reinforced Concrete Flexural Member," *Cracking in concrete,* pp. 87 - 117.

[40] M. A. Al-Saawani, A. K. El-Sayed and A. I. Al-Negheimish, "Crack Width Prediction for Concrete Beams Strengthened with Carbon FRP Composites," *J. Compos. Constr.,* pp. 04017023-(1-14), 2017.

[41] Committee-224, "Control of Cracking in Concrete Structures," ACI, 2001.

[42] Committee-318, "Building Code Requirements for Structural Concrete," ACI, 2007.

[43] Committee-224, "Cracking of Concrete Members in Direct Tension," ACI, 1997.

[44] P.-L. Ng, V. Gribniak, R. Jakubovskis and A. Rimkus, "Tension stiffening approach for deformation assessment of flexural reinforced concrete members under compressive axial load," *fib wiley: Structural Concrete,* p. 1–13, 2019.

[45] CEN, "Eurocode 2: Design of concrete structures," EUROPEAN STANDARD, Brussels, 2002.

[46] EUROCODE, "Eurocode Applied.com," [Online]. Available: https://eurocodeapplied.com/design/en1992. [Accessed 2021].

[47] JASCE, "Standard Specifications For Concrete Structures - 2007 "DESIGN"," JASCE, Tokyo, 2007.

[48] N. SHARMA, S. SAURABH, V. JOSHI and A. S. SANTHI, "ESTIMATION OF ERROR IN DEFLECTION OF A SIMPLY SUPPORTED BEAM," *International Journal of Civil, Structural, Environmental and Infrastructure Engineering, Research and Development (IJCSEIERD),* pp. Vol. 3, Issue 3, 113-118, 2013.

[49] H.-b. ZHU, Y.-q. XU and X. LI, "Fatigue Behavior of Reinforced Concrete T-beam," *Journal of Highway and Transportation Research and Development,* pp. 8(3): 46-51, 2014.

[50] C. Zhou, Z. Zhu, Z. Wang and H. Qiu, "Deterioration of concrete fracture toughness and elastic modulus under simulated acid-sulfate environment," *Construction and Building Materials,* p. 176 490–499, 2018.

[51] H. G. Russell, Control of Concrete Cracking in Bridges, Glenview: National Academy of Sciences, 2017.

[52] V. Gribniak, V. Cervenka and G. Kaklauskas, "Deflection prediction of reinforced concrete beams by design codes and computer simulation," *Elsevier: Engineering Structures,* p. 56 (2013) 2175–2186, 2013.

[53] A. Farsi, A. D. Pullen, J. P. Latham, J. Bowen, M. Carlsson, E. H. Stitt and M. Marigo, "Full deflection profile calculation and Young's modulus optimisation for engineered high performance materials," *Nature/SCIENTIFIC REPORTS,* pp. Rep. 7, 46190, 2017.

[54] V. A. P. C. G. K. A. R. A. S. Gribniak, "Effect of Arrangement of Tensile Reinforcement on Flexural Stiffness and Cracking," *Engineering Structures,* p. 124 (June): 418–28, 2016.

[55] V. Gribniak, A. Rimkus, A. P. Caldentey and A. Sokolov, "Cracking of Concrete Prisms Reinforced with Multiple Bars in Tension–the Cover Effect," *Engineering Structures,* 2020.

[56] V. Gribniak, A. Rimkus, L. Torres and R. Jakstaite, "Deformation Analysis of Reinforced Concrete Ties: Representative Geometry," *Structural Concrete,* pp. 634 - 647, 2016.

10 Appendix

10.1 Solution of Equations (SOE)

$\sum M@R_1 = 0$

$Deck\colon -6.72\frac{kN}{m}(1.1\ m)(0.5x1.1\ m) = -4.07\ kN.m$

$Curb\colon -3.08\ \mathrm{kN}\ (0.9\ \mathrm{m}) = -2.78\ kN.m$

$Ballast\colon -5.7\frac{kN}{m}(0.7\ m)(0.5x0.7\ m) = -1.4\ kN.m$

$Deck\colon 6.72\frac{kN}{m}(3.7\ m)(0.5x3.7\ m) = 46.00\ kN.m$

$Ballast\colon 5.7\frac{kN}{m}(3.3\ m)(0.5x3.3\ m) = 31.04\ kN.m$

$Ties\colon 1.3\frac{kN}{m}(2.6\ m)(0.5x2.6\ m) = 4.39\ kN.m$

$Rail\colon 3\mathrm{kN}\ (0.5455\ \mathrm{m}) = 1.64\ kN.m$

$Rail\colon 3\ \mathrm{kN}\ (2.05\ \mathrm{m}) = 6.16\ kN.m$

$Curb\colon 3.08\ \mathrm{kN}\ (3.5\ \mathrm{m}) = 10.78\ kN.m$

91.77 kN.m

SoE 10-1: Configuration of dead load on flange

$V_c = -6.72\frac{kN}{m}(0\ m) = 0$

$V_{d1} = 0\ \mathrm{kN} - 6.72\frac{kN}{m}(0.2\ m) = -1.34\ kN$

$V_{d_2} = -1.34\ kN - 3.08\ kN = -4.42\ kN$

$V_e = -4.42\ kN - 6.72\frac{kN}{m}(0.2\ m) = -5.76\ kN$

$V_A = -5.76\ kN - (6.72 + 5.7)\frac{kN}{m}(0.7\ m) = -14.45\ kN$

$V_{R1} = -14.45\ kN + 35.30\ kN = 20.85\ kN$

$V_{f1} = 20.85\ kN - (6.72 + 5.7 + 1.3)\frac{kN}{m}(0.5545\ m) = 13.37\ kN$

$V_{f2} = 13.37\ kN - 3.0\ kN = 10.37\ kN$

$V_{g1} = 10.37\ kN - (6.72 + 5.7 + 1.3)\frac{kN}{m}(1.509\ m) = -10.33\ kN$

$V_{g2} = -10.33\ kN - 3.0\ kN = -13.33\ kN$

$V_B = -13.33\ kN - (6.72 + 5.7 + 1.3)\frac{kN}{m}(0.5545\ m) = -20.81\ kN$

$V_{R2} = -20.81\ kN + 35.30\ kN = 14.49\ kN$

$V_h = 14.49\ kN - (6.72 + 5.7)\frac{kN}{m}(0.7\ m) = 5.80\ kN$

$V_{i_1} = 5.80\ kN - 6.72\frac{kN}{m}(0.2\ m) = 4.46\ kN$

$V_{i_2} = 4.46\ kN - 3.08\ kN = 1.38\ kN$

$V_j = 1.38\ kN - 6.72\frac{kN}{m}(0.2\ m) = -0.04\ kN \approx 0$

SoE 10-2: Computation of dead load shear on flange

$M_c = (0\ kN)(0\ m) = 0$

$M_d = 0 - 0.5(0.2\ m)(1.34\ kN) = -0.13\ kN.m$

$M_e = -0.13\ kN.m - 0.5(0.2\ m)(4.42 + 5.76)kN \quad = -1.15\ kN.m$
$M_A = -1.15\ kN.m - 0.5(0.7\ m)(5.76 + 14.45)kN \quad = -8.22\ kN$
$M_f = -8.22\ kN.m + 0.5(0.5455\ m)(20.85 + 13.37)kN \quad = 1.11\ kN$
$M_k = 1.11\ kN.m + 0.5(0.76\ m)(10.37)kN \quad = 5.05\ kN.m$
$M_g = 5.05\ kN.m - 0.5(1.509\ m - 0.76\ m)(10.33)kN \quad = 1.18\ kN.m$
$M_B = 1.18\ kN.m - 0.5(0.5455\ m)(13.33 + 20.81)kN \quad = -8.13\ kN$
$M_h = -8.13\ kN.m + 0.5(0.7\ m)(14.49 + 5.80)kN \quad = -1.03\ kN$
$M_i = -1.03\ kN.m + 0.5(0.2\ m)(5.80 + 4.46)kN \quad = 0.0\ kN$
$M_j = 00\ kN.m + 0.5(0.2\ m)(1..38)kN \quad = 0.14 \approx 0$

SoE 10-3: Computation of dead load moment on flange

$$\rho_0 = \left[1 - \sqrt{1 - \left(\frac{2m_{sd}}{\emptyset\varphi f_c' bd^2}\right)}\right]\frac{0.85 f_c'}{f_y}$$
$$ñ_0 = \left[1 - \sqrt{1 - \left(\frac{2 * 10360}{0.9 * 0.85 * (40 * 10^6) * 1 * 0.22^2}\right)}\right]\frac{0.85(40 * 10^6)}{420 * 10^6}$$
$$\rho_0 = \left[1 - \sqrt{1 - \left(\frac{2 * 10360}{0.9 * 0.85 * (40 * 10^6) * 1 * 0.22^2}\right)}\right]\frac{0.85(40 * 10^6)}{420 * 10^6}$$
$\rho_0 = [1 - 0.933]0.081$
$\rho_0 = [1 - 0.993]0.081$
$\rho_0 = [0.007]0.081$
$\rho_0 = 0.000567$
$\rho_0 \approx 0.0006$

SoE 10-4: Computation of flange dead load steel ratio

$$\rho_0 = \left[1 - \sqrt{1 - \left(\frac{2m_{sd}}{\emptyset\varphi f_c' bd^2}\right)}\right]\frac{0.85 f_c'}{f_y}$$
$$\rho_0 = \left[1 - \sqrt{1 - \left(\frac{2 * 200710}{0.9 * 0.85 * \left(40 * 10^6\right) * 1 * 0.22^2}\right)}\right]\frac{0.85(40 * 10^6)}{420 * 10^6}$$
$\rho_0 = [1 - 0.854]0.081$
$\rho_0 = [0.146]0.081$
$\rho_0 = 0.011826$
$\rho_0 \approx 0.012$
$\rho_0 \approx 1.2\%$

SoE 10-5: Computation of flange live load steel ratio

$Deck: -6.72\frac{kN}{m}(1.1\ m)(0.5x1.1\ m) \quad = -4.07\ kN.m$
$Curb: -3.08$ kN (0.9 m) $\quad = -2.77\ kN.m$
$Ballast: -5.7\frac{kN}{m}(0.7\ m)(0.5x0.7\ m) \quad = -1.40\ kN.m$

$$Deck: 6.72\frac{kN}{m}(3.7\ m)(0.5x3.7\ m) \quad = 46.00\ kN.m$$
$$Ballast: 5.7\frac{kN}{m}(3.3\ m)(0.5x3.3\ m) \quad = 31.04\ kN.m$$
$$Ties: 1.3\frac{kN}{m}(2.6\ m)(0.5x2.6\ m) \quad = 4.39\ kN.m$$
$$Rail + Live\ loads: 295.01\text{kN}\ (0.5455\ \text{m}) \quad = 160.93\ kN.m$$
$$Rail\ + Live\ loads: 295.01\ \text{kN}\ (2.0545\ \text{m}) \quad = 606.10\ kN.m$$
$$Curb: 3.08\ \text{kN}\ (3.5\ \text{m}) \quad = 10.78\ kN.m$$
$$= \boldsymbol{851.00\ kN.m}$$

SoE 10-6: Configuration of dead and live loads on flange

$$V_c = -6.72\frac{kN}{m}(0\ m) \quad = 0$$
$$V_{d1} = 0\ \text{kN} - 6.72\frac{kN}{m}(0.5 * 0.4\ m) \quad = -1.34\ kN$$
$$V_{d_2} = -1.34\ kN - 3.08\ kN \quad = -4.42\ kN$$
$$V_e = -4.42\ kN - 6.72\frac{kN}{m}(0.5 * 0.4\ m) \quad = -5.76\ kN$$
$$V_A = -5.76\ kN - (6.72 + 5.7)\frac{kN}{m}(0.7\ m) \quad = -14.45\ kN$$
$$V_{R1} = -14.45\ kN + 327.31\ kN \quad = 312.86\ kN$$
$$V_{f1} = 312.83\ kN - (6.72 + 5.7 + 1.3)\frac{kN}{m}(0.5545\ m) \quad = 305.38\ kN$$
$$V_{f2} = 305.38\ kN - 295.01\ kN \quad = 10.37\ kN$$
$$V_{g1} = 10.37\ kN - (6.72 + 5.7 + 1.3)\frac{kN}{m}(1.5090\ m) \quad = -10.33\ kN$$
$$V_{g2} = -10.33\ kN - 295.01\ kN \quad = -305.34\ kN$$
$$V_B = -305.34\ kN - (6.72 + 5.7 + 1.3)\frac{kN}{m}(0.5545\ m) \quad = -312.82\ kN$$
$$V_{R2} = -312.82\ kN + 327.31\ kN \quad = 14.49\ kN$$
$$V_h = 14.49\ kN - (6.72 + 5.7)\frac{kN}{m}(0.7\ m) \quad = 5.80\ kN$$
$$V_{i_1} = 5.80\ kN - 6.72\frac{kN}{m}(0.5 * 0.4\ m) \quad = 4.46\ kN$$
$$V_{i_2} = 4.46\ kN - 3.08\ kN \quad = 1.38\ kN$$
$$V_j = 1.38\ kN - 6.72\frac{kN}{m}(0.5 * 0.4\ m) \quad = 0.036\ kN \approx 0$$

SoE 10-7: Computation of dead and live loads shear on flange

$$M_c = (0\ kN)(0\ m) \quad = 0$$
$$M_d = 0 - 0.5(0.2\ m)(1.34\ kN) \quad = -0.13\ kN.m$$
$$M_e = -0.13\ kN.m - 0.5(0.2\ m)(4.42 + 5.76)kN \quad = -1.15\ kN.m$$
$$M_A = -1.15\ kN.m - 0.5(0.7\ m)(5.76 + 14.45)kN \quad = -8.22\ kN.m$$
$$M_f = -8.22\ kN.m + 0.5(0.5455\ m)(312.86 + 305.38)kN \quad = 160.40\ kN.m$$
$$M_k = 160.40\ kN.m + 0.5(0.756\ m)(10.37)kN \quad = 164.32\ kN.m$$
$$M_g = 164.32\ kN.m - 0.5(1.5090\ m - 0.756\ m)(10.33\ kN) \quad = 160.43\ kN.m$$
$$M_B = 160.43\ kN.m - 0.5(0.5455\ m)(305.34 + 312.82)kN \quad = -8.17\ kN.m$$
$$M_h = -8.17\ kN.m + 0.5(0.7\ m)(14.49 + 5.80)kN \quad = -1.07\ kN.m$$

$M_i = -1.07\ kN.m + 0.5(0.2\ m)(5.80 + 4.46)kN \qquad = 0.04\ kN.m$
$M_j = 0.04\ kN.m + 0.5(0.2\ m)(1.38)kN \qquad = 0.10\ kN.m \approx 0$

SoE 10-8: Computation of dead and live loads moment on flange

$$\rho_0 = \left[1 - \sqrt{1 - \left(\frac{2M_{sd}}{\emptyset\varphi f_c^{'}bd^2}\right)}\right]\frac{0.85f_c^{'}}{f_y}$$
$$\rho_0 = \left[1 - \sqrt{1 - \left(\frac{2 * 207040}{0.9 * 0.85 * \left(40 * 10^6\right) * 1 * 0.22^2}\right)}\right]\frac{0.85(40 * 10^6)}{420 * 10^6}$$
$$\rho_0 = [1 - 0.849]0.081$$
$$\rho_0 = [0.151]0.081$$
$$\rho_0 = 0.012231$$
$$\rho_0 \approx 0.012$$
$$\rho_0 = 1.2\%$$

SoE 10-9: Computation of flange dead and live loads steel ratio

10.2 Appendicular table (Tablapp)

These are tables of reference used to provide detailed information as referenced in the text.

10.2.1 For T-section

Unfactored Loads: Dead Load + a percentage of Live Load to E_c and I_g

%LL	DL + a %LL (N/m)	*l* (m)	E_c (N/m^2)	$E_{c,eff}$ (N/m^2)	I_g (m^4)	I_e (m^4)	Δ (m)	Δ (mm)	% Incre. of Δ (%Δ)	%Δ_{acc}
0.0	61270.00	10	30000000000		0.078547232		0.0034	3.4	0.00	0.00
2.5	66085.75	10	30000000000		0.078547232		0.0037	3.7	8.82	8.82
5.0	70901.50	10	30000000000		0.078547232		0.0039	3.9	5.41	14.23
7.5	75717.25	10	30000000000		0.078547232		0.0042	4.2	7.69	21.92
10.0	80533.00	10	30000000000		0.078547232		0.0045	4.5	7.14	29.06
12.5	85348.75	10	30000000000		0.078547232		0.0047	4.7	4.44	33.50
15.0	90164.50	10	30000000000		0.078547232		0.005	5.0	6.38	39.88
17.5	94980.25	10	30000000000		0.078547232		0.0052	5.2	4.00	43.88
20.0	99796.00	10	30000000000		0.078547232		0.0055	5.5	5.77	49.65
22.5	104611.75	10	30000000000		0.078547232		0.0058	5.8	5.45	55.10
25.0	109427.50	10	30000000000		0.078547232		0.006	6.0	3.45	58.55
27.5	114243.25	10	30000000000		0.078547232		0.0063	6.3	5.00	63.55
30.0	119059.00	10	30000000000		0.078547232		0.0066	6.6	4.76	68.31
32.5	123874.75	10	30000000000		0.078547232		0.0068	6.8	3.03	71.34
35.0	128690.50	10	30000000000		0.078547232		0.0071	7.1	4.41	75.75
37.5	133506.25	10	30000000000		0.078547232		0.0074	7.4	4.23	79.98
40.0	138322.00	10	30000000000		0.078547232		0.0076	7.6	2.70	82.68
42.5	143137.75	10	30000000000		0.078547232		0.0079	7.9	3.95	86.63
45.0	147953.50	10	30000000000		0.078547232		0.0082	8.2	3.80	90.43
47.5	152769.25	10	30000000000		0.078547232		0.0084	8.4	2.44	92.87
50.0	157585.00	10	30000000000		0.078547232		0.0087	8.7	3.57	96.44
52.5	162400.75	10	30000000000		0.078547232		0.009	9.0	3.45	99.89
55.0	167216.50	10	30000000000		0.078547232		0.0092	9.2	2.22	102.11
57.5	172032.25	10	30000000000		0.078547232		0.0095	9.5	3.26	105.37
60.0	176848.00	10	30000000000		0.078547232		0.0098	9.8	3.16	108.53

62.5	181663.75	10	30000000000		0.078547232		0.0100	10.0	2.04	110.57
65.0	186479.50	10	30000000000		0.078547232		0.0103	10.3	3.00	113.57
67.5	191295.25	10	30000000000		0.078547232		0.0106	10.6	2.91	116.48
70.0	196111.00	10	30000000000		0.078547232		0.0108	10.8	1.89	118.37
72.5	200926.75	10	30000000000		0.078547232		0.0111	11.1	2.78	121.15
75.0	205742.50	10	30000000000		0.078547232		0.0114	11.4	2.70	123.85
77.5	210558.25	10	30000000000		0.078547232		0.0116	11.6	1.75	125.60
80.0	215374.00	10	30000000000		0.078547232		0.0119	11.9	2.59	128.19
82.5	220189.75	10	30000000000		0.078547232		0.0122	12.2	2.52	130.71
85.0	225005.50	10	30000000000		0.078547232		0.0124	12.4	1.64	132.35
87.5	229821.25	10	30000000000		0.078547232		0.0127	12.7	2.42	134.77
90.0	234637.00	10	30000000000		0.078547232		0.013	13.0	2.36	137.13
92.5	239452.75	10	30000000000		0.078547232		0.0132	13.2	1.54	138.67
95.0	244268.50	10	30000000000		0.078547232		0.0135	13.5	2.27	140.94
97.5	249084.25	10	30000000000		0.078547232		0.0138	13.8	2.22	143.16
100.0	253900.00	10	30000000000		0.078547232		0.014	14.0	1.45	144.61

Tablapp 10-1: The EcIg detailed deflection table for unfactored dead and live loads

Unfactored Loads: Dead Load + a percentage of Live Load to E_c and I_e										
%LL	**DL + a %LL (N/m)**	***l* (m)**	**E_c (N/m^2)**	**$E_{c,eff}$ (N/m^2)**	**I_g (m^4)**	**I_e (m^4)**	**Δ (m)**	**Δ (mm)**	**% Incre. of Δ (%Δ)**	**%Δ_{acc}**
0.0	61270.00	10	30000000000			0.1028664163	0.0026	2.6	0.00	0.00
2.5	66085.75	10	30000000000			0.1028664163	0.0028	2.8	7.69	7.69
5.0	70901.50	10	30000000000			0.1028664163	0.0030	3.0	7.14	14.83
7.5	75717.25	10	30000000000			0.1028664163	0.0032	3.2	6.67	21.50
10.0	80533.00	10	30000000000			0.1028664163	0.0034	3.4	6.25	27.75
12.5	85348.75	10	30000000000			0.1028664163	0.0036	3.6	5.88	33.63
15.0	90164.50	10	30000000000			0.1028664163	0.0038	3.8	5.56	39.19
17.5	94980.25	10	30000000000			0.1028664163	0.004	4.0	5.26	44.45
20.0	99796.00	10	30000000000			0.1028664163	0.0042	4.2	5.00	49.45
22.5	104611.75	10	30000000000			0.1028664163	0.0044	4.4	4.76	54.21
25.0	109427.50	10	30000000000			0.1028664163	0.0046	4.6	4.55	58.76
27.5	114243.25	10	30000000000			0.1028664163	0.0048	4.8	4.35	63.11
30.0	119059.00	10	30000000000			0.1028664163	0.005	5.0	4.17	67.28
32.5	123874.75	10	30000000000			0.1028664163	0.0052	5.2	4.00	71.28
35.0	128690.50	10	30000000000			0.1028664163	0.0054	5.4	3.85	75.13
37.5	133506.25	10	30000000000			0.1028664163	0.0056	5.6	3.70	78.83
40.0	138322.00	10	30000000000			0.1028664163	0.0058	5.8	3.57	82.40
42.5	143137.75	10	30000000000			0.1028664163	0.006	6.0	3.45	85.85
45.0	147953.50	10	30000000000			0.1028664163	0.0062	6.2	3.33	89.18
47.5	152769.25	10	30000000000			0.1028664163	0.0064	6.4	3.23	92.41
50.0	157585.00	10	30000000000			0.1028664163	0.0066	6.6	3.12	95.53
52.5	162400.75	10	30000000000			0.1028664163	0.0069	6.9	4.55	100.08
55.0	167216.50	10	30000000000			0.1028664163	0.0071	7.1	2.90	102.98
57.5	172032.25	10	30000000000			0.1028664163	0.0073	7.3	2.82	105.80
60.0	176848.00	10	30000000000			0.1028664163	0.0075	7.5	2.74	108.54
62.5	181663.75	10	30000000000			0.1028664163	0.0077	7.7	2.67	111.21
65.0	186479.50	10	30000000000			0.1028664163	0.0079	7.9	2.60	113.81
67.5	191295.25	10	30000000000			0.1028664163	0.0081	8.1	2.53	116.34
70.0	196111.00	10	30000000000			0.1028664163	0.0083	8.3	2.47	118.81
72.5	200926.75	10	30000000000			0.1028664163	0.0085	8.5	2.41	121.22
75.0	205742.50	10	30000000000			0.1028664163	0.0087	8.7	2.35	123.57
77.5	210558.25	10	30000000000			0.1028664163	0.0089	8.9	2.30	125.87
80.0	215374.00	10	30000000000			0.1028664163	0.0091	9.1	2.25	128.12

82.5	220189.75	10	30000000000			0.1028664163	0.0093	9.3	2.20	130.32
85.0	225005.50	10	30000000000			0.1028664163	0.0095	9.5	2.15	132.47
87.5	229821.25	10	30000000000			0.1028664163	0.0097	9.7	2.11	134.58
90.0	234637.00	10	30000000000			0.1028664163	0.0099	9.9	2.06	136.64
92.5	239452.75	10	30000000000			0.1028664163	0.0101	10.1	2.02	138.66
95.0	244268.50	10	30000000000			0.1028664163	0.0103	10.3	1.98	140.64
97.5	249084.25	10	30000000000			0.1028664163	0.0105	10.5	1.94	142.58
100.0	253900.00	10	30000000000			0.1028664163	0.0107	10.7	1.90	144.48

Tablapp 10-2: The E_cI_e detailed deflection table for unfactored dead and live loads

Unfactored Loads: Dead Load + a percentage of Live Load to E_c and I_e										
%LL	**DL + a %LL (N/m)**	***l* (m)**	**E_c (N/m^2)**	**$E_{c,eff}$ (N/m^2)**	**I_g (m^4)**	**I_e (m^4)**	**Δ (m)**	**Δ (mm)**	**% Incre. of Δ (%Δ)**	**%Δ_{acc}**
0.0	61270.00	10		996000000000	0.078547232		0.0001	0.10	0.00	0.00
2.5	66085.75	10		996000000000	0.078547232		0.0001	0.10	0.00	0.00
5.0	70901.50	10		996000000000	0.078547232		0.0001	0.10	0.00	0.00
7.5	75717.25	10		996000000000	0.078547232		0.0001	0.10	0.00	0.00
10.0	80533.00	10		996000000000	0.078547232		0.0001	0.10	0.00	0.00
12.5	85348.75	10		996000000000	0.078547232		0.0001	0.10	0.00	0.00
15.0	90164.50	10		996000000000	0.078547232		0.0002	0.20	100.00	100.00
17.5	94980.25	10		996000000000	0.078547232		0.0002	0.20	0.00	100.00
20.0	99796.00	10		996000000000	0.078547232		0.0002	0.20	0.00	100.00
22.5	104611.75	10		996000000000	0.078547232		0.0002	0.20	0.00	100.00
25.0	109427.50	10		996000000000	0.078547232		0.0002	0.20	0.00	100.00
27.5	114243.25	10		996000000000	0.078547232		0.0002	0.20	0.00	100.00
30.0	119059.00	10		996000000000	0.078547232		0.0002	0.20	0.00	100.00
32.5	123874.75	10		996000000000	0.078547232		0.0002	0.20	0.00	100.00
35.0	128690.50	10		996000000000	0.078547232		0.0002	0.20	0.00	100.00
37.5	133506.25	10		996000000000	0.078547232		0.0002	0.20	0.00	100.00
40.0	138322.00	10		996000000000	0.078547232		0.0002	0.20	0.00	100.00
42.5	143137.75	10		996000000000	0.078547232		0.0002	0.20	0.00	100.00
45.0	147953.50	10		996000000000	0.078547232		0.0002	0.20	0.00	100.00
47.5	152769.25	10		996000000000	0.078547232		0.0003	0.30	50.00	150.00
50.0	157585.00	10		996000000000	0.078547232		0.0003	0.30	0.00	150.00
52.5	162400.75	10		996000000000	0.078547232		0.0003	0.30	0.00	150.00
55.0	167216.50	10		996000000000	0.078547232		0.0003	0.30	0.00	150.00
57.5	172032.25	10		996000000000	0.078547232		0.0003	0.30	0.00	150.00
60.0	176848.00	10		996000000000	0.078547232		0.0003	0.30	0.00	150.00
62.5	181663.75	10		996000000000	0.078547232		0.0003	0.30	0.00	150.00
65.0	186479.50	10		996000000000	0.078547232		0.0003	0.30	0.00	150.00
67.5	191295.25	10		996000000000	0.078547232		0.0003	0.30	0.00	150.00
70.0	196111.00	10		996000000000	0.078547232		0.0003	0.30	0.00	150.00
72.5	200926.75	10		996000000000	0.078547232		0.0003	0.30	0.00	150.00
75.0	205742.50	10		996000000000	0.078547232		0.0003	0.30	0.00	150.00
77.5	210558.25	10		996000000000	0.078547232		0.0004	0.40	33.33	183.33
80.0	215374.00	10		996000000000	0.078547232		0.0004	0.40	0.00	183.33
82.5	220189.75	10		996000000000	0.078547232		0.0004	0.40	0.00	183.33
85.0	225005.50	10		996000000000	0.078547232		0.0004	0.40	0.00	183.33
87.5	229821.25	10		996000000000	0.078547232		0.0004	0.40	0.00	183.33
90.0	234637.00	10		996000000000	0.078547232		0.0004	0.40	0.00	183.33
92.5	239452.75	10		996000000000	0.078547232		0.0004	0.40	0.00	183.33
95.0	244268.50	10		996000000000	0.078547232		0.0004	0.40	0.00	183.33
97.5	249084.25	10		996000000000	0.078547232		0.0004	0.40	0.00	183.33
100.0	253900.00	10		996000000000	0.078547232		0.0004	0.40	0.00	183.33

Tablapp 10-3: The $E_{c,eff}I_g$ detailed deflection table for unfactored dead and live loads

Unfactored Loads: Dead Load + a percentage of Live Load to $E_{c,eff}$ and I_e										
%LL	**DL + a %LL (N/m)**	**l (m)**	**E_c (N/m^2)**	**$E_{c,eff}$ (N/m^2)**	**I_g (m^4)**	**I_e (m^4)**	**Δ (m)**	**Δ (mm)**	**% Incre. of Δ (%Δ)**	**%Δ_{acc}**
0.0	61270.00	10		996000000000		0.1028664163	0.0001	0.10	0.00	0.00
2.5	66085.75	10		996000000000		0.1028664163	0.0001	0.10	0.00	0.00
5.0	70901.50	10		996000000000		0.1028664163	0.0001	0.10	0.00	0.00
7.5	75717.25	10		996000000000		0.1028664163	0.0001	0.10	0.00	0.00
10.0	80533.00	10		996000000000		0.1028664163	0.0001	0.10	0.00	0.00
12.5	85348.75	10		996000000000		0.1028664163	0.0001	0.10	0.00	0.00
15.0	90164.50	10		996000000000		0.1028664163	0.0001	0.10	0.00	0.00
17.5	94980.25	10		996000000000		0.1028664163	0.0001	0.10	0.00	0.00
20.0	99796.00	10		996000000000		0.1028664163	0.0001	0.10	0.00	0.00
22.5	104611.75	10		996000000000		0.1028664163	0.0001	0.10	0.00	0.00
25.0	109427.50	10		996000000000		0.1028664163	0.0001	0.10	0.00	0.00
27.5	114243.25	10		996000000000		0.1028664163	0.0001	0.10	0.00	0.00
30.0	119059.00	10		996000000000		0.1028664163	0.0002	0.20	100.00	100.00
32.5	123874.75	10		996000000000		0.1028664163	0.0002	0.20	0.00	100.00
35.0	128690.50	10		996000000000		0.1028664163	0.0002	0.20	0.00	100.00
37.5	133506.25	10		996000000000		0.1028664163	0.0002	0.20	0.00	100.00
40.0	138322.00	10		996000000000		0.1028664163	0.0002	0.20	0.00	100.00
42.5	143137.75	10		996000000000		0.1028664163	0.0002	0.20	0.00	100.00
45.0	147953.50	10		996000000000		0.1028664163	0.0002	0.20	0.00	100.00
47.5	152769.25	10		996000000000		0.1028664163	0.0002	0.20	0.00	100.00
50.0	157585.00	10		996000000000		0.1028664163	0.0002	0.20	0.00	100.00
52.5	162400.75	10		996000000000		0.1028664163	0.0002	0.20	0.00	100.00
55.0	167216.50	10		996000000000		0.1028664163	0.0002	0.20	0.00	100.00
57.5	172032.25	10		996000000000		0.1028664163	0.0002	0.20	0.00	100.00
60.0	176848.00	10		996000000000		0.1028664163	0.0002	0.20	0.00	100.00
62.5	181663.75	10		996000000000		0.1028664163	0.0002	0.20	0.00	100.00
65.0	186479.50	10		996000000000		0.1028664163	0.0002	0.20	0.00	100.00
67.5	191295.25	10		996000000000		0.1028664163	0.0002	0.20	0.00	100.00
70.0	196111.00	10		996000000000		0.1028664163	0.0002	0.20	0.00	100.00
72.5	200926.75	10		996000000000		0.1028664163	0.0003	0.30	50.00	150.00
75.0	205742.50	10		996000000000		0.1028664163	0.0003	0.30	0.00	150.00
77.5	210558.25	10		996000000000		0.1028664163	0.0003	0.30	0.00	150.00
80.0	215374.00	10		996000000000		0.1028664163	0.0003	0.30	0.00	150.00
82.5	220189.75	10		996000000000		0.1028664163	0.0003	0.30	0.00	150.00
85.0	225005.50	10		996000000000		0.1028664163	0.0003	0.30	0.00	150.00
87.5	229821.25	10		996000000000		0.1028664163	0.0003	0.30	0.00	150.00
90.0	234637.00	10		996000000000		0.1028664163	0.0003	0.30	0.00	150.00
92.5	239452.75	10		996000000000		0.1028664163	0.0003	0.30	0.00	150.00
95.0	244268.50	10		996000000000		0.1028664163	0.0003	0.30	0.00	150.00
97.5	249084.25	10		996000000000		0.1028664163	0.0003	0.30	0.00	150.00
100	253900.00	10		996000000000		0.1028664163	0.0003	0.30	0.00	150.00

Tablapp 10-4:: The $E_{c,eff}I_e$ detailed deflection table for unfactored dead and live loads

Unfactored Loads: Dead Load + a percentage of Live Load to $E_{c,eff}$ and I_e										
%LL	**DL + a %LL (N/m)**	***l* (m)**	**E_c (N/m^2)**	**$E_{c,eff}$ (N/m^2)**	**I_g (m^4)**	**I_e (m^4)**	**Δ (m)**	**Δ (mm)**	**% Incre. of Δ (%Δ)**	**%Δ_{acc}**
0.0	61270.00	10		996000000000		0.1028664163	0.0001	0.10	0.00	0.00
2.5	66085.75	10		996000000000		0.1028664163	0.0001	0.10	0.00	0.00
5.0	70901.50	10		996000000000		0.1028664163	0.0001	0.10	0.00	0.00
7.5	75717.25	10		996000000000		0.1028664163	0.0001	0.10	0.00	0.00
10.0	80533.00	10		996000000000		0.1028664163	0.0001	0.10	0.00	0.00
12.5	85348.75	10		996000000000		0.1028664163	0.0001	0.10	0.00	0.00
15.0	90164.50	10		996000000000		0.1028664163	0.0001	0.10	0.00	0.00
17.5	94980.25	10		996000000000		0.1028664163	0.0001	0.10	0.00	0.00
20.0	99796.00	10		996000000000		0.1028664163	0.0001	0.10	0.00	0.00
22.5	104611.75	10		996000000000		0.1028664163	0.0001	0.10	0.00	0.00
25.0	109427.50	10		996000000000		0.1028664163	0.0001	0.10	0.00	0.00
27.5	114243.25	10		996000000000		0.1028664163	0.0001	0.10	0.00	0.00
30.0	119059.00	10		996000000000		0.1028664163	0.0002	0.20	100.00	100.00
32.5	123874.75	10		996000000000		0.1028664163	0.0002	0.20	0.00	100.00
35.0	128690.50	10		996000000000		0.1028664163	0.0002	0.20	0.00	100.00
37.5	133506.25	10		996000000000		0.1028664163	0.0002	0.20	0.00	100.00
40.0	138322.00	10		996000000000		0.1028664163	0.0002	0.20	0.00	100.00
42.5	143137.75	10		996000000000		0.1028664163	0.0002	0.20	0.00	100.00
45.0	147953.50	10		996000000000		0.1028664163	0.0002	0.20	0.00	100.00
47.5	152769.25	10		996000000000		0.1028664163	0.0002	0.20	0.00	100.00
50.0	157585.00	10		996000000000		0.1028664163	0.0002	0.20	0.00	100.00
52.5	162400.75	10		996000000000		0.1028664163	0.0002	0.20	0.00	100.00
55.0	167216.50	10		996000000000		0.1028664163	0.0002	0.20	0.00	100.00
57.5	172032.25	10		996000000000		0.1028664163	0.0002	0.20	0.00	100.00
60.0	176848.00	10		996000000000		0.1028664163	0.0002	0.20	0.00	100.00
62.5	181663.75	10		996000000000		0.1028664163	0.0002	0.20	0.00	100.00
65.0	186479.50	10		996000000000		0.1028664163	0.0002	0.20	0.00	100.00
67.5	191295.25	10		996000000000		0.1028664163	0.0002	0.20	0.00	100.00
70.0	196111.00	10		996000000000		0.1028664163	0.0002	0.20	0.00	100.00
72.5	200926.75	10		996000000000		0.1028664163	0.0003	0.30	50.00	150.00
75.0	205742.50	10		996000000000		0.1028664163	0.0003	0.30	0.00	150.00
77.5	210558.25	10		996000000000		0.1028664163	0.0003	0.30	0.00	150.00
80.0	215374.00	10		996000000000		0.1028664163	0.0003	0.30	0.00	150.00
82.5	220189.75	10		996000000000		0.1028664163	0.0003	0.30	0.00	150.00
85.0	225005.50	10		996000000000		0.1028664163	0.0003	0.30	0.00	150.00
87.5	229821.25	10		996000000000		0.1028664163	0.0003	0.30	0.00	150.00
90.0	234637.00	10		996000000000		0.1028664163	0.0003	0.30	0.00	150.00
92.5	239452.75	10		996000000000		0.1028664163	0.0003	0.30	0.00	150.00
95.0	244268.50	10		996000000000		0.1028664163	0.0003	0.30	0.00	150.00
97.5	249084.25	10		996000000000		0.1028664163	0.0003	0.30	0.00	150.00
100	253900.00	10		996000000000		0.1028664163	0.0003	0.30	0.00	150.00

Tablapp 10-5: The $E_{c,eff}I_e$ detailed deflection table for unfactored dead and live loads

Synchronized summary of all deflections calculated										
Deflection Summary				**Statistics**						
$\Delta[E_cI_g]$ (mm)	**$\Delta[E_cI_e]$ (mm)**	**$\Delta[E_{c,eff}I_g]$ (mm)**	**$\Delta[E_{c,eff}I_e]$ (mm)**	**$\sum\Delta$ (mm)**	**n**	**Δ[Ave] (mm)**	**n-1**	**variance**	**standard deviation**	**C_v (%)**
3.4	2.6	0.1	0.1	6.20	4	*1.55*	3	2.2	1.5	95.31
3.7	2.8	0.1	0.1	6.70	4	*1.68*	3	2.6	1.6	95.93
3.9	3.0	0.1	0.1	7.10	4	*1.78*	3	2.9	1.7	96.05
4.2	3.2	0.1	0.1	7.60	4	*1.90*	3	3.4	1.8	96.55
4.5	3.4	0.1	0.1	8.10	4	*2.03*	3	3.9	2.0	96.98
4.7	3.6	0.1	0.1	8.50	4	*2.13*	3	4.3	2.1	97.04
5.0	3.8	0.2	0.1	9.10	4	*2.28*	3	4.7	2.2	95.26
5.2	4.0	0.2	0.1	9.50	4	*2.38*	3	5.1	2.3	95.38
5.5	4.2	0.2	0.1	10.00	4	*2.50*	3	5.7	2.4	95.79
5.8	4.4	0.2	0.1	10.50	4	*2.63*	3	6.4	2.5	96.16
6.0	4.6	0.2	0.1	10.90	4	*2.73*	3	6.9	2.6	96.23
6.3	4.8	0.2	0.1	11.40	4	*2.85*	3	7.6	2.8	96.56
6.6	5.0	0.2	0.2	12.00	4	*3.00*	3	8.2	2.9	95.22
6.8	5.2	0.2	0.2	12.40	4	*3.10*	3	8.7	3.0	95.31
7.1	5.4	0.2	0.2	12.90	4	*3.23*	3	9.5	3.1	95.63
7.4	5.6	0.2	0.2	13.40	4	*3.35*	3	10.3	3.2	95.93
7.6	5.8	0.2	0.2	13.80	4	*3.45*	3	11.0	3.3	95.99
7.9	6.0	0.2	0.2	14.30	4	*3.58*	3	11.8	3.4	96.26
8.2	6.2	0.2	0.2	14.80	4	*3.70*	3	12.8	3.6	96.51
8.4	6.4	0.3	0.2	15.30	4	*3.83*	3	13.3	3.6	95.28
8.7	6.6	0.3	0.2	15.80	4	*3.95*	3	14.2	3.8	95.54
9.0	6.9	0.3	0.2	16.40	4	*4.10*	3	15.4	3.9	95.64
9.2	7.1	0.3	0.2	16.80	4	*4.20*	3	16.2	4.0	95.7
9.5	7.3	0.3	0.2	17.30	4	*4.33*	3	17.2	4.1	95.92
9.8	7.5	0.3	0.2	17.80	4	*4.45*	3	18.3	4.3	96.14
10.0	7.7	0.3	0.2	18.20	4	*4.55*	3	19.2	4.4	96.18
10.3	7.9	0.3	0.2	18.70	4	*4.68*	3	20.3	4.5	96.38
10.6	8.1	0.3	0.2	19.20	4	*4.80*	3	21.5	4.6	96.57
10.8	8.3	0.3	0.2	19.60	4	*4.90*	3	22.4	4.7	96.6
11.1	8.5	0.3	0.3	20.20	4	*5.05*	3	23.4	4.8	95.8
11.4	8.7	0.3	0.3	20.70	4	*5.18*	3	24.7	5.0	95.99
11.6	8.9	0.4	0.3	21.20	4	*5.30*	3	25.4	5.0	95.12
11.9	9.1	0.4	0.3	21.70	4	*5.43*	3	26.7	5.2	95.31
12.2	9.3	0.4	0.3	22.20	4	*5.55*	3	28.1	5.3	95.5
12.4	9.5	0.4	0.3	22.60	4	*5.65*	3	29.1	5.4	95.55
12.7	9.7	0.4	0.3	23.10	4	*5.78*	3	30.6	5.5	95.72
13.0	9.9	0.4	0.3	23.60	4	*5.90*	3	32.0	5.7	95.89
13.2	10.1	0.4	0.3	24.00	4	*6.00*	3	33.1	5.8	95.92
13.5	10.3	0.4	0.3	24.50	4	*6.13*	3	34.6	5.9	96.08
13.8	10.5	0.4	0.3	25.00	4	*6.25*	3	36.2	6.0	96.23
14.0	10.7	0.4	0.3	25.40	4	*6.35*	3	37.4	6.1	96.26

Tablapp 10-6: Summary of all deflections and statistics

10.2.2 Rectangular section

Unfactored Loads: Dead Load + a percentage of Live Load to E_c and I_g										
%LL	**DL + a %LL (N/m)**	***l*** **(m)**	**E_c (N/m^2)**	**$E_{c,eff}$ (N/m^2)**	**I_g (m^4)**	**I_e (m^4)**	**Δ (m)**	**Δ (mm)**	**% Incre. of Δ (%Δ)**	**$\%\Delta_{acc}$**
0.0	61270.00	10	30000000000		0.041666667		0.0064	6.4	0.00	0.00
2.5	66085.75	10	30000000000		0.041666667		0.0069	6.9	7.81	7.81
5.0	70901.50	10	30000000000		0.041666667		0.0074	7.4	7.25	15.06
7.5	75717.25	10	30000000000		0.041666667		0.0079	7.9	6.76	21.82
10.0	80533.00	10	30000000000		0.041666667		0.0084	8.4	6.33	28.15
12.5	85348.75	10	30000000000		0.041666667		0.0089	8.9	5.95	34.10
15.0	90164.50	10	30000000000		0.041666667		0.0094	9.4	5.62	39.72
17.5	94980.25	10	30000000000		0.041666667		0.0099	9.9	5.32	45.04
20.0	99796.00	10	30000000000		0.041666667		0.0104	10.4	5.05	50.09
22.5	104611.75	10	30000000000		0.041666667		0.0109	10.9	4.81	54.90
25.0	109427.50	10	30000000000		0.041666667		0.0114	11.4	4.59	59.49
27.5	114243.25	10	30000000000		0.041666667		0.0119	11.9	4.39	63.88
30.0	119059.00	10	30000000000		0.041666667		0.0124	12.4	4.2	68.08
32.5	123874.75	10	30000000000		0.041666667		0.0129	12.9	4.03	72.11
35.0	128690.50	10	30000000000		0.041666667		0.0134	13.4	3.88	75.99
37.5	133506.25	10	30000000000		0.041666667		0.0139	13.9	3.73	79.72
40.0	138322.00	10	30000000000		0.041666667		0.0144	14.4	3.6	83.32
42.5	143137.75	10	30000000000		0.041666667		0.0149	14.9	3.47	86.79
45.0	147953.50	10	30000000000		0.041666667		0.0154	15.4	3.36	90.15
47.5	152769.25	10	30000000000		0.041666667		0.0159	15.9	3.25	93.40
50.0	157585.00	10	30000000000		0.041666667		0.0164	16.4	3.14	96.54
52.5	162400.75	10	30000000000		0.041666667		0.0169	16.9	3.05	99.59
55.0	167216.50	10	30000000000		0.041666667		0.0174	17.4	2.96	102.55
57.5	172032.25	10	30000000000		0.041666667		0.0179	17.9	2.87	105.42
60.0	176848.00	10	30000000000		0.041666667		0.0184	18.4	2.79	108.21
62.5	181663.75	10	30000000000		0.041666667		0.0189	18.9	2.72	110.93
65.0	186479.50	10	30000000000		0.041666667		0.0194	19.4	2.65	113.58
67.5	191295.25	10	30000000000		0.041666667		0.0199	19.9	2.58	116.16
70.0	196111.00	10	30000000000		0.041666667		0.0204	20.4	2.51	118.67
72.5	200926.75	10	30000000000		0.041666667		0.0209	20.9	2.45	121.12
75.0	205742.50	10	30000000000		0.041666667		0.0214	21.4	2.39	123.51
77.5	210558.25	10	30000000000		0.041666667		0.0219	21.9	2.34	125.85
80.0	215374.00	10	30000000000		0.041666667		0.0224	22.4	2.28	128.13
82.5	220189.75	10	30000000000		0.041666667		0.0229	22.9	2.23	130.36
85.0	225005.50	10	30000000000		0.041666667		0.0234	23.4	2.18	132.54
87.5	229821.25	10	30000000000		0.041666667		0.0239	23.9	2.14	134.68
90.0	234637.00	10	30000000000		0.041666667		0.0244	24.4	2.09	136.77
92.5	239452.75	10	30000000000		0.041666667		0.0249	24.9	2.05	138.82
95.0	244268.50	10	30000000000		0.041666667		0.0254	25.4	2.01	140.83
97.5	249084.25	10	30000000000		0.041666667		0.0259	25.9	1.97	142.80
100.0	253900.00	10	30000000000		0.041666667		0.0264	26.4	1.93	144.73

Tablapp 10-7: The E_cI_g detailed deflection table for unfactored dead and live loads for the rectangular beam

Unfactored Loads: Dead Load + a percentage of Live Load to E_c and I_e										
%LL	DL + a %LL (N/m)	*l* (m)	E_c (N/m^2)	$E_{c,eff}$ (N/m^2)	I_g (m^4)	I_e (m^4)	Δ (m)	Δ (mm)	% Incre. of Δ (%Δ)	%Δ_{acc}
0.0	61270.00	10	30000000000			0.038481401205	0.0069	6.9	0.00	0.00
2.5	66085.75	10	30000000000			0.038481401205	0.0075	7.5	8.7	8.70
5.0	70901.50	10	30000000000			0.038481401205	0.008	8	6.67	15.37
7.5	75717.25	10	30000000000			0.038481401205	0.0085	8.5	6.25	21.62
10.0	80533.00	10	30000000000			0.038481401205	0.0091	9.1	7.06	28.68
12.5	85348.75	10	30000000000			0.038481401205	0.0096	9.6	5.49	34.17
15.0	90164.50	10	30000000000			0.038481401205	0.0102	10.2	6.25	40.42
17.5	94980.25	10	30000000000			0.038481401205	0.0107	10.7	4.9	45.32
20.0	99796.00	10	30000000000			0.038481401205	0.0113	11.3	5.61	50.93
22.5	104611.75	10	30000000000			0.038481401205	0.0118	11.8	4.42	55.35
25.0	109427.50	10	30000000000			0.038481401205	0.0123	12.3	4.24	59.59
27.5	114243.25	10	30000000000			0.038481401205	0.0129	12.9	4.88	64.47
30.0	119059.00	10	30000000000			0.038481401205	0.0134	13.4	3.88	68.35
32.5	123874.75	10	30000000000			0.038481401205	0.014	14	4.48	72.83
35.0	128690.50	10	30000000000			0.038481401205	0.0145	14.5	3.57	76.40
37.5	133506.25	10	30000000000			0.038481401205	0.0151	15.1	4.14	80.54
40.0	138322.00	10	30000000000			0.038481401205	0.0156	15.6	3.31	83.85
42.5	143137.75	10	30000000000			0.038481401205	0.0161	16.1	3.21	87.06
45.0	147953.50	10	30000000000			0.038481401205	0.0167	16.7	3.73	90.79
47.5	152769.25	10	30000000000			0.038481401205	0.0172	17.2	2.99	93.78
50.0	157585.00	10	30000000000			0.038481401205	0.0178	17.8	3.49	97.27
52.5	162400.75	10	30000000000			0.038481401205	0.0183	18.3	2.81	100.08
55.0	167216.50	10	30000000000			0.038481401205	0.0189	18.9	3.28	103.36
57.5	172032.25	10	30000000000			0.038481401205	0.0194	19.4	2.65	106.01
60.0	176848.00	10	30000000000			0.038481401205	0.0199	19.9	2.58	108.59
62.5	181663.75	10	30000000000			0.038481401205	0.0205	20.5	3.02	111.61
65.0	186479.50	10	30000000000			0.038481401205	0.021	21	2.44	114.05
67.5	191295.25	10	30000000000			0.038481401205	0.0216	21.6	2.86	116.91
70.0	196111.00	10	30000000000			0.038481401205	0.0221	22.1	2.31	119.22
72.5	200926.75	10	30000000000			0.038481401205	0.0227	22.7	2.71	121.93
75.0	205742.50	10	30000000000			0.038481401205	0.0232	23.2	2.2	124.13
77.5	210558.25	10	30000000000			0.038481401205	0.0237	23.7	2.16	126.29
80.0	215374.00	10	30000000000			0.038481401205	0.0243	24.3	2.53	128.82
82.5	220189.75	10	30000000000			0.038481401205	0.0248	24.8	2.06	130.88
85.0	225005.50	10	30000000000			0.038481401205	0.0254	25.4	2.42	133.30
87.5	229821.25	10	30000000000			0.038481401205	0.0259	25.9	1.97	135.27
90.0	234637.00	10	30000000000			0.038481401205	0.0265	26.5	2.32	137.59
92.5	239452.75	10	30000000000			0.038481401205	0.027	27	1.89	139.48
95.0	244268.50	10	30000000000			0.038481401205	0.0276	27.6	2.22	141.70
97.5	249084.25	10	30000000000			0.038481401205	0.0281	28.1	1.81	143.51
100.0	253900.00	10	30000000000			0.038481401205	0.0286	28.6	1.78	145.29

Tablapp 10-8: The E_cI_e detailed deflection table for unfactored dead and live loads for the rectangular beam

Unfactored Loads: Dead Load + a percentage of Live Load to $E_{c,eff}$ and I_g										
%LL	**DL + a %LL (N/m)**	***l* (m)**	**E_c (N/m^2)**	**$E_{c,eff}$ (N/m^2)**	**I_g (m^4)**	**I_e (m^4)**	**Δ (m)**	**Δ (mm)**	**% Incre. of Δ (%Δ)**	**%Δ_{acc}**
0.0	61270.00	10		25000000000	0.041666667		0.0077	7.7	0.00	0.00
2.5	66085.75	10		25000000000	0.041666667		0.0083	8.3	7.79	7.79
5.0	70901.50	10		25000000000	0.041666667		0.0089	8.9	7.23	15.02
7.5	75717.25	10		25000000000	0.041666667		0.0095	9.5	6.74	21.76
10.0	80533.00	10		25000000000	0.041666667		0.0101	10.1	6.32	28.08
12.5	85348.75	10		25000000000	0.041666667		0.0107	10.7	5.94	34.02
15.0	90164.50	10		25000000000	0.041666667		0.0113	11.3	5.61	39.63
17.5	94980.25	10		25000000000	0.041666667		0.0119	11.9	5.31	44.94
20.0	99796.00	10		25000000000	0.041666667		0.0125	12.5	5.04	49.98
22.5	104611.75	10		25000000000	0.041666667		0.0131	13.1	4.80	54.78
25.0	109427.50	10		25000000000	0.041666667		0.0137	13.7	4.58	59.36
27.5	114243.25	10		25000000000	0.041666667		0.0143	14.3	4.38	63.74
30.0	119059.00	10		25000000000	0.041666667		0.0149	14.9	4.20	67.94
32.5	123874.75	10		25000000000	0.041666667		0.0155	15.5	4.03	71.97
35.0	128690.50	10		25000000000	0.041666667		0.0161	16.1	3.87	75.84
37.5	133506.25	10		25000000000	0.041666667		0.0167	16.7	3.73	79.57
40.0	138322.00	10		25000000000	0.041666667		0.0173	17.3	3.59	83.16
42.5	143137.75	10		25000000000	0.041666667		0.0179	17.9	3.47	86.63
45.0	147953.50	10		25000000000	0.041666667		0.0185	18.5	3.35	89.98
47.5	152769.25	10		25000000000	0.041666667		0.0191	19.1	3.24	93.22
50.0	157585.00	10		25000000000	0.041666667		0.0197	19.7	3.14	96.36
52.5	162400.75	10		25000000000	0.041666667		0.0203	20.3	3.05	99.41
55.0	167216.50	10		25000000000	0.041666667		0.0209	20.9	2.96	102.37
57.5	172032.25	10		25000000000	0.041666667		0.0215	21.5	2.87	105.24
60.0	176848.00	10		25000000000	0.041666667		0.0221	22.1	2.79	108.03
62.5	181663.75	10		25000000000	0.041666667		0.0227	22.7	2.71	110.74
65.0	186479.50	10		25000000000	0.041666667		0.0233	23.3	2.64	113.38
67.5	191295.25	10		25000000000	0.041666667		0.0239	23.9	2.58	115.96
70.0	196111.00	10		25000000000	0.041666667		0.0245	24.5	2.51	118.47
72.5	200926.75	10		25000000000	0.041666667		0.0251	25.1	2.45	120.92
75.0	205742.50	10		25000000000	0.041666667		0.0257	25.7	2.39	123.31
77.5	210558.25	10		25000000000	0.041666667		0.0263	26.3	2.33	125.64
80.0	215374.00	10		25000000000	0.041666667		0.0269	26.9	2.28	127.92
82.5	220189.75	10		25000000000	0.041666667		0.0275	27.5	2.23	130.15
85.0	225005.50	10		25000000000	0.041666667		0.0281	28.1	2.18	132.33
87.5	229821.25	10		25000000000	0.041666667		0.0287	28.7	2.14	134.47
90.0	234637.00	10		25000000000	0.041666667		0.0293	29.3	2.09	136.56
92.5	239452.75	10		25000000000	0.041666667		0.0299	29.9	2.05	138.61
95.0	244268.50	10		25000000000	0.041666667		0.0305	30.5	2.01	140.62
97.5	249084.25	10		25000000000	0.041666667		0.0311	31.1	1.97	142.59
100.0	253900.00	10		25000000000	0.041666667		0.0317	31.7	1.93	144.52

Tablapp 10-9: The $E_{c,eff}I_g$ detailed deflection table for unfactored dead and live loads for the rectangular beam

Unfactored Loads: Dead Load + a percentage of Live Load to $E_{c,eff}$ and I_e										
%LL	DL + a %LL (N/m)	*l* (m)	E_c (N/m^2)	$E_{c,eff}$ (N/m^2)	I_g (m^4)	I_e (m^4)	Δ (m)	Δ (mm)	% Incre. of Δ (%Δ)	%Δ_{acc}
0.0	61270.00	10		25000000000		0.038481401205	0.0083	8.3	0.0	0.00
2.5	66085.75	10		25000000000		0.038481401205	0.0089	8.9	7.2	7.23
5.0	70901.50	10		25000000000		0.038481401205	0.0096	9.6	7.9	15.10
7.5	75717.25	10		25000000000		0.038481401205	0.0102	10.2	6.3	21.35
10.0	80533.00	10		25000000000		0.038481401205	0.0109	10.9	6.9	28.21
12.5	85348.75	10		25000000000		0.038481401205	0.0116	11.6	6.4	34.63
15.0	90164.50	10		25000000000		0.038481401205	0.0122	12.2	5.2	39.80
17.5	94980.25	10		25000000000		0.038481401205	0.0129	12.9	5.7	45.54
20.0	99796.00	10		25000000000		0.038481401205	0.0135	13.5	4.7	50.19
22.5	104611.75	10		25000000000		0.038481401205	0.0142	14.2	5.2	55.38
25.0	109427.50	10		25000000000		0.038481401205	0.0148	14.8	4.2	59.61
27.5	114243.25	10		25000000000		0.038481401205	0.0155	15.5	4.7	64.34
30.0	119059.00	10		25000000000		0.038481401205	0.0161	16.1	3.9	68.21
32.5	123874.75	10		25000000000		0.038481401205	0.0168	16.8	4.4	72.56
35.0	128690.50	10		25000000000		0.038481401205	0.0174	17.4	3.6	76.13
37.5	133506.25	10		25000000000		0.038481401205	0.0181	18.1	4.0	80.15
40.0	138322.00	10		25000000000		0.038481401205	0.0187	18.7	3.3	83.46
42.5	143137.75	10		25000000000		0.038481401205	0.0194	19.4	3.7	87.20
45.0	147953.50	10		25000000000		0.038481401205	0.02	20.0	3.1	90.29
47.5	152769.25	10		25000000000		0.038481401205	0.0207	20.7	3.5	93.79
50.0	157585.00	10		25000000000		0.038481401205	0.0213	21.3	2.9	96.69
52.5	162400.75	10		25000000000		0.038481401205	0.022	22.0	3.3	99.98
55.0	167216.50	10		25000000000		0.038481401205	0.0226	22.6	2.7	102.71
57.5	172032.25	10		25000000000		0.038481401205	0.0233	23.3	3.1	105.81
60.0	176848.00	10		25000000000		0.038481401205	0.0239	23.9	2.6	108.39
62.5	181663.75	10		25000000000		0.038481401205	0.0246	24.6	2.9	111.32
65.0	186479.50	10		25000000000		0.038481401205	0.0252	25.2	2.4	113.76
67.5	191295.25	10		25000000000		0.038481401205	0.0259	25.9	2.8	116.54
70.0	196111.00	10		25000000000		0.038481401205	0.0265	26.5	2.3	118.86
72.5	200926.75	10		25000000000		0.038481401205	0.0272	27.2	2.6	121.50
75.0	205742.50	10		25000000000		0.038481401205	0.0278	27.8	2.2	123.71
77.5	210558.25	10		25000000000		0.038481401205	0.0285	28.5	2.5	126.23
80.0	215374.00	10		25000000000		0.038481401205	0.0292	29.2	2.5	128.69
82.5	220189.75	10		25000000000		0.038481401205	0.0298	29.8	2.1	130.74
85.0	225005.50	10		25000000000		0.038481401205	0.0305	30.5	2.4	133.09
87.5	229821.25	10		25000000000		0.038481401205	0.0311	31.1	2.0	135.06
90.0	234637.00	10		25000000000		0.038481401205	0.0318	31.8	2.3	137.31
92.5	239452.75	10		25000000000		0.038481401205	0.0324	32.4	1.9	139.20
95.0	244268.50	10		25000000000		0.038481401205	0.0331	33.1	2.2	141.36
97.5	249084.25	10		25000000000		0.038481401205	0.0337	33.7	1.8	143.17
100	253900.00	10		25000000000		0.038481401205	0.0344	34.4	2.1	145.25

Tablapp 10-10: The $E_{c,eff}I_e$ detailed deflection table for unfactored dead and live loads for the rectangular beam

Synchronized summary of all deflections calculated										
Deflection Summary				**Statistics**						
$\Delta[E_cI_g]$ (mm)	**$\Delta[E_cI_e]$ (mm)**	**$\Delta[E_{c,eff}I_g]$ (mm)**	**$\Delta[E_{c,eff}I_e]$ (mm)**	**$\sum\Delta$ (mm)**	**n**	**Δ[Ave] (mm)**	**n-1**	**variance**	**standard deviation**	**C_v (%)**
6.4	6.9	7.7	8.3	29.30	4	7.33	3	0.5	0.7	9.96
6.9	7.5	8.3	8.9	31.60	4	7.90	3	0.6	0.8	9.64
7.4	8.0	8.9	9.6	33.90	4	8.48	3	0.7	0.8	9.92
7.9	8.5	9.5	10.2	36.10	4	9.03	3	0.8	0.9	9.83
8.4	9.1	10.1	10.9	38.50	4	9.63	3	0.9	1.0	9.89
8.9	9.6	10.7	11.6	40.80	4	10.20	3	1.1	1.0	10.12
9.4	10.2	11.3	12.2	43.10	4	10.78	3	1.1	1.1	9.87
9.9	10.7	11.9	12.9	45.40	4	11.35	3	1.3	1.1	10.07
10.4	11.3	12.5	13.5	47.70	4	11.93	3	1.4	1.2	9.86
10.9	11.8	13.1	14.2	50.00	4	12.50	3	1.6	1.3	10.04
11.4	12.3	13.7	14.8	52.20	4	13.05	3	1.7	1.3	9.97
11.9	12.9	14.3	15.5	54.60	4	13.65	3	1.9	1.4	10.01
12.4	13.4	14.9	16.1	56.80	4	14.20	3	2.0	1.4	9.95
12.9	14.0	15.5	16.8	59.20	4	14.80	3	2.2	1.5	9.99
13.4	14.5	16.1	17.4	61.40	4	15.35	3	2.3	1.5	9.93
13.9	15.1	16.7	18.1	63.80	4	15.95	3	2.5	1.6	9.97
14.4	15.6	17.3	18.7	66.00	4	16.50	3	2.7	1.6	9.91
14.9	16.1	17.9	19.4	68.30	4	17.08	3	2.9	1.7	10.05
15.4	16.7	18.5	20.0	70.60	4	17.65	3	3.1	1.7	9.9
15.9	17.2	19.1	20.7	72.90	4	18.23	3	3.3	1.8	10.02
16.4	17.8	19.7	21.3	75.20	4	18.80	3	3.5	1.9	9.89
16.9	18.3	20.3	22.0	77.50	4	19.38	3	3.8	1.9	10
17.4	18.9	20.9	22.6	79.80	4	19.95	3	3.9	2.0	9.88
17.9	19.4	21.5	23.3	82.10	4	20.53	3	4.2	2.0	9.99
18.4	19.9	22.1	23.9	84.30	4	21.08	3	4.4	2.1	9.94
18.9	20.5	22.7	24.6	86.70	4	21.68	3	4.7	2.2	9.97
19.4	21.0	23.3	25.2	88.90	4	22.23	3	4.9	2.2	9.93
19.9	21.6	23.9	25.9	91.30	4	22.83	3	5.2	2.3	9.96
20.4	22.1	24.5	26.5	93.50	4	23.38	3	5.4	2.3	9.92
20.9	22.7	25.1	27.2	95.90	4	23.98	3	5.7	2.4	9.95
21.4	23.2	25.7	27.8	98.10	4	24.53	3	5.9	2.4	9.91
21.9	23.7	26.3	28.5	100.40	4	25.10	3	6.3	2.5	10
22.4	24.3	26.9	29.2	102.80	4	25.70	3	6.6	2.6	10.02
22.9	24.8	27.5	29.8	105.00	4	26.25	3	6.9	2.6	9.99
23.4	25.4	28.1	30.5	107.40	4	26.85	3	7.2	2.7	10.01
23.9	25.9	28.7	31.1	109.60	4	27.40	3	7.5	2.7	9.97
24.4	26.5	29.3	31.8	112.00	4	28.00	3	7.8	2.8	10
24.9	27.0	29.9	32.4	114.20	4	28.55	3	8.1	2.8	9.96
25.4	27.6	30.5	33.1	116.60	4	29.15	3	8.5	2.9	9.99
25.9	28.1	31.1	33.7	118.80	4	29.70	3	8.7	3.0	9.95
26.4	28.6	31.7	34.4	121.10	4	30.28	3	9.2	3.0	10.03

Tablapp 10-11: Rectangular section deflection and statistics summary

10.2.3 For T- and rectangular sections combined

%LL	$(\Delta E_cI_g)_T$	$(\Delta E_cI_g)_R$	$(\Delta E_cI_e)_T$	$(\Delta E_cI_e)_R$	$(\Delta E_{c,eff}I_g)_T$	$(\Delta E_{c,eff}I_g)_R$	$(\Delta E_{c,eff}I_e)_T$	$(\Delta E_{c,eff}I_e)_R$	$(\Delta_{Ave})_T$	$(\Delta_{Ave})_R$	Δ_η
0.0	2.2	3.7	1.8	3.2	0.4	3.7	0.3	3.2	1.18	3.45	*2.32*
2.5	2.7	4.6	2.3	4.0	0.5	4.6	0.4	4.0	1.48	4.30	*2.89*
5.0	3.3	5.6	2.7	4.8	0.6	5.6	0.5	4.8	1.78	5.20	*3.49*
7.5	3.8	6.5	3.2	5.6	0.7	6.5	0.6	5.6	2.07	6.05	*4.06*
10.0	4.4	7.4	3.7	6.4	0.8	7.4	0.7	6.4	2.40	6.90	*4.65*
12.5	4.9	8.4	4.1	7.2	0.9	8.4	0.7	7.2	2.65	7.80	*5.23*
15.0	5.5	9.3	4.6	8.0	1.0	9.3	0.8	8.0	2.98	8.65	*5.82*
17.5	6.0	10.2	5.0	8.8	1.1	10.2	0.9	8.8	3.25	9.50	*6.38*
20.0	6.6	11.2	5.5	9.6	1.2	11.2	1.0	9.6	3.58	10.40	*6.99*
22.5	7.1	12.1	5.9	10.4	1.3	12.1	1.1	10.4	3.85	11.25	*7.55*
25.0	7.7	13.0	6.4	11.2	1.4	13.0	1.2	11.2	4.18	12.10	*8.14*
27.5	8.2	14.0	6.9	12.0	1.5	14.0	1.2	12.0	4.45	13.00	*8.73*
30.0	8.8	14.9	7.3	12.8	1.6	14.9	1.3	12.8	4.75	13.85	*9.30*
32.5	9.3	15.8	7.8	13.6	1.7	15.8	1.4	13.6	5.05	14.70	*9.88*
35.0	9.9	16.8	8.2	14.4	1.8	16.8	1.5	14.4	5.35	15.60	*10.48*
37.5	10.4	17.7	8.7	15.2	1.9	17.7	1.6	15.2	5.65	16.45	*11.05*
40.0	11.0	18.6	9.2	16.0	2.0	18.6	1.7	16.0	5.98	17.30	*11.64*
42.5	11.5	19.6	9.6	16.8	2.1	19.6	1.7	16.8	6.23	18.20	*12.22*
45.0	12.1	20.5	10.1	17.6	2.2	20.5	1.8	17.6	6.55	19.05	*12.80*
47.5	12.6	21.4	10.5	18.4	2.3	21.4	1.9	18.4	6.83	19.90	*13.37*
50.0	13.2	22.4	11.0	19.2	2.4	22.4	2.0	19.2	7.15	20.80	*13.98*
52.5	13.7	23.3	11.5	20.0	2.5	23.3	2.1	20.0	7.45	21.65	*14.55*
55.0	14.3	24.2	11.9	20.8	2.6	24.2	2.2	20.8	7.75	22.50	*15.13*
57.5	14.8	25.2	12.4	21.6	2.7	25.2	2.2	21.6	8.03	23.40	*15.72*
60.0	15.4	26.1	12.8	22.4	2.8	26.1	2.3	22.4	8.33	24.25	*16.29*
62.5	15.9	27.0	13.3	23.2	2.9	27.0	2.4	23.2	8.63	25.10	*16.87*
65.0	16.4	28.0	13.7	24.0	3.0	28.0	2.5	24.0	8.90	26.00	*17.45*
67.5	17.0	28.9	14.2	24.8	3.1	28.9	2.6	24.8	9.23	26.85	*18.04*
70.0	17.5	29.8	14.7	25.6	3.2	29.8	2.7	25.6	9.53	27.70	*18.62*
72.5	18.1	30.8	15.1	26.4	3.3	30.8	2.7	26.4	9.80	28.60	*19.20*
75.0	18.6	31.7	15.6	27.2	3.4	31.7	2.8	27.2	10.10	29.45	*19.78*
77.5	19.2	32.6	16.0	28.0	3.5	32.6	2.9	28.0	10.40	30.30	*20.35*
80.0	19.7	33.6	16.5	28.8	3.6	33.6	3.0	28.8	10.70	31.20	*20.95*
82.5	20.3	34.5	17.0	29.6	3.7	34.5	3.1	29.6	11.03	32.05	*21.54*
85.0	20.8	35.4	17.4	30.4	3.8	35.4	3.2	30.4	11.30	32.90	*22.10*
87.5	21.4	36.4	17.9	31.2	3.9	36.4	3.3	31.2	11.63	33.80	*22.72*
90.0	21.9	37.3	18.3	32.0	4.0	37.3	3.3	32.0	11.88	34.65	*23.27*
92.5	22.5	38.2	18.8	32.8	4.1	38.2	3.4	32.8	12.20	35.50	*23.85*
95.0	23.0	39.2	19.3	33.6	4.2	39.2	3.5	33.6	12.50	36.40	*24.45*
97.5	23.6	40.1	19.7	34.4	4.3	40.1	3.6	34.4	12.80	37.25	*25.03*
100	24.1	41.0	20.2	35.2	4.4	41.0	3.7	35.2	13.10	38.10	*25.60*

Tablapp 10-12: Deflections, percent increment in deflection, and accumulated percentage of increment in deflection of all stiffnesses the experimented rectangular section

10.3 Appendicular figure (Figapp)

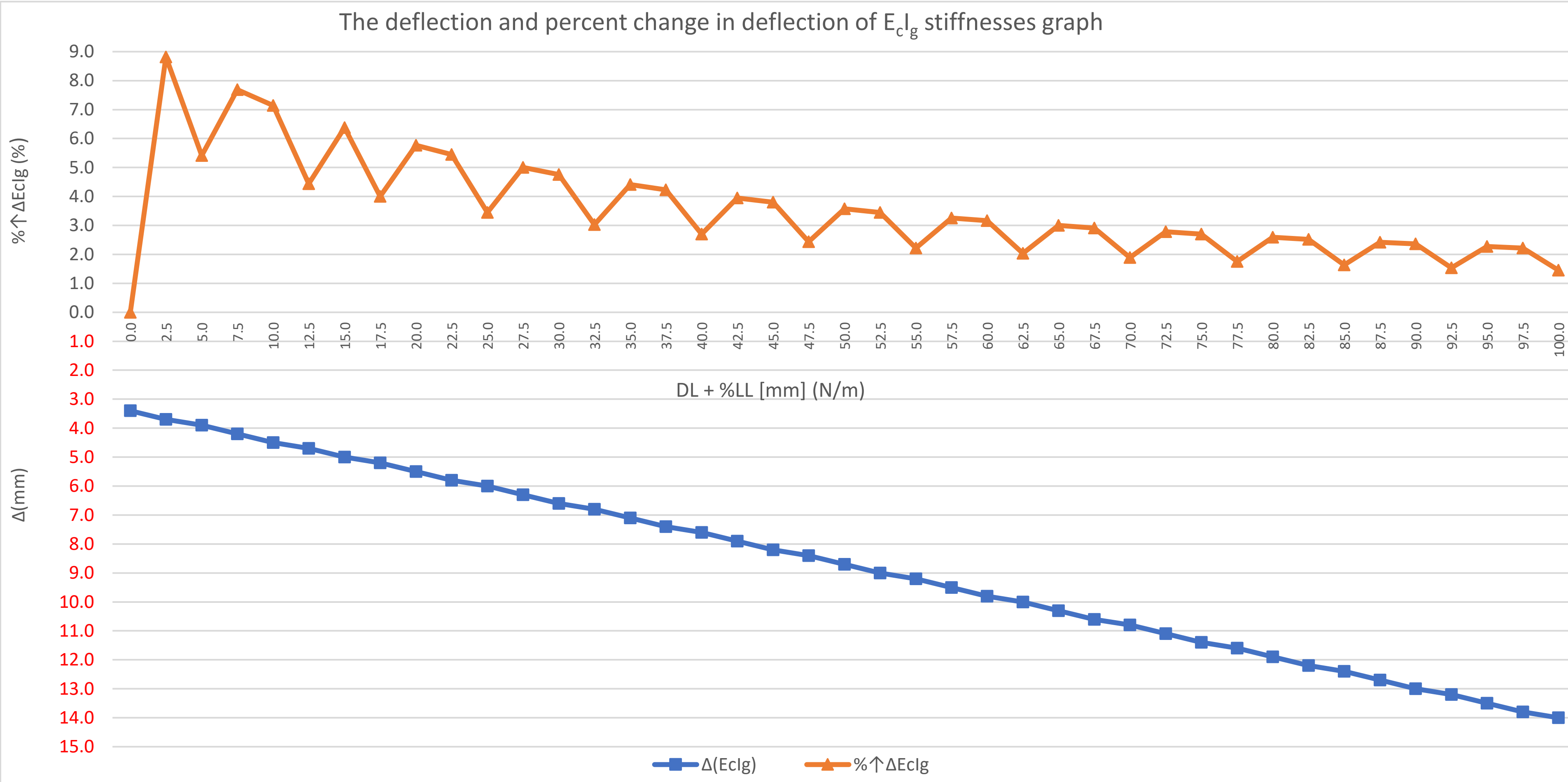

FigApp 10-1: Graphical representation of deflection and percent change in load

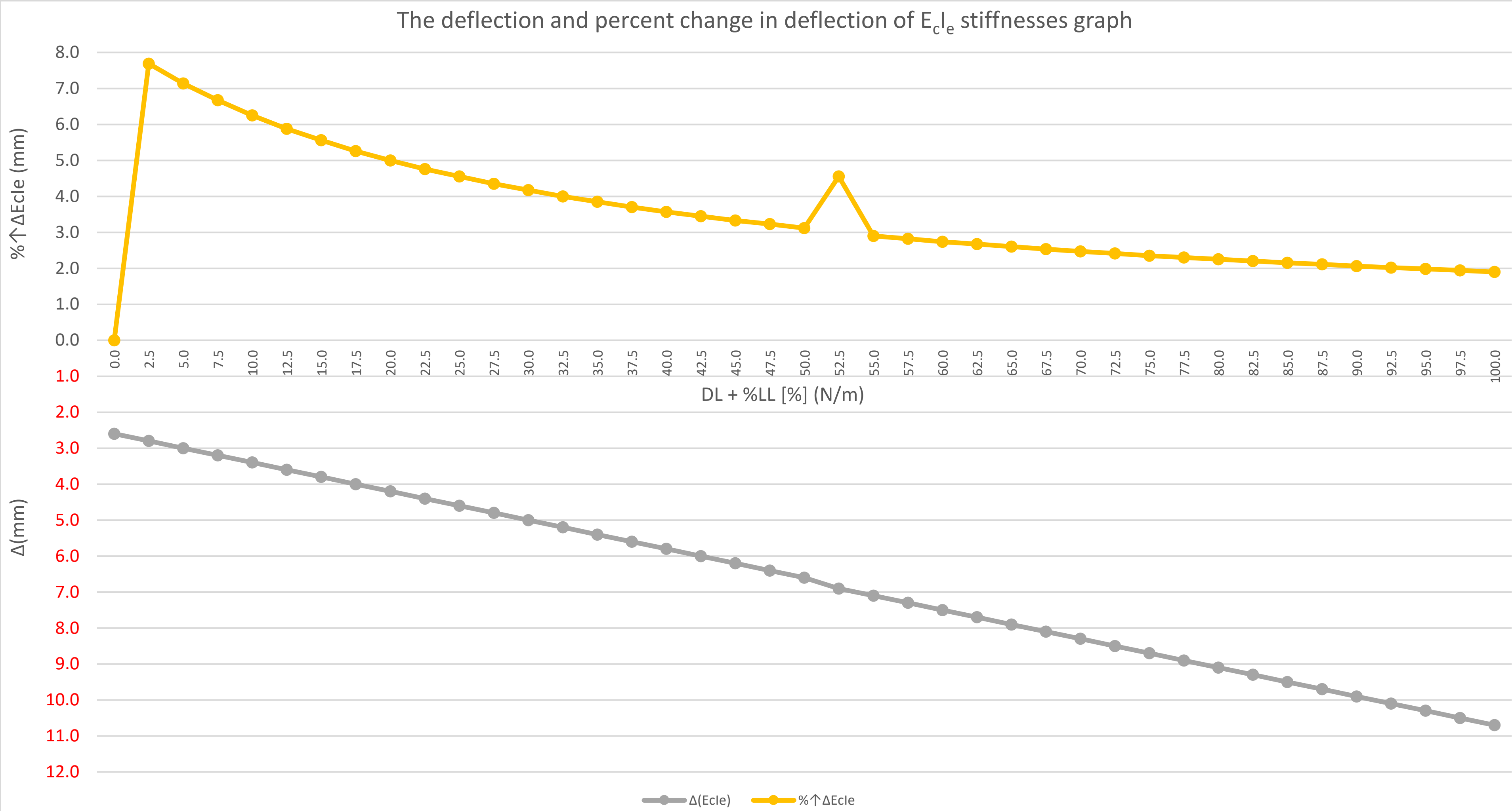

FigApp 10-2: Graphical representation of deflection and percent change in load for Tablapp 10-2

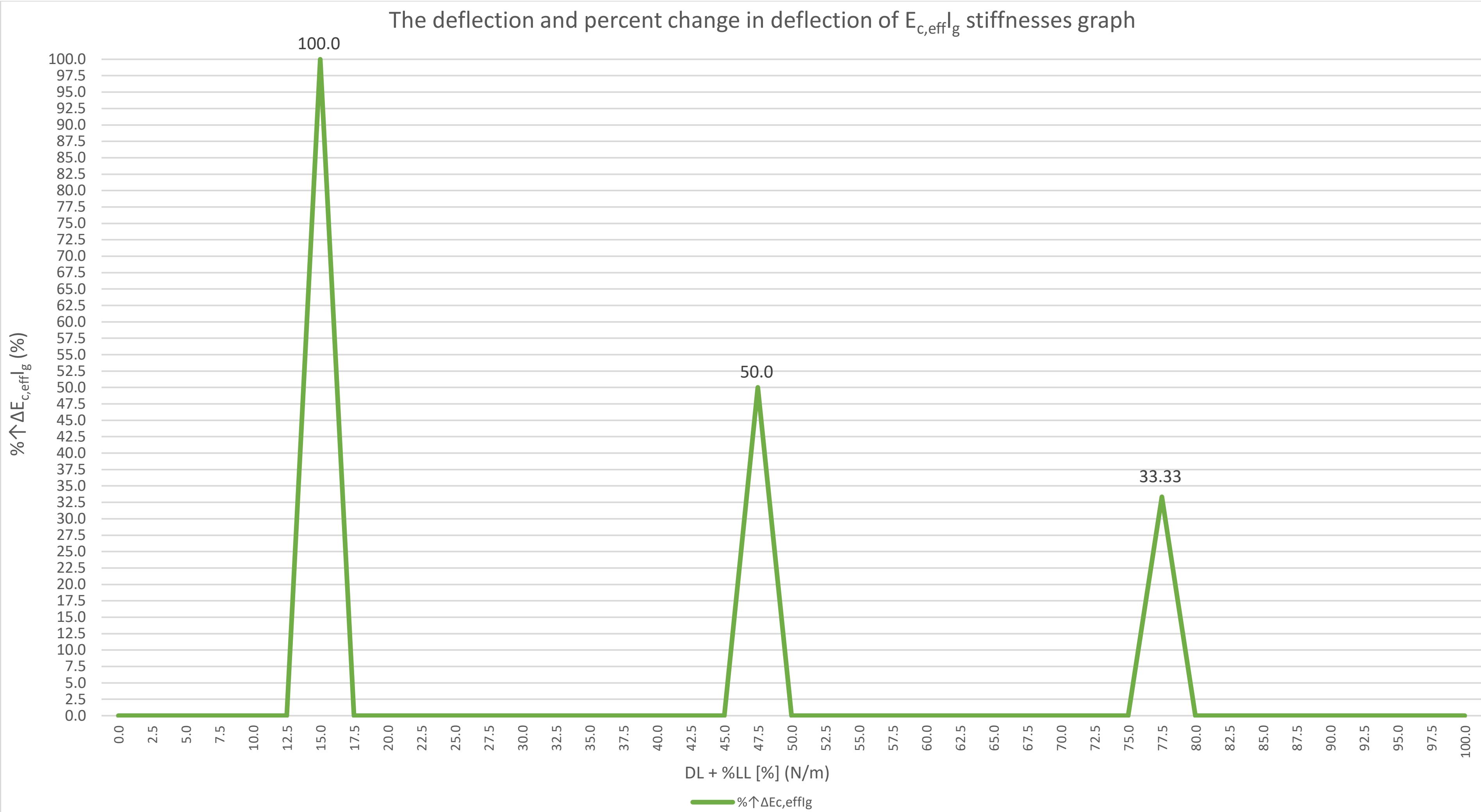

FigApp 10-3: View of the effect of percent increment in load on the increment in deflection (Tablapp 10-3)

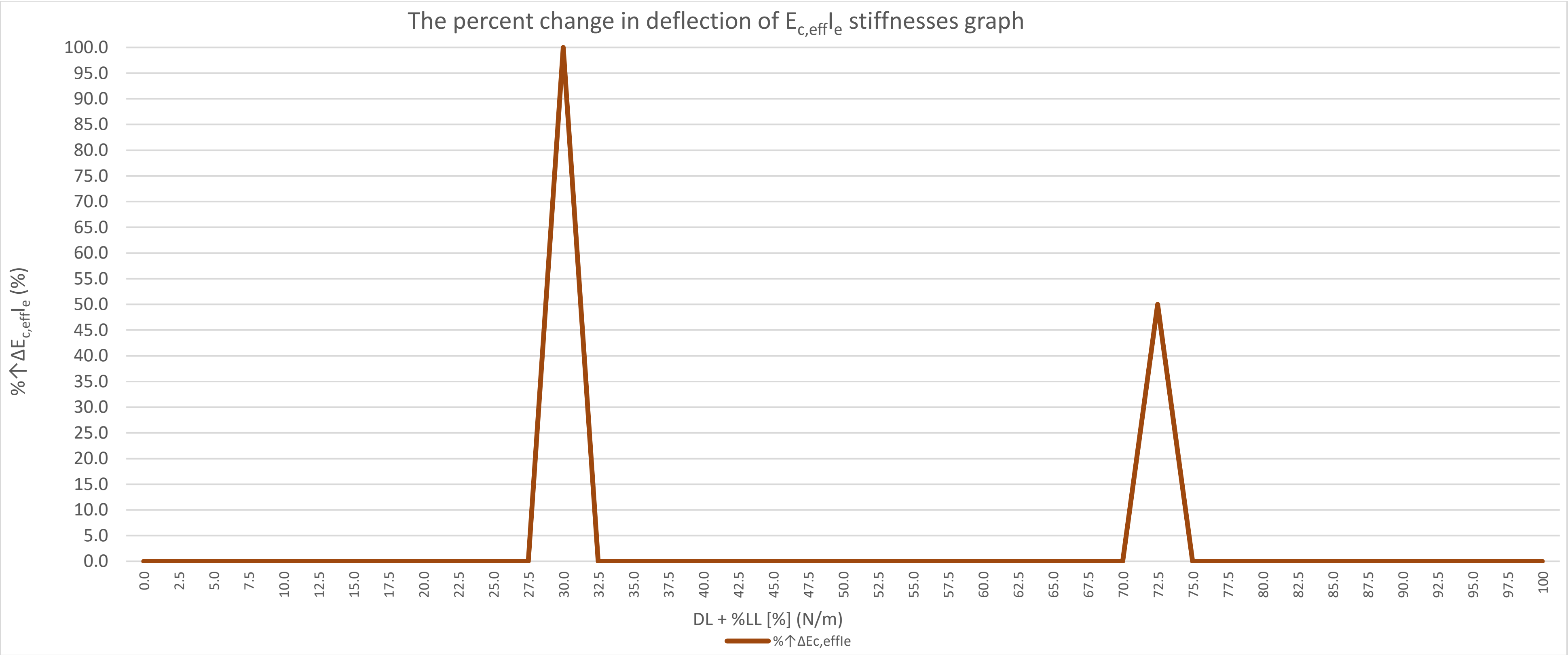

FigApp 10-4: View of the effect of percent increment in load on the increment in deflection (Tablapp 10-4)

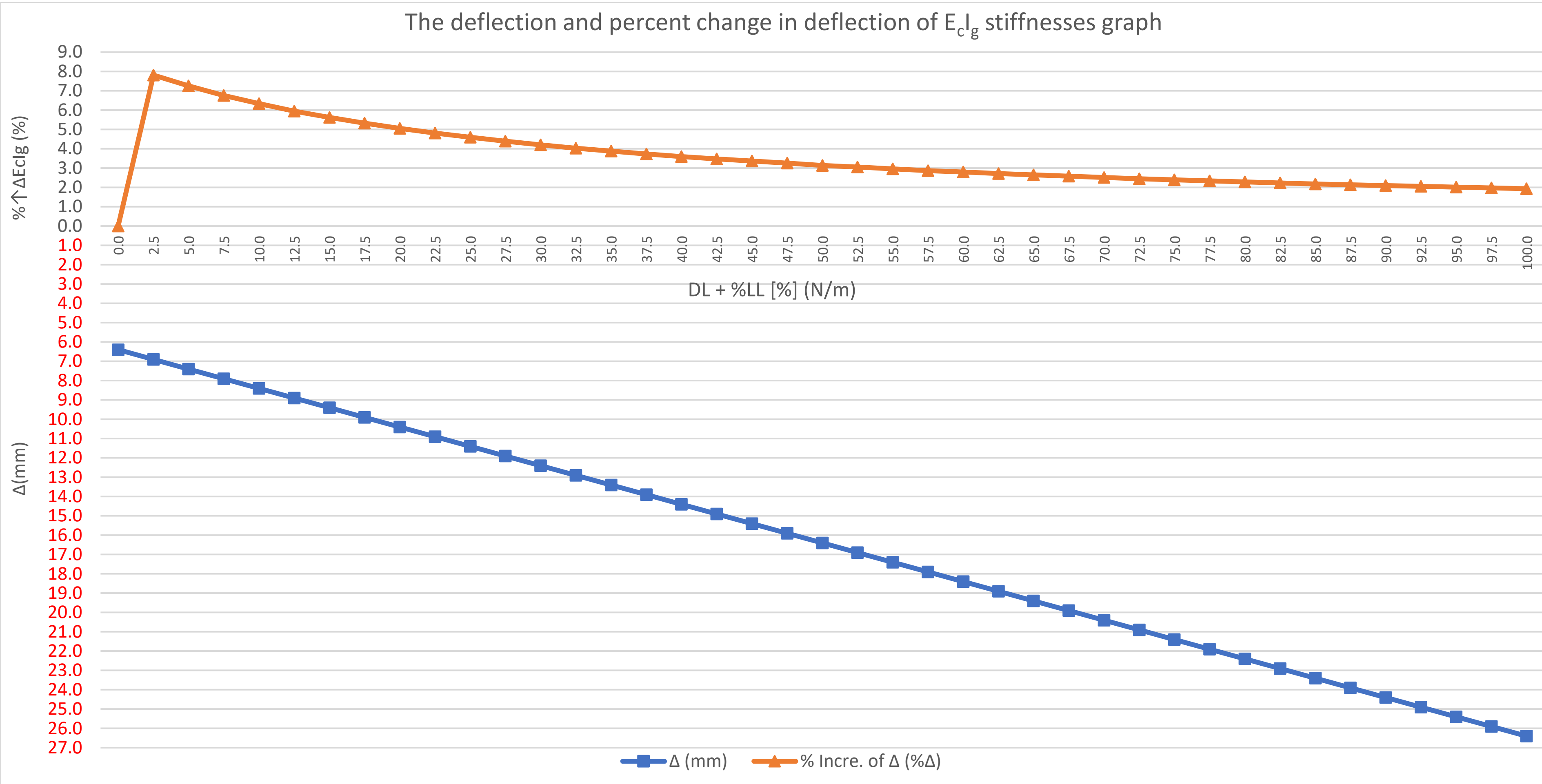

FigApp 10-5: Graphical representation of deflection and percent change in deflection

Supplementary Data

Bridges serve a pivotal role in the land transport sector of every establishment. A fully road-connected road service eases transportation of goods and passengers in the locale concerned. A 2013 inspection data from the Ethiopian Road Authority (ERA) shows that there were 4344 road-crossing structures back then.

#	**Bridge Type**	**Qty**
1	RC Slab Culvert	1878
2	RC Deck Girder	1089
3	PC Box Girder	6
4	RC Box Culvert	874
5	PC Deck Girder	3
6	Masonry Arch	353
7	RC Arch	20
8	RC Deck Girder and RC Slab Culvert	19
9	Steel Panel/Bailey	36
10	Steel Girder/ Composite	8
11	Steel Truss	4
12	RC Box Girder	35
13	Steel Truss and RCDG	3
14	RC Box Girder and RCDG	8
15	RC Rigid Frame	3
16	RC Arch and RCDG	1
17	Extradosed Cable	1
18	Pipe/Steel/RC	2
19	Steel Truss and Box Girder	1
	Total	**4344**

Table 10-1: Summary of all Ethiopian bridges (types and quantities) as of 2013

During the same period of assessment, 3743 bridges were assessed and a total of 11498 defects recorded. Of this, crack is being the most predominantly occurring defect with a frequency of 2498. This further stresses the severe unpredictability of cracks as contained in this work.

Defects				
Cracking	2498		Displacement / Bulging	94
Peel Off	1034		Displacement	22
Rebar Exposure	1122		Parts Missing	19
Honey Comb	1493		Potholes	283
Void	749		Blocked	273
Peel Off / Stone deterioration	484		Rutting	154
Scour	775		Bolt Missing	12
Erosion	521		Depression	191
Deformation	224		Pipe damage	53
Missing	263		Main damage	24
Inlet Damage	26		Anchor Damage	16
Wave	166		Bed Damage	7
Water Leakage	866		Unusual Movement	3
Noise	53		Wearing	1
Corrosion	68		Paint Peel Off	4
Sub-total	**10342**		**Sub-total**	**1156**
		11498		

Table 10-2: Summary defects of all Ethiopian bridges (types and quantities) as of 2013

In Liberia, the most viable railway line is operated by ArcelorMittal Liberia (AML), a subsidiary of the world steel giant ArcelorMittal. As a student of railway engineering, research works would be undertaken to investigate civil defects, line improvement mechanism/strategies, etc. and help strengthen national policies. Mining operations along the AML line is made possible through the many civil structures (as of 2019):

No.	Location from Buchanan (KM)	Bridge Type	Bridge Description	Special Description	# of Spans	Span Length (m)	Total Length (m)	Essence to the Railway line
1	2.500	Reinforced Concrete	Overpass (Road Bridge)	Grand Bassa County			0	Not used by the railway line
2	6.100	Reinforced Concrete	Overpass (Road Bridge)	Grand Bassa County			0	Not used by the railway line
3	9.272	Reinforced Concrete	Reinforced Concrete	Grand Bassa County	1	12	**12**	Used by the railway line
4	18.800	Reinforced Concrete	Overpass (Road Bridge)	Grand Bassa County			0	Not used by the railway line
5	19.463	Steel Bridge	Steel Truss Bridge (Deck Truss)	Grand Bassa County	1	42	**42**	Used by the railway line
6	35.937	Reinforced Concrete	Reinforced Concrete	Grand Bassa County	2	11 - 11	**22**	Used by the railway line
7	84.854	Steel Bridge	Plate Girder & Steel Deck Truss Bridge	Grand Bassa County	3	20 - 42 - 20	**82**	Used by the railway line
8	87.635	Reinforced Concrete	Reinforced Concrete	Grand Bassa County	2	11 - 11	**22**	Used by the railway line
9	91.182	Steel Bridge	Steel Truss Bridge (Deck Truss)	**St. John River boundary** of Grand Bassa and Bong Counties	3	42 - 42 - 42	**126**	Used by the railway line
10	95.983	Reinforced Concrete	Reinforced Concrete	Bong county	2	11 - 11	**22**	Used by the railway line
11	100.744	Reinforced Concrete	Reinforced Concrete	Bong county	2	11 - 11	**22**	Used by the railway line
12	108.208	Reinforced Concrete	Reinforced Concrete	Bong county	1	14	**14**	Used by the railway line
13	111.336	Reinforced Concrete	Reinforced Concrete	Bong county	2	11 - 11	**22**	Used by the railway line
14	114.114	Reinforced Concrete	Reinforced Concrete	Bong county	2	11 - 11	**22**	Used by the railway line
15	126.118	Steel Bridge	Plate Girder	Bong county	3	20 - 20 - 20	**60**	Used by the railway line
16	138.539	Reinforced Concrete	Reinforced Concrete	Bong county	1	14	**14**	Used by the railway line
17	158.469	Steel Bridge	Plate Girder + Steel Through Truss	**St. Paul River -** boundary of Bong and Nimba Counties	4	14 - 40 - 40 - 14	**108**	Used by the railway line
18	190.867	Reinforced Concrete	Overpass (Road Bridge)	Nimba County	1	12	**12**	Not used by the railway line
19	190.100	Reinforced Concrete	Overpass (Road Bridge)	Nimba County			0	Not used by the railway line
20	203.010	Reinforced Concrete	Overpass (Road Bridge)	Nimba County			0	Not used by the railway line
21	209.570	Reinforced Concrete	Reinforced Concrete Frame	Nimba County	1	14	**14**	Used by the railway line
22	209.700	Reinforced Concrete	Overpass (Road Bridge)	Nimba County			0	Not used by the railway line
23	209.941	Steel Bridge	Steel Truss (Through Truss)	Nimba County	1	40	**40**	Used by the railway line
24	212.695	Steel Bridge	Plate Girder	Nimba County	2	20 - 20	**40**	Used by the railway line
25	217.626	Reinforced Concrete	Reinforced Concrete	Nimba County	3	11 - 11 - 11	**33**	Used by the railway line
26	231.870	Steel Bridge	Steel Bridge (Deck Truss)	Nimba County	1	42	**42**	Used by the railway line
27	232.200	Reinforced Concrete	Overpass (Road Bridge)	Nimba County			0	Not used by the railway line
						Total Length	**759**	

10-3: Summary of all bridges (types, location, span, quantities, and usability) of all bridges along the AML's Buchanan-Tokadeh line as of 2019 (Court.: A. Denton)

END OF THESIS